



UNIVERSITY OF TRENTO

International Doctoral School in Biomolecular Sciences
XXV cycle

p53 FUNCTIONAL INTERACTIONS: THE STUDY OF A NEW CROSSTALK WITH ESTRADIOL PATHWAY IN TRANSCRIPTIONAL RESPONSES TO CHEMOTHERAPEUTICS

Tutor: Dr. **ALBERTO INGA**
Advisor: Dr. **YARI CIRIBILLI**
Centre for Integrative Biology, CIBIO
Laboratory of Transcriptional Networks

Ph.D. Thesis of
MATTIA LION
Centre for Integrative Biology, CIBIO
Laboratory of Transcriptional Networks

Academic year 2012-2013

INDEX

ABSTRACT	5
PRIMARY TASK.....	7
<i>p53 FUNCTIONAL INTERACTIONS: INTERACTION BETWEEN p53 AND ESTRADIOL PATHWAYS IN TRANSCRIPTIONAL RESPONSES TO CHEMOTHERAPEUTICS</i>	7
INTRODUCTION.....	8
Mechanisms of transcriptional regulation	8
The tumor suppressor p53: Structure, Regulation and Function	10
Structure, Regulation and Function of Estrogen Receptors	13
The intricate p53 and ERs crosstalk	16
METHODS	21
RESULTS.....	26
Validation of the experimental approach: p53, ER activation under the different treatment protocols and impact on cell growth	26
Different stimuli or concentrations led to different transcriptome changes: microarray results followed by pathway and ontology analyses	28
Genome-wide transcriptome analyses identify a combinatorial effect between genotoxic stress and proliferation stimulus in response to DOX and E2	39
A cooperative regulation enhanced the expression of genes involved in differentiation, cell-cell communication and cell adhesion or inflammatory response	43
Genotoxic stress plays an important role in the synergy with ER: Nutlin-3a treatment synergizes with estradiol pathway only on a subset of genes	47
Silencing of p53 in MCF7 cells establishes a direct role of p53 in doxorubicin and nutlin responsiveness of the target genes	48
MCF7 vector and p53i clones did not reproduce the cooperation between p53 and estradiol pathway at the experimental conditions	51

The transcriptional responsiveness of INPP5D, TLR5 and KRT15 is associated with p53 and ER response elements	53
DISCUSSION	57
Conclusions and implications	64
SECONDARY TASK.....	66
<i>p53 FUNCTIONAL INTERACTIONS: IMPACT OF COFACTORS AND SMALL MOLECULES ASSAYED USING A SIMPLIFIED YEAST-BASED SCREENING SYSTEM</i>	66
INTRODUCTION	67
MATERIALS AND METHODS.....	71
RESULTS and DISCUSSION.....	73
Small-volume, dual-luciferase assay in yeast	73
Genetic modifications at the <i>ABC</i> transporter system.....	75
Gap repair cloning of MDM4 and 53BP1 genes in yeast	76
Impact of nutlin and RITA in the functional interactions between wild type p53 and MDM4.....	77
Functional interaction between p53 and 53BP1	78
REFERENCES	81
APPENDIX.....	91
Interaction between p53 and estradiol pathways in transcriptional responses to chemotherapeutics.	91
<i>p53 Transactivation and the Impact of Mutations, Cofactors and Small Molecules Using a Simplified Yeast- Based Screening System</i>	141

ABBREVIATIONS and ACRONYMS	
53BP1	p53-binding protein 1
5FU	5-fluorouracil
AF-1/2	activation function 1/2
ChIP	chromatin immunoprecipitation assay
DBD	DNA-binding domain
DEGs	differentially expressed genes
DMSO	dimethyl sulfoxide
DOX	doxorubicin
DSBs	DNA double strand breaks
E2	17 β -estradiol
EMT	epithelial–mesenchymal transition
ERE	estrogen receptor response element
ERs	Estrogen Receptors
EtOH	ethanol
FC	fold change
FDR	false discovery rate
GEO	Gene Expression Omnibus database repository
GO	Gene Ontology
IgG	Immunoglobulin G
IP	immunoprecipitation
IPA	Ingenuity Pathway Analysis
LU	light unit
MCF7 p53i	MCF7 clone silenced for p53
MCF7 vector	control MCF7 clone
MDMX	MDM4
N	undefined aminoacid
NES	nuclear export signal
NLS	nuclear localization signal
nutlin	Nutlin-3a
O/N	overnight
OD	tetramerization domain
OD ₆₀₀	optical density
p	p-value
p53-RE	p53 response element
PBS	Phosphate Buffered Saline
PI	protease inhibitors
PIGF	placental growth factor
PDR	pleiotropic drug resistance
PFT α	pifithrin- α
PIGF	placental growth factor
PLB	Passive Lysis Buffer
PRD	proline-rich domain
qPCR	quantitative real-time PCR
R	purine
REs	Response Elements
RITA	reactivation of p53 and induction of tumor cell apoptosis
RLU	relative light unit
RSAT	Regulatory Sequence Analysis Tool

RTCA	Real-Time Cell Analyzer
SD	synthetic medium
SERDs	selective estrogen receptor down-regulators
SERMs	selective estrogen receptor modulators
SDS	Sodium Dodecyl Sulphate
SM	second messenger
ssDNA	Salmon sperm DNA
TAD1/2	Transactivation domain 1/2
TE	Tris-EDTA buffer
TFs	Transcription Factors
TSS	transcription start site
VEGFR1	vascular endothelial growth factor 1
W	Adenine or Thymine
Y	pyrimidine
YPDA	yeast peptone dextrose adenine

ABSTRACT

BACKGROUND Objective of this thesis has been the analysis of the sequence specific transcription factor p53, a critical tumor suppressor protein, specifically, the crosstalk (or functional interactions) with other transcription factors, namely, the estrogen receptors, and the modeling in reconstituted assays of the interaction of p53 with positive and negative cofactors (e.g. MDM4 and 53BP1) and the impact of small molecules, including chemotherapeutic drugs, on such interactions. Previous reports have revealed a complex, often negative, crosstalk between p53 and estrogen receptors (ERs) related in part to the physical interaction between the two proteins. An example of transcriptional cooperation mediated by cognate, non-canonical *cis*-elements was instead discovered for the angiogenesis related VEGFR1, FLT1 promoter.

MAIN TASK Transcriptional cooperation between p53 and ERs was sought out on a global scale using the human breast adenocarcinoma MCF7 cells as a model and transcriptome analyses. Cells were subjected to single or combinatorial treatments with the chemotherapeutic agent doxorubicin (able to induce p53 protein stabilization) and the ER ligand 17 β -estradiol (E2). 201 differentially expressed genes, that showed limited responsiveness to either doxorubicin treatment or ER ligand alone, but were up-regulated in a greater than additive manner following combined treatment were identified. Among sixteen genes chosen for validation using quantitative real-time PCR (qPCR), seven (INPP5D, TLR5, KRT15, EPHA2, GDNF, NOTCH1, SOX9) were confirmed to be novel direct targets of p53, based on responses in stable MCF7 clone cells silenced for p53, or cooperative targets of p53 and ER. Based on exposure to 5-fluorouracil (another genotoxic drug) and nutlin-3a (a non-genotoxic p53-specific activator), the combined response identified genes that were consistently regulated, although with different kinetics (e.g. INPP5D, CDH26, KRT15), while others (e.g. TLR5, SOX9) were treatment selective.

Promoter pattern searches and chromatin IP experiments for the INPP5D, TLR5, KRT15 genes were also performed to interrogate a direct, *cis*-mediated p53 and ERs regulation. While these analyses confirmed the identification of novel direct p53 targets, the important contribution of ER in their transcriptional modulation and

the role of non-canonical response elements, the correlation between occupancy levels and gene expression varied.

SECONDARY TASK Using a newly developed miniaturized yeast-based assay, functional interactions between p53 and its regulators MDM4 and 53BP1 was investigated. MDM4 was confirmed as a p53 negative regulator and the impact of nutlin-3a or RITA (apoptosis inducer through p53 binding) on the p53-MDM4 interaction was explored. Instead, no stimulatory effect of the p53 co-activator 53BP1 was detected.

CONCLUSIONS Collectively, the results indicate that combinatorial activation of p53 and ER can induce novel gene expression programs which have implications for cell-cell communications, adhesion, cell differentiation, development and inflammatory responses as well as cancer treatments. The yeast-based assay represents a versatile tool to study p53 interactions with cofactors.

PRIMARY TASK

p53 FUNCTIONAL INTERACTIONS:

**INTERACTION BETWEEN p53 AND ESTRADIOL
PATHWAYS IN TRANSCRIPTIONAL RESPONSES
TO CHEMOTHERAPEUTICS**

INTRODUCTION

Mechanisms of transcriptional regulation

Transcription is one of the first steps that takes place in gene expression and must be tightly regulated to be adequately robust, accurate, tailored and responsive to temporal, spatial, and physiological signals and changes.

About the 10% of the encoded genes are thought to be transcription factors (TFs) that in eukaryotes can recognize short sequences, called response elements (REs) ¹. A *cis*-regulatory region, usually the promoter of a gene, is composed by a series of these short DNA sequence motifs, often in multiple copies or partially overlapping with each other, that can be bound by general or sequence-specific transcription factors ^{2, 3}. Multiple TFs can bind simultaneously this array of REs determining the gene expression and its regulation. The number of combinations of TFs and REs at the level of a *cis*-regulatory region can be vast and not easy to determine ¹. Indeed many factors participate in the process of the recognition of a RE by a sequence-specific transcription factor. Cellular condition is extremely important because it implies post-transcriptional and post-translational modifications, concentration of the TF within the cell and interactions with components of the basal transcriptional machinery and its specific cofactors. In particular, post-translational modifications play an important role in modulating the behavior of a TF, in terms of differential recruitment of partners, nuclear exclusion or shuttling, change of binding affinity and site preference as well as change in transactivation/transrepression activity. Chromatin state and landscape also directly contribute to transcriptional modulation, making DNA more or less accessible and increasing or reducing the genomic region that can be recognized and bound by a TF. Equally important is also the “quality” of the response element sequences that determines the selectivity and specificity of TF recognition. The activity of a TF can in addition be modulated when it interacts or cooperates with other transcription factors present in close proximity ^{1, 2, 4}.

REs are usually found at the level of the promoter near the transcription start site but they might be also present in enhancers or other genomic regions many base pairs away from the promoter. TFs are usually active as dimers or tetramers. This is thought to increase the binding specificity due to the fact that the total sequence length recognized is longer. That could explain why REs are usually

composed by two half-sites, where half-site is defined as the minimal sequence recognized by a monomer or dimer, in case of a dimeric or a tetrameric TF, respectively ^{1, 2}. Indeed, RE sequences are very short and the probability to identify one of them in the human genome by chance is extremely high. Taking into account that mismatches can be tolerated especially in certain positions of the RE, the probability increases considerably. The majority of them are just spurious sequences not bound by the specific TF. The factors mentioned above and the capacity of a TF to dimerize or tetramerize contribute to discriminate between a random sequence and a *cis*-element ². Base pair changes can of course affect the binding selectivity of a TF although it can still recognize and bind these degenerate binding sites expanding the variety of different modulations and regulations that can take place on those promoters.

When two different TFs bind a *cis*-regulatory region two different scenarios can occur, either interaction or synergy. Interaction between two different transcription factors is called heterodimerization and it can be preassembled or assembled at the level of the promoter itself. Heterosynergy, instead, does not require a direct interaction between the two TFs, as shown in Figure 1. Synergy is a mechanism that allows a stronger transcriptional response and ensures a better discrimination of signal from a background noise due to the presence of similar binding sites in the genome. Synergy, as part of cooperation between two TFs, allows the integration of information coming from different signal transduction pathways. But the mechanisms that control such synergy are still poorly understood. The transcriptional machinery (or mediator) is recruited simultaneously and more efficiently by two TFs than by only one. Many factors control the simultaneous binding of the mediator, including the geometry of the promoter, the shapes of the transactivation domains and the ability of the TFs to recruit in concert the transcriptional machinery ².

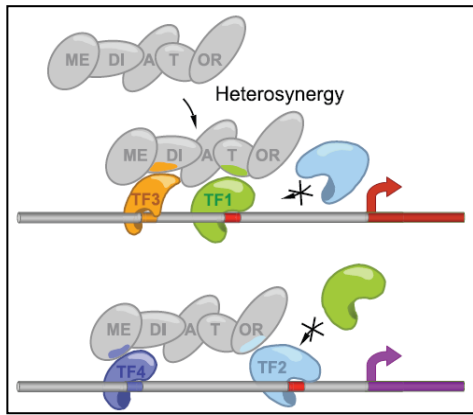


Figure 1. Schematic cartoon showing heterosynergy. The mediator complex (basal transcriptional machinery) is more efficiently recruited at the level of the promoter by two or more TFs instead of one. Georges et al., 2010.

The tumor suppressor p53: Structure, Regulation and Function

The sequence-specific transcription factors p53 and estrogen receptors are considered master regulators because they directly or indirectly control a myriad of biological functions.

p53 is well-known as “the guardian of the genome” and it controls several responses to stress, mostly related to genome stability, cell cycle and growth control, apoptosis, senescence and angiogenesis ^{5, 6}. Nevertheless, p53 can regulate many other biological processes including autophagy, energy metabolism, mTOR signaling, immune responses, cell motility and migration, cell-cell communication, in part through the modulation of several microRNA genes or the control of microRNA maturation ⁵⁻⁹ (Figure 2).

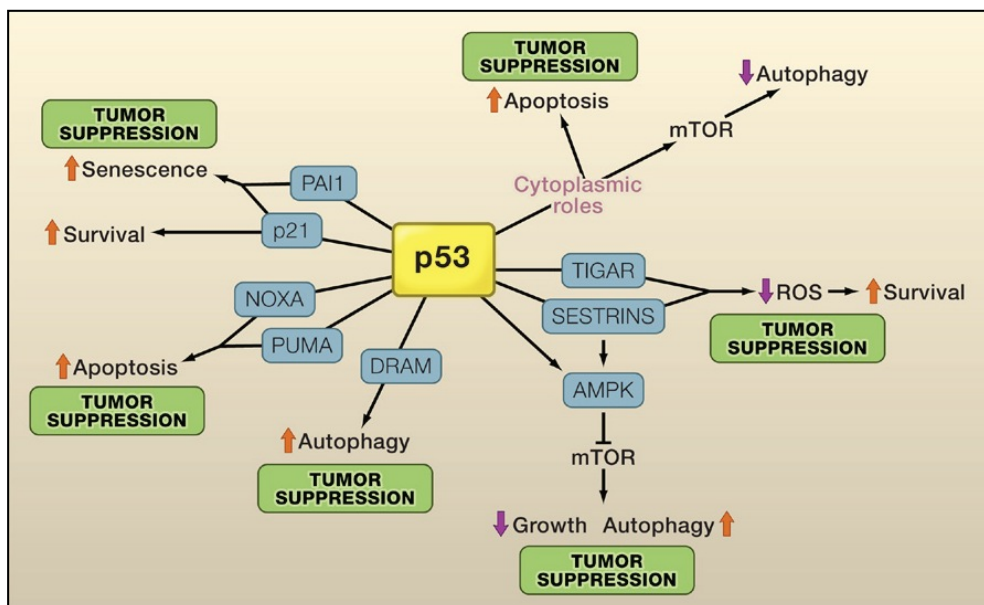


Figure 2. Chart summarizing the main p53 functions. Vousden and Prives, 2009

p53 is mainly a tumor suppressor and it must be maintained at low levels in unstressed conditions. The RING-finger ubiquitin E3 ligase MDM2 is its primary negative regulator. The short half-life of p53 is in fact due to a continuous ubiquitylation and degradation by proteasomes. During stress condition instead its ubiquitylation is suppressed in favor of its stability and homotetramers formation. p53 tetramers can transactivate target genes through the binding of p53 response elements (p53-REs). The tumor suppressor activity can be achieved also outside the nucleus. In this case p53 translocates to the mitochondria and triggers apoptosis program, interacting directly with anti-apoptotic proteins (Mcl-1, Bcl-xL). According to its function, it is not surprising to find p53 mutated in about the 50% of the tumors known and its function is probably altered or inactive in the rest of the cancer types ⁵.

A p53 monomer can be divided in three main functional domains: a transactivation domain (N-terminal region), a DNA-binding domain (central core) and a tetramerization domain (C-terminal region), although the protein organization is more complex. Indeed the N-terminal portion of the protein consists of three domains, two transactivation domains (TAD1 and TAD2) required for the activation of the transcription of target genes and the interaction with other factors (TFs, acetyltransferases and MDM2) ^{5, 12, 13}, and the SH3 domain, a proline-rich region (PRD) required for protein-protein interactions, for example with SIN3. SIN3 is involved in protection of p53 degradation, but also can participate as chromatin modifying enzyme in p53-mediated gene repression ^{14, 15}. The p53-RE within promoters is recognized by the DNA-binding domain (DBD), located in the central portion of the protein. The majority of the mutations occurs at the level of the DBD, highlighting the importance for tumor cells of escaping the binding of the targeted REs. The C-terminal region carries the tetramerization domain (OD), a nuclear localization signal (NLS), a nuclear export signal (NES) and a regulatory domain important for the DNA binding (Figure 3) ^{5, 7}.

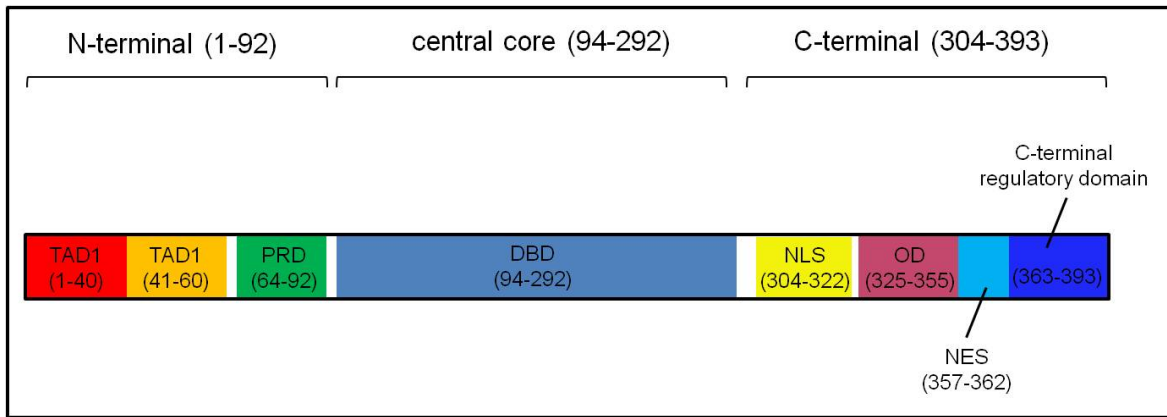


Figure 3. Scheme showing the different p53 domains according to references 5,12,13. Numbers indicate amino acid residues of the different domains within the protein.

Post-translational modifications play a crucial role in modulating p53 activity. The p53 protein is modified by as many as 50 individual post-translational modifications. Many of these occur in response to genotoxic or non-genotoxic stresses and show interdependence, in a way that one or more modifications can nucleate subsequent events. The most common ones reported include phosphorylation, acetylation, ubiquitylation, sumoylation, neddylation and some evidences of glycosylation and ribosylation as well ⁵. In the same cellular context p53 can be activated but different post-translational modifications can occur leading to a different transactivation response.

As a sequence-specific TF, p53 recognizes a consensus sequence composed of two decamers infrequently divided by a spacer. p53 binds as a tetramer the consensus sequence 5'-RRRCWWGYYY(N)_nRRRCWWGYYY-3', where N is the spacer (0-13 nt), R a purine, Y a pyrimidine and W either adenine or thymine ⁸⁻¹¹. Each dimer contacts directly six nucleotides within the decamer; one monomer binds the 1/4-site RRRCW and the other monomer the 1/4-site WGYYY. When p53 is bound to the target DNA a conformational change occurs in the protein so that the orientation of the transactivation domains might be affected, in favor of the transcriptional machinery recruitment. The decamers can be oriented either head-to-head or head-to-tail. The core CWWG sequence of the decamer plays a crucial role in determining the level of transactivation, owing the strongest positional effect. C and G are essential and required for p53 recognition and CATG is thought to be required for the strongest level of transactivation. CAAG and CTTG are usually associated with a lower activity and CTAG with an inhibitory function. The flanking purines and pyrimidines are also important in modulating the

transactivation activity, and in particular the two inner nucleotides with GG/CC as the most active and AG/CT the least active. The spacer instead seems to have a more transactivation-repressing function; the longer is the spacer (>2) the weaker is the transactivation. Non-canonical p53-REs have also been annotated, consisting of $\frac{1}{2}$ - (a decamer) and $\frac{3}{4}$ -sites (a decamer + $\frac{1}{4}$ -site). The p53 protein is able to bind also those REs, most probably as a tetramer where one dimer –in the case of $\frac{1}{2}$ sites- or one dimer + a monomer –in the case of $\frac{3}{4}$ sites- establish specific DNA contacts⁸⁻¹¹. In these cases the non-consensus portion of the DNA sequence can be bound through non-specific p53 interactions. The role these non-canonical p53-REs can have in the p53 transcriptional network is still under investigation but the contribution on expanding the p53 universe has been demonstrated. Specifically, it has been shown that p53 can use those non-canonical REs to regulate gene expression through the interaction with other transcription factors. These interactions might be positive or negative according to different cellular conditions⁸⁻¹¹.

Structure, Regulation and Function of Estrogen Receptors

Estrogen receptors (ERs) belong to the Class I of nuclear receptor transcription factors that exert hormonal responses through the activation of many biological pathways, mainly stimulating proliferation. ERs are carrying out their roles not only in women but also in men, being master regulators essential for development and maintenance of normal sexual and reproductive functions, but also playing a role in the cardiovascular, musculoskeletal, immune, and central nervous systems. The hormone estrogen can be bound by two different ER subtypes, ER α and ER β , with different and non-redundant functions and distinct tissue expression patterns. In particular, at the promoter level of proliferative genes, ER α and ER β seem to have opposite actions and the overall balance of both signaling reflects the proliferative stimulus due to the hormone. Indeed the ratio between the two proteins, when simultaneously expressed within the same cellular context, seems to determine the overall estrogen responsiveness. ER α and ER β are also transcribed from different genes located on different chromosomes¹⁶⁻¹⁸.

The classical mechanism through which ERs transactivate their targets is in a ligand-dependent fashion, directly contacting DNA after ER dimerization. Ligand-bound ERs can also regulate gene expression through protein-protein interaction

with other TFs (indirect DNA binding, tethered pathway); in this particular case promoters do not require to harbor estrogen receptor response elements (EREs). A third mechanism due to ER ligands, occurring within seconds or minutes, includes the activation of kinases and phosphatases without involving direct gene regulation. This non-genomic pathway with rapid effects requires the binding of the hormone to a receptor usually associated with the membrane (either ER or another receptor) or a signal activates ERs in the cytoplasm; the final outcome involves signaling cascades initiated via second messengers (SM) affecting the ion or nitric oxide levels in the cytoplasm (physiological effect). All these mechanisms are depicted in Figure 4 together with the so-called ligand-independent pathway that includes the activation of ERs through non-canonical signaling, such as growth factor signaling. Once kinases are active, ERs can be phosphorylated and dimerize in order to directly bind and transactivate the target genes¹⁶⁻¹⁸.

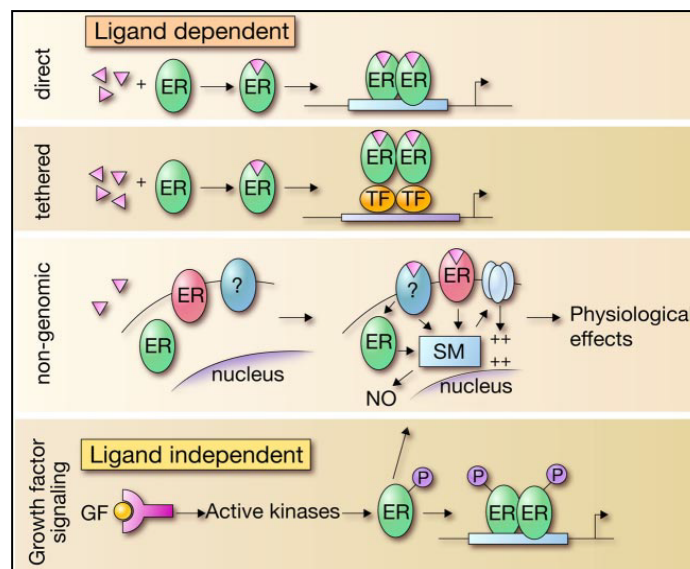


Figure 4. Different molecular ER pathways. Heldring et al., 2007

ER activity can also be modulated by post-translational modifications, including phosphorylation, acetylation, sumoylation and ubiquitination. Functional ER domains are quite well evolutionary conserved and ER α and ER β share a high level of homology (Figure 5). Among the six domains, the most conserved one is the central DNA-binding domain, containing two cysteine-cysteine zinc-fingers, that shares approximately the 98% of amino acid similarity (C domain). A ligand binding domain is also present (E/F domain) and within it the activation function-2 (AF-2) region drives the ligand-dependent transcriptional activation. At the N-

terminal portion of the protein (A/B domain with poor homology, 16%) an activation function-1 (AF-1) region is involved in the ligand-independent activity, capacity considered either absent or negligible for ER β . The AF regions seem to be involved in transcription directly interacting with the transcriptional machinery. AF-2 is able to recruit coregulators and adaptor proteins that together with the N-terminal region of the protein regulate gene transcription. Conformation of the ligand binding domain is usually altered upon binding to ligand and is involved in dimerization together with the C domain. The conformational change allows also the recruitment of co-activator proteins. The hinge domain (or D domain) has also a role in dimerization and in binding to chaperone heat-shock proteins^{19, 20}.

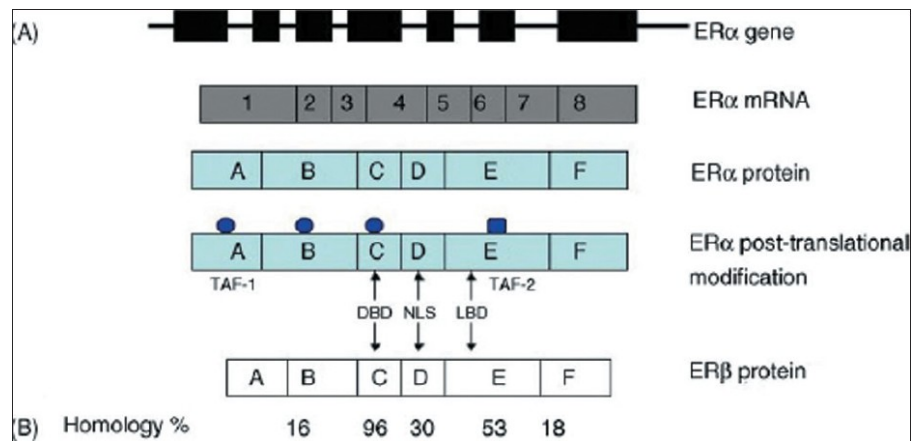


Figure 5. ER structure, including the functional domains and the degree of homology.

Abdulkareem and Zurmi, 2012.

ERs are also sequence-specific transcription factors and they bind the estrogen response element (ERE) sequence 5'-GGTCANNNTGACC-3', where N could be any nucleotide. When the receptor contacts an ERE the conformation of the ER alters. The affinity with which ER α binds an ERE is modulated by extra nucleotides flanking the basal ERE (5'-AGGTCANNNTGACCT-3'). The canonical ERE is a perfect palindrome, and with the additional nucleotides it forms a 15 bp palindromic inverted repeat. Imperfect palindromic EREs differ in one or more nucleotides and are less responsive to ERs. Non-palindromic EREs seem to be present in the majority of ER responsive genes. The consensus half-site ERE is thought to be the minimal target site for ER, and other transcription factors as well as cofactors could be required to promote the binding and transcriptional modulation²¹⁻²².

The intricate p53 and ERs crosstalk

p53 and ERs appeared to be master regulators that participate in the regulation of different biological functions and are activated by different signaling pathways. However, there are many evidences that suggest an intricate and not yet well-understood crosstalk between these two diverse networks. This crosstalk can be due for instance to direct interaction between p53 and the ERs, with the more frequently described outcome being repression of p53 activity. ER α binds p53 repressing its transcriptional function. This could be a way used in some abnormal cellular growth to suppress anti-proliferative genes, such as genes involved in cell-cycle arrest and apoptosis, and enhancing the ER responsive proliferative ones. That could also explain why the majority of ER-positive breast cancers still express wild type p53. Many of ER-negative breast cancers, instead, express mutant p53. Experiments performed in breast adenocarcinoma-derived MCF7 cell line (p53 wild type and positive for ER α) showed that ER α physically binds the promoter-bound p53 on p53 response elements. The interaction was mapped and seems to be due to AF-2 region of ER α and the C-terminal regulatory domain of p53 and such interaction can be relieved by stress-dependent post-translational modifications of p53, obtained for instance with ionizing radiation²⁴⁻²⁷. Some observations also link a physical interaction with the inhibition of ER α transcriptional activity. p53 interacts ER α in multiple domains repressing its function^{28, 29}. ER α and p53 can therefore be considered respective coregulators.

However, the p53/ER interaction can also result in mutual positive regulation at the level of target gene expression level. For example, estradiol and ER α can act through the canonical, estrogen-dependent pathway to positively modulate wild type and mutant p53 protein levels. The logical explanation can be attributed to a control mechanism that estrogen-dependent cells use to avoid cell death when the level of estrogen is low due to the reduction of p53 activity^{30, 31}. p53 on the other side can directly up-regulate ER α gene expression through elements located in the promoter³². This, again, supports the findings of a correlation between the presence of wild type p53 and ER-positive breast cancer along with a correlation between mutant p53 and ER-negative breast cancer^{33, 34}. Most of these studies addressing p53/ER interaction were performed in breast cancer cell lines, underlining the importance of the regulation of the activity and expression of p53 and ERs in tumors. Many of the studies particularly were performed in MCF7 or

MCF7-derived cell lines. The different results obtained can in part be attributed to the cellular context on one side and on the other side to the target genes considered and to the signaling context created.

The two transcription factors can also share some coregulators, such as p300 and MDM2. Some studies, in particular, emphasized the role of the p53 negative regulator MDM2 for the ER activity, showing both the inhibition³⁵ and the positive regulation³⁶ of ER α . In breast cancer cells MDM2 can interact with ER α and p53 to form a ternary complex promoting ER α turnover through, most probably, its ubiquitin-ligase activity; and cellular stress can stabilize ER α and abolish its degradation³⁵. The ternary complex appeared to protect p53 from functional deactivation of MDM2 due to the binding of ER α to the p53 N-terminal region³⁷. Other reports in breast cancer cells show instead a positive modulation of ER α -mediating gene expression and estrogen-responsiveness mediated by a direct MDM2-ER α interaction not involving p53³⁶.

Recently, a transcriptional cooperation between activated p53 and ligand-bound ERs at the promoter of the vascular endothelial growth factor receptor-1 (VEGFR-1, FLT1 gene) has also been uncovered³⁸⁻⁴¹. Vascular endothelial growth factor (VEGF) participates in angiogenesis and vasculogenesis processes and it can bind two principal transmembrane receptors, named VEGFR-1 and VEGFR-2. Many cell types in addition to endothelial cells express these two receptors on their surface, including also some tumor cells. FLT1 gene can be in fact up-regulated by hypoxia; and VEGFB and placental growth factor (PIGF), usually overexpressed in pathological conditions, can be its specific ligands. Blood vessels formation is a critical step during tumor development and cancer cells must find a way how to regulate expression of genes involved in angiogenesis. In this particular case, the transcriptional cooperation arises only in the presence of a specific SNP in the promoter of the VEGFR-1 gene. The C>T transition (GGACACCGCTC \rightarrow GGACATGCTC) changes a critical mismatch that generates a $\frac{1}{2}$ -site p53-RE, named as p53RE-T, responsive to p53. When the SNP occurs the FLT1 promoter can be modulated in response to genotoxic stress, resulting in a possible biological diversity within a population. An additional angiogenesis gene can therefore be part of p53 target genes and expand the p53 transcriptional network. The p53 responsiveness leads however to a weak FLT1 transactivation. A higher level of responsiveness, called synergy, can be instead achieved when ligand-activated

ERs act in *cis* at the level of the VEGFR-1 promoter (Figure 6). ERs can bind the FLT-1 promoter through two ½-site EREs located in close proximity of the ½-site p53-RE. The first ½-site ERE annotated was the one located 225 bp upstream the ½-site p53-RE (GGTCAGgaTcACT) and a second one is instead located 145 bp downstream the ½-site p53-RE (GGTCAGgagcggC)³⁸⁻⁴¹.

Consequently, the p53/ER functional interaction appeared to be dependent only on non-canonical *cis*-promoter REs for both transcription factors. Occupancy analysis, suggested that p53 was required for ER recruitment to the two ½-site EREs and therefore for ER-dependent transcription. ½-site EREs are located within 250 bp, a sufficient distance to assure the positioning of a nucleosome and assuring a topographical proximity³⁸⁻⁴¹.

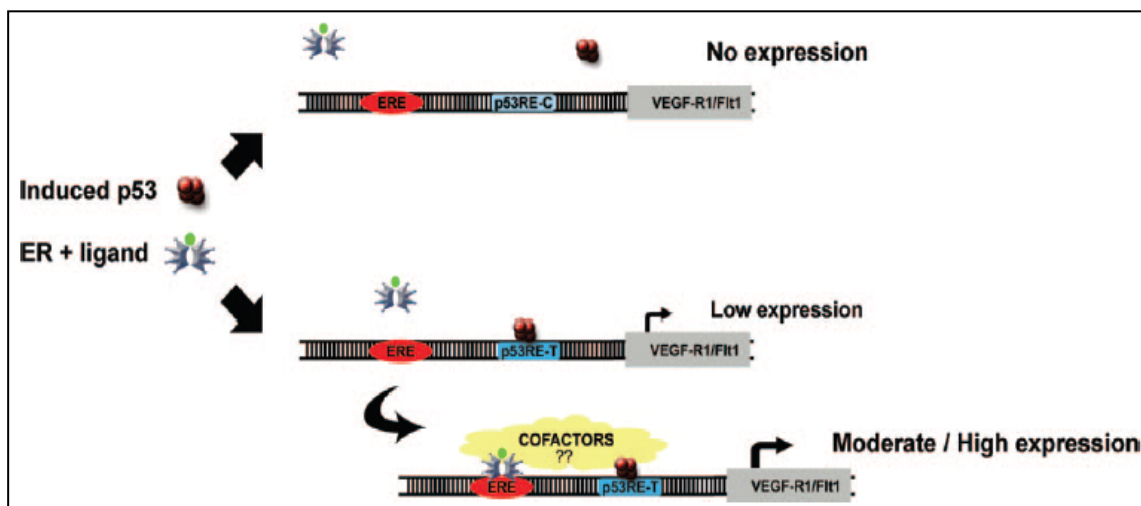


Figure 6. Example of mechanism of transcriptional synergy between p53 and ERα at the level of the FLT1 promoter. Menendez et al., 2007.

Based in part on these findings, non-canonical p53 REs, consisting of ½- or ¾-sites, can be included in the p53 target network providing for moderate or weak p53 responsiveness, but at the same time for the opportunity of conditional, context-dependent transactivation¹¹. Also in the case of ERs, the anatomy of an estrogen receptor element (ERE) can also deeply influence the binding affinity as well as the gene expression²¹⁻²³. Hence, p53 and ER networks need to maintain enough plasticity to adapt their transcriptional response according to the cellular context.

Investigation of general functional interactions between the tumor suppressor p53 and ligand-bound estrogen receptors, and specifically, a positive

transcriptional cooperation mediated by *cis* response elements, became the focus of this work. For this reason, the hypothesis that FLT1 would not be a unique example of a synergistic transcriptional cooperation between p53 and ERs mediated through non-canonical, but possibly also through canonical REs, was sought out.

Transcriptome analyses were performed using the above mentioned breast adenocarcinoma-derived MCF7 cell line. The specific MCF7 clone employed is p53 wild type, positive for ER α and weakly positive for ER β ³⁸. A genome-wide transcriptome analysis was performed to address cooperation between the two TFs on a global scale. Cells were cultured in an estrogen-depleted medium allowing the possibility to add ER ligand when needed. In normal condition p53 level is barely detectable in MCF7 cells and p53 requires to be activated and stabilized to function properly. This allowed the simultaneous treatment of MCF7 cells with ER and p53 activators. Whole-genome expression changes were determined following exposures to doxorubicin (DOX) and 5-Fluorouracil (5FU), genotoxic chemotherapeutic drugs commonly used in cancer therapy and to study p53-dependent responses, two different concentrations of 17 β -estradiol (E2) as ER ligand, and the combination of DOX and E2 to systematically compare whole-genome expression changes.

Despite the awaited responsiveness of well-established p53 target genes, a different impact after 10 hours-treatment with DOX or 5FU was observed, confirming previous reports showing that each cell type has a distinct response to drugs treatment as well as each genotoxic compound might lead to a different expression change that underlies the mechanisms of action of these agents ^{42, 43}. This limited overlap between DOX and 5FU differentially expressed genes confirmed previous studies that were however based on experiments conducted with different cell lines or endpoints. E2-concentration-dependent changes in gene expression were also different. Results obtained with both concentrations of E2 reflect expected estrogen response, comprising differentiation, proliferation, survival and hormonal responses. The higher E2 concentration, named as pharmacological concentration, had a more general repressive effect with also some unexpected functional regulations. The analysis was therefore focused on treatments with DOX and the lower E2 concentration (physiological concentration).

Finally, 201 genes that were up-regulated with a more than additive effect after DOX and E2 treatment were identified and these 201 genes showed a predicted functional enrichment for cellular differentiation and development, cell-cell communication, cell adhesion, and inflammation responses. For ten out of sixteen genes examined further, the synergistic transactivation was statistically validated using a quantitative real time PCR (qPCR) approach. An extensive analysis was performed including also nutlin-3a (a non-genotoxic drug, used as MDM2 antagonist) as direct p53 activator⁴⁴.

Two out of the ten genes showed the synergistic transcriptional cooperation after the combined treatment with all the p53 activators used (DOX, 5FU or nutlin-3a) and E2 administration. Using MCF7 cells with reduced p53 expression, it was also addressed that p53 participates directly in the modulation of their expression and in the cooperation with ER, and three new p53 target genes (GDNF, KRT15, SOX9) were discovered. The *cis*-mediated cooperation at the level of the promoter of three of those genes was studied, performing a chromatin immunoprecipitation assay. KRT15 expression appeared to be regulated in *cis* through p53 and ER α response elements. However, chromatin immunoprecipitation does not provide temporal resolution for different TFs that can occupy promoters in a population of cells. Dissection of the mechanism that regulates the synergistic expression at the level of the promoter of the genes identified is part of future directions. This might be addressed using mutant ERs that lack some protein functions, such as tethering mechanism and binding affinity.

METHODS

This section reflects my personal contribution to the work. The complete description of the Materials and Methods can be found in the manuscript enclosed (p100).

Cell lines and culture conditions

The human breast adenocarcinoma-derived MCF7 cell lines were normally maintained in Dulbecco's modified Eagle's (DMEM) supplemented with 10% fetal bovine serum (FBS), 2mM glutamine, 100 units/ml penicillin, and 100 µg/ml streptomycin at 37°C under 5% CO₂.

For the experiments performed in estrogen-depleted medium MCF7 cells were instead maintained in DMEM without phenol red supplemented with 10% charcoal filtered FBS for two days before seeding onto 6-well plates, 100 or 150 mm Petri dishes or E-Plates 16 (Roche Applied Science, Milan, Italy).

Human breast adenocarcinoma cells MCF7 stably expressing shRNA to p53 from the pSUPER vector, designated as "MCF7-p53i", or only carrying pSUPER vector as a control ("MCF7-vector")⁶³ were cultured in DMEM medium supplemented with 10% FBS, 100 U/ml of penicillin, 100 µg/ml of streptomycin (Invitrogen, Carlsbad, CA) and 0.2 µg/ml of puromycin at 37°C under 5% CO₂.

Cells treatment

MCF7 cells were cultured in estrogen-depleted medium and treated for 10 or 24 hours with 1.5 µM doxorubicin (DOX) or 375 µM 5-fluorouracil (5FU) or 10 µM Nutlin-3a for p53 stabilization and/or 10⁻⁹/10⁻⁷ M 17β-estradiol ERs activation. Dimethyl sulfoxide (DMSO) and ethanol (EtOH) were included as control in the mock condition. All the treatments were done on cells at 70-80% of confluence.

Microarray data analysis and functional annotation clustering

In order to select differentially expressed genes (DEGs), every condition corresponding to a treatment was first compared to the mock. Three different thresholds were set in order to select differentially expressed genes for each comparison: a) t-test unpaired unequal variance p value < 0.01; b) Rank Product percentage of false positive (pfp) < 0.05; c) absolute log₂ (fold change) > log₂ (2) .

Genes up-regulated by the concomitant treatment of doxorubicin and E2 (10^{-9} M) with more than an additive effect were identified among those satisfying the condition $\log_2[\text{FC}_{\text{double treatment}}] > 2$ subtracting the two fold changes corresponding to the single treatments to the fold change corresponding to the double treatment and selecting those with a positive result: $(\log_2 [\text{FC}_{\text{double treatment}}] - \log_2[\text{FC}_{\text{doxo}}] - \log_2[\text{FC}_{\text{E2}}]) > 0.1$.

Functional annotation clustering analyses were performed using the Ingenuity Pathway Analysis (IPA, <http://www.ingenuity.com>) as well as DAVID (<http://david.abcc.ncifcrf.gov/>)⁴⁵ (enrichment score ≥ 1.5 , medium classification stringency) with default settings. Results from DAVID functional cluster were then summarized as a Table with the indicated enrichment score. Results from IPA Canonical Pathways and Upstream Regulators are presented as screen snapshots. In particular, the IPA Upstream Regulator analysis presented in the first three columns names and function of upstream regulators that may be responsible for gene expression changes and their relative expression (Fold Change) observed in the data set. Predicted activity of these regulators with IPA-provided statistical assessment is included in column 4 and 5. A partial list of gene names and the total number in each group is also provided along with the Fisher's Exact Test results of the extent of overlap between DEGs and total number of genes considered as targets of the upstream regulator. In the IPA Canonical Pathways are instead displayed pathways as bar chart. The $-\log(\text{p value})$ results of a right-tailed Fisher's Exact Test is indicated. The ratio, calculated as number of genes in a given pathways that meet cut-off criteria divided by the total number of genes that make up the pathway, is overlaid as an orange line. The first 10 top pathways are shown.

Western blot analysis

Proteins were extracted using RIPA (RadioImmunoPrecipitation Assay) buffer supplemented with protease inhibitors and quantified using the BCA protein assay kit (Thermo Scientific, Pierce Protein Research Products, Milan, Italy). Proteins separated on 12% SDS-PAGE gels were transferred to a nitrocellulose membrane (GE Healthcare, Milan, Italy) using an iBlot® Dry Blotting System (Invitrogen™, Life Technology) and checked by Ponceau S staining. Membranes were blocked using 5% skim milk + PBS-Tween20 (0.1%) for 1 hour at room temperature and

then probed with the primary antibodies in 1% skim milk + PBS-Tween 20. Immune complexes were visualized using Amersham ECL™ Advance Western Blotting Detection Kit (GE Healthcare) or SuperSignal West Pico Chemiluminescent Substrate (Thermo Scientific, Rockford, IL, USA). The relative molecular mass values of the immunoreactive bands were determined using PageRuler™ Plus Prestained Protein Ladder (Fermentas, Milan, Italy).

Quantitative Real Time PCR (qPCR)

MCF7 cells, MCF7 p53i and vector were seeded onto 6-well plates and allowed to reach 70–80% of confluence before treating them with different drugs as described before. 10 or 24 hours after the treatment cells were washed twice with PBS and harvested using 1X trypsin (BioWhittaker®, Lonza). Total RNA was extracted using the RNeasy mini Kit (Qiagen®) according to the manufacturer's instructions and quantified using the NanoDrop spectrophotometer. For quantitative real time PCR experiments 1 µg of total RNA was reverse transcribed in 20 µl of reaction using the 'RevertAid™ First Strand cDNA Synthesis Kit' (Fermentas, Milan, Italy) or TaqMan reverse transcription reagents from Applied Biosystems (Foster City, CA). qPCR was carried out using 384-well plates in a final volume of 10 µl either on a CFX384 Touch™ Real-Time PCR Detection Systems (Bio-Rad, Milan, Italy) or on ABI prism HT7900 system (Applied Biosystems). KAPA Probe FAST qPCR Kit/TaqMan Universal PCR Master Mix (Applied Biosystems, Branchburg, USA) or KAPA SYBR® FAST qPCR Kit (Kapa Biosystems, Resnova, Rome, Italy) was used to perform the reaction together with TaqMan® Gene Expression Assays (Applied Biosystem™, Life Technology, Milan, Italy) or primers purchased from Eurofins (MWG, Operon, Ebersberg, Germany).

Relative mRNA quantification was obtained using the comparative Ct method ($\Delta\Delta C_t$), where glyceraldehyde 3-phosphate dehydrogenase (GAPDH), β -2microglobulin (B2M) or β -actin genes served as internal controls. Calculations were performed using Qbase^{PLUS} software (Biogazelle) that uses the geNorm method [39] to evaluate the expression stability of candidate reference genes.

A statistical analysis considering the \log_2 of the fold of induction was used to confirm the synergistic effect. The means of two normally distributed populations composed of $\log_2 [FC_{\text{double treatment}}]$ and $\log_2 [FC_{\text{doxo}}] + \log_2 [FC_{E2}]$ were analysed

using a t-test approach ($p < 0.05$). Quantitative real time PCR for ChIP samples is described in the next session.

Promoter pattern search

An *in silico* analysis was performed in order to identify putative canonical or non-canonical p53 and ER α response elements (REs) couples with a maximum distance of around 500 bp within the promoters of the selected genes. Three different approaches were used and combined together: a) manual pattern matching analysis ($\frac{1}{2}$ p53 RE: RRRCWWGYYY; $\frac{1}{2}$ ER α RE: (A)GGTCA, TGACC(T) or GGCTA) b) pattern matching analysis with $\frac{1}{2}$ site position weight matrixes derived from TransFac using the online Regulatory Sequence Analysis Tool (RSAT)⁶⁴ and c) R tool analysis using TransFac matrixes.

Chromatin immunoprecipitation (ChIP) assay

MCF7 cells were cultured in estrogen-depleted conditions in a 150 mm Petri dish and treated for 10 hrs with doxorubicin and/or the physiological concentration of E2 (10^{-9} M). Cells were cross-linked in 1% formaldehyde for 10 minutes at room temperature and the reaction was then quenched with glycine to a final concentration of 0.125 M for 5 minutes. Cells were then washed twice with cold PBS and scraped using PBS plus protease inhibitors (PI). Pellet was resuspended in 500 μ l of lysis buffer (1% SDS, 0.1 mg/ml ssDNA, PI 1x) and centrifuged for 10 minutes at 14-15°C. Pellet was then resuspended in 500 μ l of sonication solution buffer (0.25% SDS, 200 mM NaCl, 0.1 mg/ml ssDNA, PI 1x) and sonicated using the Misonix S4000 Sonicator (Misonix Inc., Farmingdale, NY, USA) in order to obtain DNA fragments in a range of 200-500 bp. After removal from the supernatant of the non-specific binding using Dynabeads[®] Protein G (Life Technology), immunoprecipitation (IP) was performed using 1 μ g of the appropriate antibody on 150 μ l of sample diluted 10 times with dilution buffer (16.7 mM Tris HCl, 0.01% SDS, 1.1% Triton X-100, 1.2 mM EDTA, 167 mM NaCl, 0.1 mg/ml ssDNA, PI 1x) + 40 μ l of agarose beads o/n at 4°C. 15 μ l of sample was also collected (1/10) as input (In). After many steps of washing the IP, crosslinks were reversed firstly in elution buffer (50 mM Tris HCl, 1 mM EDTA, 1% SDS) at 65°C for 10 minutes and then in TE 1x + 0.65% SDS for 10 minutes at 65°C. The collected solutions were incubated at 65°C o/n as well as the input samples +

elution buffer + TE 1x + 0.65% SDS. After RNase A and proteinase K treatment DNA was purified using PCR purification kit supplied by Qiagen®.

The purified DNAs were used for quantitative real time PCR analysis. Input samples were used for the normalisation and the fold enrichment was calculated over the mock condition in order to obtain a $\Delta\Delta C_t$ value. IgG DNAs were not taken into account for the normalisation step. qPCR was carried out using 384-well plates in a final volume of 10 μ l on a CFX384 Touch™ Real-Time PCR Detection Systems (Bio-Rad, Milan, Italy). KAPA SYBR® FAST qPCR Kit (Kapa Biosystems,) was used to perform the reaction together with primers purchased from Eurofins (MWG Operon, Ebersberg, Germany).

Cell proliferation assay

Toxicity of the chemicals and drugs used for the experimental approach was tested using the Real-Time Cell Analyzer (RTCA) DP supplied by Roche Applied Science, Milan, Italy. Cells were seeded onto an E-Plate 16 and allowed to reach 70–80% of confluence (checked by cell index value, almost 22-24 hours) before treating them with different drugs as described in *Cells treatment*. The proliferation rate was checked in the first 10 hours of treatment. A cell index normalization was imposed at the time point before the drugs administration. Mock condition was used as baseline. The experiment was conducted in triplicate for each condition.

RESULTS

This section presents an extended summary of the results included in the accompanying manuscript (p92 Lion et al.). For clarity some of the Figures of the manuscripts are also reproduced here. The complete description of the Materials and Methods can be found in the manuscript (p100). The Methods section in the thesis body reflects my personal contribution to the work. Specifically, I was not involved in the experimental part of the microarray analysis (RNA extraction, labeling and hybridization) and the processing of data acquisition. I did all the other data analyses and experiments described here and in the paper.

Validation of the experimental approach: p53, ER activation under the different treatment protocols and impact on cell growth

The functional effect of the drugs used in the experiments carried out was checked in this model system, the breast adenocarcinoma-derived MCF7 cells (p53 wild type; ER α - and weakly ER β positive). The validation was performed both by western blot and quantitative real time PCR (qPCR) analysis.

p53 was stabilized after treatment with doxorubicin (DOX), 5-Fluorouracil (5FU) and nutlin-3a (nutlin) and its endogenous levels increased in comparison to mock or E2 condition. The ER α protein levels in total extract did not change after any of the 10 hour-stimuli used (Figure R1A).

Gene expression of the canonical p53 target p21/CDKN1A¹⁰ and the canonical ER α target pS2/TFF1²² was tested to confirm their mutual transcriptional activation by qPCR (Figure R1B&C). p21 was indeed induced only when p53 activators were administered whereas pS2 only in the presence of E2. Fold of induction may differ according to the type of treatment. Notably, nutlin treatment resulted in higher relative p21 expression that was increased 1.5 fold with the addition of E2 (Figure R1C).

Absence of a real toxicity during the 10 hours-administration of the p53 activator drugs or E2 alone was confirmed by monitoring cell number and surface attachment in real time using Xcelligence (Figure R2). Nutlin and 5FU treatments were slightly toxic compared to the mock condition used as baseline. The combination of a p53 activator with E2 increased the overall cell index value, consistent with a role of estradiol in promoting proliferation.

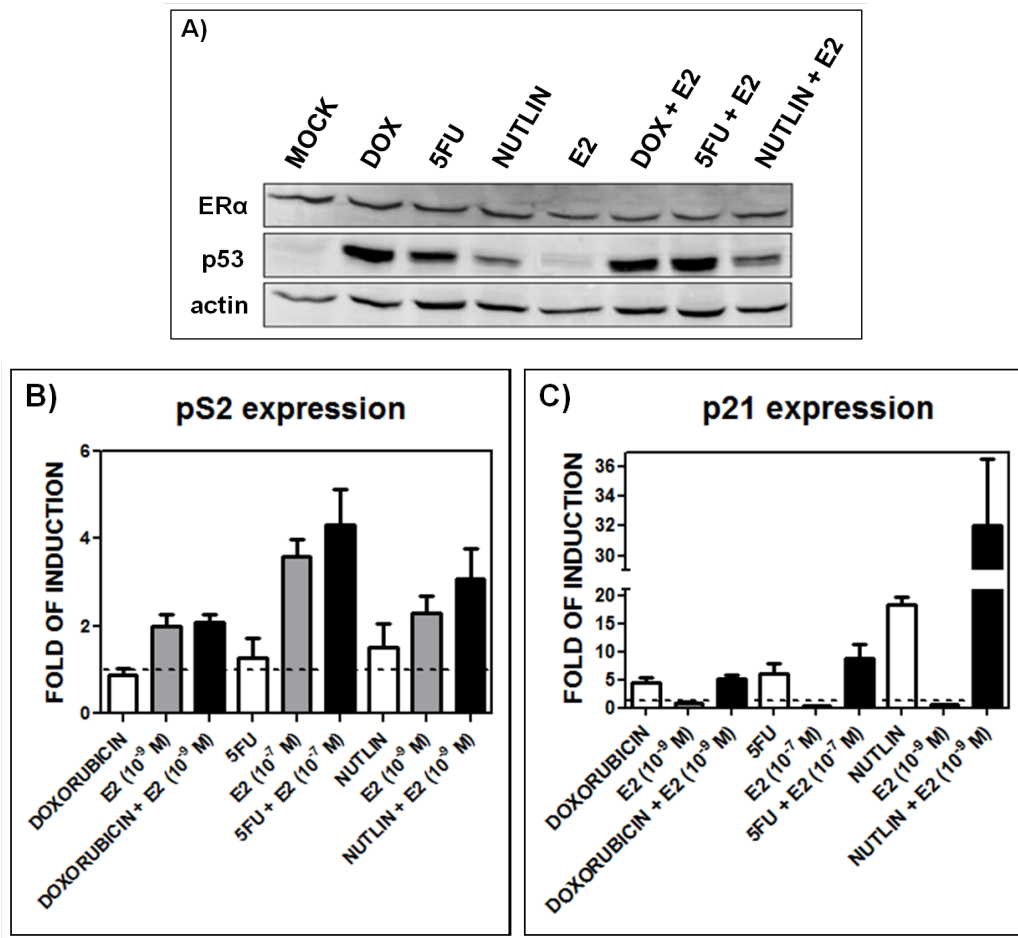


Figure R1. p53 and ERα protein levels and transactivation activities upon DOX, 5FU, nutlin, E2 single or combined treatments. A) Western blot analysis showing p53 and ERα protein levels 10 hours after the indicated treatments at the following doses: DOX, 1.5 μM; 5FU, 375 μM, nutlin, 10 μM; E2, 10⁻⁹ M. Figures B-C) qPCR results for the p53 target gene p21¹⁰ (B) and the ERα target gene pS2/TFF1²² (C). Presented in the bar graphs are fold-induction relative to the mock condition and the standard errors of three biological and two technical replicates for each condition. For qPCR, GAPDH, B2M and β-actin housekeeping genes served as internal controls.

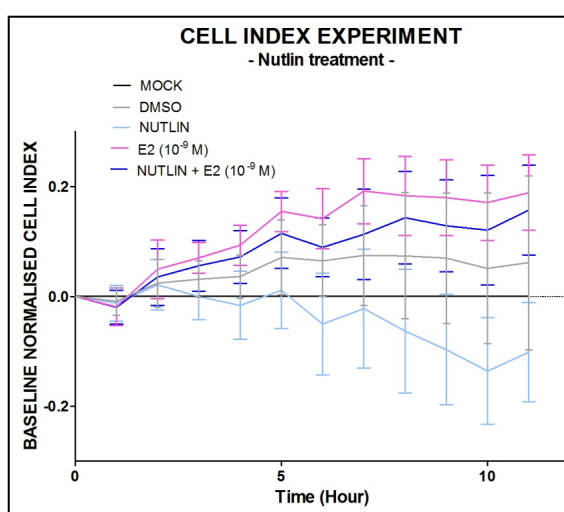
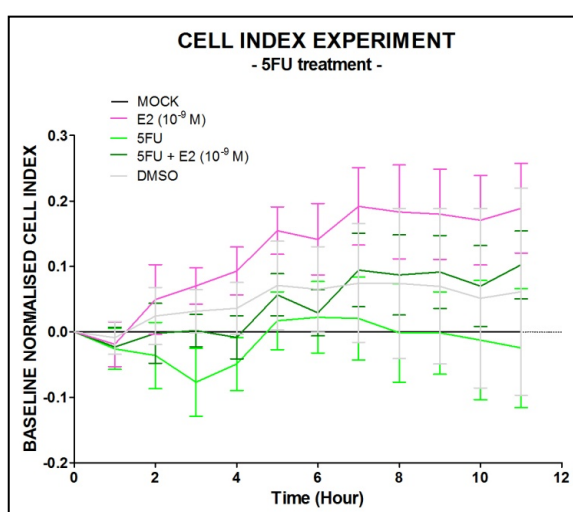
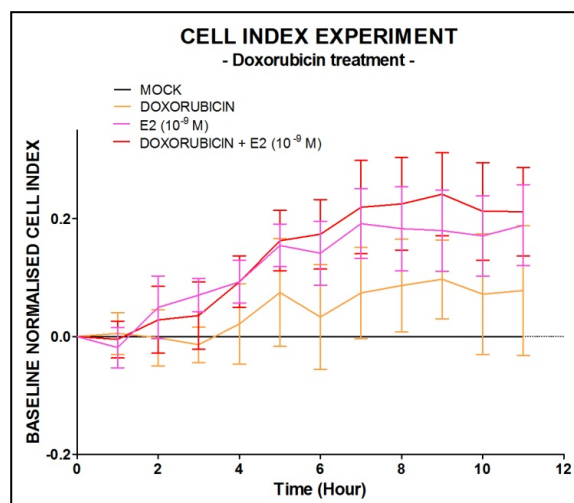


Figure R2. Cell Index Analysis to follow up treatment-specific toxicity. Impact of the chemicals and drugs used in the experimental approach was tested using the Real-Time Cell Analyzer (RTCA) DP supplied by Roche Applied Science, Milan, Italy. Cells were seeded onto an E-Plate 16 and allowed to reach 70–80% of confluence (checked by cell index value at ~22-24 hours) before treating them with drugs as described in the Methods section. The proliferation rate was checked in the first 10 hours of treatment. A cell index normalization was imposed at the time point before drug administration. Mock condition was used as baseline. Presented are the average and standard deviation of three replicates for each condition. A) 1.5 μM doxorubicin B) 375 μM 5-fluorouracil, C) 10 μM nutlin +/- 10^{-9} M 17β -estradiol (E2).

Different stimuli or concentrations led to different transcriptome changes: microarray results followed by pathway and ontology analyses

Global gene expression profiling was determined using an Agilent 4x44k platform (see p100 Material and Methods in *Lion et al.*) upon single treatment with specific chemotherapeutic agents (DOX or 5FU) or with the ER ligand 17β -estradiol (E2), using two different concentrations. The two different E2 concentrations tested are referred respectively to physiological (10^{-9} M) and pharmacological dosage (10^{-7}

M). Statistical analysis of the microarray data was performed as described in Material and Methods (p100). Complete raw and normalized data are available on the GEO Gene Expression Omnibus database repository (GEO, <http://www.ncbi.nlm.nih.gov/geo/>; GEO accession: GSM591738).

To further investigate functional annotation clusters for each specific treatment, data from the lists of differentially expressed genes (score cut off ≥ 2) were analyzed using the tools Ingenuity Pathway Analysis (IPA, <http://www.ingenuity.com>) and DAVID (<http://david.abcc.ncifcrf.gov/>⁴⁵). These analyses allowed to decide the p53 activator and the concentration of E2 to use in the investigation of p53/ER cooperation.

DOX and 5FU treatments stabilize and activate p53, although with a different pattern in terms of protein levels (Figure R1A), and extent of induction of its target gene p21 (Figure R1C). A different impact on gene expression was instead observed. Figure R3 and R4 clearly show the differences in transcriptome changes in terms of gene numbers after the two genotoxic drug administrations. Both treatments led to a more extensive repression of gene expression, particularly emphasized by the 10 hr-stimulus of 5FU. Only a small number of differentially expressed genes (DEGs) is shared between the two treatments with the two agents; specifically only 2.3% of the up-regulated and 10.9% of the down-regulated DOX DEGs are in common with up- and down-regulated 5FU DEGs. Considering the predicted transactivation behavior of 373 genes that are included in the IPA p53 signaling pathway, on average a correlation coefficient of 0.59 between DOX and 5FU DEGs was calculated (Figure R5). Gene ontology (GO), pathway enrichment and network analysis were therefore used in the selection phase of the chemotherapeutic drug treatment that resulted in a more distinct signature of p53 activation. The translation of the large amount of data coming from microarray analysis into a biological interpretation can offer a more general insight into the cellular mechanisms elicited from a given condition. The analyses performed in Figure R6 (using DEGs filtered with the parameters highlighted in Materials and Methods) compare the microarray results obtained with the two chemotherapeutics. Overall, doxorubicin treatment resulted mainly in enrichment for the p53-pathway/signaling activation, including regulation of transcription, cell cycle and mitosis, cell response to stress, DNA damage checkpoint and response, BRCA1 function, apoptosis and ATM pathway. Both DAVID and IPA analyses

confirm this enrichment. Hence, for the further genome-wide experiments the analysis was focused on DOX genotoxic stimulus only.

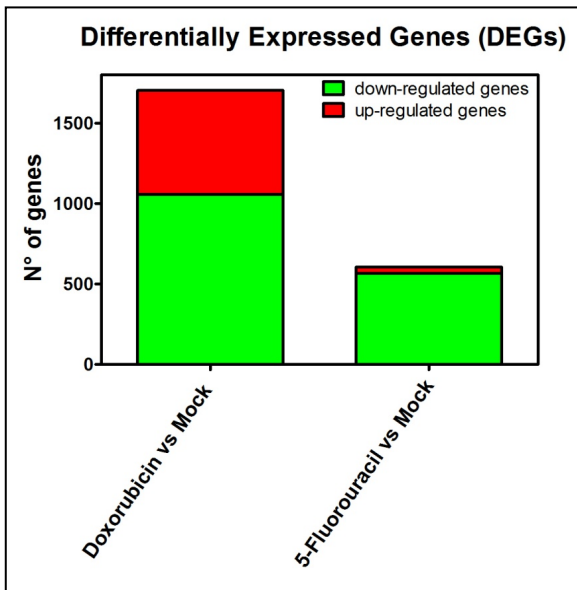


Figure R3. 2 colors-stacked bar graph showing the total number of DEGs and the up- and down-regulated genes in every condition.

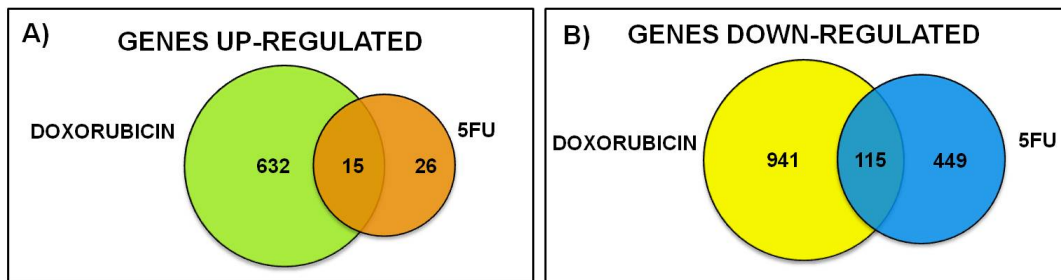


Figure R4 A&B) Venn diagrams showing the number of DEGs in common between different conditions.

IPA p53 signalling	DOX DEGs	5FU DEGs	IPA p53 signalling	DOX DEGs	5FU DEGs	IPA p53 signalling	DOX DEGs	5FU DEGs	
ABCC1	Inhibited	-0.538263076	-0.997195609	CDT1	Inhibited	-0.832829068	-0.39670714	FOXO3	Activated
ACSL3	Inhibited	-2.407540763	-2.407540763	CENPF	Inhibited	-1.627870703	-1.76636831	FUBP1	Inhibited
ACTA2	Activated	4.004325354	2.826416674	CEP55	Inhibited	-1.139363343	-1.775776519	FXD3	Activated
ACTB	Inhibited	-0.15859598	-2.237771056	CES2	Activated	0.850993167	0.340809181	GADD45A	Activated
AEN	Activated	1.695171738	1.535674055	CFAR	Inhibited		-0.633016248	GART	Activated
AIFM2	Activated		0.875357178	CHD3	Inhibited		-0.393182675	GDF15	Activated
AK1	Activated	1.171771408	0.535011594	CHEK1	Inhibited	-1.328637001	0.792066656	GLB1	Activated
AKAP12	Inhibited		0.545574467	CHEK2	Inhibited	-0.83063511	0.665640959	GLPR1	Activated
ANXA1	Activated	-0.504728642	-0.11803344	CHUK	Inhibited		0.15524852	GML	Activated
ANXA2	Activated	0.47063644	0.646309143	CKAP2	Activated	-1.28868807	-0.600256396	GNL3	Activated
ANXA4	Activated	1.306636852	-0.22341571	CKS1B	Inhibited			GPR87	Activated
APAF1	Activated	0.627790471	-0.733591115	CLIC4	Activated		1.191456514	GSR	Activated
APOL1	Activated	0.678002974	0.835475929	CLU	Activated			GSTM1	Activated
AR	Inhibited	-0.676328074	-0.525870286	COL14A1	Activated	0.65054612		H19	Inhibited
ARL6IP1	Inhibited	0.556361686	0.556361686	COL1A1	Activated	0.343451096		H2AFX	Inhibited
ARPC1B	Inhibited		0.20750708	COL4A1	Activated		0.381875069	HBEGF	Activated
ATF3	Activated	4.519071854	1.337118699	COL9A1	Activated			HDAC2	Activated
ATP1A1	Activated	0.700569119	-0.625806566	CPOX	Activated	-0.237324034	-0.430638269	HDAC3	Activated
AURKA	Inhibited	-0.465747143	-1.37889402	CSTF1	Inhibited	-1.33937264		HDAC5	Activated
AURKB	Inhibited	-0.74811186	-1.213812476	CTNNB1	Inhibited		-0.983184683	HIF1A	Inhibited
BAI1	Activated			CTSD	Activated	0.460715879	0.410335642	HK2	Inhibited
BAK1	Activated	-0.910195442	0.782812856	CTSK	Activated	0.667003222		HLA-B	Inhibited
BAX	Activated	1.200341919	1.000273002	CX3CL1	Activated	0.408862769	0.293066649	HMGB1	Inhibited
BBC3	Activated	0.892525873	1.526030344	CYP24A1	Activated	0.573994435	0.739555537	HMGN2	Activated
BCL2	Inhibited	-1.100866278		CYTB	Inhibited	-0.352009565	0.519737367	HMMR	Inhibited
BCL2A1	Activated	-0.356614063	-0.251798216	DBF4	Inhibited	-0.199381458	-0.417473438	HMOX1	Activated
BCL3	Inhibited	-1.889020732		DDB2	Activated	1.476159238	0.952071012	HRAS	Activated
BHLHE40	Activated	-1.204550996		DDIT3	Activated	1.995683246	0.418363983	HS3ST1	Inhibited
BID	Activated		-0.217780948	DDR1	Activated			HSP90AB1	Inhibited
BIK	Activated			DGKA	Activated	-0.150938702	-0.723900971	HSPA1L	Inhibited
BIRC5	Inhibited	-0.46593278	-0.696378354	DHFR	Inhibited			HSPA8	Inhibited
BNIP3	Activated			DICER1	Activated		0.811321269	HTT	Activated
BRCA1	Inhibited	-1.001956309	-1.215563236	DKK1	Activated	-2.507319481		ID1	Activated
BTG1	Activated		-0.846437949	DNMT1	Inhibited	-0.301469484	-0.795415146	ID2	Inhibited
BTG2	Activated	2.179960299	1.442597687	DRAM1	Activated		1.541597793	IER3	Activated
BUB1	Inhibited	-1.577737386	-2.200480302	DSN1	Inhibited	-1.204981691	-0.221506038	IGF1R	Inhibited
BUB1B	Inhibited	-2.607541277	-2.23956246	DUSP1	Activated	0.472350074		IGFBP3	Activated
C12orf5	Activated	1.730679985	1.957101086	DUSP5	Activated	4.541958479	-0.797380396	IL6	Inhibited
CASP3	Inhibited	0.726440326		DUT	Inhibited		-0.450930656	INHBA	Activated
CASP4	Activated	-0.21555022		DYRK1A	Inhibited	0.452097265	0.920792207	IPO7	Inhibited
CASP6	Activated		-0.13864259	EDN1	Activated	-0.74992835	0.80485994	IQCBI	Inhibited
CASP8	Activated	-1.756438401	-0.478839522	EFNA1	Activated	-0.936098228	-0.271396205	IRF5	Activated
CAT	Activated		-1.125233977	EGFR	Activated	-0.334769905	-0.904715915	IRF7	Activated
CAV1	Activated	-0.966017309	-0.179761388	EGR1	Inhibited	1.63359935		IRF9	Activated
CCNA2	Inhibited	-2.017172873	-0.860184914	EGR3	Inhibited		-0.278897166	IRS1	Inhibited
CCNB1	Inhibited	-0.897166375	-0.868701308	EI24	Activated	1.599853637		ISG15	Activated
CCNE2	Inhibited			EIF2B1	Activated	0.585671695		ITGA2	Inhibited
CCNG1	Activated	0.92222449	0.907407724	ELF4	Inhibited	0.568999757	0.432805065	ITGB4	Inhibited
CCNG2	Activated	0.999011068		ENG	Inhibited		0.943246802	JMJD1C	Inhibited
CCNK	Activated	0.89896589	1.854246782	EPHA2	Activated	1.623661741	-0.438597944	JUNB	Activated
CD44	Inhibited			ERCC1	Activated	0.505337773		KIAA0101	Inhibited
CD82	Activated	0.678358493		ESR1	Activated			KIF23	Inhibited
CDC20	Inhibited	-0.975762624	-1.049481275	EZH2	Inhibited	0.471311514	-1.461082552	KLK3	Inhibited
CDC25A	Inhibited			EZR	Activated		0.524631205	KRT15	Activated
CDC25C	Inhibited	-0.723758332	-1.462283366	FAM3C	Inhibited	0.475880179		KRT8	Activated
CDC6	Inhibited	-0.571355074	0.679508491	FAS	Activated	3.855303289	3.875498635	LATS2	Activated
CDC7	Inhibited	-1.022260254	-0.819012452	FASN	Inhibited	-0.2253003	-0.900539826	LBR	Inhibited
CDK1	Inhibited	-0.261801386	-0.223497599	FDXR	Activated	2.602247776	1.177726877	LDHA	Inhibited
CDK4	Inhibited	-0.44589815	-0.274971918	FEN1	Inhibited			LGALS3	Inhibited
CDKN1A	Activated	2.400613865	3.196023083	FHL2	Activated	-0.74919159	-0.64324637	LIF	Activated
CDKN1B	Activated			FKBP3	Inhibited		-0.786260883	MAD1L1	Inhibited
CDKN2A	Inhibited	0.589617068	0.988920951	FOSL1	Activated	2.392503058	1.066919858	MAD2L1	Inhibited

IPA p53 signalling	DOX DEGs	5FU DEGs	IPA p53 signalling	DOX DEGs	5FU DEGs	IPA p53 signalling	DOX DEGs	5FU DEGs			
MCL1	Activated	0.596825281	1.079961129	PPM1D	Activated	1.128419483	0.933573254	SON	Inhibited	-0.640536335	-0.797310068
MCM2	Inhibited	-0.728208874	-0.650749764	PPP1R15A	Activated			SPATA18	Activated	2.640456403	0.809805174
MCM3	Inhibited	-0.856285716	-2.186825477	PPP3CA	Inhibited	-0.661815509	-0.445449081	SPHK1	Inhibited	1.69102181	-6.496906416
MCM4	Inhibited		-0.96013177	PRC1	Inhibited	-0.929066916	-1.659821127	ST14	Activated	0.979189974	-0.400824092
MCM6	Inhibited	-0.592895302	-0.836794381	PRIM1	Inhibited	-0.978944222	-0.230338901	STAG1	Activated	-0.918058535	-0.701147171
MCM7	Inhibited	-0.535587343	-0.520503333	PRKAB1	Activated	1.272054291		STK17A	Activated		0.932668442
MDM2	Activated	0.95774379	1.613840639	PRKAB2	Activated	0.754750216	1.51559211	STMN1	Inhibited		-0.695382529
MDM4	Activated	-0.83581699	0.83891691	PRKCA	Inhibited	-0.81844632	-3.019278317	STRN3	Inhibited		0.59921936
MED13L	Inhibited	0.677872071	0.174089909	PRODH	Activated	1.500380241	0.544201781	TAGLN2	Activated	0.419976329	
MET	Inhibited	-1.100760568	0.518108976	PSEN1	Activated	0.654063614		TANK	Inhibited		0.484112443
MFAP2	Activated	0.572695107		PSEN2	Inhibited			TAP1	Activated	2.014585718	-0.164384429
MGMT	Inhibited			PTEN	Activated		1.307975158	TAP2	Inhibited	0.589580594	0.794689661
MGST2	Inhibited	-0.452162686	-0.668907935	PTP4A1	Inhibited	1.561360804	1.270117172	TBXAS1	Inhibited		
MIR17HG	Inhibited	-0.350410909	-1.088517405	PTPRA	Inhibited	-0.230722391	-0.497271757	TCF7L2	Inhibited	-1.002576791	-0.838969683
MMP9	Inhibited	-0.120992391	0.713719266	PTTG1	Activated	-0.50529428	-1.297809095	TCL1A	Inhibited		0.624428102
MSH2	Activated	-0.911108862	-1.623318618	PVRL3	Inhibited	-0.446152901	-0.380711582	TERT	Inhibited		0.511414176
MSH6	Inhibited	-0.857828164	-0.719624799	PVT1	Activated		0.565876158	TFPI2	Activated	0.896984728	
MS11	Activated	-0.33146512	-0.27972118	PYCARD	Activated	0.268514043		TGFA	Activated	2.003750616	-0.859068511
MUC2	Activated	0.710619835	0.744251412	RAD23A	Activated	-0.552256778	0.236453854	TGFB2	Activated	-2.065210924	
MX1	Activated	-1.608283751	-1.07712331	RAD54B	Inhibited	-0.886198103	-0.680602199	TGFBR2	Inhibited	-0.505571473	-0.680602199
MYBL2	Inhibited		0.24891855	RALY	Inhibited	-0.265882994	0.213451288	THBD	Inhibited	1.624085673	0.495027673
MYC	Inhibited		0.587675891	RARRES3	Activated	0.930764914	0.496806886	THBS1	Activated	-0.451756291	
MYO6	Activated	-0.151529838	-1.579289397	RB1	Inhibited	0.495085177		THBS2	Activated		1.000425221
NCAPG	Inhibited	-1.338644735	-1.595115373	RECQL4	Inhibited		0.618203191	TIMP3	Inhibited		
NDC80	Inhibited	-2.173439285	-1.541644844	RFC3	Inhibited	2.123535093	1.316974784	TMEM97	Inhibited	0.345822099	1.446146724
NDRG1	Activated		-0.687623716	RFC4	Activated	-0.830024695		TMSB15A	Activated	0.978373345	
NEDD8	Activated		0.812762829	RFXWD2	Activated	-0.306942706	-0.304029836	TNFRSF10A	Activated	2.46056377	0.751355205
NEK2	Inhibited	-1.621555535	-1.406827348	RGS16	Activated	2.066341365	-0.296222449	TNFRSF10B	Activated	3.565575465	3.075944407
NFKBIA	Activated	-0.896634053		RNF144B	Activated	-2.228530496	-0.111968921	TNFRSF10C	Activated	3.596247219	2.757058444
NME1	Activated			RPRM	Activated	-1.044437661	-1.288319781	TNFSF10	Activated	0.368229994	0.719208883
NOL3	Inhibited	-1.487041482		RPS27L	Activated	1.490631202	1.27272038	TNFSF9	Activated	0.909473252	0.525538933
NOS3	Inhibited	0.454513959	0.976876598	RPSA	Inhibited	-0.306942706		TOP2A	Inhibited	-0.562086364	-2.509055122
NOTCH1	Activated	2.308592158	1.303768493	RRM2	Inhibited	-0.445033208	0.720311719	TOP2B	Activated	-0.756742902	-0.908642708
NUP153	Inhibited	-0.995434703	-0.490841715	RRM2B	Activated	1.274512502	0.481264005	TP53	Activated		-1.968585378
OSGIN1	Activated	-0.539374569	0.896955584	RUNX2	Inhibited	-2.085488547	-0.219133933	TP53BP2	Inhibited	0.517411018	-0.390710496
OTX1	Activated	0.75372948		S100A2	Activated		0.645113157	TP53I3	Activated	2.251100989	1.245478616
PANK1	Activated	1.105144856	0.84415379	S100A4	Activated		1.231227261	TP53INP1	Activated	1.428009663	0.904517099
PARK2	Activated	1.016808125	1.040504807	SAT1	Activated	1.449654947	0.333333333	TP63	Inhibited	-3.43064015	-1.683324434
PARP2	Inhibited	-2.079687244	-0.779597945	SCN3B	Activated	0.303030303		TP73	Activated		0.469383887
PBK	Inhibited	-1.323688345	0.419865532	SCO2	Activated		0.510937919	TPX2	Inhibited	-1.364477675	-1.534532037
PCBP4	Activated	0.859202689	0.897770911	SEI1L	Activated		1.7289195	TRAF4	Activated		0.596553887
PCNA	Activated	1.359150102	0.924062941	SERPINB2	Activated	0.664612263	0.515345555	TRIO	Activated	-0.22933567	0.439533611
PDHX	Inhibited	0.608597044		SERPINE2	Activated	2.070331531		TSC2	Activated	0.84037618	-0.191454905
PDK1	Inhibited	-0.233880878	-1.417137	SESN1	Activated	1.434521985	2.096630192	TSG101	Inhibited		
PDRG1	Inhibited	-0.244418834	0.870461889	SESN2	Activated	2.116544942	1.689084134	TTK	Inhibited	-2.13915695	-1.673284453
PERP	Activated	-0.138429802	0.235644942	SFN	Activated	1.198646862	0.82479514	TWIST1	Inhibited	0.664044003	0.798692714
PFKFB3	Inhibited		2.818539604	SHC1	Activated	-0.575489527		UBE2B	Inhibited	0.853484655	-0.701147171
PFKM	Inhibited		0.280944134	SHISA5	Activated			UBE2C	Inhibited	-1.270146186	-0.725883424
PFKP	Inhibited	-0.202871054	-1.368759792	SIAH1	Activated	-0.685908909	-0.25420737	UIMC1	Activated	-0.66002013	-0.191454905
PGM3	Inhibited	-0.398777778	-0.962276603	SIRT1	Inhibited	0.558580191	-0.262183594	UNC5A	Activated	0.700909091	0.636281129
PHLDA3	Activated	0.690638899	1.783855048	SIVA1	Activated		0.117171717	VCAN	Activated	0.447330869	0.899199303
PLAU	Inhibited	-0.607070707	1.769561713	SLC16A1	Inhibited	0.944351199	0.480874657	VDR	Activated	1.275728977	
PLK1	Inhibited	-2.010654467	-1.830550118	SLC19A1	Inhibited	-1.374195632	-0.31908747	VEGFA	Inhibited	0.893841848	1.06240024
PLK2	Activated	-1.060139519	0.669741786	SLC2A1	Inhibited		0.47348693	WDHD1	Inhibited	-0.457259711	-0.939439119
PLXNB2	Activated		-0.780240688	SLPI	Activated	0.628756163	0.771103105	WWP1	Inhibited	-0.869820023	0.389720629
PMAIP1	Activated	2.859806538	2.267715178	SMAD6	Activated	0.765704716		XAF1	Inhibited	-0.285558136	0.495826217
PML	Activated	0.84023669	0.575974677	SMAD7	Inhibited	-0.319794692	0.657114084	XPC	Activated	1.432049261	0.662862811
PODXL	Inhibited		-0.34382057	SMC2	Inhibited	-0.637169727	-1.214388484	XPO1	Inhibited	-0.678263248	-0.432308468
POLA1	Inhibited	-0.432903202	-1.362539959	SMC3	Inhibited	-0.656053199	-0.527792271	XRCC5	Activated	0.681816219	
POLB	Activated		0.394080972	SMC4	Inhibited	-1.09842678	-0.882085475	ZFP36L1	Activated	0.681816219	0.662862811
POLD1	Inhibited	-0.588446172	-0.966835697	SMURF1	Activated			ZMAT3	Activated	1.046462541	0.972081876
POLD2	Inhibited		0.394080972	SNAI1	Inhibited	3.960361837	0.808454023				
POLE2	Inhibited	-1.049295705	-0.400931433	SOD2	Activated	0.561947251	0.865923282				

Figure R5. Predicted transactivation behavior of genes related to IPA p53 pathway. Activated state=■; Inhibited state=■. DEGs values (log₂): FC>2=■; FC<-2=■; -2<FC<2=■. From the log₂ FC values coming from the array analysis a correlation coefficient between the DOX and 5FU treatment was calculated using Pearson correlation.

R6 A) DAVID ANALYSIS

DOXORUBICIN FUNCTIONAL ANNOTATION CLUSTER	
Annotation Cluster	score
regulation of transcription	8.53
components of cytoskeleton	7.59
cell cycle/mitosis	7.28
components of nuclear lumen/nucleoplasm	6.77
cellular response to stress/DNA damage stimulus	5.97
constituent parts of chromosomes/condensed chromosome kinethocore	5.07
proteins with zinc finger domain/C ₂ H ₂ -like	4.23
regulation of apoptosis	3.43
components of microtubule cytoskeleton	2.93
DNA damage/cell cycle checkpoint	2.74
components of chromosome segregation	2.68
positive regulation of transcription	2.66
basic-leucine zipper (bZIP) transcription factors	2.65
regulation of programmed cell death	2.62
negative regulation of transcription	2.57
proteins with BTB/POZ domain	1.95
GTPase regulator activity	1.93
regulation of meiotic cell cycle	1.90
p53/ATM cell signalling pathway	1.86
constituent parts of nuclear chromosomes	1.84
tube development	1.79
response to radiation	1.75
double-strand break repair	1.74
hemopoiesis/myeloid cell differentiation	1.74
negative regulation of transferase activity	1.68
positive regulation of cell migration	1.68
regulation of cell growth	1.66
nucleotide-binding	1.66
DNA damage response, signal transduction by p53 class mediator	1.62
growth factor activity	1.53
ovulation cycle process	1.51
regulation of DNA metabolic process / DNA replication	1.50

5-FLUOROURACIL FUNCTIONAL ANNOTATION CLUSTER	
Annotation Cluster	score
cell cycle/mitosis	15.22
components of microtubule cytoskeleton	9.25
nucleotide-binding	5.52
components of the condensed chromosome kinethocore	5.39
regulation of cell cycle	4.87
proteins with pleckstrin homology (PH) domain	4.40
proteins involved in the microtubule-based movement	3.78
proteins involved in the microtubule cytoskeleton organization	3.69
regulation of small GTPase mediated signal transduction	3.60
proteins involved in the microtubule motor activity	3.47
GTPase regulator activity	3.28
components of nuclear lumen/nucleoplasm	3.16
proteins involved in ubiquitin-like modifier processing, activation, conjugation or deconjugation	3.09
components of chromosome segregation	2.82
establishment of spindle localization	2.51
serine/threonine-protein kinases	2.40
proteins of G1/S transition of mitotic cell cycle	2.05
cytoskeletal protein binding	2.03
proteins with bromodomains	2.01
lipid binding	2.01
negative regulation of cell cycle process	2.00
cytoskeleton organization	2.00
proteins with tetrapeptide repeats	1.80
proteins with zinc finger/RanBP2-type domain	1.79
DNA damage response, cell cycle checkpoint	1.73
signaling pathway from G-protein families	1.70
chromosome organization	1.64
proteolysis/protein catabolic process	1.64
cellular component of morphogenesis	1.62
protein kinases C-like, phorbol ester/diacylglycerol binding	1.55
regulation of phosphate metabolic process/transferase activity	1.52

R6 B) DOXORUBICIN & 5-FLUOROURACIL COMPARISON (IPA UPSTREAM REGULATOR ANALYSIS)

Analysis	Upstream Regulator	Fold Change	Molecule Type	Predicted Activation State	Activation z-score	Notes	p-value of overlap	Target molecules in dataset
5FU analysis	KDM5B		transcription regulator	Activated	2,125	bias	4,87E-06	↑BUB1B, ↑DLGAP5, ↑ECT2, ↑HMMR, ↑NICM3, ...all 14
5FU analysis	CDKN2A	0,989	transcription regulator	Activated	2,157	bias	4,33E-03	↑CDC25C, ↑CDKN2C, ↑ITGAV, ↑MDM2, ↑PLN, ...all 10
5FU analysis	TP53	↓-1,969	transcription regulator	Activated	4,221		2,36E-07	↑ACSL3, ↑ACTB, ↑ANLN, ↑ASK1, ↑BCL2L11, ...all 48
DOX analysis	CEBPB	↑1,240	transcription regulator	Activated	2,167		3,25E-01	↑BCL2, ↑CDC42EP3, ↑CEBPA, ↑CSF1R, ↑F8, ...all 13
DOX analysis	GATA1		transcription regulator	Activated	2,219		1,82E-01	↑ANK1, ↑BCL2L11, ↑BMP6, ↑GP1BA, ↑NFE2, ...all 6
DOX analysis	RUVBL1		transcription regulator	Activated	2,236		5,43E-02	↑FAM53C, ↑GADD45B, ↑HIST1H4A (includes o...all 7
DOX analysis	ETS1		transcription regulator	Activated	2,372		1,14E-01	↑CCNE1, ↑CDKN1A, ↑CSF1R, ↑CTGF, ↑EGRI, ...all 15
DOX analysis	IRF3	0,613	transcription regulator	Activated	2,378		4,23E-01	↑ANXA4, ↑ARG2, ↑CDH11, ↑HLA-F, ↑IRF7, ...all 8
DOX analysis	HOXA5	0,983	transcription regulator	Activated	2,449		3,31E-04	↑CDKN1A, ↑EGRI, ↑GADD45B, ↑KLF10, ↑MDM2, ...all 6
DOX analysis	PGR		ligand-dependent nuclear receptor	Activated	2,488		2,69E-02	↑CDKN1A, ↑CDKN1C, ↑CEBPB, ↑DST, ↑GAS6, ...all 18
DOX analysis	CDKN2A	0,590	transcription regulator	Activated	2,512		3,48E-05	↑ASF1B, ↑BAX, ↑BCL2, ↑BLM, ↑CCNA2, ↑C...all 25
DOX analysis	EP300		transcription regulator	Activated	2,572		4,38E-01	↑ACTA1, ↑BAX, ↑CCNE1, ↑CDKN1A, ↑CEBPA, ...all 11
DOX analysis	CREBBP		transcription regulator	Activated	2,586		6,21E-02	↑BCL2, ↑CDKN1A, ↑EGRI, ↑FGFR3, ↑FOS, ...all 11
DOX analysis	STAT1		transcription regulator	Activated	2,598		5,81E-02	↑BCL2L11, ↑CASP8, ↑CDKN1A, ↑FAS, ↑FOS, ...all 14
DOX analysis	FOXO3		transcription regulator	Activated	2,765		5,80E-03	↑BCL2L11, ↑CASP8, ↑CDC42EP3, ↑CDKN1A, ...all 16
DOX analysis	MYCN	↓-1,475	transcription regulator	Activated	2,786		1,00E-00	↑BAX, ↑CAVI, ↑CDH11, ↑CDKN1A, ↑CTGF, ...all 18
DOX analysis	FOXO4		transcription regulator	Activated	2,798		1,62E-04	↑CDC42EP3, ↑CDKN1A, ↑CTGF, ↑GADD45A, ...all 9
DOX analysis	KDM5B		transcription regulator	Activated	2,851		2,76E-04	↑ANKRD36B, ↑AP4S1, ↑BUB1B, ↑CAVI, ↑CD...all 21
DOX analysis	SMAD4	-0,297	transcription regulator	Activated	3,003		3,90E-04	↑CCNE1, ↑CDC42EP3, ↑CDKN1A, ↑CTGF, ...all 23
DOX analysis	TP73	0,172	transcription regulator	Activated	3,139		1,83E-06	↑ADA, ↑AEN, ↑BAX, ↑BCL2L11, ↑CDKN1A, ...all 23
DOX analysis	HIF1A		transcription regulator	Activated	3,248		3,11E-02	↑ANGPTL4, ↑BCL2, ↑CAVI, ↑CDKN1A, ↑CO...all 27
DOX analysis	TP53	0,179	transcription regulator	Activated	6,348		1,51E-20	↑ACTA2, ↑ADA, ↑ADCK3, ↑AEN, ↑AK1, ...all 138
5FU analysis	FOXO1		transcription regulator	Inhibited	-2,720	bias	1,42E-03	↑ANLN, ↑BCL2L11, ↑DLGAP5, ↑KIF11, ↑KIF1...all 11
DOX analysis	FOXM1	-0,348	transcription regulator	Inhibited	-2,804		2,64E-03	↑BUB1B, ↑CAVI, ↑CCNA2, ↑CDKN1A, ↑CE...all 10
DOX analysis	SP11		transcription regulator	Inhibited	-2,200		2,68E-01	↑BAX, ↑CSF1R, ↑FES, ↑FOS, ↑IL1R2, ↑NCF1, ...all 8
DOX analysis	E2F2	↓-1,612	transcription regulator	Inhibited	-2,121		1,64E-03	↑BCL2, ↑CCNA2, ↑CCNE1, ↑CDC4A, ↑CDK...all 11
DOX analysis	MDM2	↑1,050	transcription regulator	Inhibited	-2,073		5,99E-06	↑BAX, ↑BCL2, ↑CCNA2, ↑CDKN1A, ↑KAT2B, ...all 12
DOX analysis	TCF4		transcription regulator	Inhibited	-2,000		8,55E-02	↑CDKN1A, ↑DKK1, ↑ID2, ↑MIA, ↑MYC, ↑SGK1, ...all 6

R6 C) DOXORUBICIN & 5-FLUOROURACIL COMPARISON (IPA CANONICAL PATHWAYS)

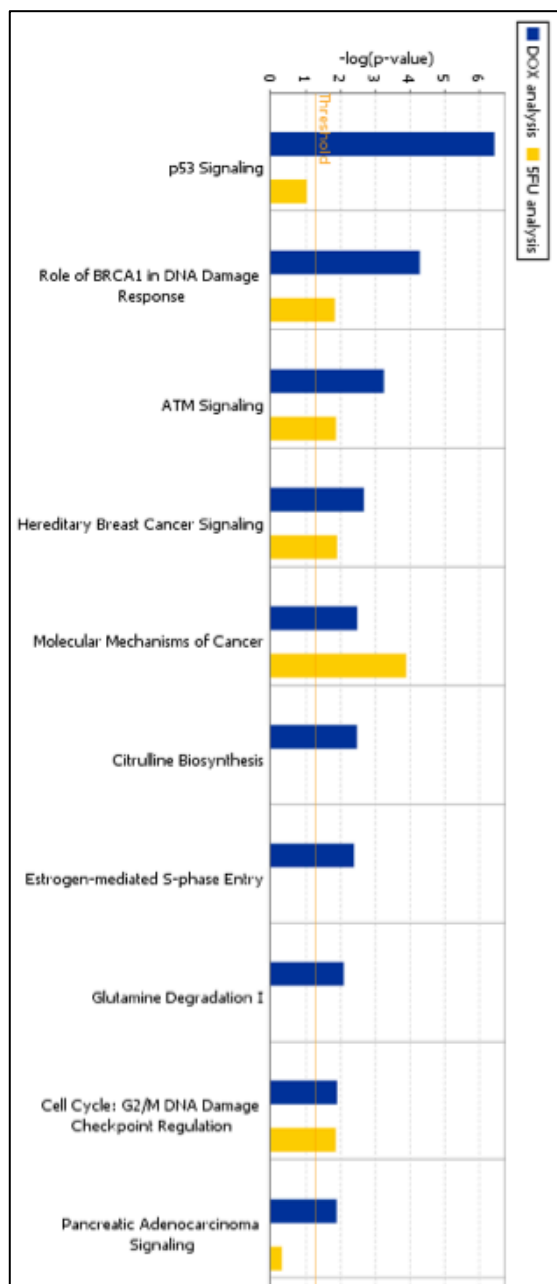


Figure R6 DOX and 5FU functional annotation clustering. Analyses were performed using the Ingenuity Pathway Analysis (IPA, <http://www.ingenuity.com>) as well as DAVID (<http://david.abcc.ncifcrf.gov/>⁴⁵) (enrichment score ≥ 1.5 , medium classification stringency) with default settings starting from the lists of differentially expressed genes corresponding to the treatment: doxorubicin (1.5 μM) and 5FU (375 μM). Results from DAVID functional cluster are summarized as a table with the indicated enrichment score. Results from IPA Canonical Pathways and Upstream Regulators are presented as screen snapshots.

A different response after the treatment with two concentrations of 17 β -estradiol was also awaited. The purpose of the data analysis was to decide between the physiological (10⁻⁹ M) and pharmacological (10⁻⁷ M) E2 concentration to further investigate the interaction between p53 and an estradiol pathway related to a more canonical ER signature. An analysis similar to the one performed above for DOX and 5FU treatment was followed. Different transcriptome responses were identified for the E2 doses (Figure R7&8). The lower E2 concentration (10⁻⁹ M) resulted in the same number of up- and down-regulated DEGs, whereas the pharmacological concentration (10⁻⁷ M) was generally more repressive (Figure R7); although a bigger number of differentially expressed genes was shared (Figure R8A&B). Indeed comparing the predicted transactivation behavior of 76 genes included in the IPA ER signaling pathway, the two treatments resulted in a comparable response (DEGs not filtered using p-value or FDR). Among the 76 genes a high correlation coefficient of 0.89 between the two conditions was identified (Figure R9).

It is not surprising that both concentrations of E2 resulted in DEGs exhibiting functional clusters enrichment (DAVID and IPA analyses, Figure R10) that reflects expected estrogen responses, including induced differentiation, proliferation, survival, hormonal responses and inhibition of p53 and SMARCB1 (Figure R10B). Unexpected functional clusters were however observed after 10⁻⁷ M E2 treatment, including positive regulation of apoptosis and negative regulation of cell growth as well as inhibition of SP1 (Figure R10A&B). Therefore, the analysis was focused on 10⁻⁹ M E2 stimulus, since it resulted in a signature much closer to that of typical estrogen responses (Figure R10).

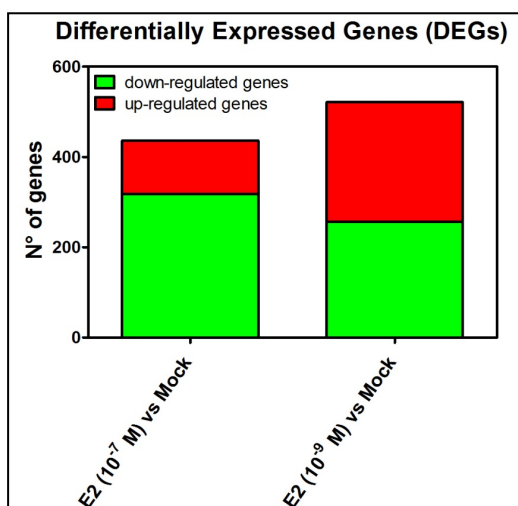


Figure R7. 2 colors-stacked bar graph showing the total number of DEGs and the up- and down-regulated genes in every condition.

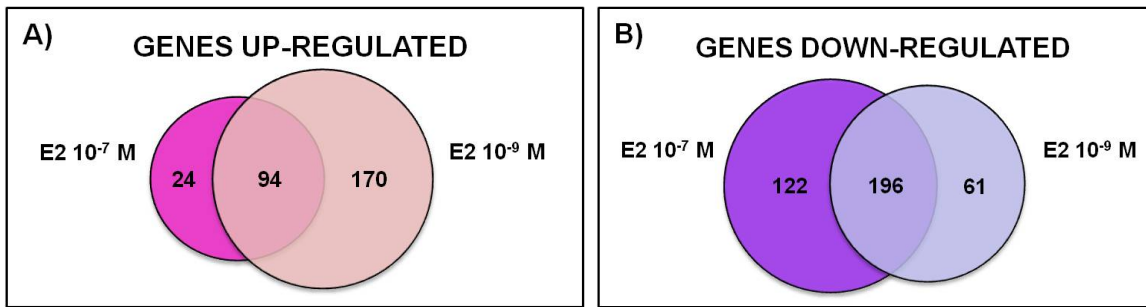


Figure R8 A&B) Venn diagrams showing the number of DEGs in common between different conditions.

IPA ER signalling	E2 (10 ⁻⁹ M) DEGs	E2 (10 ⁻⁷ M) DEGs	IPA ER signalling	E2 (10 ⁻⁹ M) DEGs	E2 (10 ⁻⁷ M) DEGs
ABCG2	Inhibited	-0.87	IL6	Inhibited	-0.89
ADA	Activated	0.84	IRS1	Activated	0.06
BCAS3	Activated		KCTD6	Activated	0.38
BIRC5	Activated		KISS1	Activated	
BMP4	Activated	0.35	LDLR	Activated	0.38
C3	Activated	0.45	LOXL4	Activated	
C8orf4	Inhibited	-0.88	LTB	Inhibited	2.70
CCL2	Inhibited	-0.44	MAPK12	Inhibited	0.10
CCL4	Inhibited	-0.86	MDM2	Activated	0.73
CCND1	Activated	1.12	MMD	Activated	-0.82
CDKN1A	Activated	-0.67	MYB	Activated	2.50
CEBPA	Activated	0.35	MYC	Activated	-0.51
CRABP2	Activated	-0.69	NCOA1	Activated	
CSAD	Activated	0.20	NCOA3	Activated	-0.76
CTSD	Activated	1.12	NQO1	Inhibited	
CXCL12	Activated	4.18	NRF1	Inhibited	0.15
CXCL3	Inhibited	0.08	OXT	Activated	-0.41
CYP1A1	Activated	-2.80	PDCD4	Inhibited	
CYP1B1	Activated	0.65	PGR	Activated	3.89
CYP7A1	Inhibited	-0.44	PRLR	Activated	0.29
E2F1	Activated	1.03	PTEN	Inhibited	
EDN1	Inhibited	0.95	RARA	Activated	0.70
EFNA1	Inhibited	-1.95	RPRM	Inhibited	-0.96
EGFR	Activated	0.07	SCARB1	Activated	0.98
ENO1	Activated	0.30	SIRT1	Activated	
ERBB2	Inhibited	-0.61	SMAD6	Activated	-0.42
ESR1	Inhibited	-0.32	SNAI1	Activated	0.80
F12	Activated	0.62	TERT	Activated	0.93
FAM100A	Activated	0.23	TFF1	Activated	0.79
FBLN1	Activated	0.20	TGFA	Activated	0.96
FOS	Activated	2.23	TGFB3	Activated	-2.04
FST	Activated	0.79	TGM2	Activated	2.48
GPAM	Activated		TNF	Inhibited	-1.02
GREB1	Activated	2.53	TNFAIP3	Inhibited	
H19	Activated	1.03	TP53	Activated	0.16
IER3	Inhibited	-0.78	VEGFA	Activated	1.00
IFI27	Activated		VEGFC	Inhibited	-0.83
IGF1R	Activated	0.88	WISP2	Activated	1.80

Figure R9 Predicted transactivation behavior of genes related to IPA ER pathway. Activated state=■; Inhibited state=■. DEGs values (log₂): FC>2=■; FC<-2=■; -2<FC<2=■. From the log₂ FC values coming from the array analysis a correlation coefficient between the E2 10⁻⁹ M and E2 10⁻⁷ M treatment was calculated using Pearson correlation.

R10 A) DAVID ANALYSIS

E2 (10 ⁻⁸ M) FUNCTIONAL ANNOTATION CLUSTER	
Annotation Cluster	score
regulation of ossification	4.00
response to hormone stimulus	3.47
Bcl-2 proteins (BH domain)	3.46
regulation of apoptosis	3.41
negative regulation of apoptosis	3.08
insulin-like growth factor binding proteins (IGFBPs)	2.95
DNA replication	2.52
mesoderm development/ morphogenesis	2.44
cytokine binding and control of the survival, growth and differentiation of tissues and cells	2.19
positive regulation of cell differentiation/cell development	2.16
chordate embryonic development	2.07
regulation of locomotion/cell migration	2.03
positive regulation of inflammatory response/ response to external stimulus	2.00
proteins with HLH domains	1.83
nucleotide-binding	1.78
protein dimerization activity	1.70
vasculature/blood vessel development	1.68
tube development	1.64
components of membrane fraction	1.62
positive regulation of ossification	1.53
proteins with SH ₂ domains	1.52

E2 (10 ⁻⁷ M) FUNCTIONAL ANNOTATION CLUSTER	
Annotation Cluster	score
response to hormone stimulus	4.34
regulation of locomotion/cell migration	2.84
constituent parts of the plasma membrane	2.49
proteins with SH ₂ domains	2.35
glycoproteins	2.34
components of membrane fraction	2.34
developmental maturation	2.32
response to hypoxia	2.31
Bcl-2 proteins (BH domain)	1.97
vasculature/blood vessel development	1.90
lipoproteins	1.89
negative regulation of cell growth	1.85
response to wounding/inflammatory response	1.64
regulation of phosphate metabolic process	1.59
positive regulation of apoptosis	1.58
proteins with Pleckstrin homology-type domain (PH domain)	1.55
components of the extracellular region part	1.52

R10 B) E2 (10⁻⁷ M) & E2 (10⁻⁹ M) COMPARISON (IPA UPSTREAM REGULATOR ANALYSIS)

Analysis	Upstream Regulator	Log Ratio	Molecule Type	Predicted Activation State	Activation z-score	Notes	p-value of overlap	Target molecules in dataset
E2_9	ZNF217	-0.837	transcription regulator	Activated	2,000		4,22E-05	ANK3, CDKN2B, FRK, G... all 10
E2_9	ESR1	-0.545	ligand-dependent nuclear receptor	Activated	2,166		1,10E-11	ABCC5, ADORA1, BCL2, ... all 28
E2_9	NCOA3	-0.862	transcription regulator	Activated	2,207		1,70E-03	BCL2, CDC25A, CDC6 (incl... all 5
E2_9	LEF1	1.031	transcription regulator	Activated	2,213		7,05E-05	BCL2, CASP9, FGF18, MTF... all 6
E2_7	ZNF217	-0.784	transcription regulator	Activated	2,449	bias	5,80E-05	ANK3, CDKN2B, EPHX4, ... all 9
E2_9	TP53 (includes EG:220)	0.164	transcription regulator	Inhibited	-3,272		2,69E-05	AEN, BBC3, BCL2, BIK, ... all 39
E2_9	SMARCB1	-0.027	transcription regulator	Inhibited	-2,789		6,20E-03	CDC6 (includes EG:23834), ... all 8
E2_7	HIF1A	0.540	transcription regulator	Inhibited	-2,734	bias	4,09E-05	CXCR4, EGLN3, EPAS1, ... all 16
E2_7	TP53 (includes EG:220)	0.361	transcription regulator	Inhibited	-2,696		6,26E-03	BBC3, BIK, BTG2, CCNG2... all 27
E2_7	SP1	-0.177	transcription regulator	Inhibited	-2,562	bias	5,39E-03	BBC3, CDK6, CDKN2B, ... all 16
E2_9	RB1	0.128	transcription regulator	Inhibited	-2,470		8,94E-05	BCL2, CDC25A, CDC6 (in... all 16
E2_7	SMARCB1	-0.025	transcription regulator	Inhibited	-2,425		2,70E-02	CXCR4, HEV1, IMC10 (in... all 6
E2_7	NFKBIA	-0.617	transcription regulator	Inhibited	-2,213		1,94E-01	BTG2, CXCR4, IL15 (includ... all 5
E2_7	SMARCA4	0.234	transcription regulator	Inhibited	-2,200	bias	1,65E-02	ABHD2, CCR1, CDC25A, ... all 11
E2_9	CDKN2A	-0.915	transcription regulator	Inhibited	-2,155		2,06E-02	BCL2, CDC25A, CITED2, ... all 8
E2_7	CTNNB1	-0.548	transcription regulator	Inhibited	-2,069	bias	2,26E-03	AXIN2, DKK1, ID3, ID3, ... all 14

R10 C) E2 (10⁻⁷ M) & E2 (10⁻⁹ M) COMPARISON (IPA CANONICAL PATHWAYS)

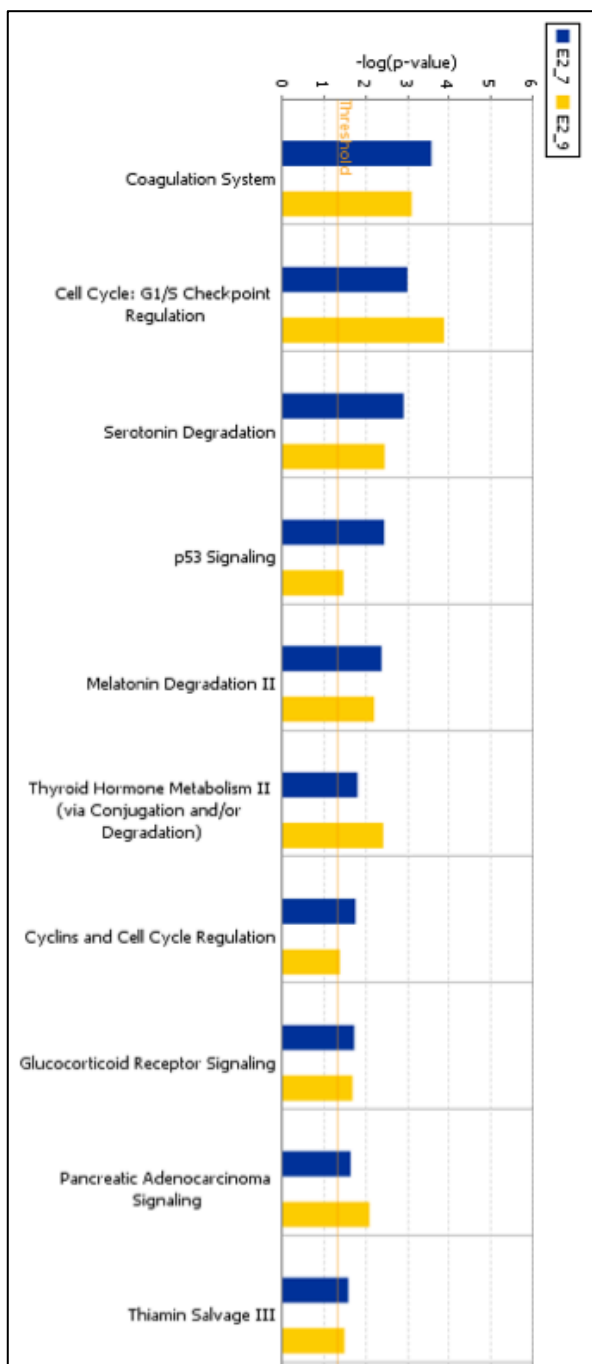


Figure R10. E2 (10⁻⁹ M) and E2 (10⁻⁷ M) functional annotation clustering. Analyses were performed using the Ingenuity Pathway Analysis (IPA, <http://www.ingenuity.com>) as well as DAVID (<http://david.abcc.ncifcrf.gov/>⁴⁵) (enrichment score ≥ 1.5 , medium classification stringency) with default settings starting from the lists of differentially expressed genes corresponding to the treatment: E2 (10⁻⁹ M) and E2 (10⁻⁷ M). Results from DAVID functional cluster are summarized as a table with the indicated enrichment score. Results from IPA Canonical Pathways and Upstream Regulators are presented as screen snapshots.

Genome-wide transcriptome analyses identify a combinatorial effect between genotoxic stress and proliferation stimulus in response to DOX and E2

Drawing upon the results obtained with FLT-1³⁸⁻⁴⁰, possible additive or cooperative interactions between p53 and ER was investigated using combination of DOX and physiological concentration of E2 (10⁻⁹ M) treatment, again with a genome scale approach.

Lingering over the doxorubicin treatment it is evident that the combined treatment shared a common pattern of DEGs in terms of overall transcriptome response (Figure R11&R13A). Furthermore 66% among the up-regulated and 75% among the down-regulated genes were common DEGs (Figure R12). The overall transcriptome changes were however heavily influenced by both treatments (Figure R13). The same could in fact be observed with E2 treatment even though they shared a smaller number of genes (24% and 13% for the up-regulated and down-regulated groups, respectively; Figure R11&R12). Indeed, IPA upstream regulator analysis indicated both TP53 and ESR1 as activated (Figure R13B&C). A large number of genes still remained univocal in the combinatorial stimulus (Figure R12). Interestingly, 66 up-regulated and 167 down-regulated DEGs were uniquely identified following DOX+E2 treatment. Conversely, for 380 up-regulated and 369 repressed DOX DEGs the differential expression was not observed in the double treatment. Only 29 up-regulated and 57 repressed DEGs were in common for the DOX and E2 single treatments, of which 27 up- and 54 down-regulated genes were also DEGs with the double treatment (Figure R12). Functional annotation clusters obtained with groups of selective genes are summarized from p110 supplemental tables in *Lion et al.*, although no relevant biological outputs were identified probably due to the small numbers of DEGs that limited the statistical power.

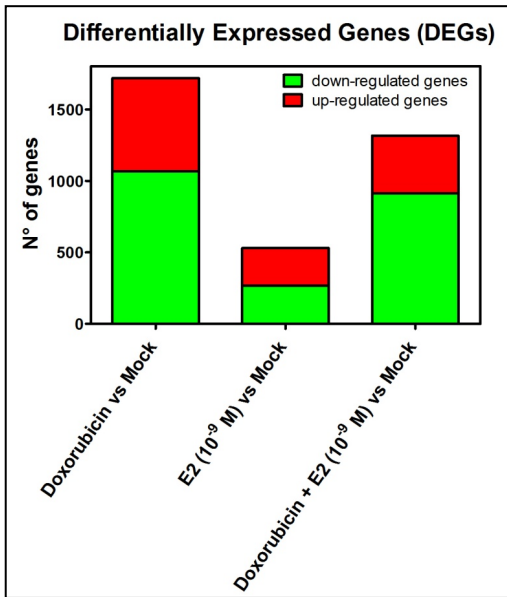


Figure R11 2 colors-stacked bar graph showing the total number of DEGs and the up- and down-regulated genes in every condition.

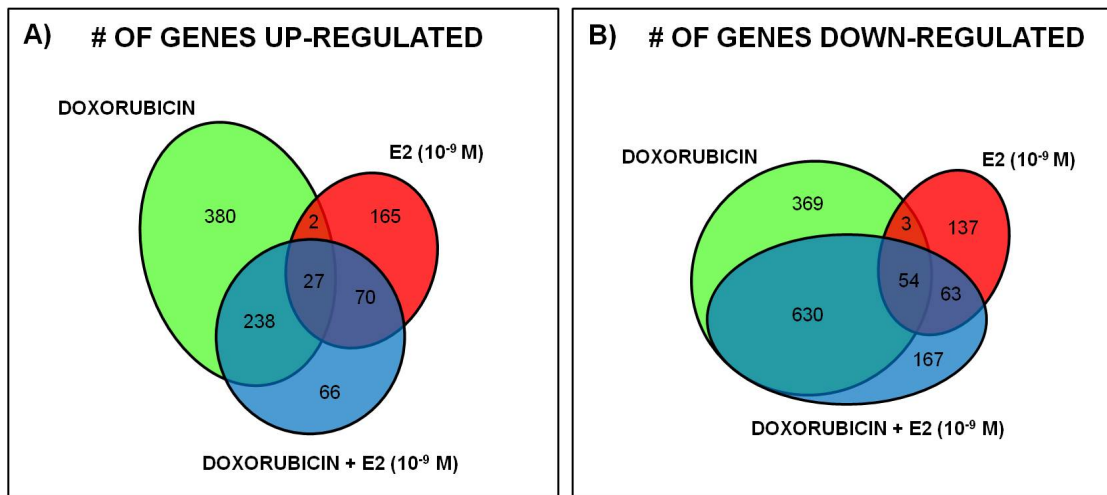


Figure R12 Specific gene signatures of the DOX+E2 combination treatment. Venn diagrams showing up-regulated genes (A) or down-regulated genes (B) comparing DOX, E2, and DOX+E2 DEGs. The number of genes differentially expressed in common or unique after doxorubicin or E2 (10⁻⁹ M) treatment or after their combination is indicated.

R13A) DOX+E2 combination treatment (DAVID ANALYSIS)

DOXORUBICIN + E2 (10 ⁻⁹ M) FUNCTIONAL ANNOTATION CLUSTER	
Annotation Cluster	score
regulation of transcription	6.48
proteins with BTB/POZ domain	4.42
basic-leucine zipper (bZIP) transcription factors	3.78
cell cycle/mitosis	3.27
components of microtubule cytoskeleton	3.63
cellular response to stress/DNA damage stimulus	3.09
proteins with zinc finger domain/C ₂ H ₂ -like	2.76
components of the nuclear chromosome part	2.69
proteins with sh3 domains	2.69
components of the condensed chromosome kinethocore	2.24
GTPase regulator activity	2.21
negative regulation of transcription from RNA pol II promoter	2.14
WNT receptor signalling pathway	2.12
components of nuclear lumen/nucleoplasm	2.10
regulation of apoptosis	2.03
positive regulation of transcription/macromolecule metabolic process	1.74
response to radiation/UV	1.62
proteins with SH ₂ domains	1.57
DNA-repair proteins/proteins with UmuC-like domain	1.53
proteins with BTB/POZ domain/Kelch-like proteins	1.52

R13 B) DOX+E2 combination treatment (IPA UPSTREAM REGULATOR ANALYSIS)

<input type="checkbox"/>	Upstream Regulator	Log Ratio	Molecule Type	Predicted Activation Status	Activation z-score	Notes	p-value of overlap	Target molecules in dataset
<input type="checkbox"/>	PP33 (includes: 56220159)	↑1.473	transcription regulator	Activated	4.605		4.31E-08	↑ACT12, ↑ADA, ... all 10
<input type="checkbox"/>	ESR1	↓-1.210	ligand-dependent nuclear receptor	Activated	3.388		4.51E-07	↑ABCC5, ↑ABCC2, ... all 36
<input type="checkbox"/>	96R	↑4.067	ligand-dependent nuclear receptor	Activated	2.043		2.67E-03	↑CDKN4, ↑SAL, ... all 18
<input type="checkbox"/>	KDM5B	↑1.058	transcription regulator	Activated	2.341		5.90E-03	↑BUB3B, ↑DUSP45, ... all 15
<input type="checkbox"/>	SMAD4	↓-1.260	transcription regulator	Activated	2.771		1.08E-02	↑CD42EP3, ↑CD, ... all 16
<input type="checkbox"/>	CDKN2A	↑1.447	transcription regulator	Activated	2.172		1.08E-02	↑BIM, ↑CDKN2, ... all 15
<input type="checkbox"/>	FOXM1	↓-0.233	transcription regulator	Inhibited	-2.224	has	5.99E-03	↑ATE2, ↑CDKN2, ... all 18
<input type="checkbox"/>	MDM2	↑1.373	transcription regulator	Inhibited	-2.194		1.87E-02	↑CDKN2, ↑CDKN4, ... all 16

R13 C) DOX+E2 combination treatment (IPA CANONICAL PATHWAYS)

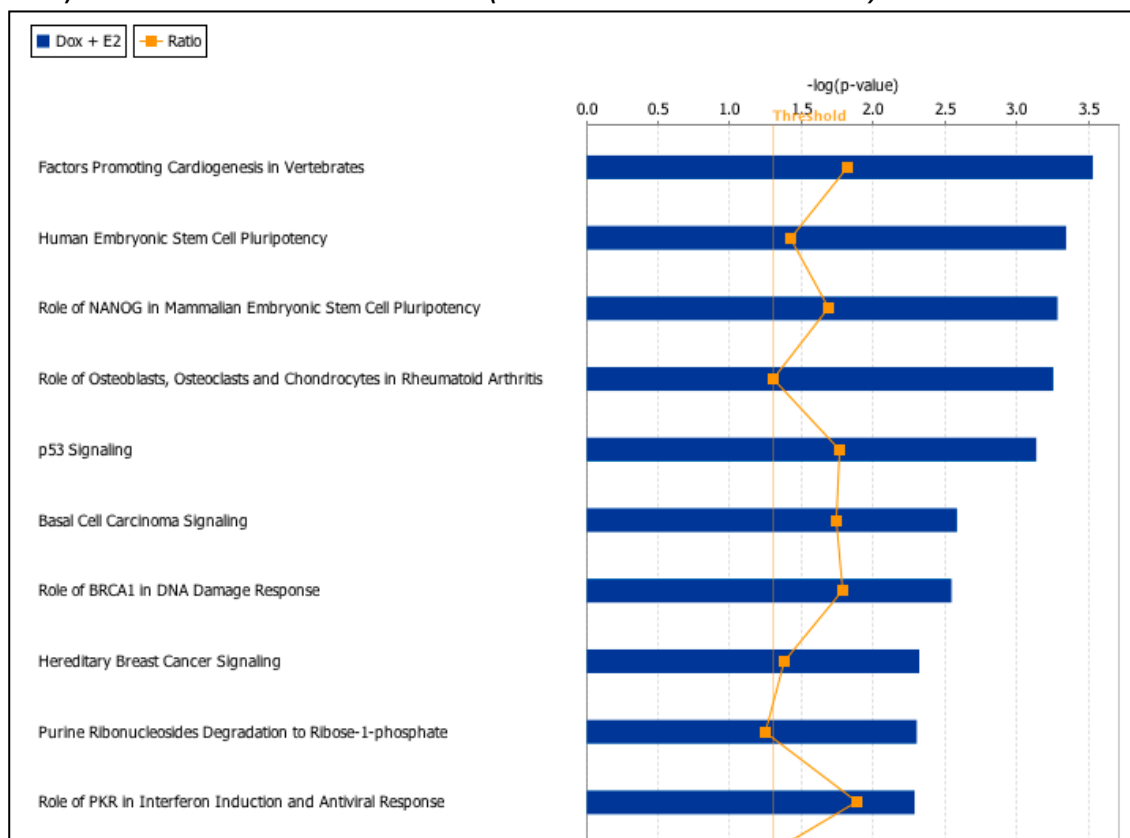


Figure R13. DOXORUBICIN + E2 (10^{-9} M) functional annotation clustering. Analyses were performed using the Ingenuity Pathway Analysis (IPA, <http://www.ingenuity.com>) as well as DAVID (<http://david.abcc.ncifcrf.gov/>⁴⁵) (enrichment score ≥ 1.5 , medium classification stringency) with default settings starting from the lists of differentially expressed genes corresponding to the treatment: doxorubicin ($1.5 \mu\text{M}$) + E2 (10^{-9} M). Results from DAVID functional cluster are summarized as a table with the indicated enrichment score. Results from IPA Canonical Pathways and Upstream Regulators are presented as screen snapshots.

The question that was raised after the genome-wide analysis was how combinatorial effect could be detected in a synergistic way. An approach based on the algebraic sum of logarithmic (\log_2) fold-changes in expression was adopted. Genes were selected considering a delta fold change with a more than an additive effect in a such way that the fold change associated to the double treatment must be greater than two (a parameter used for a more reasonable validation) and greater than the sum of the fold change associated to the single treatments (see Methods section). The delta based on the difference between the logarithmic values of the fold change of the double treatment and the sum of the single stimuli was therefore calculated and filtered ($\Delta > 0.1$). $[(\log_2[\text{FC}_{\text{double treatment}}] - \log_2[\text{FC}_{\text{DOX}}])$

$-\log_2[FC_{E2}] > 0.1]$. A Δ value equal to 0 is considered as additive effect. See p135 Supplemental Table III in *Lion et al.* for the complete list of genes.

A cooperative regulation enhanced the expression of genes involved in differentiation, cell-cell communication and cell adhesion or inflammatory response

201 up-regulated and 142 down-regulated genes met the criteria mentioned above and therefore exhibited a more than additive response following the combined p53/ER inducing treatments (see Figure R12). Analysis revealed that the functional cluster outcome appeared to be specific for the combined-treatment-specific genes, and grouped genes involved in cell-cell communication, cell adhesion, development/differentiation and inflammatory response pathways within the up-regulated genes, while cell cycle and mitosis functions were enriched in the repressed group (Figure R14). The enrichment scores were not high enough to assess if the functional clusters identified expand the p53/ER transcriptional network. It has been already addressed that ER can regulate growth and development¹⁶⁻¹⁸ and that p53 can be involved in the inflammation process^{75, 76} but the functional annotations obtained from these 201 genes can be still considered as a subclass of the DOX+E2 condition, strongly related to the synergistic cooperation analysis.

Genes from the up-regulated group were further investigated, leaving the down-regulated ones for a future study, especially since repression via *cis* elements has yet to be well established for both p53 and ER α .

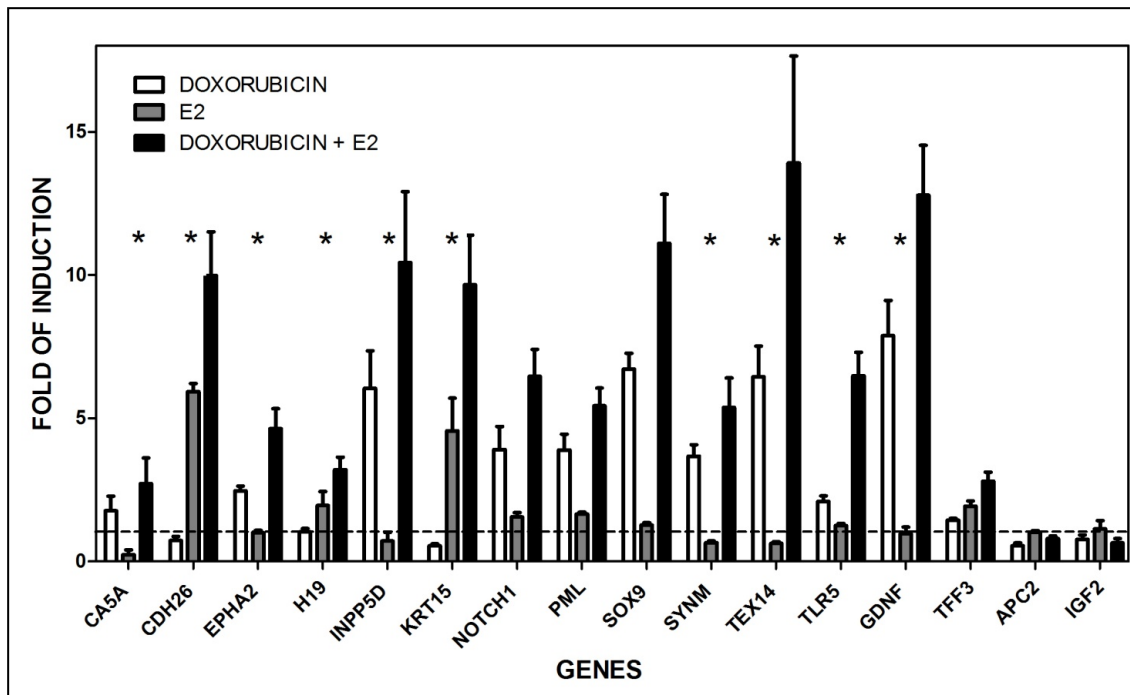
ADDITIVE EFFECT (DOXORUBICIN + E2 UP-REGULATION)		ADDITIVE EFFECT (DOXORUBICIN + E2 DOWN-REGULATION)	
FUNCTIONAL ANNOTATION CLUSTER		FUNCTIONAL ANNOTATION CLUSTER	
Annotation Cluster (201 more than additive genes)	score	Annotation Cluster (142 genes with greater than additive down-regulation)	score
ectoderm development/epithelial cell differentiation	2.94	cell cycle/mitosis	1.75
glycoproteins/proteins of the extracellular region	2.29	mitotic spindle organization/mitotic cell cycle	1.59
components of the plasma membrane	1.84		
components of the extracellular matrix/cell adhesion proteins	1.59		
inflammatory/defense response	1.55		
mesenchymal/neural crest cells differentiation	1.54		

Figure R14. DOXORUBICIN + E2 (10^{-9} M) functional annotation clustering of genes with a more than additive effect. Analyses were performed using DAVID (<http://david.abcc.ncifcrf.gov/>⁴⁵) (enrichment score ≥ 1.5 , medium classification stringency).

Some of the genes that came out from the analysis were particularly appealing for their canonical biological functions or their cellular context. From the group of 201 genes exhibiting more than additive up-regulation after combined DOX+E2

treatment, 16 that represented the main biological functions were selected for further analysis. Some are usually expressed in a different biological environment than breast cells (SOX9⁴⁶, TEX14⁴⁷, INPP5D⁷⁹) and others belong to biological pathways that can expand the p53/ER transcriptional master network (TFF3⁴⁸, CA5A⁴⁹, CDH26⁵⁰, NOTCH1⁵¹, GDNF⁵², INPP5D⁷⁹). For some, a direct or indirect functional interaction with p53 (NOTCH1⁸⁷, IGF2⁵⁴, TLR5^{75, 76}, PML⁵⁵, INPP5D⁷⁹, EPHA2⁵⁶), with ER (NOTCH1⁵⁷, CDH26^{58, 59}), or with other selected genes (IGF2 & H19⁶⁰, NOTCH1 & SOX9^{61, 62, 58}) has already been proposed.

A quantitative real time PCR (qPCR) was performed to confirm microarray results after DOX treatment with or without the addition of E2 (Figure R15). The trend of the microarray results was confirmed for the majority of the genes tested upon DOX and/or E2 treatment (see scatter plots in Figure R15). T-test analysis on the log₂ of the values obtained for relative expression confirmed for 10/16 genes the synergistic effect ($p < 0.05$) of DOX + E2 combination (see p132 supplemental tables in *Lion et al.*).



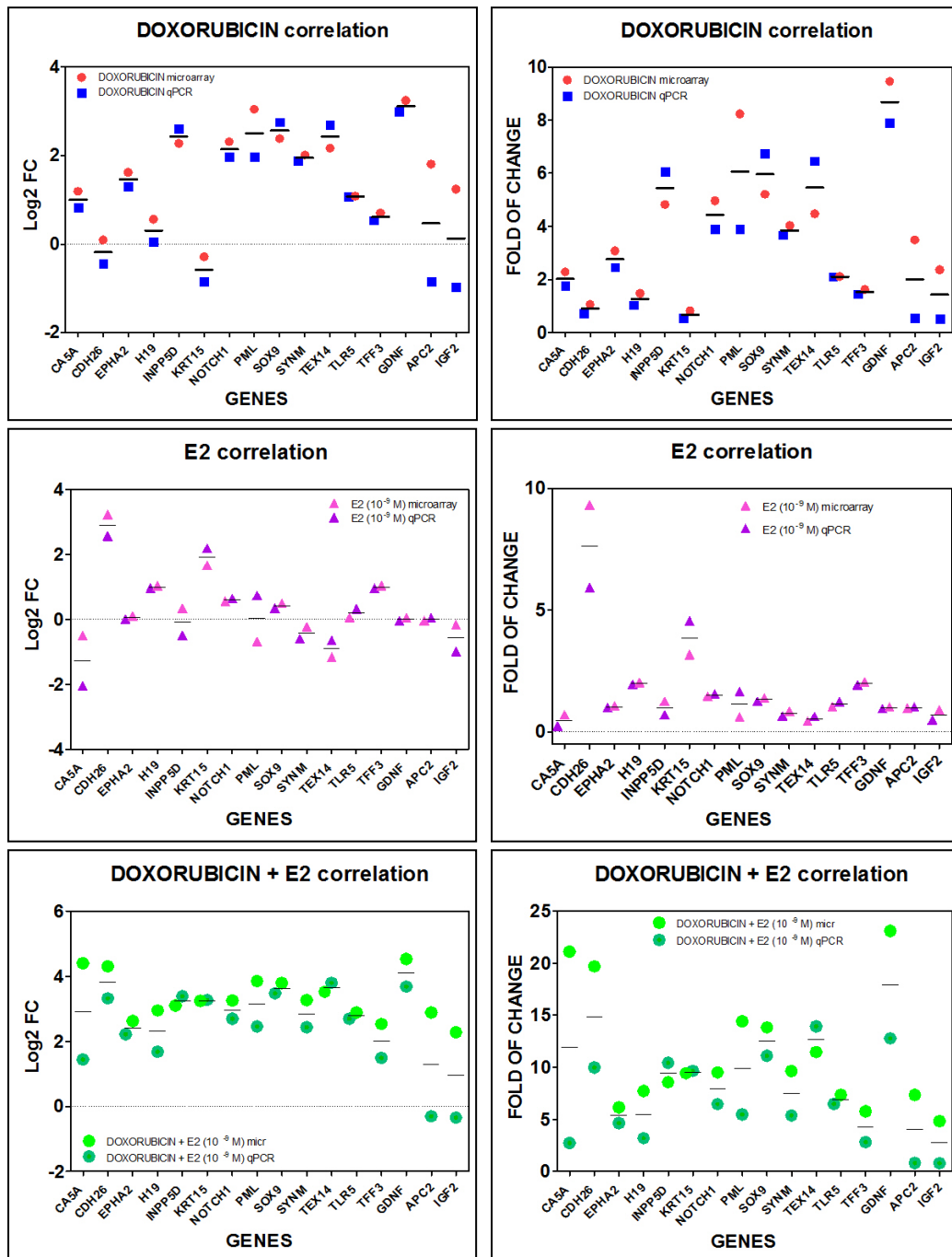


Figure R15. Treatment-selective transcriptional cooperation between doxorubicin and estradiol, correlation between microarray and qPCR analyses. qPCR reactions for the 16 chosen genes were carried out using 384-well plates in a final volume of 10 μ l using TaqMan® Gene Expression Assays (Life Technologies) with 3 biological and 2 technical replicates for each condition. GAPDH, B2M and β -actin housekeeping genes served as internal controls. Asterisks indicate statistically significant, more than additive effects in the combined treatment as described in Methods section. Same RNAs used in the microarray experiments were tested. Scatter plot graphs highlight the correlation between data coming from microarray and qPCR analyses (based on both log₂ and fold of change values). The correlation between microarray results and qPCR is shown as scatter plot generated both using the log₂ scale and the fold change conversion to better visualize the correspondence between the two methods.

Gene expression of the 16 genes was also investigated following treatment with 5FU, another commonly used genotoxic agent that results in p53 activation. The responses clearly differed between DOX and 5FU (Figure R15&R16). Speculation about the remarkable difference observed between the two chemotherapeutic targets will be discussed more extensively below in the *Discussion* chapter. Only CDH26, INPP5D, NOTCH1 were responsive to 5FU (fold change > 1.5) of which INPP5D and NOTCH1 were also DOX responsive. The synergistic effect observed after DOX+E2 administration was observed only for H19, INPP5D, and in part also for GDNF after 5FU + E2 treatment (Figure R16 and p134 supplemental table in *Lion et al.*). Unlike for DOX, the combined treatment did not affect TLR5 or EPHA2 that are already considered p53 target genes^{56, 76}. Thus, the E2 enhancing effects on expression differed between the two different inducers of p53 as discussed below in the next section.

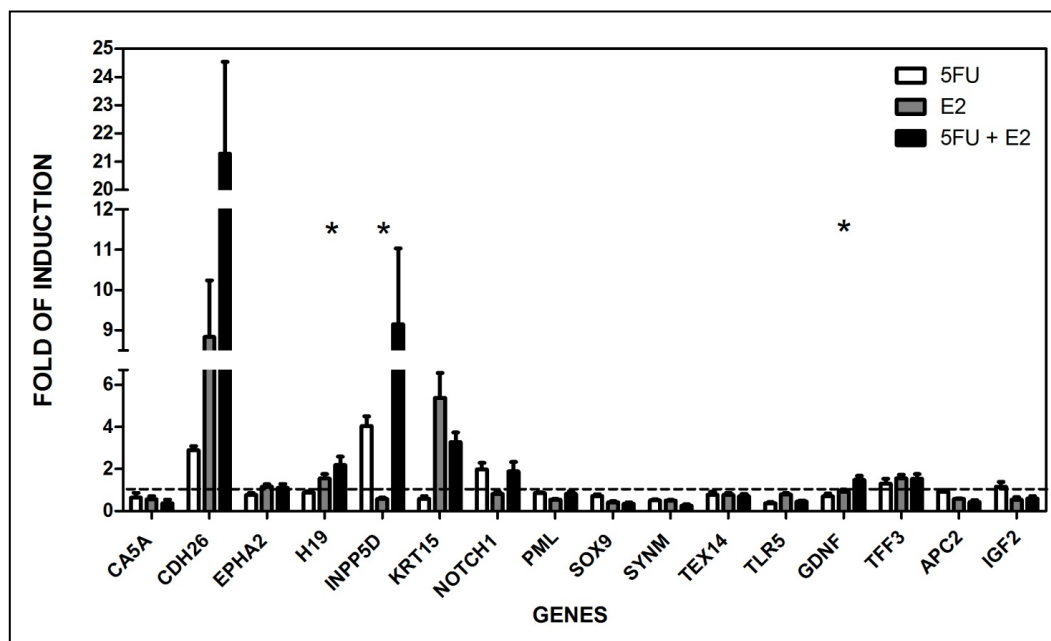


Figure R16. Treatment-selective transcriptional cooperation between 5FU stimulus and estradiol. qPCR reactions for the 16 chosen genes were carried out using 384-well plates in a final volume of 10µl using TaqMan® Gene Expression Assays (Life Technologies) with 3 biological and 2 technical replicates for each condition. GAPDH, B2M and β-actin housekeeping genes served as internal controls. Asterisks indicate statistically significant, more than additive effects in the combined treatment as described in Methods section.

Genotoxic stress plays an important role in the synergy with ER: Nutlin-3a treatment synergizes with estradiol pathway only on a subset of genes

Doxorubicin and 5FU are two different drugs acting in a different way but both creating a genotoxic stress within the cell. Genotoxic stress is an important stimulus to activate p53 protein, but it can also lead to the activation of a lot of other components or pathways, a matter that can alter the precise responses. Nutlin-3a (nutlin) on the other hand is able to directly target the complex p53-MDM2 stabilizing the tumor suppressor without inducing apparently any kind of genotoxic stress⁴⁴. For that reason MCF7 cells were treated also with nutlin alone or in combination with E2 (10^{-9} M) to check whether the results obtained using doxorubicin were reproducible. Stabilization of p53 was observed after treatment with nutlin alone or in combination with E2 as well as its transcriptional activation (Figure R1). Quantitative real time PCR analysis (Figure R17) showed an up-regulation for 6/16 genes (EPHA2, INPP5D, KRT15, NOTCH1, SOX9, TEX14) after nutlin treatment alone (fold of induction > 1.5) as obtained using doxorubicin alone apart from KRT15 that previously resulted only as an E2 responsive gene (Figure R15-17). Statistically only three genes (EPHA2, H19, INPP5D) presented a more than additive effect in the combined treatment (see p134 of supplemental tables in *Lion et al.*). These three genes were also statistically up-regulated in a synergistic way by DOX+E2 and two of those consistently exhibited transcriptional cooperation with all the p53-inducing stimuli (H19, INPP5D; see p132-134 supplemental tables in *Lion et al.*). Further analyses to investigate the p53-dependency after DOX and nutlin treatment are required to elucidate data observed in qPCR (see next paragraph).

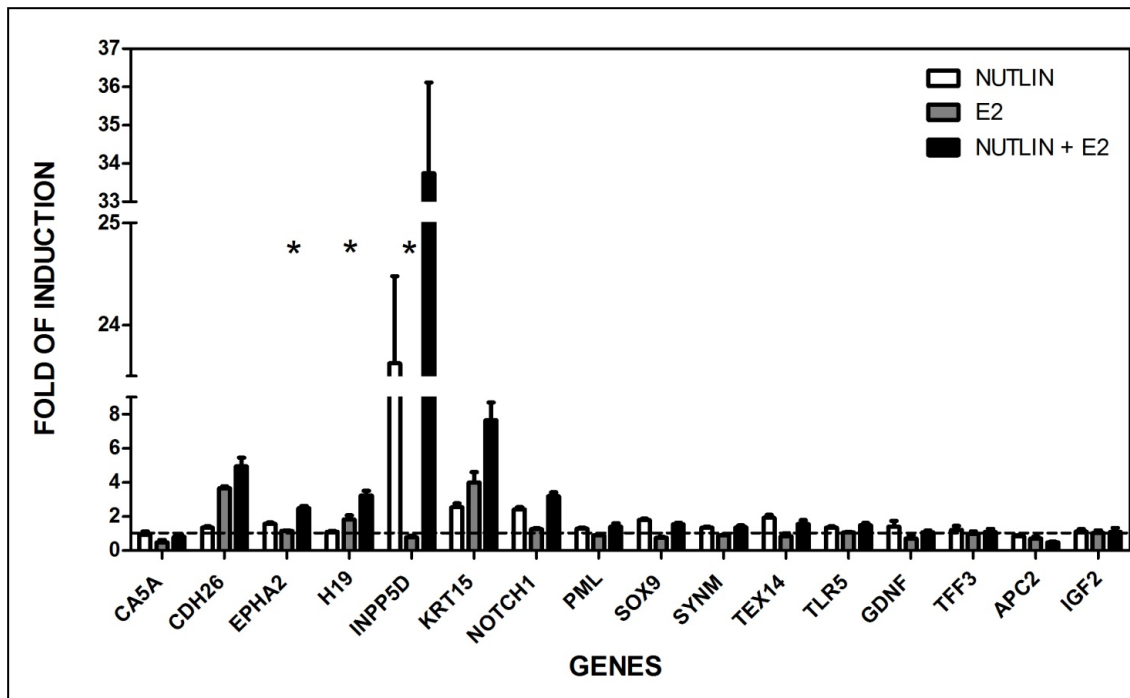


Figure R17. Treatment-selective transcriptional cooperation between nutlin stimulus and estradiol. qPCR reactions for the 16 chosen genes were carried out using 384-well plates in a final volume of 10µl using TaqMan® Gene Expression Assays (Life Technologies) with 3 biological and 2 technical replicates for each condition. GAPDH, B2M and β-actin housekeeping genes served as internal controls. Asterisks indicate statistically significant, more than additive effects in the combined treatment as described in the Methods section.

Silencing of p53 in MCF7 cells establishes a direct role of p53 in doxorubicin and nutlin responsiveness of the target genes

Many ways can be adopted to test the p53-dependency of a gene transactivation. Changing the cellular context or adding an additional drug to the treatments, for instance pifithrin-α (PFTα) that inhibits p53 function, could in principle introduce an extra bias on the experimental system. For that reason, direct p53 inducible expression of the novel genes was validated using a stable MCF7 cell line expressing shRNA to p53⁶³. MCF7 clone silenced for p53 was named as MCF7 p53i and the control MCF7 vector. Functionality of the cell model was validated both by western blot analysis and qPCR, at time point 10-hours and 24-hours stimuli (Figure R18&R19). Cells were cultured in normal medium and p53 was stabilized and activated after DOX and nutlin treatment, as expected, in MCF7 vector and it was undetectable in MCF7 p53i (Figure R18). p53 mRNA level do not vary over treatment compared to the mock condition, in the relative clone (Figure R19). ERα protein expression did not change after any of the 10 hour-stimuli used,

confirming what previously observed with the original MCF7 cell line (Figure R18). After 24-hours, however, doxorubicin repressed ER α protein levels (Figure R18) a result confirmed also by mRNA level analysis (Figure R19). This repression eventually would affect estradiol responses including the transcriptional cooperation with p53. Gene expression for the p53 target gene p21 is greatly reduced after DOX or nutlin treatment MCF7 both at 10- and 24-hour stimulus in MCF7 p53i (Figure R19). MCF7 p53i clone system was therefore confirmed to be silenced for p53, but the silencing does not totally abrogate p53 expression and transactivation activity.

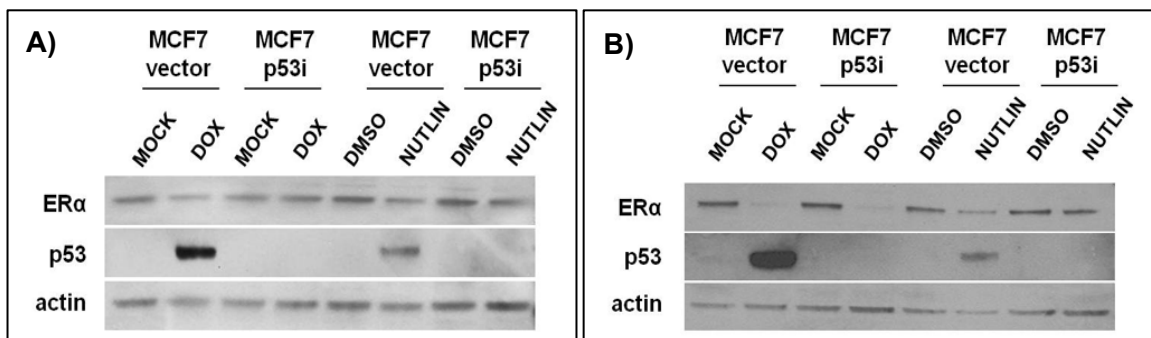


Figure R18. Changes in p53 and ER α protein levels. Western blot analysis showing p53 and ER α protein levels after 10 (A) and 24 (B) hours of DOX (1.5 μ M) or nutlin-3a (10 μ M) treatment.

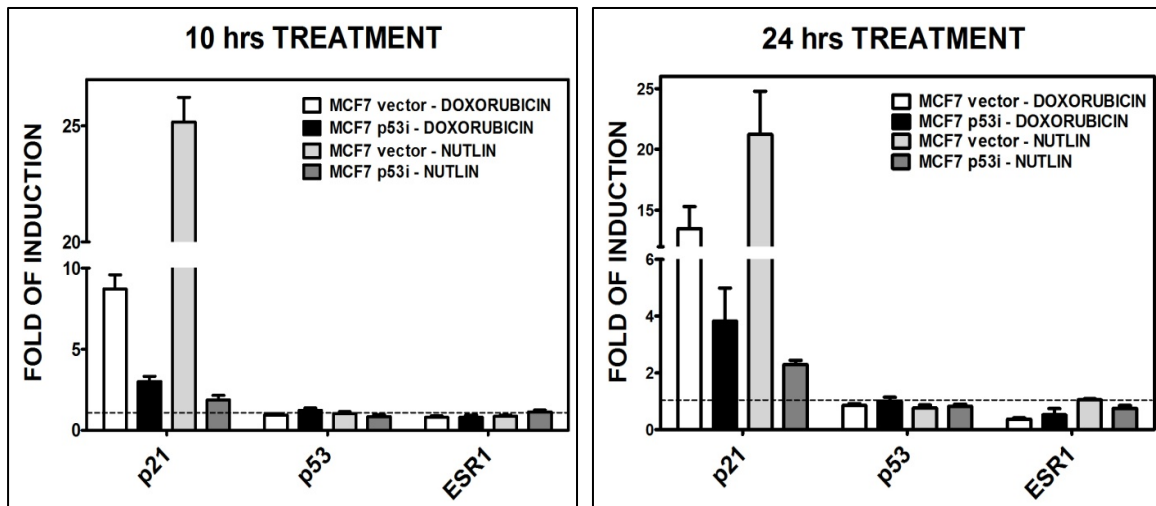


Figure R19. Changes in p21, p53 and ER α relative mRNA expression. Presented are results for p21, p53 and ER (ESR1) genes after 10 or 24 hours DOX (1.5 μ M) or nutlin-3a (10 μ M) treatment in MCF7 vector and p53i. The fold-induction relative to the mock condition for MCF7-vector or MCF7-p53i is presented (H₂O for DOX treatment or DMSO for nutlin-3a treatment).

Among the 16 genes investigated above, eight of them were selected to determine how gene expression changed in MCF7 p53i after 10- or 24-hours DOX and nutlin treatment. Nutlin treatment is an important control to discriminate between possible consequences of genotoxic effects that might occur at the gene expression level, in comparison with the quantitative real time performed previously (see Figure R15-17). At the 10-hour stimulus (the same of the previous experimental approach) EPHA2, GDNF, NOTCH1 and INPP5D were induced after either treatment in MCF7 vector cells but were non-responsive or slightly responsive in MCF7-p53i cells (Figure R20). The other five genes did not show any p53-specific responsiveness although TLR5 has been already shown to be a p53 target gene^{75, 76}.

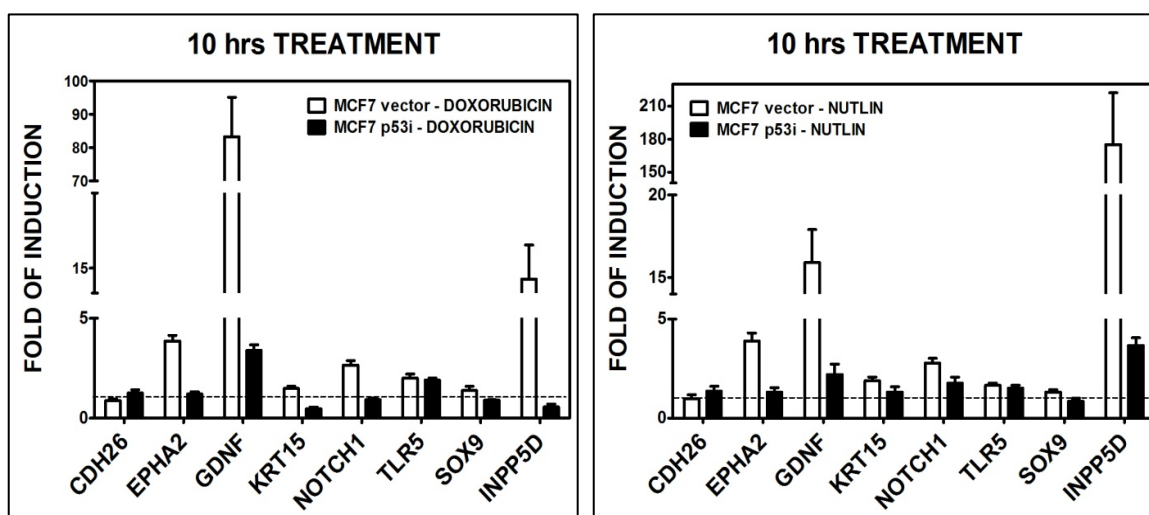


Figure R20. Changes in relative mRNA expression for the selected genes. Presented are results for eight selected genes after 10 hours DOX (1.5 μ M) or nutlin-3a (10 μ M) treatment in MCF7 vector and p53i. The fold-induction relative to the mock condition for MCF7-vector or MCF7-p53i is presented (H₂O for DOX treatment or DMSO for nutlin-3a treatment).

Then, DOX and nutlin responses after 24-hr was also examined. At this time point both treatments enhanced expression of p53, compared to the 10-hour treatment. p53-dependent induction for seven of the eight genes examined following either treatment was observed (Figure R21). DOX treatment led to a residual induction of several of the genes in the MCF7-p53i cells, while only INPP5D was slightly responsive upon nutlin treatment. The residual responsiveness was presumably due to a residual level of p53 induction in MCF7-p53i cells while the differences between DOX and nutlin could be ascribed to differences in p53 post-translational modifications elicited by the treatments or to the reduced residual levels of p53

expression observed after nutlin treatment. CDH26 gene expression offers another example of treatment dependencies as the gene was not regulated by p53 at either time point with either DOX or nutlin but was inducible by 5FU treatment alone (see Figure R16). INPP5D⁷⁹, NOTCH1⁸⁷, EPHA2⁵⁶ and TLR5^{75, 76} were established as p53 target genes and therefore confirmed what already seen in literature.

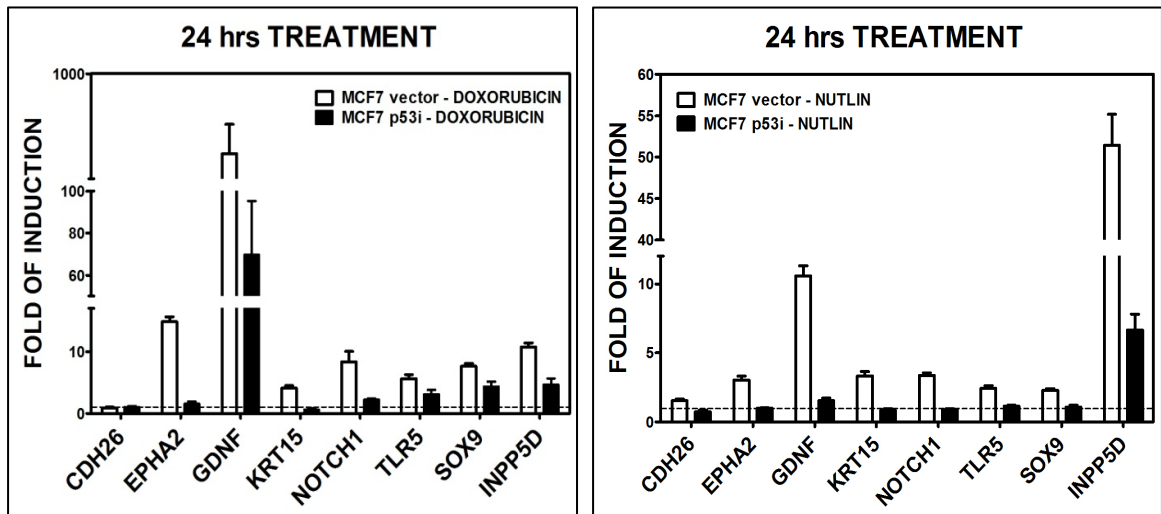


Figure R21. Changes in relative mRNA expression for the selected genes. Presented are results for eight selected genes after 24 hours DOX (1.5 μ M) or nutlin-3a (10 μ M) treatment in MCF7 vector and p53i. The fold-induction relative to the mock condition for MCF7-vector or MCF7-p53i is presented (H₂O for DOX treatment or DMSO for nutlin-3a treatment).

MCF7 vector and p53i clones did not reproduce the cooperation between p53 and estradiol pathway at the experimental conditions

MCF7 vector and p53i cells were cultured in estrogen-depleted medium and the synergistic effect after DOX or nutlin treatment in combination with E2 (10⁻⁹ M) was investigated, as previously performed for the original MCF7 clone (see Methods section). Cells were stimulated for 10 hours with one of the p53-inducing agent and/or estradiol. Gene expression of the canonical ER α target, GREB1²³, clearly shows the transrepression activity due to p53 or the genotoxic stress on ER transactivation activity (Figure R22). Nutlin indeed could not affect GREB1 expression in MCF7 p53i, probably due to the low activation of p53 protein. p21 expression was induced by DOX and nutlin in a p53-dependent manner. As expected the treatments did not affect the expression of p53 nor ESR1 (ER α). Hence, it can be hypothesized that MCF7 vector and p53i are a good model

system to study p53-dependency but there might be important differences with the original MCF7 cell line in the responses to estradiol. For example, the decrease of ER activity could also impact on the possibility to study the transcriptional cooperation with p53.

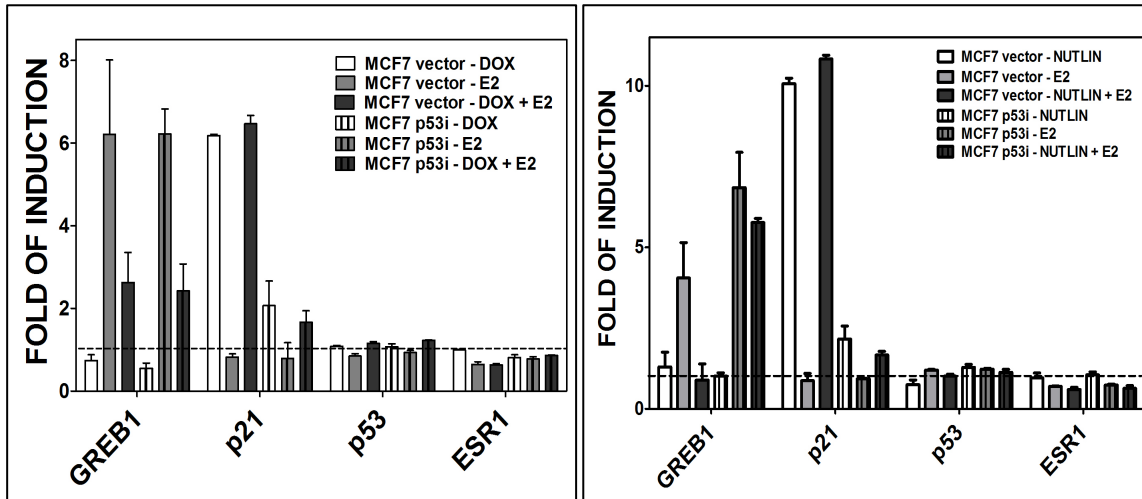


Figure R22. Changes in GREB1 mRNA expression. Presented are results after 10 hours DOX (1.5 μ M) or nutlin-3a (10 μ M) treatment and/or E2 (10⁻⁹ M) in MCF7 vector and p53i. The fold-induction relative to the mock condition for MCF7-vector or MCF7-p53i is presented (H₂O for DOX treatment or DMSO for nutlin-3a treatment).

TLR5 is an example of transcriptional cooperation observed in MCF7 vector cell line after doxorubicin treatment (Figure R23). But, as previously observed in Figure R19, the p53-dependency of TLR5 expression could not be detected after 10-hour treatment in MCF7 p53i. Consistently, a reduction in the effect of the combinatorial treatment was not observed. This is a limitation of the MCF7 p53i cell model used that does not allow easily to investigate the combinatorial role of p53 and estradiol pathway in gene transactivation at least at the 10-hour time point.

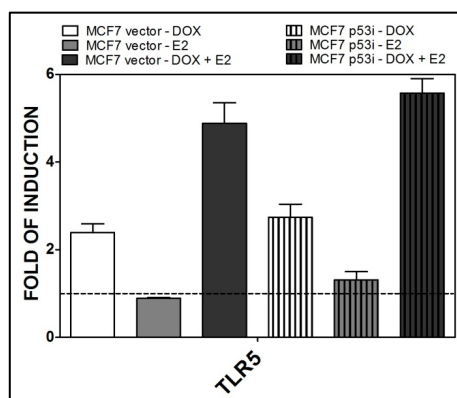


Figure R23. Changes in TLR5 mRNA expression. Presented are results after 10 hours DOX (1.5 μ M) treatment and/or E2 (10⁻⁹ M) in MCF7 vector and p53i.

An example confirming that p53 takes part in the transcriptional cooperation observed with estradiol-induced pathway is CDH26 after treatment with nutlin in combination with E2 (10^{-9} M). The combinatorial effect is completely lost in MCF7 p53i (Figure R24). In the results shown above, CDH26 was strongly E2-responsive and only 5FU responsive among the p53-inducing stimuli (see Figure R15-17). For the remaining six genes tested, the transcriptional cooperation was not reproduced (data not shown).

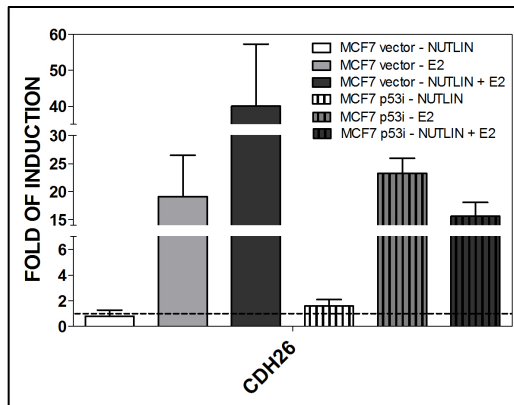


Figure R24. Changes in CDH26 and KRT15 mRNA expression. Presented are results after 10 hours nutlin-3a ($10\mu\text{M}$) treatment and/or E2 (10^{-9} M) in MCF7 vector and p53i. The fold-induction relative to the mock condition for MCF7-vector or MCF7-p53i is presented (DMSO treatment).

MCF7 clone silenced for ER α are also required to better understand the role of estrogen receptors after E2 treatment and to light up the mechanism of synergy. MCF7 cell line expressing shRNA to ER α are currently being selected.

The biological impact and expression responses due to p53 and estradiol pathway led the in-depth investigation of the promoter regions of the *INPP5D*, *TLR5A* and *KRT15* genes for the presence of canonical and non-canonical p53 and ER response elements in order to identify a more direct role of the TFs involved in the specific gene expression regulation.

The transcriptional responsiveness of INPP5D, TLR5 and KRT15 is associated with p53 and ER response elements

An in silico analysis was performed in order to identify putative canonical or non-canonical p53 and ER α response elements couples with a maximum distance of around 500bp within the promoters of the selected genes. Three different approaches were used and combined: a) manual pattern matching analysis ($\frac{1}{2}$ p53 RE: RRRCWWGYYY; $\frac{1}{2}$ ER α RE: (A)GGTCA, TGACC(T) or GGCTA) b) pattern matching analysis with $\frac{1}{2}$ site position weight matrixes derived from

TransFac using the online Regulatory Sequence Analysis Tool (RSAT) ⁶⁴ and c) R tool analysis using TransFac matrixes (see Methods section).

Putative non-canonical p53 and ER α REs couples were identified in almost all the genes' promoters selected (promoter defined as -3000bp \leftrightarrow + 2000bp from the transcription start site, TSS). The analysis was focused on the promoter regions of the *INPP5D*, *TLR5A* and *KRT15* genes and two distinct regions were identified within the promoter of each of these genes (called A & B, see Figure R25).

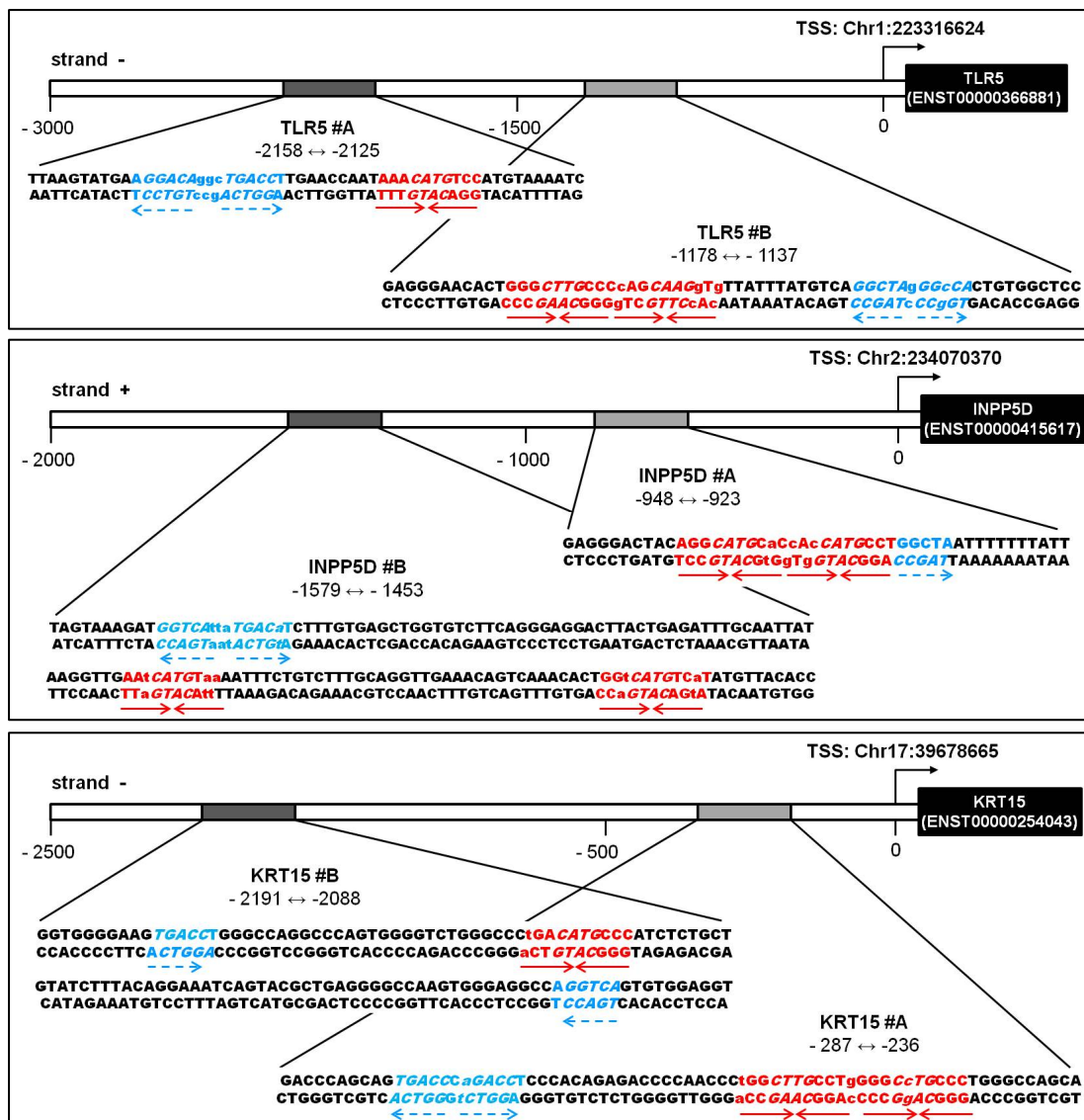
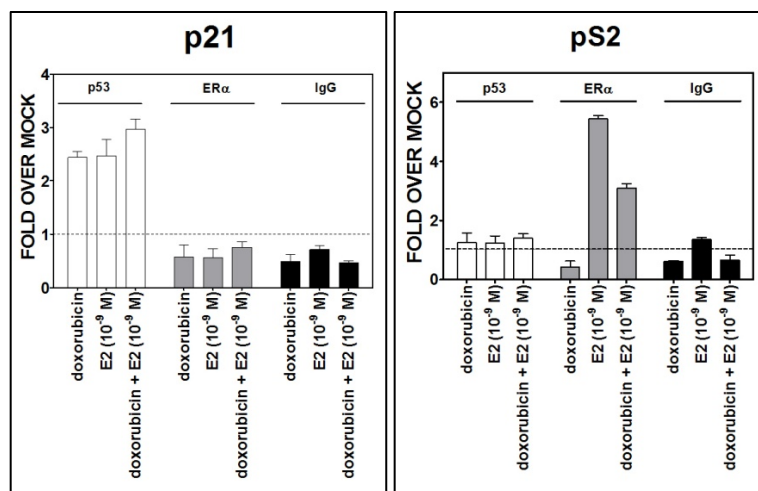


Figure R25. Predicted p53 REs and EREs at TLR5A, INPP5D and KRT15 promoter regions. Sequence, organization and position of mapped p53 and ER target sites. Promoters of selected genes were evaluated combining 3 approaches (pattern matching analysis; RSAT analysis and R tool analysis using TransFac matrixes). Blue dashed arrows mark ERE half sites, while tail-to-tail red arrows denote the p53 RE half site. The chromosomal position, strand and the distance from the transcriptional start sites are also indicated. Two promoter fragments (denoted as #A and #B) were examined separately for each gene.

The promoters were then examined by chromatin immunoprecipitation assay (ChIP) followed by qPCR for p53 and ER occupancy. Primers based on the annotated p53 and ER REs at p21 and pS2 promoters were used as controls. As expected, there was p53 occupancy at the canonical p53 target p21, as well as at the canonical ER α target pS2 (Figure R26). Interestingly, E2 led to p53 recruitment at p21 promoter (confirmed also at the level of other p53 target promoters, see p99 Figure 6B in *Lion et al.*). This might be explained with the fact that the addition of E2 after 72 hours in stripped medium could provide a proliferative stimuli that may be sensed by the cell and, therefore, resulting in enhanced p53 occupancy at some sites not necessary related to transcription. The mouse immunoglobulin G (IgG) used as negative control could give an additional explanation due to the fact that the fold over mock in the E2 condition was usually higher compared to DOX alone or DOX+E2 condition. DO-1 antibody, used to pull down p53, was also a mouse antibody.

p53 occupancy at the promoter regions was also found for the INPP5D, TLR5 and KRT15 genes following DOX treatment. However, ER α occupancy was only detected at the KRT15 promoter for fragment B (Figure R26). It appears that there is independent occupancy by the two transcription factors in that the binding of one is not required for the recruitment of the other. Thus, while transcriptional synergy is established, it could not be ascribed to effects at the level of binding, at least for the sites examined. See Discussion for further considerations, including the analysis of histone marks associated with gene activation or repression.



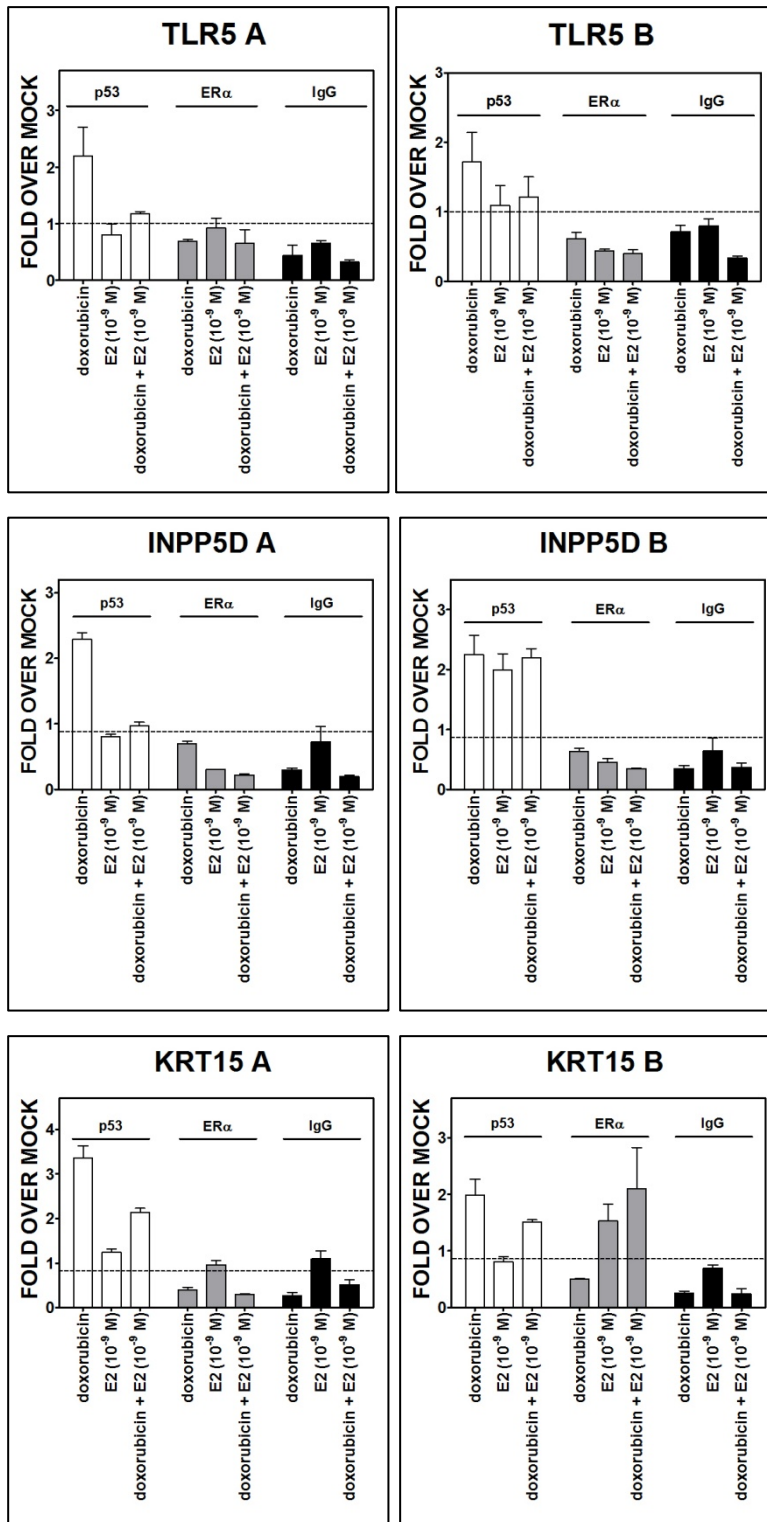


Figure R26. Relative occupancy of p53 and ERα. Chromatin Immunoprecipitation and quantitative real time PCR analyses. ChIP assays were performed using either an antibody against p53 (DO-1) or ERα (H-184) or control IgG (sc-2025). PCR was carried out in 384-well plates in a final volume of 10μl using primers designed to amplify regions containing validated REs and ERE for established p53 and ERα target genes, or to generate amplicons centered around the identified p53 REs and EREs in TLR5, INPP5D or KRT15.

DISCUSSION

Breast cancer treatment strategies involve surgery, radiotherapy, chemotherapy and hormonal/endocrine therapy⁶⁵. The latter is used specifically for estrogen receptor-positive tumors, which accounts for more than 60% of all breast cancer³². Estrogen and ERs are implicated in the development of breast cancer according to two hypotheses, one related to the stimulation of proliferation due to the effect of estrogen acting through ER, and the other one related to estrogen metabolites that can exert genotoxic stress¹⁶. ER α is a prognostic marker and therefore can also be considered a therapeutic target^{65, 66}. Genotoxic estrogen metabolites could play an important role in carcinogenesis in a ER-independent way in concert with the ER-dependent proliferation effects⁶⁵. Indeed, high doses of estrogens were extensively used in breast cancer treatment prior to the introduction of selective estrogen receptor modulators (SERMs)^{67, 68}. ER antagonist and inhibitors of estrogen synthesis are commonly used in endocrine therapy and include SERMs that can act as anti-estrogen, selective estrogen receptor down-regulators (SERDs) or aromatase inhibitors (that block specifically hormone synthesis)⁶⁸⁻⁷⁰. ER agonists, instead, are frequently used in hormonal replacement in postmenopausal women⁷¹. Endocrine therapy can however lead to unwanted side-effects; and in particular receptor agonists can increase the risk of breast cancer development⁷¹. In the context of pharmacological treatments, such as multi-drug cancer therapy or that comprises cocktails of genotoxic chemotherapeutics, the effect that endogenous or exogenous estrogen can exert in combination with other drugs must be taken into account. Doxorubicin and 5-fluorouracil are currently used as chemotherapeutic drugs in different cancer types including also breast cancers (www.chemocare.com). The information coming from the functional role of the combination of these factors in tumorigenesis might have a potential to be used in clinic for treatments of patients with ER-positive breast cancer and in general to all the other cancers dependent on steroid hormones (prostate, testicular, ovarian and endometrial tumors).

In this respect, the impact of doxorubicin on whole genome transcriptomes was determined in cells exposed or not to 17 β -estradiol. MCF7 cells were used as an experimental model of luminal-A subtype breast adenocarcinoma (p53 wild type, MDM2 positive, ER α positive, FOXA1 positive, HER2 negative)⁷². Based on previous work³⁸⁻⁴¹, genes were anticipated for which the inducible transcriptional

factors p53 and ERs could act collaboratively in *cis* at their respective REs. In fact, regardless of the mode of interaction, identifying genes that show a synergistic p53/ER response is expected to inform treatments of breast or other cancers. Overall, doxorubicin treatment resulted in profound changes in gene expression output with 647 up- and 1056 down-regulated genes and enrichment for the p53-pathway activation, including regulation of transcription, cell cycle and mitosis, DNA damage checkpoint, apoptosis and stress response. While, deeply influenced by doxorubicin, the combination treatment with E2 resulted in 66 genes uniquely responsive and a total of 201 with more than additive changes. Interestingly, gene ontology and pathway analysis suggested a significant enrichment for cell-cell communication, epithelial cell differentiation, inflammatory responses within this combinatorial up-regulated gene group. Combinatorial down-regulation was also observed for 142 genes with an enrichment for cell cycle, mitosis and metabolic functions.

16 among the 201 genes exhibiting a more than additive response were selected in order to better understand the additive responses towards p53 and estrogen inducing agents. While DOX or 5FU treatment resulted in similar p53 levels and p21 induction, there were marked differences in microarray expression after single treatments, as well as in qPCR when combined with estradiol. Previous studies have established cell type specific responses to DOX and 5FU as well as other drugs ⁷¹. A different impact on p53-induced responses and expression changes was awaited ^{42, 43} and it was confirmed in the microarray experiments as well. This huge variance has to be taken into account every time an experiment is performed. Several factors can contribute to the different responses observed. The concentration of the drug and the duration of the treatment strongly influence the expected outcome. Post-translational modification are also involved in this mechanism. Different stimuli can activate the same protein but convert the information into a different biological response. It is not surprising to expect a different impact when DOX and 5FU are also combined with estradiol pathway. To further investigate that and to confirm microarray analysis, a quantitative real-time PCR (qPCR) for the 16 selected genes was performed. Results obtained after DOX treatment are in agreement with microarray data, and ten of these genes present also a statistically significant transcriptional cooperation. 5FU treatment, instead, is not completely in line with results observed

previously with DOX stimulus and the combination with estradiol led, statistically, to a synergistic expression only for three out of sixteen genes (H19, INPP5D, GDNF). Another drug, still in clinical trial, related to p53-activation is nutlin-3a (nutlin). Nutlin was chosen to be tested in the experimental model to activate and stabilize p53 without the involvement of genotoxic stress. In fact, nutlin is thought to directly activate p53 because it inhibits the interaction of the tumor suppressor with its negative regulator MDM2 ⁴⁴. The investigation of gene expression after combination of nutlin with estradiol becomes therefore extremely interesting. qPCR analysis showed an up-regulation for six genes (EPHA2, INPP5D, KRT15, NOTCH1, SOX9, TEX14) after nutlin treatment alone, confirming a possible direct role of p53 in their gene transactivation. Also for nutlin, only three genes (EPHA2, H19, INPP5D) presented statistically a more than additive effect in the combined treatment. All together these results highlight that six genes (CDH26, EPHA2, H19, INPP5D, KRT15 and NOTCH1) showed responsiveness to E2 combined with 5FU and nutlin, but only two genes (H19, INPP5D) consistently exhibited a statistically significant transcriptional cooperation between E2 and all p53-inducing treatments (DOX, 5FU, nutlin). Notably, for the remaining eight genes (CA5A, PML, SOX9, SYNM, TEX14, TLR5, GDNF and TFF3) a dependency on the DOX+E2 treatment was observed. Results obtained after nutlin treatment must also be contextualized with possible post-translational modifications that might occur after its administration. For instance KRT15 was not responsive after DOX and 5FU treatment, but it was instead after nutlin alone. A p53 monoubiquitination that promotes its cytoplasmic localization and translocation to mitochondria upon nutlin treatment has been described ⁷⁴. The results emphasized once again the different gene expression response that can occur when different genotoxic drugs are administered and the importance of understanding the mode of action in particular when these drugs are used as p53-pathway activators.

To address the dependency on p53 as a transcriptional regulator, a panel of selected targets was investigated using a stable MCF7 clone silenced for p53 ⁶³. The p53-dependent induction after DOX and nutlin treatment was examined for eight genes and confirmed for the newly identified p53 target genes GDNF, KRT15, and SOX9 as well as the recently previously reported TLR5 ^{75, 76}, INPP5D ⁷⁹, NOTCH1 ⁸⁷ and EPHA2 ⁵⁶. CDH26 was 5FU responsive but a requirement for

p53-dependent induction was not confirmed in MCF7 cell system, highlighting once again the specificity of drug response.

The synergistic effect identified is still under investigation, in particular the mechanism through which estradiol pathway and p53 cooperate. As described in the Introduction section, results from many studies highlighted a highly complex interplay between p53 and estrogen receptors. Physical negative interaction between the two proteins, a ligand-dependent positive effect of ER on p53 protein levels, an effect of p53 on ER protein level, an indirect, negative effect of ER on p53 levels via modulation of the intronic MDM2 promoter, in cooperation with Sp1, p53-enabled ER recruitment at half sites EREs resulting in transcriptional cooperation are notable, reported functional interactions ²⁴⁻³².

Given the earlier results obtained with the FLT1 gene ³⁸⁻⁴¹, three (TLR5, INPP5D, KRT15) of the 16 genes were examined for the possibility of *cis*-interactions by assessing p53 and ER occupancy. These genes were particularly appealing for their biological functions in respect also to the canonical pathways usually controlled by p53 and ER. TLR5 gene is involved in the innate immunity and its expression has been shown to be regulated by DNA damage and p53 activation ^{75, 76}. TLR5 has been indeed very recently shown to be a p53 target gene, along with several other toll-like receptors, indicating a link between DNA damage signaling mediated by p53 and innate immunity responses leading to activation of NFκB ^{75, 76}. Results obtained so far extend this observation in MCF7 cells and reveal a contribution of the estradiol pathway in further modulating TLR5 expression in response to the combination with doxorubicin treatment. High expression of TLR5 has been reported in breast carcinomas, and the activation of its pathway through the ligand flagellin seems to inhibit cell proliferation in breast cancer ⁷⁷. INPP5D on the other side is not directly related to TLR5 but it is considered as a toll-like receptor pathway inhibitor, particularly a TLR2/TLR4 inhibitor ⁷⁸. It is also known as SHIP1, for lipid phosphatase SH2 domain-containing inositol-5'-phosphatase 1, and it has been proposed to act as tumor suppressor gene, and its expression has been previously linked to p53 status in head and neck cancer, as responsive to cisplatin treatment ^{79, 80}. p53-dependency was in fact confirmed and INPP5D was responsive to all the p53 activators used in the experiments performed and showed a more than additive transactivation in all the three combined treatments. However, it has also been shown that 5'-

phosphatase activity towards inositol is not equivalent to the PTEN function (a 3'-phosphatase) as PI(3,4)P₂ could still lead to the activation of the serine-threonine protein kinase AKT. Loss of INPP5D elevates AKT activation due to the increased of PI(3,4,5)P₃ production. Both the lipid phosphatases (PTEN and SHIP1) are instead crucial in controlling neutrophil chemotaxis through the regulation (with different receptor-regulated processes) of PI(3,4,5)P₃⁸¹. INPP5D expression is not usually observed in breast tissues but it seems restricted mostly to hematopoietic cells⁷⁹⁻⁸¹. KRT15 on the other hand is an intermediate filament type I protein responsible for the mechanical integrity of epithelial cells. KRT15, together with other keratins is a marker of epithelial differentiation, but particularly of squamous epithelia, where the p53-related protein p63 can be an important transcriptional regulator⁸². Its expression is regulated by E2 as well as nutlin in the experiments performed, and a synergistic up-regulation in DOX+E2 condition and an additive response in nutlin+E2 treatment was identified. Also, KRT15 expression is p53-dependent in the cell model used. KRT15 expression is also been observed in breast tissues and breast carcinomas. No evidences of a correlation with malignant status have been addressed, rather it has been suggested that KRT15 can be a neutral keratin whose expression can be detected also in luminal progenitors⁸³. KRT15 is often co-expressed along with KRT14 and KRT19^{82, 83}. The experiments also highlight the presence of other two keratins, named as KRT13 and KRT14, whose expression was up-regulated with a more than additive effect after combination of doxorubicin and estradiol pathway. In concert with KRT15 they might specifically have a biological impact.

It can be hypothesized that non-canonical p53 REs, consisting of ½ or ¾ sites, or ERα response element ½ sites can provide for moderate or weak responsiveness, but at the same time if they are close enough (within 500bp) they can provide a cooperative interaction between p53 and ERα. The occupancy analysis confirmed once again the direct role of p53. In fact, p53 bound directly to p53 related target sequences in the promoters of the TLR5, INPP5D and KRT15 genes. ERα occupancy was observed only at the level of KRT15 promoter gene, upon E2 single and combined treatment, supporting the evidence of a functional interaction between p53 and ER via *cis*-elements.

The absence of a detectable ERα occupancy upon combined treatments at the level of TLR5 and INPP5D promoter could be explained either by the lack of a *cis*-

mediated cooperation at the level of the promoter areas examined or with a temporal shift between transcription and transcription factors occupancy. Functional interactions with p53 could involve other members of the large superfamily of nuclear receptors including, for example, the glucocorticoid or androgen receptors, connected through a multi-protein mediator complex ³⁹. Furthermore, these initial studies suggest that for a subset of promoters, crosstalk with ER could be affected by other members of the p53 family, p63 and p73 ⁴⁰. p53 splice variants and various kinds of p53 stresses or ER activators might be expected to have different effects on the ER/p53 synergistic responses. The type of interaction that can occur between p53 and ER α might also differ between genes: ER α can in fact binds other transcription factors on a ERE-independent manner; and a non-genomic estrogen signaling pathways must also be considered. The role that ER β can exert in the modulation of the synergistic cooperation with p53 was not yet investigated and could also explain the lack of ER α occupancy at the level of the promoters chosen. Another important remark to consider is the resolution provided by immunoprecipitation assays. Dynamics of the complexes formed at the level of the promoter could not be easily detected using ChIP assays due to the fact that a temporal resolution is not provided. ChIP data do not provide kinetics and do not measure TF function at a given locus. The two proteins might not be present at the same time in the same complex after 10-hr treatment ⁸⁴. Since changes in chromatin around regulatory regions of transcribed genes can modulate the activity and cooperativity between transcription factors, chromatin status was analyzed at the TLR5, INNP5D, KRT15 genes (see Figure 7 and 8 –p101, p103- and Figure S3 –p109- in the *Lion et al* manuscript in Appendix). The same promoter regions analyzed for p53 and ER occupancy along with regions encompassing the transcription start site (TSS) were examined for changes in histone tail post-translational modifications associated with gene activation or repression using ChIP approaches. The results indicated that all three genes were in an active chromatin state even in the mock condition, which is consistent with their basal expression levels. The treatments had an impact on several histone marks, although there was not a specific signature apparent for the double treatment. (Detailed description of these results can be found in the Results and Discussion sections of the accompanying paper in Appendix).

While a positive transcriptional cooperation between ERs and p53 was described on a global scale by this study, the precise mechanisms underlying the synergistic interaction between these two transcription factors seem to be promoter dependent and need further investigation. ChIP experiments provided additional evidences for the contribution of p53 and ER α occupancy at target REs in the transcriptional cooperation. As the p53 response (doxorubicin-driven in this study) is mainly triggered through the binding to full-site p53-RE, the pursuit of non-canonical p53 REs associated in *cis*, in close proximity, with ERE sites was undertaken. The next step will involve the pursuit of the sources of interaction. A structure-function analysis will light up the mechanism behind the interaction between p53 and the estradiol pathway. ChIP data about KRT15 promoter are the first evidences that an in-*cis* p53/ER cooperation might occur and that involves a p53 half-site and half-site EREs, extending the previous findings beyond the FLT1 gene and model plasmid based systems³⁹. A structure-function analysis is necessary not only to understand the nature of the mechanisms through which these two proteins can interact but also to provide new insights about the functional processes that different mechanisms can exert. For this reason, putative identified regions of the TLR5, INPP5D and KRT15 promoters are now being cloned into a reporter plasmid that can allow to perform functional analysis. On this respect, the use of mutant ERs is planned in combination with wild-type p53 to clarify the nature and the mode of interaction between the two TFs, if it is really present. ER mutants (Figure D1) lacking either the DNA binding activity or the tethering activity or both functions will determine the type of interaction, if cooperativity is present, if the two TFs act independently and will help to dissect the general mechanism that might be different for different promoter regions.

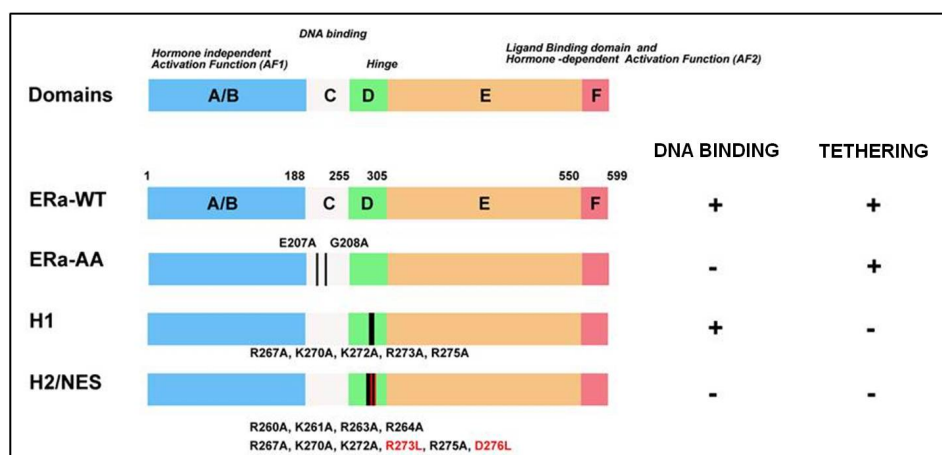


Figure D1. Scheme provided by K. Korach (unpublished results).

Conclusions and implications

Transcriptional programs within cells are continuously shaped by myriad signal transduction pathways and the architecture of promoter and enhancer sequences underlies the potential for such integration of multiple concomitant signals. Extensive transcriptional cooperation between ERs and p53 across the genome was found. Given the importance of activators of these two genes in cancer treatments, these findings provide opportunities for investigations of treatments involving many newly identified targets of synergy, although the mechanisms of synergy remain to be established. The findings are also likely relevant to understanding combined ER hormonal responses and any of the various stresses that can induce p53 as well as general biological and cancer implications.

It is still not clear, however, whether this mechanism is important for the selective regulation of the transcription of genes involved in specific biological processes that may play a role in the tumor physiology, such as progression or invasion. Possibly, the synergy might lead to increase aggressiveness or tumor metastasis (such as epithelial–mesenchymal transition, EMT) or alternatively influence inhibition of classical tumor hallmarks such as proliferation. A clear answer has not been identified yet and further studies are required. Although it is difficult to unambiguously predict phenotypic outcome, the relevance of potential interaction between p53 and estradiol pathway is extremely prominent. Despite the apparent random heterogeneity of functions that these genes exert, it cannot be discarded the possibility that their concomitant activation could result in new functions leading to yet unexplored biological consequences. Indeed there are some evidences that the expression or the function of some of the selected genes is impaired in breast cancer. For example, among the 16 candidate genes examined in depth, H19^{85, 86}, NOTCH1⁸⁷, SYNM⁸⁸, TLR5⁸⁹, and cadherins⁹⁰ are found either over-expressed or down-regulated in breast cancer. More generally many of these selected genes are somehow related to tumors. PML⁹¹, INPP5D⁹² and APC2⁹³ are thought, for instance, to be tumor suppressor genes. EPHA2, instead, has been reported to play a role in angiogenesis and tumor neovascularization as well as being a positive mediator of UV-induced and largely p53-independent apoptosis^{94, 95}. Several cadherins are usually down-regulated in tumors⁹⁰ whereas IGF2 is usually overexpressed in many types of cancers and thought to be an oncogene⁹⁶.

Finally, these findings suggest the opportunity to identify additional luminal breast tumor markers. Expression of some of the sixteen selected genes is usually weak or moderate in normal breast tissues (Human Protein Atlas, ⁹⁷). Understanding the functional roles that altered expression of those genes can play in different tissues could also aid in understanding the role that they may have in tumorigenesis. A systems biology approach could reveal the intricate scenario created by the combination of stress-dependent signaling (p53 pathway) and proliferative stimulus (estradiol pathway).

SECONDARY TASK

p53 FUNCTIONAL INTERACTIONS:
IMPACT OF COFACTORS AND
SMALL MOLECULES ASSAYED USING A
SIMPLIFIED YEAST-BASED SCREENING SYSTEM

INTRODUCTION

Inactivation of the p53 pathway in cancer frequently occurs through the expression of mutant p53 proteins. In tumors that retain wild type p53, the pathway can be altered at the level of upstream modulators, particularly the p53 negative regulators MDM2 and MDM4 (MDMX)⁵⁻¹¹. These two proteins play a crucial role during development, homeostasis, and the response to stress, through regulation of p53 activity and are very often overexpressed in many types of cancers that retain wild type p53⁹⁸⁻¹⁰⁰. They are structurally related proteins (Figure II.1), but with non-redundant functions. It is not surprising that MDM2 and MDMX are now appealing targets for cancer treatment. A combination of drugs that can inhibit both proteins at the same time represents a strategy for reactivating p53 in tumors that retain the wild type form⁹⁸⁻¹⁰⁰.

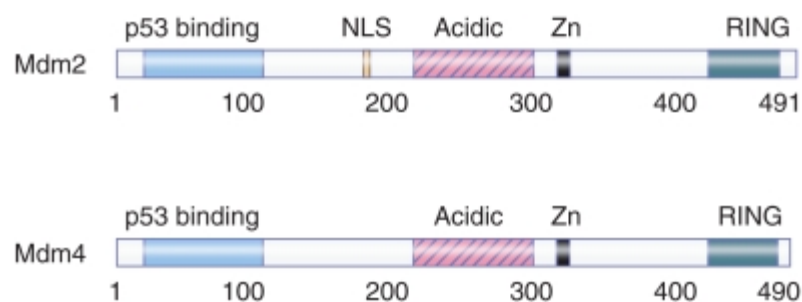


Figure II.1. Structure comparison of the MDM2 and MDMX proteins according to functional domains. Perry 2010

An intricate regulation and interaction, occurring also between MDM2 and MDMX, control the level and function of p53. The classical way through which MDM2 exerts its function is by binding the N-terminal domain of p53 and blocking the transcriptional activity, and by directly ubiquitinating p53, targeting it for the proteosomal degradation. MDM2 is indeed a RING-finger domain E3 ubiquitin ligase and it is thought to be the main p53 negative regulator. Furthermore, it also catalyzes the ubiquitination of MDMX and of itself. p53 controls its protein level and stability and therefore its activity, directly transcribing the MDM2 gene, thus generating a negative feedback loop^{7, 98-100}. MDMX expression, vice versa, is not directly upregulated by p53, although p53 occupancy in its promoter region has been reported¹⁰¹. MDMX inhibits p53 physically by binding to and masking the N-terminal domain (transactivation domain) but it does not have any appreciable ubiquitin ligase activity. Some evidences report a heterodimer formation between

MDM2 and MDMX that can prevent MDM2 autoubiquitination. MDMX binds MDM2 through its own RING-finger domain⁹⁸⁻¹⁰⁰.

DNA repair and cell cycle arrest (or apoptosis) must follow after DNA breaks, and it involves p53 activity. The affinity of p53 with its negative regulators MDM2 and MDM4 is drastically reduced when the p53 N-terminal region is phosphorylated by ATM. ATM plays its role after DNA damage and its activation (autophosphorylation) is also favored by 53BP1, as the acronym says - p53-binding protein 1-, another protein that directly binds p53. 53BP1 plays a crucial role in signaling the presence of DNA double strand breaks (DSBs)¹⁰³⁻¹⁰⁴. It is literally a sensor that detects DNA damages and lesions upstream of ATM (Figure II.2). Suppression of 53BP1 directly correlates with a decrease of ATM activation. 53BP1 participates in the organization of nuclear foci and contacts DSBs through its two tandem Tudor domains. These two domains were also reported to mediate interaction with p53 C-terminal domain¹⁰³. 53BP1 also binds p53 through its BRCT domains at the level of the DNA binding domain, acting as a co-activator, and therefore enhancing p53-mediated transcriptional activation. It is not surprising that 53BP1 can be expressed at low levels in several tumors¹⁰³⁻¹⁰⁴.

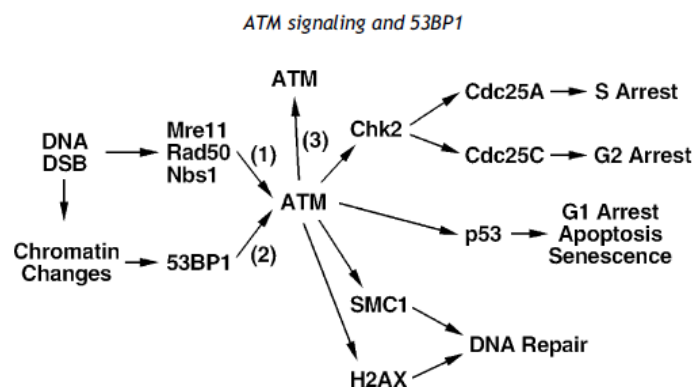


Figure II.2. The complexity of ATM signaling pathway. Zgheib et al., 2005

Yeast, as a model organism, can be easily used to investigate interactions between p53 and cofactors and to study the impact of small molecules. *Saccharomyces cerevisiae* can serve as an *in vivo* test tube to address the transactivation capacity of highly controlled p53 protein levels toward specific REs cloned upstream a quantitative reporter gene. In fact, the rheostatable control (*GAL1,10* promoter) of wild type p53 or mutant p53 cloned in a centromeric, selectable vector allows for the investigation of p53-transactivation capacity at

different protein levels. The yeast system displays advantages, including the absence of endogenous p53 and its coregulators (and consequently of p53-induced biological consequences). It is therefore a suitable system to study the factors that influence p53 function, including expression levels, mutations, cofactors and small molecules. It is also a very clean tool that allow unbiased screening opportunities for functional assays with luminescent reporters ¹⁰⁵.

In this work ¹⁰⁵ a highly defined (small-volume format) dual luciferase yeast-based functional assay was set up to investigate the impact of small molecules on p53 transactivation potential or on the functional interaction between p53 and cofactors. A specific p53 response element was placed upstream of the minimal promoter of the firefly luminescent reporter whereas the renilla luminescent report was under the control of a minimal promoter to assess sensitivity and robustness of the assay system. These yeast strains were also enhanced for chemical uptake modifying the ABC-transporters in yeast. This small-volume yeast screening system provides for rapid assessment of p53 transactivation potential and can be applied to high-throughput screening of chemicals toward a matrix of factors that can influence p53 protein levels (including small molecules), nature of the p53 REs, and level of p53-interacting proteins.

Once the potential of the yeast-based system was established, the ability of the dual luciferase assay system was examined to discriminate the functional interaction of wild type and mutant p53 when co-expressed with MDM2 or 53BP1 (lacking the N-terminal portion of 960 amino acids) and the effects of RITA (reactivation of p53 and induction of tumor cell apoptosis) and nutlin-3a (nutlin). Details are provided in the attached paper. Briefly, it appeared that co-expression of MDM2 can lead to reduced p53 transactivation at low levels of p53 protein expression, and that nutlin and RITA both relieve the MDM2-dependent inhibition of wild type p53 transactivation function similarly to what is usually observed in mammalian cells. The co-expression of 53BP1 with p53 also leads to a reduction in p53-dependent transactivation, and only RITA partially impacts p53/53BP1 functional interactions. Nutlin had no effect on the p53-53BP1 interaction. The mode of action of nutlin has been extensively described previously in the results and discussion sessions. The small molecule RITA induces p53-dependent apoptosis through p53 accumulation and subsequent activation in tumor cell lines. RITA binds the p53 N-terminus and reduces p53/MDM2 interaction. RITA and

nutlin target p53/MDM2 interaction but in a different way and they seem also to lead to a different transcriptional response ¹⁰⁶. The experiments were also extended to the p53 cofactor MDM4 as well as to the full length 53BP1 using the small-volume luciferase assay. MDM4 inhibited p53 function but both nutlin and RITA did not relieve such effect. Similarly to the truncated construct, full length 53BP1 also inhibited p53-mediated transactivation contrary to the expectation from mammalian cells' studies. Taken collectively, the yeast-based assay represents a versatile tool to study p53 interactions with cofactors and the impact of small molecules targeting those interactions.

MATERIALS AND METHODS

A more extensive description of the Materials and Methods can be also found in the manuscript enclosed (p142).

Yeast strains

Isogenic yeast strains (yLFM) containing different human p53 response element sequences cloned upstream the reporter Firefly luciferase gene were tested. yLFM PUMA/yRFM I2 yeast strain, carrying the PUMA response element upstream the Firefly luciferase gene and the Renilla ORF under the control of the minimal CYC1 promoter, was also used.

Luciferase assay in yeast

Traditional assays were performed starting from a 2 ml overnight (O/N) cultures of the appropriate yeast strain cultured in synthetic selective medium containing 2% raffinose as carbon source and the desired amount of galactose (see Results section) for the induction of the *GAL1,10* promoter that drives p53 expression. Luciferase activity was determined either using extraction of soluble proteins by mechanical lysis (glass beads, Sigma-Aldrich) and centrifugation, or permeabilizing cells using Passive Lysis Buffer 1x (PLB 1x) in agitation for 15 min at room temperature.

The newly developed miniaturized assay was performed starting from a 100 µl overnight (O/N) culture (in a 96-well plate) cultures of the appropriate yeast strain cultured in synthetic selective medium containing 2% raffinose and the desired amount of galactose (see Results section) for the induction of the *GAL1,10* promoter. Luciferase activity was determined permeabilizing cells using Passive Lysis Buffer 2x (PLB 2x) in agitation for 15 min at room temperature.

Time course experiments were performed starting from a 2 ml O/N culture in synthetic selective medium containing 2% dextrose (to prevent *GAL1,10* activation) and then switching for 6 hours to a culture containing synthetic selective medium (with 2% raffinose) and the desired amount of galactose.

Luciferase assay was conducted in a white 384-well plate using 10µl of Bright Glo reagent (Promega, Milan Italy). Optical density at 600nm (OD) was measured and used as normalizing factor. The dual luciferase assay was developed

similarly, except for the use of 10 μ l of the Firefly substrate followed by additional 10 μ l of Stop&Glow Renilla substrate to measure renilla activity.

Yeast transformants and GAP repair technique

5ml O/N yeast cultures were cotransformed with the linearized targeting pTSA_d plasmid and the gene ORF of interest or just transformed with the appropriate plasmids, using lithium acetate transformation protocol (see manuscript for further details). Transformants were then selected on a synthetic selective medium plate.

Drug treatment

2 ml O/N culture in synthetic selective medium containing 2% dextrose and a switch for 16 hours to 100 μ l of synthetic selective medium (with 2% raffinose), the desired amount of galactose and the desired drug was conducted (in a 96-well plate). RITA and Nutlin were prepared in DMSO that was included as control.

Sensitivity to cycloheximide was performed similarly with the only exception that serial dilutions (1:5) were made before transferring yeast cells to plates containing synthetic medium (SD) with different concentrations of cycloheximide (0.005, 0.01, 0.015, 0.02 ng/ μ l) using a 48-pin replicator. A rich (YPDA) and an SD control plates were spotted for comparison. Plates were incubated for two days at 30° C.

RESULTS and DISCUSSION

Small-volume, dual-luciferase assay in yeast

The yeast-based assay has been improved in efficiency and miniaturized (materials, methods, and interpretation of results obtained are extensively described in the paper attached, p141). My personal contributions were to investigate a p53 induction-time course and to perform the comparison between three different dual-luciferase yeast-based assays:

- traditional assay I (using glass beads)
- traditional assay II (using Passive Lysis Buffer 1x, PLB 1x)
- newly developed miniaturized assay (using PLB 2x)

Briefly, the finely-tuned inducible *GAL1,10* promoter (“rheostatable”) was investigated to address transcriptional response on PUMA response element that is dependent upon p53 protein levels. 4 time points (0, 6, 12 and 24 h) and two galactose concentrations (0.032% and 0.128%) were used to achieve respectively a moderate and high p53 protein levels. T=0h was in 2% dextrose that inhibits *GAL1,10* promoter function (Figure II.3). This provides robust measurement of p53-dependent transactivation. In particular, the ability of firefly and renilla luminescent proteins was shown to serve as reporters for p53 transactivation.

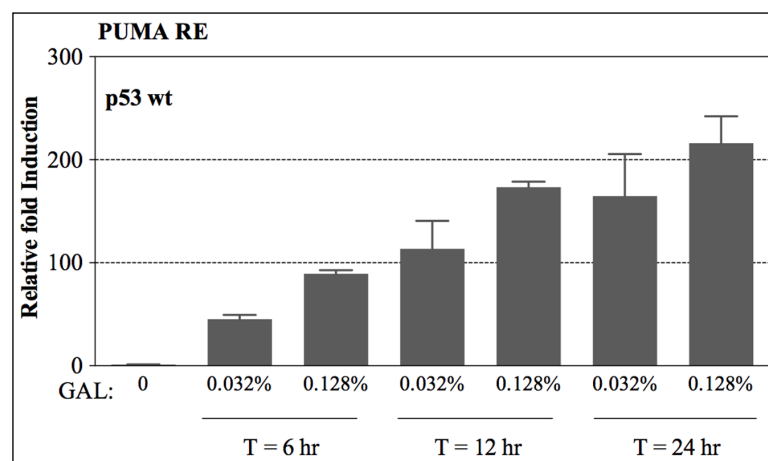


Figure II.3. p53 induction-time course. Dual luciferase reporter assay with a strain expressing wild type p53 and containing the Firefly luciferase as p53 reporter gene (PUMA RE) and the renilla luciferase as constitutive reporter. Presented are the average and standard error of the Firefly luciferase activities normalized for renilla and compared to empty vector at various time points after shifting 100 ml yeast cultures to galactose-containing media in the 96-well plate format.

The previous yeast assay system based on the 2 ml O/N cultures and soluble protein extraction to quantify luciferase activity limited the experimental opportunities. An alternative system to protein extraction was found out: cells of both the haploid and diploid strains could be permeabilized for uptake of luciferase substrate if resuspended in PLB. Also, results coming from a 2ml O/N culture or from a small culture volume (100 μ l, miniaturized system) were comparable. The transactivation potential was investigated both for wild type p53 and the Δ 368 deletion mutant lacking the regulatory domain in the p53 carboxy terminus (C-ter). All these data support the use of luminescent reporters, permeabilized cells, and small volumes to assess p53 transcriptional functions as well as providing a high-throughput format (Figure II.4 & II.5).

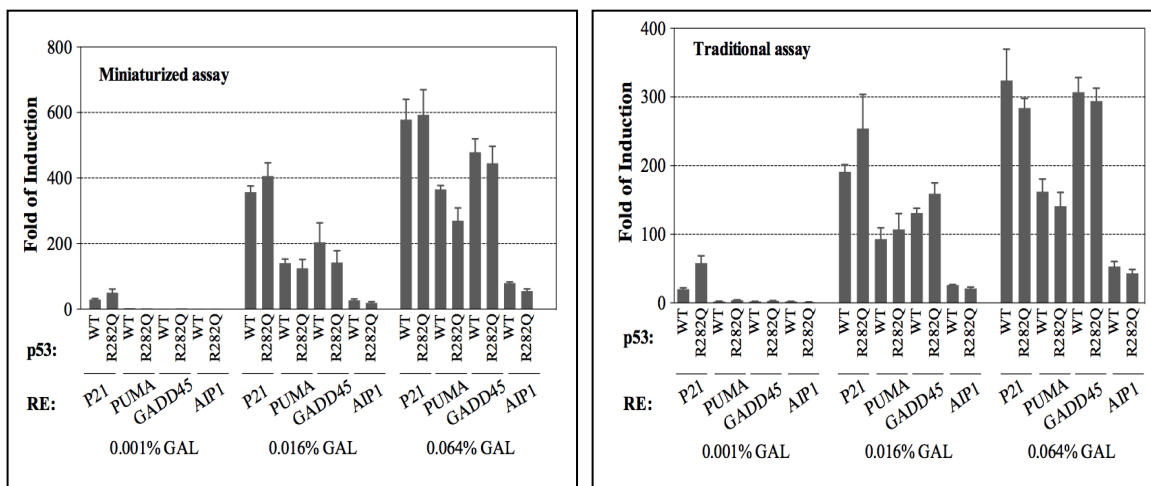


Figure II.4. Generation of a small volume format for p53 functional assays. Relative transactivation capacity of WT and the R282Q mutant p53 have been compared towards four different p53 REs obtained with the traditional assay based on 2ml liquid cultures in individual tubes (A) or with the miniaturized assay format based on 100 μ l cultures prepared directly in 96-well plates (B). p53 proteins were induced at different levels by varying the amount of galactose (indicated below the chart). A strong (p21), two moderate (PUMA, GADD45) and a weak p53 RE (AIP1) were compared.

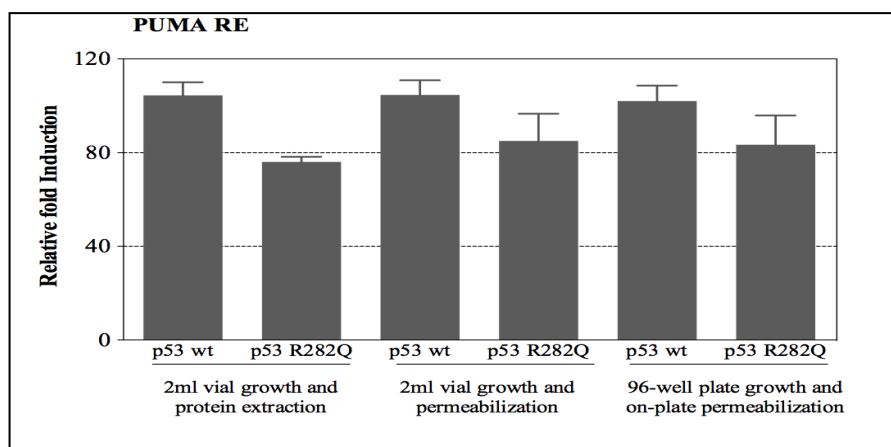


Figure II.5. Comparison of relative p53-dependent transactivation in the different assay formats. Relative transactivation capacities of WT p53 and the R282Q mutant in the “2 ml vial” experimental set-ups were measured using either protein extraction or permeabilization. Direct permeabilization of cells was conducted in a 384-well format following transfer from a 96-well growth plate that was used for cell growth. Experiments were conducted using 0.032% galactose inducer.

Genetic modifications at the ABC transporter system

Genetic modifications at the ABC transporter system could improve drug accumulation in these reporter strains and could allow the study of the impact of small molecules on p53 transactivation and interaction with other cofactor. The disruption of the cassette for the PDR (pleiotropic drug resistance) genes was the technique adopted to directly affect the ABC transporter system. Materials, methods, and interpretation of results obtained are described in the supporting information, p157. My personal contribution was the examination of cycloheximide toxicity on the ABC mutants to further investigate if drug uptake (and therefore the toxicity) was actually enhanced in the double mutant (pdr1, pdr5 mutant). Results confirmed that both PDR1 and PDR5 disruption rendered the cells more sensitive to the drug. The pdr5 mutant was the most sensitive although, surprisingly, the double mutant pdr1, pdr5 exhibited a slightly reduced sensitivity compared to pdr5 (Figure II.6). Based on these observations, all the modifications of the yeast-based assay were performed using the pdr5 mutant.

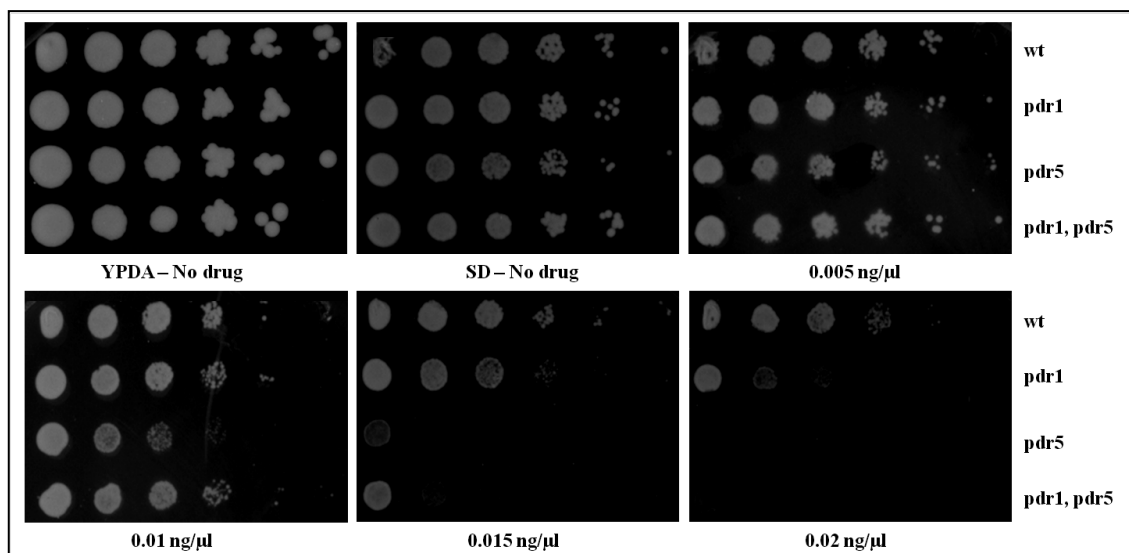


Figure II.6. Impact of genetic modifications at the ABC transporter system on cell sensitivity to cycloheximide.

Based on the experiments described by Stepanov *et. al.*, 2008, cycloheximide treatment was used to evaluate whether the disruption of *PDR1* and replacement with a *PDR1*-repressor construct, the disruption of *PDR5*, or the combined modifications would result in enhanced toxicity in the strain background. Cells from the indicated strains were resuspended in sterile water and transferred to a 96-well plate. Serial dilutions (1:5) were prepared and cells were transferred to plates containing synthetic medium (SD) with different concentrations of cycloheximide using a 48-pin replicator. A rich (YPDA) and an SD control plates were also spotted for comparison. Plates were incubated for two days at 30° C.

Gap repair cloning of MDM4 and 53BP1 genes in yeast

Gap repair is considered a simple and useful *in vivo* cloning approach in yeast. It is based on the advantage of using homologous sequences that can recombine to restore the integrity of a linearized targeting plasmid resulting at the same time in the incorporation of the selected sequence. In fact, flanking short homologous sequences are added to the selected sequence via PCR and the unpurified PCR product is cotransformed in yeast together with the linearized plasmid. The gap repair process is RAD52 dependent.

Gap repair technique was used to clone MDM4 and 53BP1 genes in the yeast expression vector pTSA_d, that is based on the centromeric pRS314, contains the *TRP1* selection marker and the transcription of the cloned cDNA is under the control of a constitutive promoter (pADH1).

Impact of nutlin and RITA in the functional interactions between wild type p53 and MDM4

In this work ¹⁰⁵, the interaction between p53 and its negative regulator MDM2 was extensively investigated. Similarly to what happens in mammalian cells, it clearly appeared that MDM2 can reduced p53 transactivation also in yeast, and that both nutlin and RITA relieve the MDM2-dependent inhibition of wild type p53 transactivation function.

Aside from the paper, I started to examine the functional interaction between p53 and the other negative regulator MDM4. The conditions utilized were similar to the ones used in the paper attached. p53 expression was therefore modulated varying the amount of galactose (0.008% or 0.024% galactose; p53 was cloned in a pLLS89 vector, containing the LEU2 selectable marker) while MDM4 expression was maintained at constitutive level. Dual luciferase assay was performed on the yeast strains carrying the PUMA response element (yLFM PUMA/yRFM I2). The effect of nutlin (20 μ M) and RITA (1 μ M) was also evaluated. A negative impact on p53 transactivation was confirmed when p53 protein was co-expressed (at different levels) with MDM4 (Figure II.7A). Nutlin treatment does not seem to have an impact on the inhibitory effect of MDM4, as previously shown in mammalian cells ⁹⁸. RITA, as already shown in the paper attached, has a severe negative impact on the firefly reporter activity that might lead to a misinterpretation of the results. The initial results suggest that RITA could not restore the negative impact of MDM4 on the p53 transactivation at the dose used (Figure II.7B).

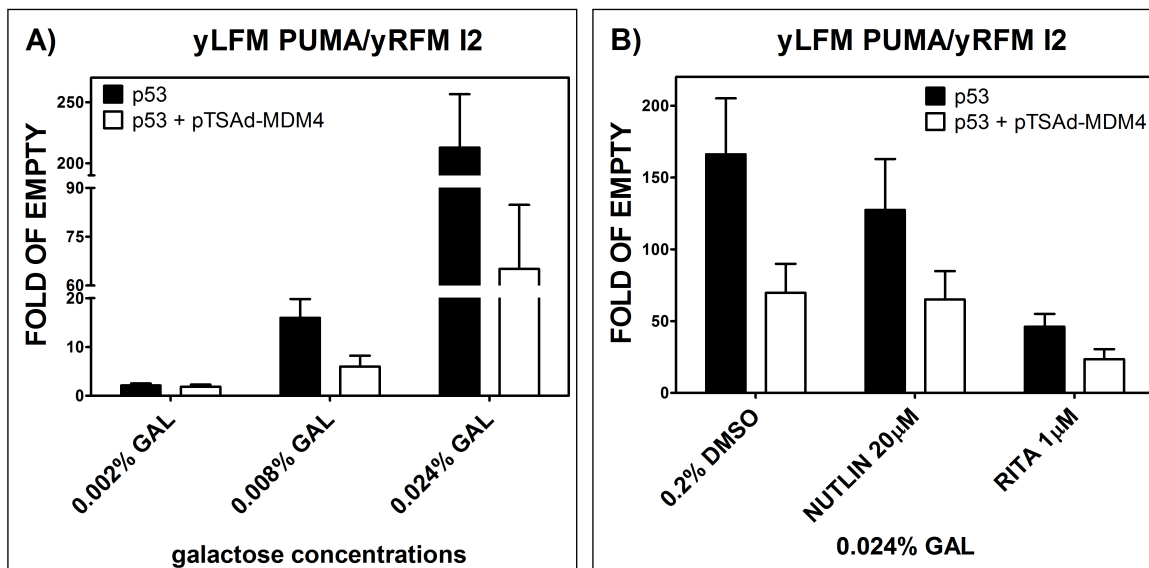


Figure II.7. Functional interactions between wild type p53 and MDM4 and the impact of nutlin and RITA. Dual-luciferase assay was performed on yeast transformed with an empty vector or with a p53-expression plasmid alone or in combination with an MDM4 expression vector. Results are plotted as average fold of reporter induction, relative to the empty vector, and standard errors of four biological repeats. A) Three galactose concentrations were used to modulate the expression of p53. B) The impact of nutlin and RITA was examined using 0.024% galactose as p53-inducer in a reporter strain containing the moderate PUMA p53 RE.

Functional interaction between p53 and 53BP1

Data obtained in this work show that the co-expression of 53BP1 (lacking the N-terminal region) with p53 also leads to a reduction in p53-dependent transactivation, and only RITA partially impacts p53/53BP1 functional interactions. Nutlin had no effect on the p53-53BP1 interaction. In mammalian cells the interaction between 53BP1 and p53 has been shown to have a positive impact on p53 transactivation activity. Hence, the results of the yeast-based assays appear to be in contrast with the expectation from mammalian cells. Since the 53BP1 expression plasmid that was used in the initial study was not full-length, to investigate whether the unexpected results were due to the absence of the N-terminal region of 53BP1 protein, a new expression plasmid was prepared containing the entire 53BP1 gene cloned in a pTSAAd vector and the pLLS89 plasmid was used to express p53. A negative impact on p53 transactivation was also observed, confirming the results obtained previously (Figure II.8). The impact of 53BP1 was slight, particularly at higher p53 expression levels. To exclude the possibility of a target-specific effect, the impact on five yLFM reporter strains was also investigated to address the control of different p53-dependent promoters.

These strains do not carry the renilla reporter gene (RE::firefly). All the data were therefore normalized using OD_{600nm} values only. Two time points were chosen (4 or 24 hours) with two different concentrations of galactose (0.008% and 0.032%). The results obtained confirmed again that no stimulatory effect of 53BP1 can be detected in yeast using this assay, and for some of the reporters an inhibitory effect of 53BP1 was observed (53BP1-effect is RE-dependent). Values obtained after 24hr from the galactose switching are lower in absolute value, due to a higher OD_{600nm} number that is not linearly correlated to firefly activity (Figure II.9).

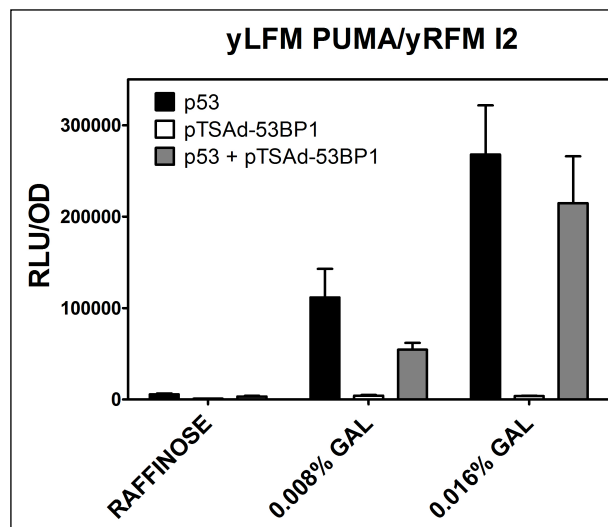


Figure II.8. Functional interactions between wild type p53 and 53BP1. Dual-luciferase assay was performed on yeast transformed with a p53-expression plasmid alone and/or in combination with a 53BP1 expression vector. Results are plotted as average of relative light unit (RLU), normalized with OD_{600nm}, and standard errors of four biological repeats. Two galactose concentrations (0.008% and 0.016%) were used to modulate the expression of p53 using a reporter strain containing the moderate PUMA p53 RE.

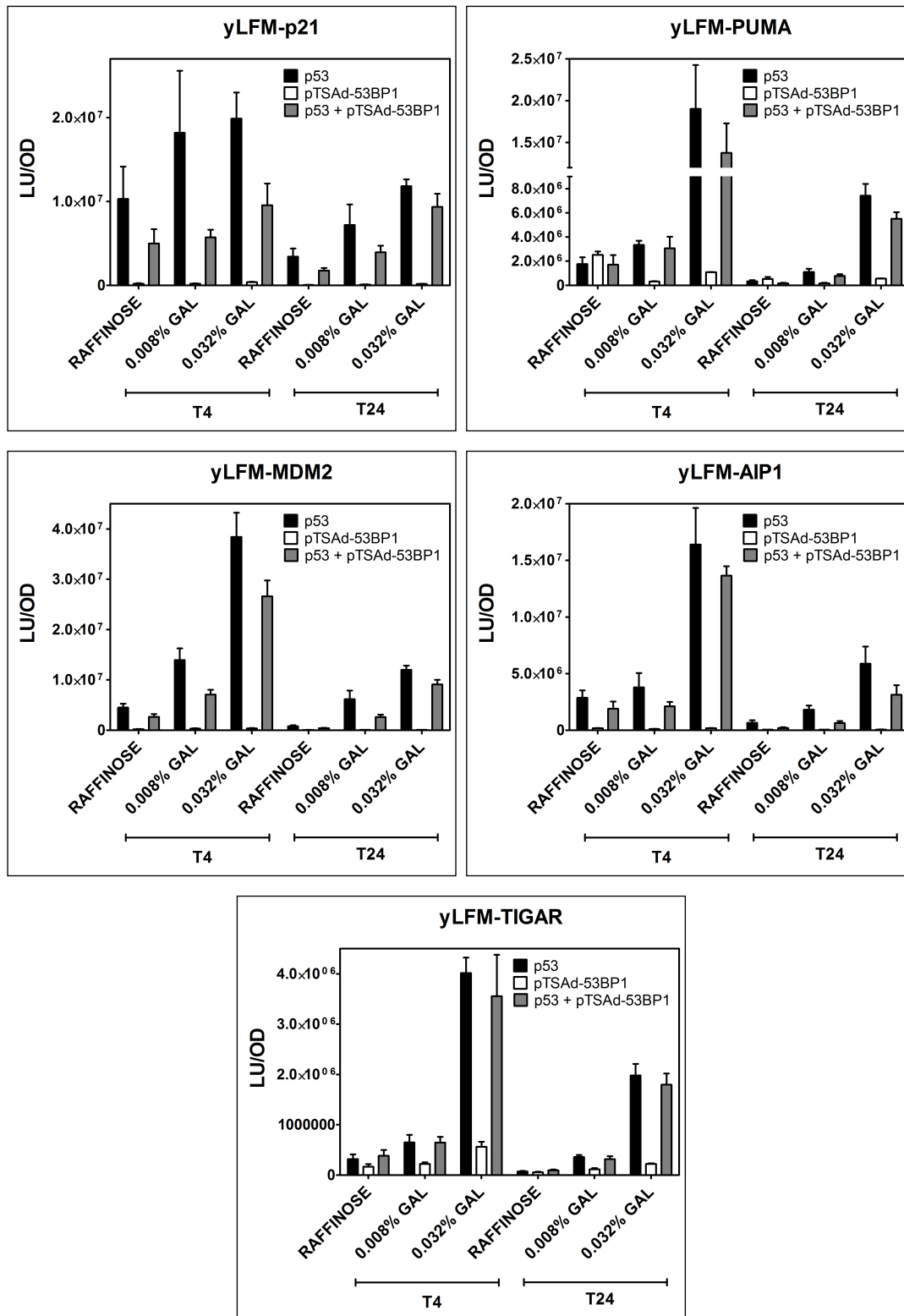


Figure II.9. Functional interactions between wild type p53 and 53BP1 on different p53-response promoters. Dual-luciferase assay was performed on yeast transformed with a p53-expression plasmid alone and/or in combination with a 53BP1 expression vector. Results are plotted as average of light unit (RLU), normalized with OD_{600nm}, and standard errors of four biological repeats. Two galactose concentrations (0.008% and 0.032%) were used to modulate the expression of p53 on five different yLFM reporter strains (p21, PUMA, TIGAR, AIP1, MDM2).

REFERENCES

1. Pan Y, Tsai C-J, Ma B, Nussinov R. Mechanisms of transcription factor selectivity. *Trends in Genetics* 2010; 26:75-83.
2. Georges AB, Benayoun BA, Caburet S, and Veiti RA. Generic binding sites, generic DNA-binding domains: where does specific promoter recognition come from? *The FASEB Journal* 2010; 24: 346-356.
3. In˜iguez-Lluhi´ JA and Pearce D. A Common Motif within the Negative Regulatory Regions of Multiple Factors Inhibits Their Transcriptional Synergy. *Molecular and cellular biology*, 2000, 20: 6040–6050.
4. Espinosa JM. Mechanisms of regulatory diversity within the p53 transcriptional network. *Oncogene* 2008; 27:4013-23.
5. Bode AM, Dong Z. Post-translational modification of p53 in tumorigenesis. *Nat Rev Cancer* 2004; 4:793-805.
6. Levine AJ, Oren M. The first 30 years of p53: growing ever more complex. *Nat Rev Cancer* 2009; 9:749-58.
7. Vousden KH, Prives C. Blinded by the Light: The Growing Complexity of p53. *Cell* 2009; 137:413-31.
8. Menendez D, Inga A, Resnick MA. Potentiating the p53 network. *Discov Med* 2010; 10:94-100.
9. Inga A, Jordan JJ, Menendez D, De Sanctis V and Resnick MA. The p53 Master Regulator and Rules of Engagement with Target Sequences. *Handbook of Cell Signalling* 2010, chapter 265: 2205-2216.
10. Wang B, Xiao Z and Ren EC. Redefining the p53 response element. *Proc Natl Acad Sci U S A*. 2009;106(34):14373-8.
11. Menendez D, Inga A, Resnick MA. The expanding universe of p53 targets. *Nat Rev Cancer* 2009; 9:724-37.
12. Brady CA, Jiang D, Mello SS, Johnson TM, Jarvis LA, Kozak MM, Kenzelmann Broz D, Basak S, Park EJ, McLaughlin ME, Karnezis AN and Attardi LD. Distinct p53 transcriptional programs dictate acute DNA-damage responses and tumor suppression. *Cell*. 2011; 145(4):571-83.
13. Xue B, Brown CJ, Dunker AK and Uversky VN. Intrinsically disordered regions of p53 family are highly diversified in evolution. *Biochim Biophys Acta*. 2013;1834(4):725-38.

14. Jack T. Zilfou, William H. Hoffman, Michael Sank, Donna L. George, and Maureen Murphy. The Corepressor mSin3a Interacts with the Proline-Rich Domain of p53 and Protects p53 from Proteasome-Mediated Degradation. *Mol Cell Biol.* 2001; 21(12): 3974–3985
15. Bansal N, Kadamb R, Mittal S, Vig L, Sharma R, Dwarakanath BS and Saluja D. Tumor suppressor protein p53 recruits human Sin3B/HDAC1 complex for down-regulation of its target promoters in response to genotoxic stress. *PLoS One.* 2011;6(10):e26156.
16. Deroo BJ, Korach KS. Estrogen receptors and human disease. *The Journal of Clinical Investigation* 2006; 116:561-70.
17. Heldring N, Pike A, Andersson S, Matthews J, Cheng G, Hartman J, et al. Estrogen Receptors: How Do They Signal and What Are Their Targets. *Physiological Reviews* 2007; 87:905-31.
18. Dahlman-Wright K, Cavailles V, Fuqua SA, Jordan VC, Katzenellenbogen JA, Korach KS, et al. International Union of Pharmacology. LXIV. Estrogen Receptors. *Pharmacological Reviews* 2006; 58:773-81.
19. Carpenter KD and Korach KS. Potential Biological Functions Emerging from the Different Estrogen Receptors. *Ann. N.Y. Acad. Sci* 2006; 1092:361-363.
20. Bolli A and Marino M. Current and future development of estrogen receptor ligands: applications in estrogen-related cancers. *Recent Pat Endocr Metab Immune Drug Discov.* 2011;5(3):210-29.
21. Klinge CM. Estrogen receptor interaction with estrogen response elements. *Nucleic Acids Res.* 2001; 29(14):2905-19.
22. Gruber CJ, Gruber DM, Gruber IML, Wieser F, Huber JC. Anatomy of the estrogen response element. *Trends in Endocrinology & Metabolism* 2004; 15:73-8.
23. Carroll JS, Brown M. Estrogen Receptor Target Gene: An Evolving Concept. *Molecular Endocrinology* 2006; 20:1707-14.
24. Konduri SD, Medisetty R, Liu W, Kaipparettu BA, Srivastava P, Brauch H, et al. Mechanisms of estrogen receptor antagonism toward p53 and its implications in breast cancer therapeutic response and stem cell regulation. *Proceedings of the National Academy of Sciences* 2010; 107:15081-6.
25. Liu W, Ip M, Podgorsak M, Das G. Disruption of estrogen receptor α -p53 interaction in breast tumors: a novel mechanism underlying the anti-tumor

- effect of radiation therapy. *Breast Cancer Research and Treatment* 2009; 115:43-50.
26. Liu W, Konduri SD, Bansal S, Nayak BK, Rajasekaran SA, Karuppaiyl SM, et al. Estrogen Receptor- α Binds p53 Tumor Suppressor Protein Directly and Represses Its Function. *Journal of Biological Chemistry* 2006; 281:9837-40.
 27. Sayeed A, Konduri SD, Liu W, Bansal S, Li F, Das GM. Estrogen Receptor α Inhibits p53-Mediated Transcriptional Repression: Implications for the Regulation of Apoptosis. *Cancer Research* 2007; 67:7746-55.
 28. Liu G, Schwartz JA, Brooks SC. p53 Down-Regulates ER-Responsive Genes by Interfering with the Binding of ER to ERE. *Biochemical and Biophysical Research Communications* 1999; 264:359-64.
 29. Yu C-L, Driggers P, Barrera-Hernandez G, Nunez SB, Segars JH, Cheng S-y. The Tumor Suppressor p53 Is a Negative Regulator of Estrogen Receptor Signaling Pathways. *Biochemical and Biophysical Research Communications* 1997; 239:617-20.
 30. Fernández-Cuesta L, Anaganti S, Hainaut P, Olivier M. Estrogen levels act as a rheostat on p53 levels and modulate p53-dependent responses in breast cancer cell lines. *Breast Cancer Research and Treatment* 2011; 125:35-42.
 31. Qin C, Nguyen T, Stewart J, Samudio I, Burghardt R and Safe S. Estrogen up-regulation of p53 gene expression in MCF-7 breast cancer cells is mediated by calmodulin kinase IV-dependent activation of a nuclear factor kappaB/CCAAT-binding transcription factor-1 complex. *Mol Endocrinol.* 2002;16(8):1793-809.
 32. Angeloni SV, Martin MB, Garcia-Morales P, Castro-Galache MD, Ferragut JA, Saceda M. Regulation of estrogen receptor-alpha expression by the tumor suppressor gene p53 in MCF-7 cells. *Journal of Endocrinology* 2004; 180:497-504.
 33. Miller LD, Smeds J, George J, Vega VB, Vergara L, Ploner A, et al. An expression signature for p53 status in human breast cancer predicts mutation transcriptional effects, and patient survival. *Proceedings of the National Academy of Sciences of the United States of America* 2005; 102:13550-5.

34. Olivier M, Langerød A, Carrieri P, Bergh J, Klaar S, Eyfjord J, et al. The clinical value of somatic TP53 gene mutations in 1,794 patients with breast cancer. *Clinical Cancer Research* 2006; 12:1157-67.
35. Duong V, Boule N, Daujat S, Chauvet J, Bonnet S, Neel H, et al. Differential Regulation of Estrogen Receptor α Turnover and Transactivation by Mdm2 and Stress-Inducing Agents. *Cancer Research* 2007; 67:5513-21.
36. Kim K, Burghardt R, Barhoumi R, Lee S-o, Liu X, Safe S. MDM2 regulates estrogen receptor α and estrogen responsiveness in breast cancer cells. *Journal of Molecular Endocrinology* 2011; 46:67-79.
37. Liu G, Schwartz JA and Brooks SC. Estrogen receptor protects p53 from deactivation by human double minute-2. *Cancer Res.* 2000 Apr 1;60(7):1810-4.
38. Ciribilli Y, Andreotti V, Menendez D, Langen J-S, Schoenfelder G, Resnick MA, et al. The Coordinated P53 and Estrogen Receptor Cis-Regulation at an FLT1 Promoter SNP Is Specific to Genotoxic Stress and Estrogenic Compound. *PLoS ONE* 2010; 5:e10236.
39. Menendez D, Inga A, Snipe J, Krysiak O, Schönfelder G, Resnick MA. A Single-Nucleotide Polymorphism in a Half-Binding Site Creates p53 and Estrogen Receptor Control of Vascular Endothelial Growth Factor Receptor 1. *Molecular and Cellular Biology* 2007; 27:2590-600.
40. Menendez D, Inga A, Resnick MA. Estrogen receptor acting in cis enhances WT and mutant p53 transactivation at canonical and non-canonical p53 target sequences. *Proceedings of the National Academy of Sciences* 2010; 107:1500-5.
41. Menendez D, Krysiak O, Inga A, Krysiak B, Resnick MA, Schönfelder G. A SNP in the flt-1 promoter integrates the VEGF system into the p53 transcriptional network. *Proceedings of the National Academy of Sciences of the United States of America* 2006; 103:1406-11.
42. Troester MA, Hoadley KA, Parker JS, Perou CM. Prediction of toxicant-specific gene expression signatures after chemotherapeutic treatment of breast cell lines. *Environ Health Perspect* 2004; 112:1607-13.
43. Barrett JR (2004) Template for Toxicants: Gene Expression Varies by Cell Type. *Environmental Health Perspectives*, 112(16): A944

44. Cheek CF, Verma CS, Baselga J, Lane DP. Translating p53 into the clinic. *Nat Rev Clin Oncol* 2011; 8:25-37.
45. Huang DW, Sherman BT, Lempicki RA. Systematic and integrative analysis of large gene lists using DAVID bioinformatics resources. *Nat Protocols* 2008; 4:44-57.
46. Staffler A, et al. Heterozygous SOX9 Mutations Allowing for Residual DNA-binding and Transcriptional Activation Lead to the Acampomelic Variant of Campomelic Dysplasia. *Human Mutation* 2010. 31(6):E1436-E1444.
47. Yatsenko AN, et al. The Power of Mouse Genetics to Study Spermatogenesis. *Journal of Andrology* 2010. 31(1):34-44.
48. Takano T, Yamada H. Trefoil factor 3 (TFF3): a promising indicator for diagnosing thyroid follicular carcinoma. *Endocrine Journal*. 2009, 56(1):9-16
49. Vullo D, Nishimori I, Innocenti A, Scozzafava A and Supuran CT. Carbonic anhydrase activators: An activation study of the human mitochondrial isoforms VA and VB with amino acids and amines. *Bioorganic & Medicinal Chemistry Letters*, 2006, 17(5):1336-1340
50. Li RW, Gasbarre LC. A temporal shift in regulatory networks and pathways in the bovine small intestine during *Cooperia oncophora* infection. *International Journal for Parasitology – Elsevier*. 2009, 39(7):813-24
51. Ferrando AA. The role of NOTCH1 signaling in T-ALL. *Hematology*. 2009, 353-61
52. Pascual A, Hidalgo-Figueroa M, Gómez-Díaz R, López-Barneo J. GDNF and protection of adult central catecholaminergic neurons. *Journal of Molecular Endocrinology*. 2011, 46(3):R83-92
53. Kim SB, Chae GW, Lee J, Park J, Tak H, Chung JH, et al. Park TG, Ahn JK, Joe CO. Activated Notch1 interacts with p53 to inhibit its phosphorylation and transactivation. *Cell Death & Differentiation*. 2007, 14(5):982-91.
54. Zhang L, Zhan Q, Zhan S, Kashanchi F, Fornace AJ Jr, Seth P, et al. Helman LJ. p53 regulates human insulin-like growth factor II gene expression through active P4 promoter in rhabdomyosarcoma cells. *DNA and Cell Biology*. 1998, 17(2):125-31

55. Kurki S, Latonen L, Laiho M. Cellular stress and DNA damage invoke temporally distinct Mdm2, p53 and PML complexes and damage-specific nuclear relocalization. *Journal of Cell Science*. 2003, 16(Pt 19):3917-25
56. Jin YJ, Wang J, Qiao C, Hei TK, Brandt-Rauf PW and Yin Y. A novel mechanism for p53 to regulate its target gene ECK in signaling apoptosis. *Molecular Cancer Research*, 2006, 4(10): 769-778
57. Hao L, Rizzo P, Osipo C, Pannuti A, Wyatt D, Cheung LW, et al. Sonenshein G, Osborne BA, Miele L. Notch-1 activates estrogen receptor-alpha-dependent transcription via IKKalpha in breast cancer cells. *Oncogene* 2010, 29(2):201-13
58. Carroll JS, Meyer CA, Song J, Li W, Geistlinger TR, Eeckhoutte J, et al. Brodsky AS, Keeton EK, Fertuck KC, Hall GF, Wang Q, Bekiranov S, Sementchenko V, Fox EA, Silver PA, Gingeras TR, Liu XS, Brown M. Genome-wide analysis of estrogen receptor binding sites. *Nature Genetics*. 2006, 38(11):1289-97
59. Lin CY, Vega VB, Thomsen JS, Zhang T, Kong SL, Xie M, et al. Chiu KP, Lipovich L, Barnett DH, Stossi F, Yeo A, George J, Kuznetsov VA, Lee YK, Charn TH, Palanisamy N, Miller LD, Cheung E, Katzenellenbogen BS, Ruan Y, Bourque G, Wei CL, Liu ET. Whole-genome cartography of estrogen receptor alpha binding sites. *PLoS Genetics*. 2007, 3(6):e87.
60. Reeve AE. Role of genomic imprinting in Wilms' tumour and overgrowth disorders. *Medical and Pediatric Oncology*. 1996, 27(5):470-5.
61. Muto A, Iida A, Satoh S and Watanabe S. The group E Sox genes Sox8 and Sox9 are regulated by Notch signaling and are required for Müller glial cell development in mouse retina. *Experimental Eye Research*, 2009, 89(4): 549-558
62. Mead TJ and Yutzey KE. Notch Pathway Regulation of Chondrocyte Differentiation and Proliferation during Appendicular and Axial Skeleton Development. *Proceedings of the National Academy of Sciences*, 2009 106(34):14420-5
63. Brummelkamp TR, Bernards R, Agami R. A system for stable expression of short interfering RNAs in mammalian cells. *Science* 2002; 296:550-3.

64. Thomas-Chollier M, Defrance M, Medina-Rivera A, Sand O, Herrmann C, Thieffry D, et al. RSAT 2011: regulatory sequence analysis tools. *Nucleic Acids Research* 2011; 39:W86-W91
65. Yue W, Wang JP, Li Y, Fan P, Liu G, Zhang N, et al. Effects of estrogen on breast cancer development: Role of estrogen receptor independent mechanisms. *International Journal of Cancer* 2010, 127: 1748-1757
66. Yager JD and Davidson NE. Estrogen carcinogenesis in breast cancer. *The New England Journal of Medicine* 2006, 354: 270-282
67. Ingle JN. Estrogen as therapy for breast cancer. *Breast Cancer Research* 2002, 4: 133-136.
68. Munster PN and Carpenter JT. Estradiol in breast cancer treatment. *Journal of American Medical Association* 2009, 302(7): 797-780.
69. Cruz Jurado J, Richart Aznar P, García Mata J, Fernández Martínez R, Peláez Fernández I, Sampedro Gimeno T, et al. Management of patients with metastatic breast cancer. *Advances in Therapy* 2011, 28(6): 50-65
70. Cazzaniga M and Bonanni B. Breast Cancer Chemoprevention: Old and New Approaches. *Journal of Biomedicine and Biotechnology* 2012; 2012:985620
71. Gustafsson J. What pharmacologists can learn from recent advances in estrogen signaling. *Trends in Pharmacological Sciences* 2003, 24(9): 479-485
72. Subik K, Lee J-F, Baxter L, Strzepek T, Costello D, Crowley P, et al. The Expression Patterns of ER, PR, HER2, CK5/6, EGFR, Ki-67 and AR by Immunohistochemical Analysis in Breast Cancer Cell Lines. *Breast Cancer: Basic and Clinical Research* 2010; 4:35
73. Héctor HV, Esteban B, Pedro CS, Cayetano VK, Immaculada BR, Menel E, et al. Transcriptional profiling of MCF7 breast cancer cells in response to 5-Fluorouracil: Relationship with cell cycle changes and apoptosis, and identification of novel targets of p53. *International Journal of Cancer* 2006, 119: 1164-1175.
74. Morselli E, Galluzzi L, Kepp O and Kroemer G. Nutlin kills cancer cells via mitochondrial p53. *Cell Cycle*. 2009;8(11):1647-8.

75. Shatz M, Menendez D and Resnick MA. The human TLR innate immune gene family is differentially influenced by DNA stress and p53 status in cancer cells. *Cancer Res.* 2012; 72(16):3948-57.
76. Menendez D, Shatz M, Azzam K, Garantziotis S, Fessler MB, Resnick MA. The Toll-Like Receptor Gene Family Is Integrated into Human DNA Damage and p53 Networks. *PLoS Genet* 2011; 7:e1001360.
77. Cai Z, Sanchez A, Shi Z, Zhang T, Liu M and Zhang D. Activation of Toll-like receptor 5 on breast cancer cells by flagellin suppresses cell proliferation and tumor growth. *Cancer Res.* 2011;71(7):2466-75.
78. Katsounas A, Trippler M, Kottlil S, Lempicki RA, Gerken G and Schlaak JF. Altered expression of SHIP, a Toll-like receptor pathway inhibitor, is associated with the severity of liver fibrosis in chronic hepatitis C virus infection. *J Infect Dis.* 2011; 204(8):1181-5.
79. Liu Q, Dumont DJ. Molecular Cloning and Chromosomal Localization in Human and Mouse of the SH2-Containing Inositol Phosphatase, INPP5D(SHIP). *Genomics* 1997; 39:109-12.
80. Kerley-Hamilton JS, Pike AM, Li N, DiRenzo J, Spinella MJ. A p53-dominant transcriptional response to cisplatin in testicular germ cell tumor-derived human embryonal carcinoma. *Oncogene* 2005; 24:6090-100.
81. Mondal S, Subramanian KK, Sakai J, Bajrami B and Luo HR. Phosphoinositide lipid phosphatase SHIP1 and PTEN coordinate to regulate cell migration and adhesion. *Mol Biol Cell.* 2012; 23(7):1219-30.
82. Badock V, Steinhilber U, Bommert K, Wittmann-Liebold B, Otto A. Apoptosis-induced cleavage of keratin 15 and keratin 17 in a human breast epithelial cell line. *Cell Death Differ* 2001; 8:308-15.
83. Celis JE, Gromova I, Cabezón T, Gromov P, Shen T, Timmermans-Wielenga V, Rank F and Moreira JM. Identification of a subset of breast carcinomas characterized by expression of cytokeratin 15: relationship between CK15+ progenitor/amplified cells and pre-malignant lesions and invasive disease. *Mol Oncol.* 2007;1(3):321-49.
84. Sikorski TW and Buratowski S. The basal initiation machinery: beyond the general transcription factors. *Curr Opin Cell Biol.* 2009;21(3):344-51
85. Berteaux N, Lottin S, Monté D, Pinte S, Quatannens B, Coll J, et al. H19 mRNA-like Noncoding RNA Promotes Breast Cancer Cell Proliferation

- through Positive Control by E2F1. *Journal of Biological Chemistry* 2005; 280:29625-36.
86. Lottin S, Adriaenssens E, Dupressoir T, Berteaux N, Montpellier C, Coll J, et al. (2002) Overexpression of an ectopic H19 gene enhances the tumorigenic properties of breast cancer cells. *Carcinogenesis*, 23(11): 1885-1895
87. Wang J, Fu L, Gu F, Ma Y. Notch1 is involved in migration and invasion of human breast cancer cells. *Oncol Rep* 2011; 26:1295-303.
88. Noetzel E, Rose M, Sevinc E, Hilgers RD, Hartmann A, Naami A, et al. Intermediate filament dynamics and breast cancer: Aberrant promoter methylation of the Synemin gene is associated with early tumor relapse. *Oncogene* 2010; 29:4814-25.
89. Cai Z, Sanchez A, Shi Z, Zhang T, Liu M, Zhang D. Activation of Toll-like Receptor 5 on Breast Cancer Cells by Flagellin Suppresses Cell Proliferation and Tumor Growth. *Cancer Research* 2011; 71:2466-75.
90. Cowin P, Rowlands TM, Hatsell SJ. Cadherins and catenins in breast cancer. *Current Opinion in Cell Biology* 2005; 17:499-508.
91. Salomoni P, Pandolfi PP. The Role of PML in Tumor Suppression. *Cell* 2002; 108:165-70.
92. Luo JM, Liu ZL, Hao HL, Wang FX, Dong ZR, Ohno R. Mutation analysis of SHIP gene in acute leukemia. *Zhongguo Shi Yan Xue Ye Xue Za Zhi* 2004; 12:420-6.
93. Zhou M-N, Kunttas-Tatli E, Zimmerman S, Zhouzheng F, McCartney BM. Cortical localization of APC2 plays a role in actin organization but not in Wnt signaling in *Drosophila*. *Journal of Cell Science* 2011; 124:1589-600.
94. Shetty P, Movva S, Pasupuleti Udayakumar D, Zhang G, Ji Z, Njauw CN, Mroz P, Tsao H. EphA2 is a critical oncogene in melanoma. *Oncogene* 2011; 30:4921-9.
95. Zhang G, Njauw C-N, Park JM, Naruse C, Asano M, Tsao H. EphA2 Is an Essential Mediator of UV Radiation-Induced Apoptosis. *Cancer Research* 2008; 68:1691-6.
96. N, Vedicherlla B, Vattam K, Venkatasubramanian S, et al. Regulation of IGF2 transcript and protein expression by altered methylation in breast

- cancer. *Journal of Cancer Research and Clinical Oncology* 2011; 137:339-45.
97. Uhlen M, Oksvold P, Fagerberg L, Lundberg E, Jonasson K, Forsberg M, et al. Towards a knowledge-based Human Protein Atlas. *Nat Biotech* 2010; 28:1248-50.
98. Pei D, Zhang Y and Zheng J. Regulation of p53: a collaboration between Mdm2 and Mdmx. *Oncotarget*. 2012;3(3):228-35.
99. Wang X. p53 regulation: teamwork between RING domains of Mdm2 and MdmX. *Cell Cycle*. 2011;10(24):4225-9.
100. Perry ME. The Regulation of the p53-mediated Stress Response by MDM2 and MDM4. *Spring Harb Perspect Biol*. 2010 Jan;2(1).
101. Nikulenkov F, Spinnler C, Li H, Tonelli C, Shi Y, Turunen M, Kivioja T, Ignatiev I, Kel A, Taipale J and Selivanova G. Insights into p53 transcriptional function via genome-wide chromatin occupancy and gene expression analysis. *Cell Death Differ*. 2012;19(12):1992-2002.
102. Roy S, Musselman CA, Kachirskaia I, Hayashi R, Glass KC, Nix JC, Gozani O, Appella E and Kutateladze TG. Structural insight into p53 recognition by the 53BP1 tandem Tudor domain. *J Mol Biol*. 2010;398(4):489-96.
103. Zgheib O, Huyen Y, DiTullio RA Jr, Snyder A, Venere M, Stavridi ES and Halazonetis TD. ATM signaling and 53BP1. *Radiother Oncol*. 2005;76(2):119-22.
104. FitzGerald JE, Grenon M and Lowndes NF. 53BP1: function and mechanisms of focal recruitment. *Biochem Soc Trans*. 2009 Aug;37(Pt 4):897-904.
105. Andreotti V, Ciribilli Y, Monti P, Bisio A, Lion M, Jordan J, Fronza G, Menichini P, Resnick MA and Inga A. p53 transactivation and the impact of mutations, cofactors and small molecules using a simplified yeast-based screening system. *PLoS One*. 2011;6(6):e20643.
106. Selivanova G. Therapeutic targeting of p53 by small molecules. *Semin Cancer Biol*. 2010; 20(1):46-56.

APPENDIX

Interaction between p53 and estradiol pathways in transcriptional responses to chemotherapeutics. (Cell Cycle, in press)

Lion *et al.*,p92

Lion *et al.*, **Supplemental Figure legends, supplemental Figures and tables**

.....p106

p53 Transactivation and the Impact of Mutations, Cofactors and Small Molecules Using a Simplified Yeast- Based Screening System

Andreotti, Ciribilli, Monti *et al.*p141

Andreotti, Ciribilli, Monti *et al.* **Supporting information**p157

Interaction between p53 and estradiol pathways in transcriptional responses to chemotherapeutics

Mattia Lion,¹ Alessandra Bisio,¹ Toma Tebaldi,² Veronica De Sanctis,² Daniel Menendez,³ Michael A. Resnick,³ Yari Ciribilli¹ and Alberto Inga^{1,*}

¹Laboratory of Transcriptional Networks; Centre for Integrative Biology (CIBIO); University of Trento; Mattarello, Trento, Italy; ²Laboratory of Translational Genomics; Centre for Integrative Biology (CIBIO); University of Trento; Mattarello, Trento, Italy; ³Chromosome Stability Group; National Institute of Environmental Health Sciences; Research Triangle Park, NC USA

Keywords: p53, estrogen receptor, synergy, synergistic cooperation, cis-element, MCF7 cells, non-canonical response elements; doxorubicin; 17-beta estradiol, nutlin

Estrogen receptors (ERs) and p53 can interact via cis-elements to regulate the angiogenesis-related VEGFR1 (FLT1) gene, as we reported previously. Here, we address cooperation between these transcription factors on a global scale. Human breast adenocarcinoma MCF7 cells were exposed to single or combinatorial treatments with the chemotherapeutic agent doxorubicin and the ER ligand 17 β -estradiol (E2). Whole-genome transcriptome changes were measured by expression microarrays. Nearly 200 differentially expressed genes were identified that showed limited responsiveness to either doxorubicin treatment or ER ligand alone but were upregulated in a greater than additive manner following combined treatment. Based on exposure to 5-fluorouracil and nutlin-3a, the combined responses were treatment-specific. Among 16 genes chosen for validation using quantitative real-time PCR, seven (INPP5D, TLR5, KRT15, EPHA2, GDNF, NOTCH1, SOX9) were confirmed to be novel direct targets of p53, based on responses in MCF7 cells silenced for p53 or cooperative targets of p53 and ER. Promoter pattern searches and chromatin IP experiments for the INPP5D, TLR5, KRT15 genes supported direct, cis-mediated p53 and/or ER regulation through canonical and noncanonical p53 and ER response elements. Collectively, we establish that combinatorial activation of p53 and ER can induce novel gene expression programs that have implications for cell-cell communications, adhesion, cell differentiation, development and inflammatory responses as well as cancer treatments.

Introduction

The transcriptional activity of a sequence-specific transcription factor (TF) can be modulated in many ways including post-transcriptional and post-translational modifications, interactions with components of the basal transcription machinery or specific cofactors as well as the chromatin state.^{1,2} Equally important is the “quality” of the response element sequences and the cooperation/interaction with other transcription factors.^{1,2}

The tumor suppressor p53, which has been described as the “guardian of the genome,” controls several biological outcomes that include cell cycle, growth, apoptosis, senescence, angiogenesis and genome stability.^{3,4} Also, it can regulate many other cellular processes such as autophagy, energy metabolism, mTOR signaling, immune responses, cell motility/migration and cell-cell communication, in part through modulation of several microRNA genes.⁵⁻⁷

The estrogen receptors (ERs) are nuclear receptor transcription factors that exert hormonal responses through the activation of proliferation pathways. While ERs are master regulators

essential for development and maintenance of normal sexual and reproductive functions, they can also play a role in the cardiovascular, musculoskeletal, immune and central nervous systems.⁸⁻¹⁰

These two diverse networks exhibit crosstalk that can be due to direct interaction between p53 and the ERs, with the more frequently described outcome being repression of p53 activity,¹¹⁻¹⁴ although p53 can also inhibit ER α .^{15,16} The inhibitory crosstalk, which can be mediated by physical interactions between the two proteins, can be relieved by stress-dependent post-translational modifications of p53.^{12,14} The p53/ER interactions can also result in mutual positive regulation at the level of target gene expression level.^{17,18} Most of the studies addressing p53/ER interaction were performed in breast cancer cell lines, implicating regulation of the activity and expression of p53 and ERs in tumorigenesis. This was supported by findings of a correlation between the presence of wild type p53 and ER-positive breast cancer and a correlation between mutant p53 and ER-negative breast cancer.^{19,20} The two transcription factors can also share co-regulators, such as p300 and MDM2. Both inhibition²¹ and positive regulation²² of ER α can result from the p53 negative regulator MDM2.

*Correspondence to: Alberto Inga; Email: inga@science.unitn.it
Submitted: 10/31/12; Revised: 03/11/13; Accepted: 03/14/13
<http://dx.doi.org/10.4161/cc.24309>

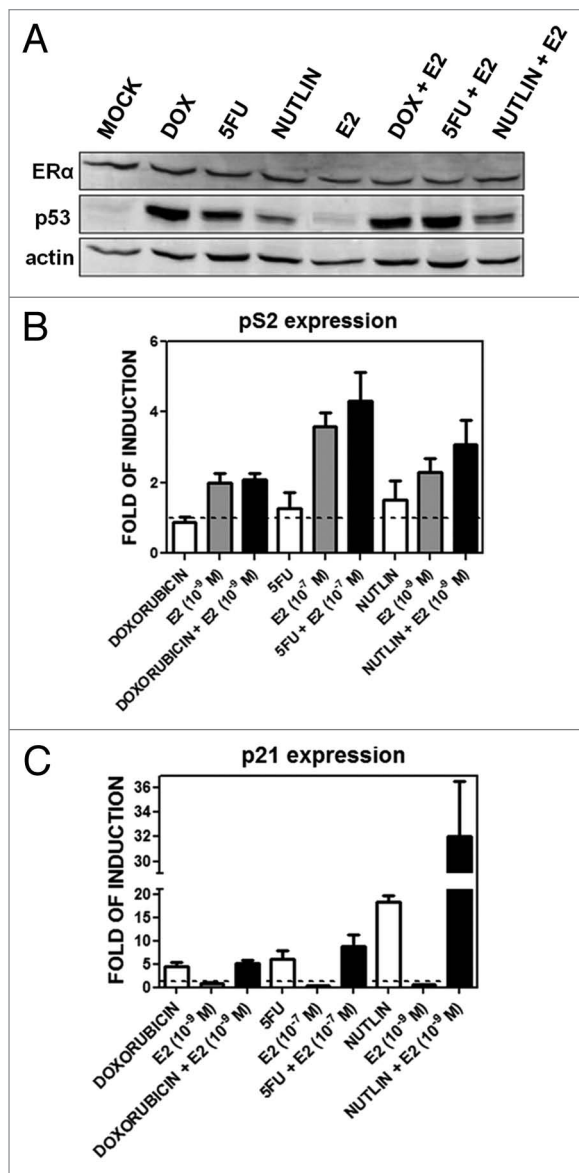


Figure 1. p53 and ER α protein levels and transactivation activities upon DOX, 5FU, nutlin-3a, E2 single or combined treatments. (A) Western blot analysis showing p53 and ER α protein levels 10 h after the indicated treatments at the following doses: DOX, 1.5 μ M; 5FU, 375 μ M, nutlin-3a, 10 μ M; E2, 10⁻⁹ M. (B and C) qPCR results for the p53 target gene p21 (B) and the ER α target gene pS2/TFF1 (C). Presented in the bar graphs are fold-induction relative to the mock condition and the standard errors of three biological and two technical replicates for each condition. GAPDH, B2M and β -actin housekeeping genes served as internal controls.

We recently identified transcriptional cooperation between activated p53 and ligand-bound ERs at the promoter of the VEGFR-1/FLT1 gene.^{23,24} The functional interaction appeared to occur through noncanonical cis-promoter REs for both transcription factors located in close proximity within the target promoter, where the p53 was a half-site created by an infrequent single nucleotide polymorphism.²⁵⁻²⁷ Neither p53 nor ER alone could significantly upregulate FLT1, but the combination resulted in synergistic activation.²⁴ We proposed that noncanonical p53 REs

consisting of 1/2 or 3/4 sites can expand the p53 target network providing for moderate or weak p53 responsiveness, but at the same time providing the opportunity of conditional, context-dependent transactivation.^{5,25,27} Also, in the case of ERs the structural organization of the response element (ERE) has been shown to influence the binding affinity as well as the modulation of the expression of target genes. The consensus half-site ERE is considered the minimal target site for ERs, and other transcription factors as well as cofactors can promote binding and transcriptional modulation.²⁸⁻³⁰

Based on our finding at the FLT1 locus, we have taken a global approach to address whether similar scenarios might exist elsewhere in the genome using breast adenocarcinoma-derived MCF7 cells. Whole-genome expression changes were determined following combinations of exposures to doxorubicin (DOX), a genotoxic chemotherapeutic drug commonly used in cancer therapy that induces p53, and the ER ligand 17 β -estradiol (E2). We identified 201 genes for which combined DOX/E2 treatment led to greater than additive upregulation. The genes were involved in cellular differentiation/development, extracellular matrix, cell adhesion and inflammation responses. For 10 out of 16 genes examined further, the synergistic transactivation was validated using quantitative real-time PCR. Using MCF7 cells with reduced p53 expression, we demonstrated that p53 participates directly in the modulation of their expression and in the cooperation with ER, and we discovered three new p53 target genes (GDNF, KRT15, SOX9). The cis-mediated cooperation at the level of the promoter of three of the 16 genes was interrogated by chromatin immunoprecipitation. KRT15 expression appeared to be regulated in cis through p53 and ER α response elements.

Results

Genome-wide transcriptome analyses identify a combinatorial effect of p53 and ERs activation in response to DOX and E2. We established the utility of our MCF7 cell system for detecting p53 and/or ER responses following treatment with DOX and/or the ER ligand E2. The chemotherapeutic agent 5-fluorouracil (5FU) and the non-genotoxic MDM2 inhibitor nutlin-3a³¹ were included to further support p53-specific effects on gene expression. The ER α protein levels in total extracts did not change after any of the 10-h stimuli used, while p53 protein was stabilized by DOX, 5FU and nutlin-3a but not by E2 (Fig. 1A). Both pathways were activated based on qPCR analysis of expression of the standard p53 target p21/CDKN1A and the ER α target pS2/TFF1 genes (Fig. 1B and C). p21 was induced to similar levels by DOX and 5FU, while E2 had no effect on expression. Nutlin-3a treatment resulted in higher relative p21 expression that was increased 1.5-fold with the addition of E2 (Fig. 1C). pS2/TFF1 was upregulated only in the presence of E2 and as a function of its concentration (10⁻⁷ or 10⁻⁹ M) with no further increase with DOX, 5FU or nutlin-3a (Fig. 1B). Under these conditions, there was no apparent toxicity for the p53 activator drugs or E2 alone while the combination of a p53 activator with E2 increased the overall cell index value, consistent with a role for estradiol in promoting proliferation (Fig. S1).

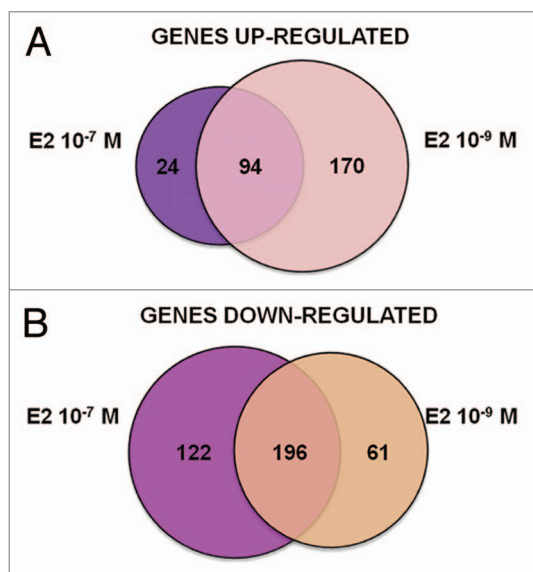


Figure 2. Graphical overview of E2 treatment-specific transcriptome changes. Differentially expressed genes (DEGs) were identified by Agilent microarray feature extraction, bioinformatics and statistical analyses, as described in the “Materials and Methods” section. Presented are Venn diagrams showing the number of upregulated (A) or downregulated (B) DEGs specific or in common between the different treatments with E2, 10⁻⁹ M and 10⁻⁷ M.

Global gene expression profiling and statistical analysis of the microarray were performed as described in “Materials and Methods.” MCF7 cells cultured in estrogen-depleted media were subjected to single or combined treatments with DOX (1.5 μM) and E2 (at a pharmacological concentration 10⁻⁷ M, or a more physiological concentration 10⁻⁹ M). Gene ontology (GO), pathway enrichment and network analyses were conducted using DAVID (<http://david.abcc.ncifcrf.gov/>)³² as well as the Ingenuity Pathway Analysis (IPA, www.ingenuity.com).

Differences in transcriptome responses were identified in relation to the E2 doses (Fig. 2A and B). The lower E2 concentration (10⁻⁹ M) resulted in the same number of up and downregulated DEGs, whereas the pharmacological concentration (10⁻⁷ M) was generally more repressive. Both concentrations of E2 resulted in differentially expressed genes (DEGs) exhibiting functional clusters enrichment that reflect expected estrogen-induced differentiation, proliferation, survival, hormonal responses and inhibition of p53 and SMARCB1 (Table S1A and B). Unexpected functional clusters were observed after 10⁻⁷ M E2, including positive regulation of apoptosis and negative regulation of cell growth as well as inhibition of SP1 (Table S1B). Therefore, we decided to focus our analysis on 10⁻⁹ M E2, since it resulted in a signature much closer to that of typical estrogen responses (Table S1A).

The clusters identified with DOX DEGs were consistent with genotoxic stress and p53 pathway activation, including cell cycle and apoptosis regulation, modulation of transcription, regulation of DNA damage checkpoints, BRCA1 functions and ATM signaling (Table S1C).

Next, we focused on the DOX + E2 (10⁻⁹ M) treatments to examine crosstalk between p53 and ERs. The overall

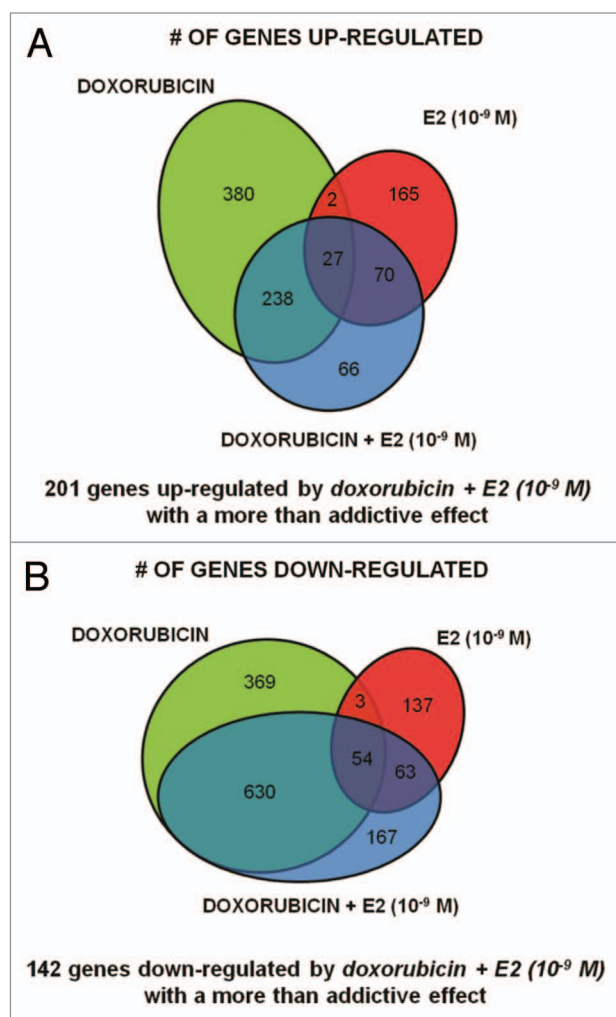


Figure 3. Specific gene signatures of the DOX+E2 combination treatment. Venn diagrams showing upregulated genes (A) or downregulated genes (B) comparing DOX, E2 and DOX + E2 DEGs. The number of genes differentially expressed in common or unique after doxorubicin or E2 (10⁻⁹ M) treatment or after their combination is indicated.

transcriptome changes were heavily influenced by both treatments (Table S1D), although a greater overlap was observed between DEGs for DOX and DOX + E2 for both upregulated (66%) and downregulated (75%) genes (Fig. 3A and B). There was much less overlap between E2 and DOX + E2 DEGs (24% and 13% for the upregulated and downregulated groups, respectively). Stem cell pluripotency appeared as a distinctive IPA pathway (Table S1D). Interestingly, 66 upregulated and 167 downregulated DEGs were uniquely identified following DOX + E2 treatment. Conversely, for 380 upregulated and 369 repressed DOX DEGs the differential expression was not observed in the double treatment. Only 29 upregulated and 57 repressed DEGs were in common for the DOX and E2 single treatments, of which 27 up and 54 downregulated genes were also DEGs with the double treatment (Fig. 3A and B). The functional annotation clusters obtained with these gene groups are summarized in Table S1E–H, although the small numbers limited the statistical power.

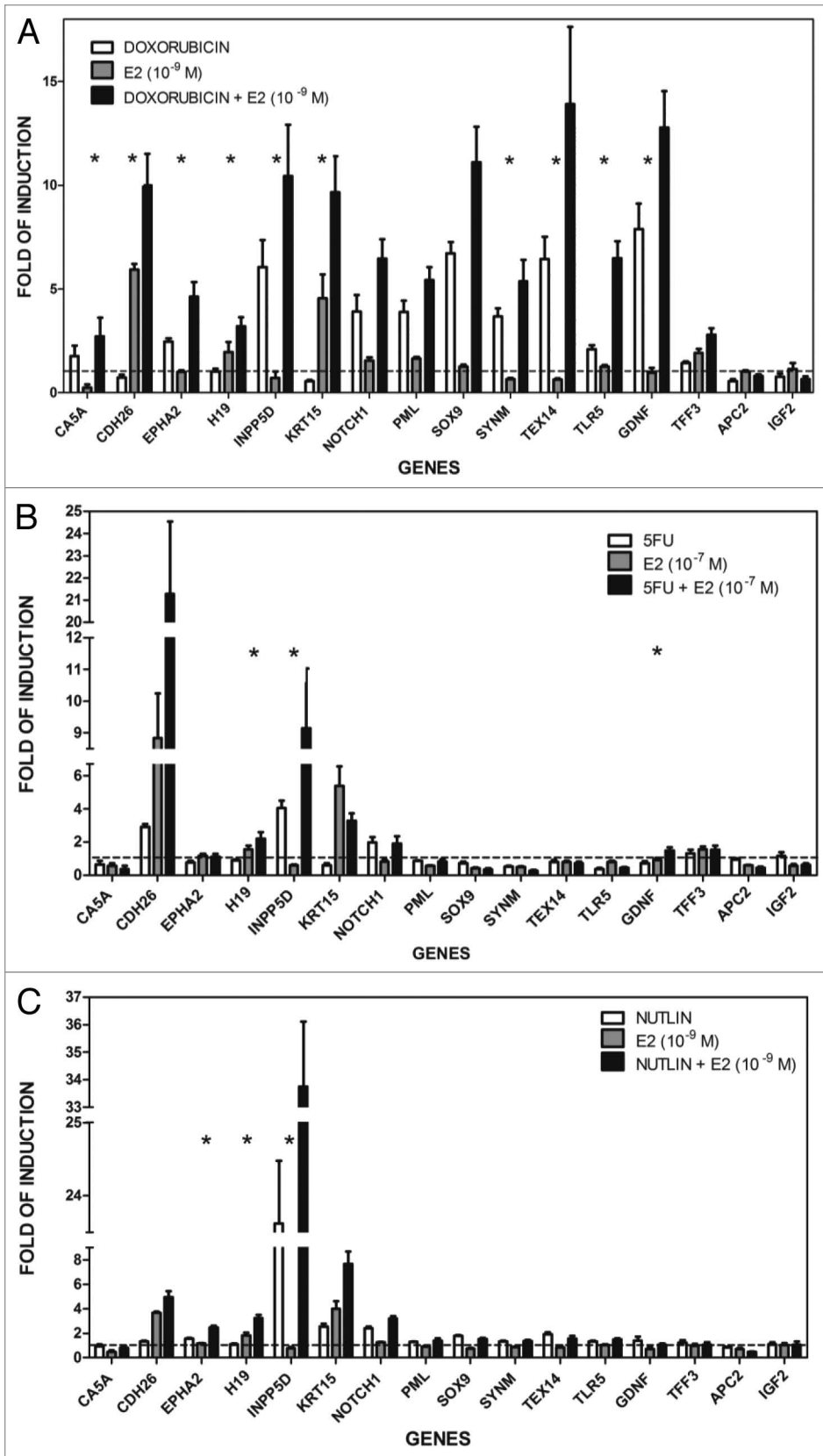


Figure 4. Treatment-selective transcriptional cooperation between p53-inducing stimuli and estradiol. qPCR reactions for the 16 chosen genes were performed using 384-well plates in a final volume of 10 μ l using TaqMan[®] Gene Expression Assays with 3 biological and 2 technical replicates for each condition. GAPDH, B2M and β -actin housekeeping genes served as internal controls. Asterisks indicate statistically significant, more than additive effects in the combined treatment as described in the “Materials and Methods.” The same RNAs used in the microarray experiments were tested in (A and B), where the experiment served also as a validation of the array results, while all results in (C) were obtained from independent treatment and RNA extractions.

Methods,” we adopted a conservative approach based on the algebraic sum of logarithmic (\log_2) fold-change in expression. Statistical analysis for synergistic impact of combined treatments is presented in Table S3.

Notably, 201 upregulated and 142 downregulated genes met these criteria and exhibited a greater than additive response following the combined p53/ER-inducing treatments (Fig. 3). Analysis revealed enrichment for cell-cell communication, cell adhesion, development/differentiation and inflammatory response pathways (Table S11) for the upregulated genes, while cell cycle and mitosis functions were enriched in the repressed group (Table S1J). We chose to pursue further the genes from the upregulated group, especially since repression via cis elements has yet to be established for p53 and ER α interactions (Table S3).

From the group of 201 genes exhibiting more than additive upregulation after combined DOX+E2 treatment (bold, Table S3), 16 that represented the main biological functions were selected for further analysis (Table S1I). Some are usually expressed in a different biological environment than breast cells (TEX14, SOX9, INPP5D), and others belong to biological pathways that can expand the

Cooperative p53, ER-mediated upregulation of genes involved in differentiation, cell-cell communication, adhesion and inflammatory response. As described in the “Materials and

p53/ER transcriptional master network (TFF3, CA5A, CDH26, NOTCH1, GDNF, INPP5D) (see Table S2A for references). For some, a direct or indirect functional interaction with p53

(NOTCH1, IGF2, TLR5 PML, INPP5D, EPHA2), with ER (NOTCH1, CDH26), or with other selected genes (IGF2 and H19, NOTCH1 and SOX9) has already been proposed (Table S2A). A summary of functional interactions predicted by text mining of the literature is shown in Figure S2 (<http://stitch.embl.de/>).³³

Quantitative real-time PCR (qPCR) was performed to confirm the microarray results after DOX treatment with or without the addition of E2 (Fig. 4A). The trend of the microarray results was confirmed for 14/16 genes upon DOX and/or E2 treatment. T-test analysis on the \log_2 of the values obtained for relative expression confirmed for 10/16 genes the synergistic effect ($p < 0.05$) of DOX + E2 combination (Fig. 4A; Table S2A).

Expression of the 16 genes was also investigated following treatment with 5FU, another commonly used genotoxic agent that results in p53 activation. The responses clearly differed between DOX and 5FU (Fig. 4A and B). Only CDH26, INPP5D, NOTCH1 were responsive to 5FU (Fig. 4B); of these INPP5D and NOTCH1 were also DOX-responsive. The synergistic effects observed after DOX + E2 administration were also observed for H19, INPP5D and, in part, also for GDNF after 5FU + E2 (10^{-7} M) (Fig. 4B; Table S2B). Unlike for DOX, the combined treatment did not affect TLR5 or EPHA2, which are p53 target genes.^{34,35} Thus, the E2 enhancing effects on expression differ between two different inducers of p53.

Nutlin-3a treatment can synergistically cooperate with E2, but only on a subset of genes. Unlike genotoxic stress, nutlin-3a can directly activate p53. It targets the complex p53-MDM2, which results in p53 stabilization and activation without apparently inducing any kind of genotoxic stress.³¹ Given the difference in mechanism of p53 activation, we investigated possible interactions between E2 (10^{-9} M) and p53 following nutlin-3a treatment.

Among the 16 genes described above, the following six were upregulated by nutlin-3a treatment alone (fold-induction > 1.5 ; Fig. 4C) based on qPCR: EPHA2, INPP5D, KRT15, NOTCH1, SOX9, TEX14. The KRT15 gene was not responsive to DOX or 5FU (Fig. 4A and B), possibly indicating a differential effect of genotoxic post-translational modifications on p53-targeted expression. Only EPHA2, H19 and INPP5D showed a greater than additive effect for nutlin-3a + E2 (Fig. 4C; Table S2C). The synergy was also found for the H19 and INPP5D genes with E2 + DOX or 5FU and for EPHA2 with DOX + E2 (Figs. 4A and B).

Silencing of p53 in MCF7 cells establishes a direct role of p53 in doxorubicin responsiveness of the target genes. We validated direct p53 inducible expression of the novel genes using a stable MCF7 cell line expressing shRNA to p53.³⁶ As shown in Figure 5A, the p53 protein level in MCF7-p53i is greatly reduced based on western blot analysis and gene expression of the p53 target gene p21, as compared with the control cells ("MCF7 vector") after DOX treatment. Neither the p53 nor the ER α mRNA levels are changed after 10-h treatment with DOX or nutlin-3a (Fig. 5A). Expression of 8 of the 16 genes was determined at 10 h after DOX or nutlin-3a treatment of MCF7-p53i and -vector cells cultured in normal medium (Fig. 5B). EPHA2, GDNF, NOTCH1 and INPP5D were induced after either treatment of

the MCF7 vector cells but were non-responsive or only slightly responsive in MCF7-p53i cells. The other five genes did not show any p53-specific responsiveness, although TLR5 is a p53 target.³⁵

We also examined DOX and nutlin-3a responses after 24 h. Both treatments enhanced expression of p53. However, DOX repressed ER α levels both at the protein and mRNA level, which would affect estradiol responses including the transcriptional cooperation with p53 at that time point (Fig. 5C). There was p53-dependent induction for seven of the eight genes following either treatment (Fig. 5D). DOX treatment led to residual induction of several of the genes in the MCF7-p53i cells, while only INPP5D was slightly responsive upon nutlin-3a treatment (Fig. 5D). This was presumably due to the low amount of p53 expression. CDH26 gene expression offers another example of treatment dependencies, as the gene was not regulated by p53 at either time point with either DOX or nutlin-3a, but was inducible by 5FU treatment alone (Fig. 4B and Fig. 5B and D).

The transcriptional responsiveness of INPP5D, TLR5 and KRT15 is associated with p53 and ER response elements. The biological impact and expression responses due to p53 plus estradiol led us to investigate in depth the promoter regions of the *INPP5D*, *TLR5* and *KRT15* genes for the presence of canonical and noncanonical p53 and ER response elements. An in silico search identified two distinct regions within the promoter of each of these genes (called A and B in Fig. 6) containing at least one putative $\frac{1}{2}$ -site p53 RE and one putative $\frac{1}{2}$ -site ERE (Fig. 6A).

The promoters were also examined by ChIP qPCR for p53 and ER occupancy. As expected, there was p53 occupancy at the canonical p53 target REs of the p21, PUMA and BAX genes (Fig. 6B). Interestingly, E2 led to p53 recruitment at these promoters. p53 occupancy at the promoter regions was also found for the INPP5D, TLR5 (fragment A) and KRT15 genes (Fig. 6C–E) following DOX treatment. However, we were only able to detect ER α occupancy at the KRT15 promoter for fragment B (Fig. 6E) as well as the canonical ER α target pS2 (Fig. 6A). It appears that there is independent occupancy by the two transcription factors, in that the binding of one is not required for the recruitment of the other.

Histone marks associated with DOX and/or E2 treatment. While transcriptional synergy was established, it could not be ascribed to levels of p53 or ER binding, at least for the sites examined. Since changes in chromatin around regulatory regions of transcribed genes can modulate the activity and cooperativity between transcription factors, we analyzed chromatin status at the TLR5, INPP5D, KRT15 genes as well as at the control genes CDKN1A and TFF1. Promoter regions containing putative or known p53 REs and EREs along with regions encompassing the transcription start site (TSS) were examined for changes in histone tail post-translational modifications as well as total histones employing ChIP approaches and the same experimental conditions used to address p53 and ER occupancy.

Treatment with DOX resulted in a significant increase of the dimethylation H3K9me2 mark, which is associated with repression, for all tested genes. The increases were generally restricted to regions upstream of the TSS, but in the case of INPP5D and KRT15 were visible also at TSS. However, E2 treatment alone

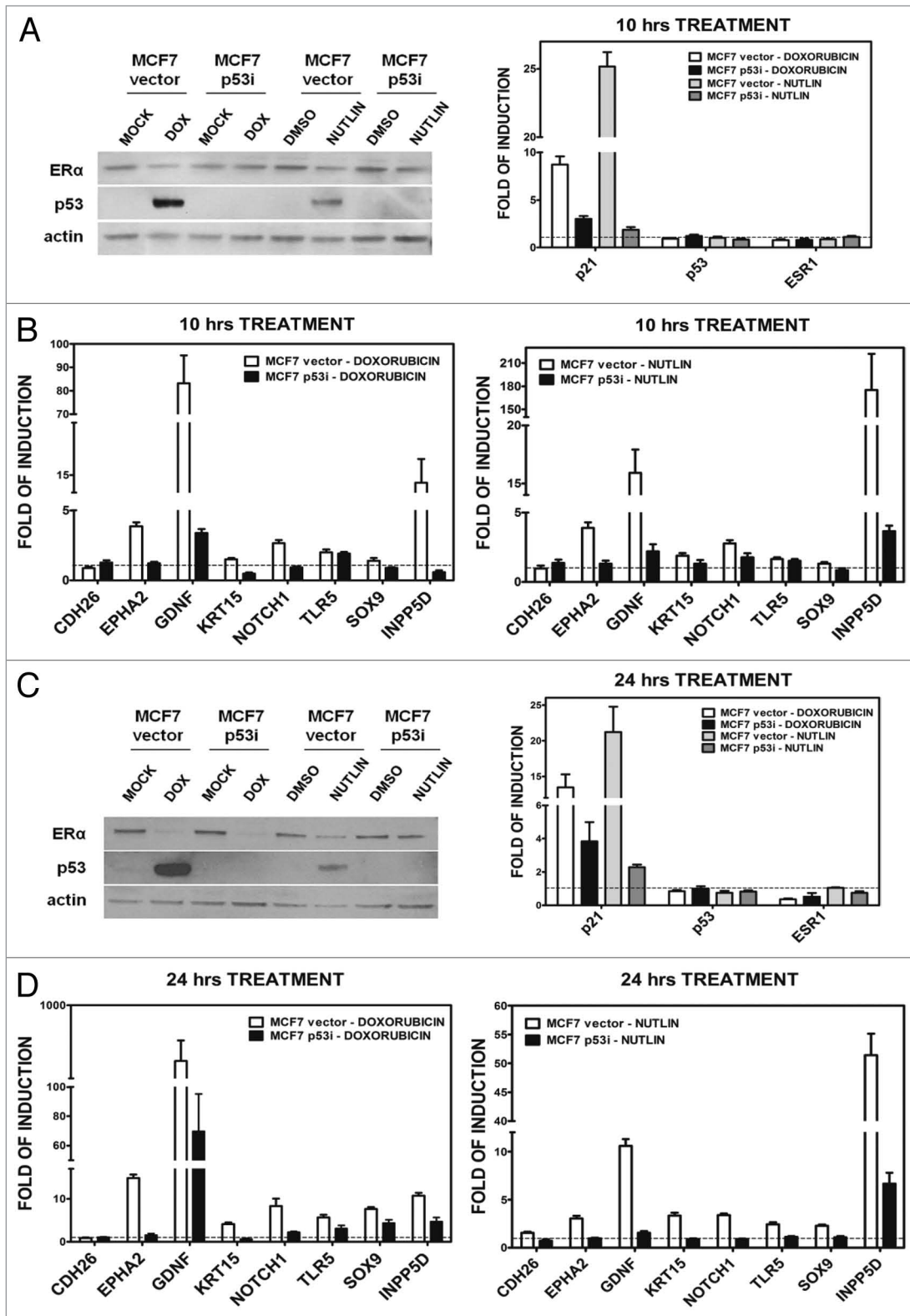


Figure 5. Changes in p53 and ERα protein levels and relative expression. Presented are results for p21, p53 and ER genes and of eight selected genes after 10 or 24 h DOX (1.5 μM) or nutlin-3a (10 μM) treatment in MCF7 vector and p53i. (**A and C**), left panel: western blot analysis showing p53 and ERα protein levels after 10 (**A**) and 24 h (**C**) of treatment. (**A and C**) right panel: qPCR results for the p53 target gene p21, the p53 and ERα (ESR1) genes after 10 (**A**) and 24 (**C**) hours of treatment. (**B and D**) qPCR results for the indicated eight genes after 10 or 24 h of treatment (left panels, DOX; right panels, nutlin). The fold-induction relative to the mock condition for MCF7-vector or MCF7-p53i is presented (H₂O for DOX treatment or DMSO for nutlin-3a treatment).

led to only a small increase in H3K9me2 at some sites and E2 was capable of reducing the DOX effect (Fig. 7A). No major changes were observed for the H3K4me2 mark, which is associated with active transcription. However, DOX treatment resulted in a slight increase at the TSS for TFF1 and INPP5D. E2 treatment was associated with an increase at TFF1 and CDKN2A TSS (Fig. 7B).

There were increases associated with DOX and DOX + E2 treatments in H3 and H4 acetylation marks, corresponding mainly to open chromatin, in the region surrounding the p53 RE present -2.2 Kb from CDKN1A TSS (Fig. 8A and B). The E2 treatment led to an increase in H3 acetylation at TFF1 TSS and H4 acetylation both at the TSS and in the ERE-containing sequence located -250 bp upstream from TSS. In both genes, these modifications are consistent with the enhanced transcription observed after DOX or E2 treatments. DOX counteracted the effect of E2 on these marks in TFF1. No significant changes were observed for the TLR5 and INPP5D genes, except for a consistent decrease in acetylation for INPP5D after combined treatment (Fig. 8A and B). For KRT15, the E2 and DOX + E2 treatments led to an increase in acetyl marks, especially near the TSS.

The total levels of H3 were also examined (Fig. S3). They appeared to be reduced near the TSS of the CDKN1A and TFF1 genes with all treatments. For KRT15, the same trend was observed for all three regions analyzed. However, no changes were observed for the promoters of TLR5 and INPP5D, and an apparent increase was detected at TSS, particularly after DOX treatment.

Overall, our results indicate that all the genes analyzed were in an active chromatin state even in the mock condition, which is consistent with their basal expression levels. The treatments had an impact on several histone marks, although there was not a specific signature apparent for the double treatment.

Discussion

We have addressed the consequences of DOX and E2 on whole genome transcriptomes using p53 wild type and ER α -positive MCF7 cells as an experimental model of luminal-A subtype breast adenocarcinoma.³⁷ Based on our previous work, we anticipated genes for which the inducible transcription factors p53 and ERs could act collaboratively in cis at their respective REs. Regardless of the mode of interaction, identifying genes for which there is a synergistic p53/ER response is expected to inform treatments of breast or other cancers. Therapeutic protocols often include modulation of either or both transcription factors, using p53-inducing drugs, such as DOX or 5FU, as well as ER antagonists or inhibitors of estrogen synthesis (www.chemocare.com).^{9,38} Other examples of crosstalk between different drugs in breast and other cancer types have been recently reported.³⁹⁻⁴¹ Those findings exemplify the relevance of examining the impact of combinatorial treatments at the genome level.

DOX treatment resulted in dramatic changes in gene expression with 647 upregulated and 1056 downregulated genes and enrichment for the p53-pathway activation. While, strongly

influenced by DOX, combined treatment with E2 resulted in 66 genes uniquely responsive and a total of 201 upregulated genes with greater than additive changes. Based on ontology and pathway analysis, the upregulated genes with greater than additive responses were enriched for cell-cell communication, epithelial cell differentiation and inflammatory response. Greater than additive downregulation was observed for 142 genes with enrichment for cell cycle, mitosis and metabolic functions (Table S1). Thus, we have identified interesting candidates for increased responses to genotoxic plus estrogen treatments.

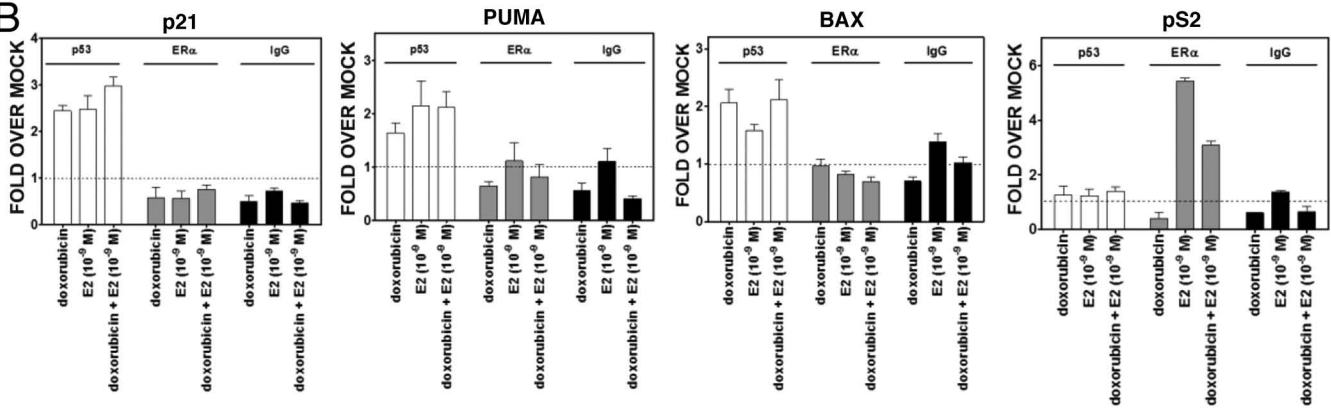
We chose to focus on 16 upregulated genes in order to better understand the greater than additive responses toward p53 and estrogen inducing agents. While DOX or 5FU treatment resulted in similar p53 levels and p21 induction, there were marked differences in expression after single treatments, as well as when combined with estradiol (summarized in Table S4). Previous studies have established cell type-specific responses to DOX and 5FU as well as other drugs.⁴² Notably, only H19 and INPP5D consistently exhibited transcriptional cooperation between E2 and DOX, 5FU and nutlin treatments. Using p53-deficient MCF7 cells, the dependency on p53 was examined for eight genes and confirmed for the newly identified p53 target genes GDNF, KRT15, and SOX9 as well as the previously reported TLR5,³⁵ INPP5D,⁴³ NOTCH1 (49) and EPHA2.³⁴ CDH26 was 5FU-responsive (Fig. 4B), but a requirement for p53-dependent induction was not confirmed in our cell system, highlighting once again the specificity of drug response.

Given our earlier results with the FLT1 gene,^{23,24} we examined three of the 16 genes for the possibility of cis interactions by assessing p53 and ER occupancy. p53 bound directly to p53-related target sequences in the promoters of the TLR5, INPP5D and KRT15 genes. We further confirmed their p53-dependent induction after DOX and nutlin-3a treatment using MCF7 cells silenced for p53. TLR5 gene is involved in innate immunity,³⁵ INPP5D affects regulation of inositol signaling^{43,44} and showed a more than additive transactivation in all three combined treatments. KRT15 is an intermediate filament type I protein responsible for the mechanical integrity of epithelial cells,⁴⁵ and its expression is regulated by E2. Direct evidence for possible functional interaction between p53 and ER via cis-elements was only established for the KRT15 gene, which also showed ER α occupancy upon E2 single treatment. There are several reasons that might explain a lack of detectable ER α occupancy upon combined treatments, if it truly contributes to the greater than additive gene responses. Included is the possibility of a role for ER β , which was not examined. Also, the type of interaction that can occur between p53 and ER α might differ between genes. ER α can in fact bind other transcription factors in an ERE-independent manner.^{9,10} Furthermore, non-genomic estrogen signaling pathways^{9,10} must also be considered for their contribution to the observed transcriptional cooperation. This might be particularly relevant in the early phase of E2 responses. The sources of interaction would be interesting to pursue in future structure-function analyses. Importantly we establish that the in-cis p53/ER cooperation involves a p53 half-site and half-site EREs, extending our previous findings beyond the FLT1 gene and model plasmid-based systems.²⁶

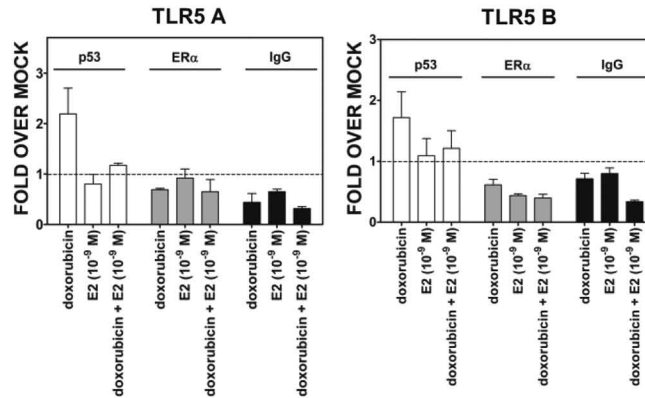
A

GENE		putative REs couples (p53 REs and ERαs)	chromosome coordinates & distance form TSS	strand
TLR5 (ENST00000366881) TSS: 223316624	#A	AGG a CAGGCTGACCTTGAACCAATAAACATGTCC ←-----→	chr1: 223318749-223318782 -2158 ↔ -2125	-
	#B	GGG C TTGCCcCAGCAAGgTgTTATTTATGTCA GGC TAGGg c CA ←-----→	chr1: 223317761-223317803 -1178 ↔ -1137	-
INPP5D (ENST00000415617) TSS: 234070370	#A	AGGCATG C aC a C a CATGCCTGG C TA ←-----→	chr2: 234069422-234069447 -948 ↔ -923	+
	#B	GGTCATTATG A c T CTTTGTGAGCTGGTGTCTTCAGGGAGGAC ←-----→ TTACTGAGATTGCAATTATAAGGTTGA A tCATG T aaAATTTCTGT ←-----→ CTTTGCAGGTTGA A ACAGTCA A ACACTGG C ATG T Ca T ←-----→	chr2:234068791-234068917 -1579 ↔ -1453	+
KRT15 (ENST00000254043) TSS: 39678665	#A	TG A CC a G A CC T CC C ACAGAGACCC C AA C C t GG C TTG C CTG ←-----→ GGG C cTG C CC ←-----→	chr17: 39678901-39678952 -287 ↔ -236	-
	#B	TG A CTGG C CCAG G CC C AGTGGG G CTGG C CC t G A CATG C CC ←-----→ ATCTCTGCTGTATCTTTACAG A ATCAGTACGCTGAGGG G CC A GTGGGAGG C CCAGG T CA ←-----→	chr17: 39680753-39680856 -2191 ↔ -2088	-

B



C



D

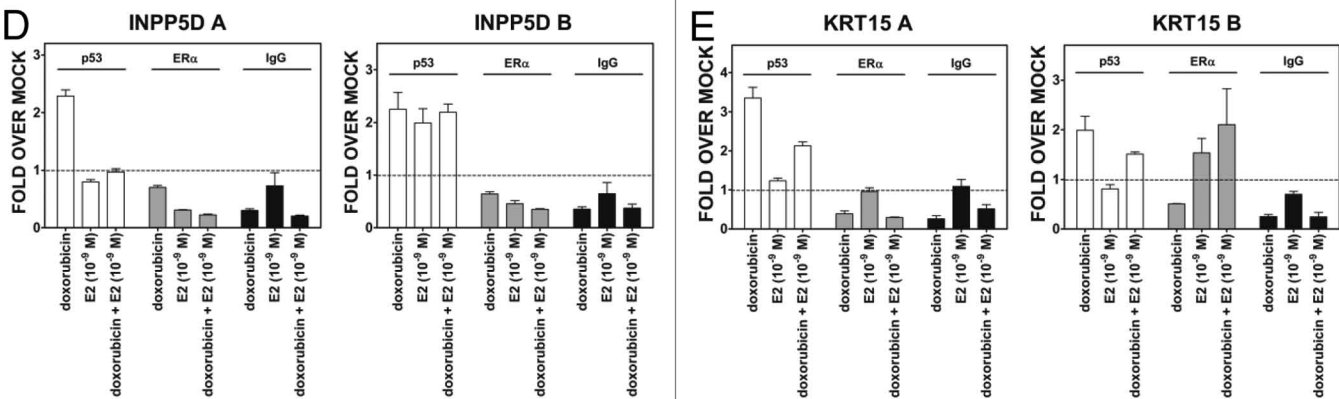


Figure 6 (See opposite page). Predicted p53 REs and ERs and relative occupancy of p53 and ER at TLR5A, INPP5D and KRT15 promoter regions. (A) Sequence, organization and position of mapped p53 and ER target sites. Promoters of selected genes were evaluated combining three approaches (see “Materials and Methods” for details). Red arrows mark ERE half sites, while tail-to-tail blue arrows denote the p53 RE half site. The chromosomal position, strand and the distance from the transcriptional start sites are also indicated. Two promoter fragments (denoted as #A and #B) were examined separately for each gene. (B–E) Chromatin immunoprecipitation and quantitative real-time PCR analyses. ChIP assays were performed using either an antibody against p53 (DO-1, Santa Cruz) or ER α (H-184) or control IgG (sc-2025). PCR was performed in 384-well plates in a final volume of 10 μ l using primers designed to amplify regions containing validated REs and ERE for established p53 and ER α target genes (B), or to generate amplicons centered around the identified p53 REs and ERs in TLR5 (C), INPP5D (D) or KRT15 (E).

p53 and ER occupancy levels were examined and did not correlate directly with the observed cooperation in expression. In our experiments the same time point (10 h) was chosen both for transcriptome and ChIP assays. Possibly, chromatin changes had occurred earlier that would influence the subsequent expression. However, in a comparison of the impact of DOX and DOX + E2 treatments in MCF7 cells, there was also a lack of correlation between p53 occupancy and transactivation levels⁴⁶ for the case of ChIP analysis at 4 h and qPCR 12 h.

We also investigated changes in chromatin, since drug treatments could elicit epigenetic changes related to transcriptional reprogramming and DNA damage responses. Chromatin could change in a gene-specific manner without a direct correlation to TF occupancy levels of expression. The H3K4me2 mark is usually associated with actively transcribed genes and positioned around the TSS and the promoter area,⁴⁷ and H3K9me2 is associated with gene silencing, especially when the mark is widespread along the gene. H3K9me2 can also be associated with openness/gene activity when present at the 5' region of a gene⁴⁷ and can reflect changes elicited by DNA damage responses.^{48,49}

p53 and ER have been functionally and physically related to proteins involved in chromatin methyl mark changes, such as G9a and LSD1.^{50–55} However, the outcome of the induced epigenetic changes is variable. For example, G9a, considered the major euchromatin H3K9 methyltransferase, can act both as corepressor and as a coactivator for nuclear receptor functions, in cooperation with CARM1 and p300.⁵⁰ Notably, both CARM1 and p300 can be recruited by p53 contributing to transcriptional activation.⁵¹ Acetylation marks at H3 and H4 histone tails are considered chromatin activation markers. Both p53 and ER can recruit histone acetyltransferases contributing to gene activation.^{51,56,57}

Thus, the complexity of histone tail epigenetic changes cannot be easily related to alterations of transcription. However, the results obtained allowed us to propose that all genes analyzed are in an active chromatin state already in the mock condition. While treatments had an impact on histone marks, a specific signature of increased promoter openness after double treatment was not evident.

There are other mechanisms that can account for transcriptional cooperation that would be interesting to pursue. Functional interactions with p53 could involve other members of the large superfamily of nuclear receptors, including, for example, the glucocorticoid or androgen receptors, connected through a multi-protein mediator complex. Furthermore, our initial studies suggest that for a subset of promoters, crosstalk with ER could be affected by p63 and p73 members of the p53 family.²⁶ p53 splice variants and various kinds of p53 stress or ER activators might be expected to affect the ER/p53 synergistic responses.

p53 activators can vary in their impact on p53 post-translational modifications and alter transcriptome responses.^{58,59} It is important to note that, while p53 has been implicated, there may be other reasons for the genotoxic stress/ER synergistic responses.

Overall, we have found extensive transcriptional cooperation between ERs and p53 across the genome. Given the importance of activators of these two genes in cancer treatments, these findings provide opportunities for investigations of treatments involving many newly identified targets of synergy, although the mechanisms of synergy remain to be established. The findings are also relevant to understanding combined ER hormonal responses and any of the many^{4,6} stresses that can induce p53 as well as general biological and cancer implications. Although it is difficult to predict phenotypic outcome, the relevance of potential p53/ER biological outcomes is apparent. For example, among the 16 genes examined in depth, H19,⁶⁰ NOTCH1,⁶¹ SYNM,⁶² TLR5⁶³ and cadherins⁶⁴ are found either overexpressed or downregulated in breast cancer. The synergy might lead to increased aggressiveness or tumor metastasis (such as EMT) or, alternatively, influence inhibition of classical tumor hallmarks such as proliferation. EPHA2 has been reported to play a role in angiogenesis and tumor neovascularization as well as being a positive mediator of UV-induced and largely p53-independent apoptosis, but it can also affect oncogenesis in melanocytes.^{65,66} Other genes, such as PML,⁶⁷ INPP5D⁶⁸ and APC2⁶⁹ are thought to be tumor suppressor genes. Cadherins are usually downregulated in tumors,⁶⁴ whereas IGF2 is often overexpressed in many types of cancers and thought to be an oncogene.⁷⁰

Finally, our findings suggest the opportunity to identify additional luminal breast tumor markers. Expression of some of the 16 selected genes is usually weak or moderate in breast tissues (Human Protein Atlas).⁷¹ Understanding the functional roles that altered expression of those genes can play in different tissues could also aid in understanding the role that they may have in tumorigenesis.

Materials and Methods

Cell lines and treatments. The human breast adenocarcinoma-derived MCF7 cell line (p53 wild type; ER α , ER β -weakly positive) was obtained from ICLC and maintained in Dulbecco's modified Eagle's (DMEM), 10% FBS, 2 mM glutamine, 100 units/ml penicillin and 100 μ g/ml streptomycin. Estrogen-depleted medium consisted of DMEM without phenol red supplemented with 10% charcoal filtered FBS. MCF7 cells stably expressing an shRNA targeting p53 (MCF7-p53i), or control cells (MCF7-vector), were kindly provided by Dr. Agami.³⁶ Media and reagents were supplied by BioWhittaker[®] or Invitrogen. MCF7

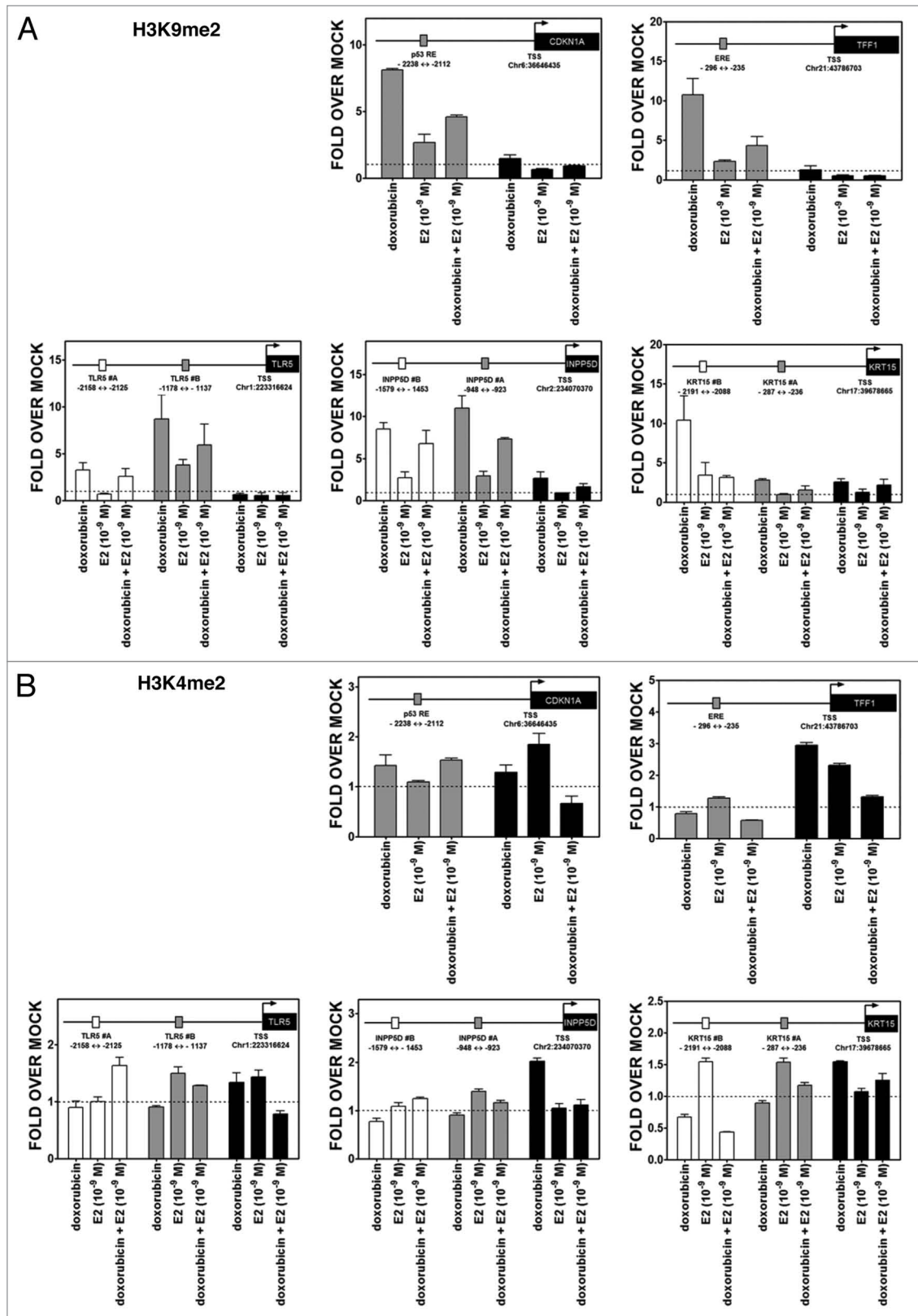


Figure 7. Treatment-induced histone methylation changes at TLR5A, INPP5D and KRT15 promoter regions. Chromatin immunoprecipitation assays were performed using antibodies against H3K9me2 (07–441, Millipore) (A) or HeK4me2 (07–030) (B). IgG was used as control (sc-2027, Santa Cruz). Two or three regions of the promoter containing established or predicted p53 REs and EREs and the TSS were examined by quantitative PCR analysis. The distance from TSS of the promoter portions is indicated (see also Fig. 6A). Presented for each amplicon are average and standard deviation of changes relative to the mock condition. The colors of the bars indicate the promoter regions that were amplified and match the boxes that are placed in the schematic drawing of the genes on the top of each figure. The distance from TSS of the promoter regions that were examined is indicated.

cells were treated with 1.5 μM doxorubicin (DOX) or 375 μM 5-fluorouracil (5FU) or 10 μM nutlin-3a for p53 stabilization, $\pm 10^{-9}/10^{-7}$ M 17 β -estradiol. Stock solutions were dissolved in 100% DMSO for 5FU (0.5 M) and nutlin-3a (10 mM), H₂O for DOX (10 mM) and 100% EtOH for E2 (10⁻³ M). DOX, 5FU and E2 were purchased from Sigma-Aldrich®; Nutlin-3a was obtained from Alexis® Biochemicals (Enzo Life Sciences). All treatments were done with cells at 70–80% confluence.

Antibodies and western blot analysis. Antibodies used for ChIP assays and western blotting analysis were: p53 (DO-1), ER α (H-184), Actin (I-19 or C-11) and IgG (sc-2025 or sc-2027) (Santa Cruz Biotechnology®) Anti-dimethyl-Histone H3 (Lys9) (07–441), anti-dimethyl-Histone H3 (Lys4) (07–030), anti-acetyl-Histone H3 (06–599), anti-acetyl-Histone H4 (06–866), anti-Histone H3 (06–755) antibodies (Millipore). Proteins were extracted using RIPA buffer supplemented with protease inhibitors and quantified using the BCA assay (Thermo Scientific, Pierce Protein Research Products). Proteins separated on 12% SDS-PAGE gels were transferred to a nitrocellulose membrane (GE Healthcare) using an iBlot® Dry Blotting System (Invitrogen™, Life Technology) and checked by Ponceau S staining. Membranes were blocked using 5% skim milk + PBS-Tween20 (0.1%) for 1 h at RT and probed with primary antibodies in 1% skim milk + PBS-Tween20. Immune complexes were visualized using Amersham ECL™ Advance WB Detection Kit (GE Healthcare) or SuperSignal West Pico Chemiluminescent Substrate (Thermo Scientific). The relative molecular mass of the immunoreactive bands was determined using PageRuler™ Plus Prestained Protein Ladder (Fermentas).

Microarray hybridization and scanning, data acquisition and analysis. Cells were seeded and treated on 10 cm Petri dishes. Total RNA was extracted from 3–7 biological replicates using the Agilent Total RNA Isolation Mini Kit (Agilent Technologies) according to the manufacturer's protocol. RNA was quantified using the NanoDrop spectrophotometer (NanoDrop Technologies), and quality was checked by gel electrophoresis as well as Agilent 2100 Bioanalyzer. Details on labeling, hybridization, analysis of TIFF images by Agilent Feature Extraction and the R software environment for statistical computing and the Bioconductor library of biostatistical packages are provided with the Gene Expression Omnibus (GEO) (www.ncbi.nlm.nih.gov/geo/) submission (GSE24065). Briefly, hybridization, blocking and washing were performed according to Agilent protocol "One-Color Microarray-Based Gene Expression Analysis (Quick Amp Labeling)." Hybridized microarray slides (Agilent-014850 Whole Human Genome Microarray 4 × 44 K G4112F-Probe Name version) were then scanned with an Agilent DNA Microarray Scanner (G2505C) at 5-micron resolution with the manufacturer's software (Agilent ScanControl 8.1.3).

The scanned TIFF images were analyzed numerically for data extraction, background correction and flagging of non-uniform features using the Agilent Feature Extraction Software version 10.7.7.1 according to the Agilent standard protocol GE1_107_Sep09. The output of Feature Extraction was analyzed with the R software environment for statistical computing and the

Bioconductor library of biostatistical packages. Probes with low signals were removed in order to filter out the constantly unexpressed genes and keep only probes flagged as present in the majority of replicates in at least one condition. Signal intensities across arrays were normalized with the quantile normalization algorithm. In order to select differentially expressed genes, every condition corresponding to a treatment was first compared with the mock treatment. Three thresholds were set in order to select differentially expressed genes for each comparison: (1) t-test unpaired unequal variance p value < 0.01; (2) rank product percentage of false positive (pfp) < 0.05;⁷² (3) absolute log₂ (fold change) > log₂(2).

Using the DAVID resource,³² a functional annotation clustering analysis (enrichment score ≥ 1.5 , medium classification stringency) was performed on the lists of differentially expressed genes corresponding to each treatment.

Genes upregulated by the concomitant treatment of doxorubicin and E2 (10⁻⁹ M) with more than an additive effect were identified among those satisfying the condition $\log_2[\text{FC}_{\text{double treatment}}] > 2$ (a parameter allowing us for a more reasonable validation) subtracting the 2-fold changes corresponding to the single treatments to the fold change corresponding to the double treatment and selecting those with a positive result: $(\log_2[\text{FC}_{\text{double treatment}}] - \log_2[\text{FC}_{\text{DOX}}] - \log_2[\text{FC}_{\text{E2}}]) > 0.1$ (Table S2).

Quantitative real-time PCR (qPCR). One μg of total RNA was reverse transcribed in 20 μl of reaction using the "RevertAid™ First Strand cDNA Synthesis Kit" (Fermentas) or TaqMan reverse transcription reagents from Applied Biosystems. qPCR was performed using 384-well plates in a final volume of 10 μl either on a CFX384 Touch™ Real-Time PCR Detection Systems (Bio-Rad) or on the ABI prism HT7900 system (Applied Biosystems). KAPA Probe FAST qPCR Kit/TaqMan Universal PCR Master Mix (Applied Biosystems) or KAPA SYBR® FAST qPCR Kit (Kapa Biosystems, Resnova) was used to perform the reaction together with TaqMan® Gene Expression Assays (Applied Biosystem™, Life Technology) or primers purchased from Eurofins (MWG, Operon). Relative mRNA quantification was obtained using the comparative Ct method ($\Delta\Delta\text{Ct}$), where glyceraldehyde 3-phosphate dehydrogenase (GAPDH), β -2microglobulin (B2M) or β -actin genes served as internal controls. Calculations were performed using QbasePLUS software (Biogazelle) that uses the geNorm method⁷³ to evaluate the expression stability of candidate reference genes.

A statistical analysis considering the log₂ of the fold-induction was used to confirm the synergistic effect. The means of two normally distributed populations composed of $\log_2[\text{FC}_{\text{double treatment}}]$ and $\log_2[\text{FC}_{\text{DOX}}] + \log_2[\text{FC}_{\text{E2}}]$ were analyzed using a t-test approach ($p < 0.05$). The logarithmic values can flatten the differences between the fold change values on one hand but, on the other hand, can make the results of our analysis more robust. The sum of logarithms is comparable to the multiplication of the fold changes and the subtraction of logarithms to the ratio of the fold-changes.

Promoter pattern searches. An in silico analysis was performed in order to identify putative canonical or non-canonical p53 and ER α response elements (REs) couples with a maximum

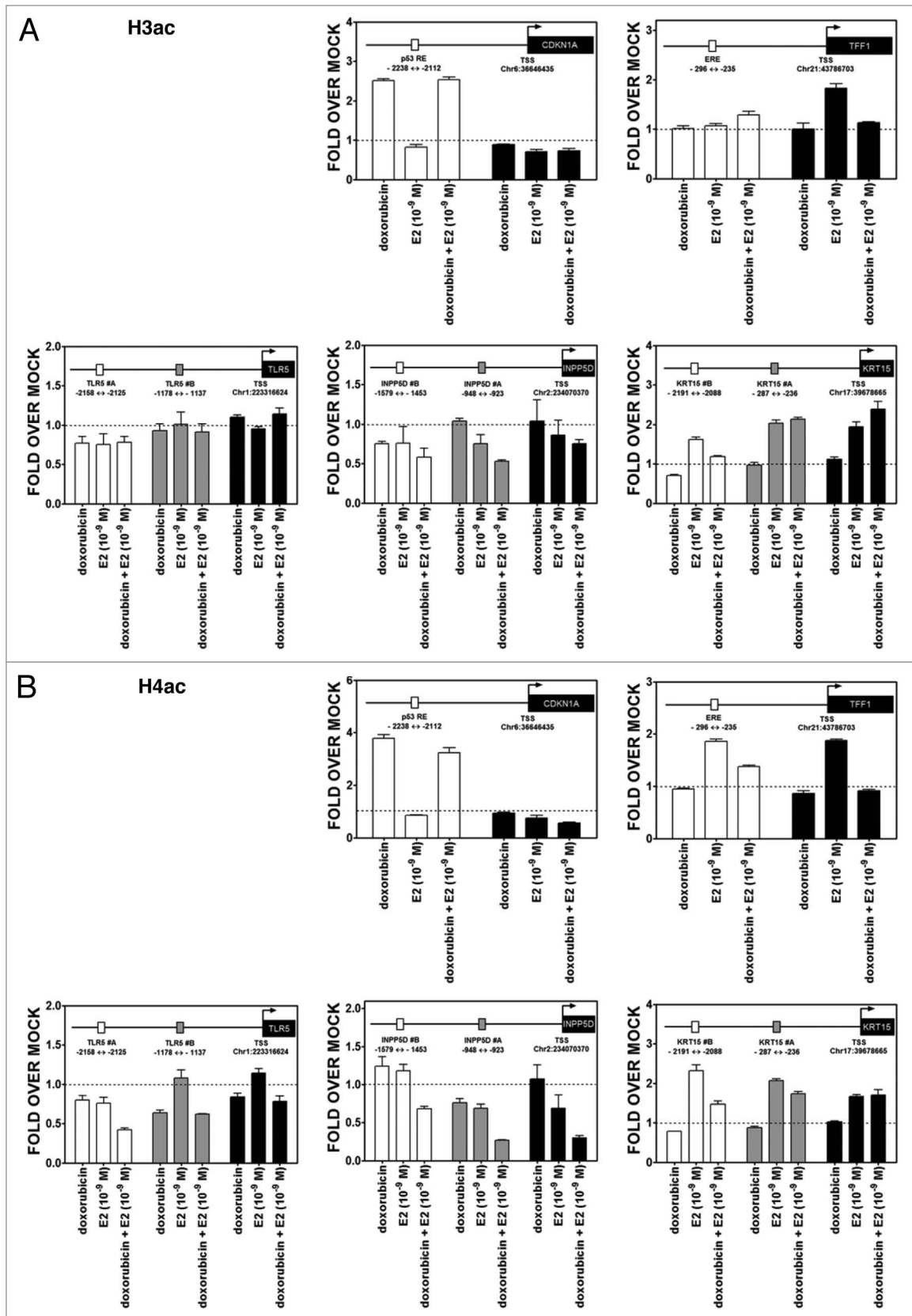


Figure 8. Treatment-induced histone acetylation changes at TLR5A, INPP5D and KRT15 promoter regions. Chromatin immunoprecipitation assays were performed using antibodies against pan-H3Ac (06–599, Millipore) (A) or pan-H4Ac (06–866) (B), as described for Figures 6 and 7. The colors of the bars indicate the promoter regions that were amplified and match the boxes that are placed in the schematic drawing of the genes on the top of each figure. The distance from TSS of the promoter regions that were examined is indicated.

distance of around 500 bp within the promoters of the selected genes. Three different approaches were used and combined: (1) pattern matching analysis ($\frac{1}{2}$ p53 RE: RRRCWWGYYY; $\frac{1}{2}$ ER α RE: (A)GGTCA, TGACC(T) or GGCTA), (2) RSAT analysis⁷⁴ and (3) R tool analysis using TransFac matrixes.

Chromatin immunoprecipitation (ChIP) assay. MCF7 cells were cultured in estrogen-depleted conditions in a 150-mm Petri dish and treated for 10 h with DOX and/or the physiological concentration of E2 (10^{-9} M). The procedure for crosslinking, sonication, IP and analysis followed a previously described protocol.^{23,24,35}

Disclosure of Potential Conflicts of Interest

No potential conflicts of interest were disclosed.

References

1. Espinosa JM. Mechanisms of regulatory diversity within the p53 transcriptional network. *Oncogene* 2008; 27:4013-23; PMID:18278067; <http://dx.doi.org/10.1038/onc.2008.37>
2. Pan Y, Tsai CJ, Ma B, Nussinov R. Mechanisms of transcription factor selectivity. *Trends Genet* 2010; 26:75-83; PMID:20074831; <http://dx.doi.org/10.1016/j.tig.2009.12.003>
3. Bode AM, Dong Z. Post-translational modification of p53 in tumorigenesis. *Nat Rev Cancer* 2004; 4:793-805; PMID:15510160; <http://dx.doi.org/10.1038/nrc1455>
4. Levine AJ, Oren M. The first 30 years of p53: growing ever more complex. *Nat Rev Cancer* 2009; 9:749-58; PMID:19776744; <http://dx.doi.org/10.1038/nrc2723>
5. Menendez D, Inga A, Resnick MA. Potentiating the p53 network. *Discov Med* 2010; 10:94-100; PMID:20670604
6. Vousden KH, Prives C. Blinded by the Light: The Growing Complexity of p53. *Cell* 2009; 137:413-31; PMID:19410540; <http://dx.doi.org/10.1016/j.cell.2009.04.037>
7. Vousden KH, Ryan KM. p53 and metabolism. *Nat Rev Cancer* 2009; 9:691-700; PMID:19759539; <http://dx.doi.org/10.1038/nrc2715>
8. Dahlman-Wright K, Cavailles V, Fuqua SA, Jordan VC, Katzenellenbogen JA, Korach KS, et al. International Union of Pharmacology. LXIV. Estrogen receptors. *Pharmacol Rev* 2006; 58:773-81; PMID:17132854; <http://dx.doi.org/10.1124/pr.58.4.8>
9. Deroo BJ, Korach KS. Estrogen receptors and human disease. *J Clin Invest* 2006; 116:561-70; PMID:16511588; <http://dx.doi.org/10.1172/JCI27987>
10. Heldring N, Pike A, Andersson S, Matthews J, Cheng G, Hartman J, et al. Estrogen receptors: how do they signal and what are their targets. *Physiol Rev* 2007; 87:905-31; PMID:17615392; <http://dx.doi.org/10.1152/physrev.00026.2006>
11. Konduri SD, Medisetty R, Liu W, Kaiparettu BA, Srivastava P, Brauch H, et al. Mechanisms of estrogen receptor antagonism toward p53 and its implications in breast cancer therapeutic response and stem cell regulation. *Proc Natl Acad Sci USA* 2010; 107:15081-6; PMID:20696891; <http://dx.doi.org/10.1073/pnas.1009575107>
12. Liu W, Ip MM, Podgorsak MB, Das GM. Disruption of estrogen receptor α -p53 interaction in breast tumors: a novel mechanism underlying the anti-tumor effect of radiation therapy. *Breast Cancer Res Treat* 2009; 115:43-50; PMID:18481172; <http://dx.doi.org/10.1007/s10549-008-0044-z>

13. Liu W, Konduri SD, Bansal S, Nayak BK, Rajasekaran SA, Karuppaiyl SM, et al. Estrogen receptor- α binds p53 tumor suppressor protein directly and represses its function. *J Biol Chem* 2006; 281:9837-40; PMID:16469747; <http://dx.doi.org/10.1074/jbc.C600001200>
14. Sayeed A, Konduri SD, Liu W, Bansal S, Li F, Das GM. Estrogen receptor α inhibits p53-mediated transcriptional repression: implications for the regulation of apoptosis. *Cancer Res* 2007; 67:7746-55; PMID:17699779; <http://dx.doi.org/10.1158/0008-5472.CAN-06-3724>
15. Liu G, Schwartz JA, Brooks SC. p53 down-regulates ER-responsive genes by interfering with the binding of ER to ERE. *Biochem Biophys Res Commun* 1999; 264:359-64; PMID:10529369; <http://dx.doi.org/10.1006/bbrc.1999.1525>
16. Yu CL, Driggers P, Barrera-Hernandez G, Nunez SB, Segars JH, Cheng Sy. The tumor suppressor p53 is a negative regulator of estrogen receptor signaling pathways. *Biochem Biophys Res Commun* 1997; 239:617-20; PMID:9344880; <http://dx.doi.org/10.1006/bbrc.1997.7522>
17. Fernández-Cuesta L, Anaganti S, Hainaut P, Olivier M. Estrogen levels act as a rheostat on p53 levels and modulate p53-dependent responses in breast cancer cell lines. *Breast Cancer Res Treat* 2011; 125:35-42; PMID:20221692; <http://dx.doi.org/10.1007/s10549-010-0819-x>
18. Angeloni SV, Martin MB, Garcia-Morales P, Castro-Galache MD, Ferragut JA, Saceda M. Regulation of estrogen receptor- α expression by the tumor suppressor gene p53 in MCF-7 cells. *J Endocrinol* 2004; 180:497-504; PMID:15012604; <http://dx.doi.org/10.1677/joc.0.1800497>
19. Miller LD, Smeds J, George J, Vega VB, Vergara L, Ploner A, et al. An expression signature for p53 status in human breast cancer predicts mutation status, transcriptional effects, and patient survival. *Proc Natl Acad Sci USA* 2005; 102:13550-5; PMID:16141321; <http://dx.doi.org/10.1073/pnas.0506230102>
20. Olivier M, Langerød A, Carrieri P, Bergh J, Klaar S, Eystjord J, et al. The clinical value of somatic TP53 gene mutations in 1,794 patients with breast cancer. *Clin Cancer Res* 2006; 12:1157-67; PMID:16489069; <http://dx.doi.org/10.1158/1078-0432.CCR-05-1029>
21. Duong V, Boule N, Daujat S, Chauvet J, Bonnet S, Neel H, et al. Differential regulation of estrogen receptor α turnover and transactivation by Mdm2 and stress-inducing agents. *Cancer Res* 2007; 67:5513-21; PMID:17545634; <http://dx.doi.org/10.1158/0008-5472.CAN-07-0967>
22. Kim K, Burghardt R, Barhoumi R, Lee SO, Liu X, Safe S. MDM2 regulates estrogen receptor α and estrogen responsiveness in breast cancer cells. *J Mol Endocrinol* 2011; 46:67-79; PMID:21169420

Acknowledgments

We thank Dr. Valentina Adami for technical assistance with the microarray experiments. This work was partially supported by the Italian Association for Cancer Research, AIRC (#IG9086 to AI), by CIBIO start-up funds and by the Intramural Research Program of the NIEHS (to D.M. and M.A.R.: Z01 ES065079). M.L. is a Ph.D. Fellow of the International Doctorate in Biomolecular Sciences, University of Trento. Y.C. is supported by a Marie-Curie/Autonomous-Province-of-Trento (PAT) co-fund grant (#40101712).

Supplemental Materials

Supplemental materials may be found here:
www.landesbioscience.com/journals/cc/article/24309

23. Ciribilli Y, Andreotti V, Menendez D, Langen JS, Schoenfelder G, Resnick MA, et al. The coordinated p53 and estrogen receptor cis-regulation at an FLT1 promoter SNP is specific to genotoxic stress and estrogenic compound. *PLoS ONE* 2010; 5:e10236; PMID:20422012; <http://dx.doi.org/10.1371/journal.pone.0010236>
24. Menendez D, Inga A, Snipe J, Krysiak O, Schönfelder G, Resnick MA. A single-nucleotide polymorphism in a half-binding site creates p53 and estrogen receptor control of vascular endothelial growth factor receptor 1. *Mol Cell Biol* 2007; 27:2590-600; PMID:17242190; <http://dx.doi.org/10.1128/MCB.01742-06>
25. Menendez D, Inga A, Resnick MA. The expanding universe of p53 targets. *Nat Rev Cancer* 2009; 9:724-37; PMID:19776742; <http://dx.doi.org/10.1038/nrc2730>
26. Menendez D, Inga A, Resnick MA. Estrogen receptor acting in cis enhances WT and mutant p53 transactivation at canonical and noncanonical p53 target sequences. *Proc Natl Acad Sci USA* 2010; 107:1500-5; PMID:20080630; <http://dx.doi.org/10.1073/pnas.0909129107>
27. Menendez D, Krysiak O, Inga A, Krysiak B, Resnick MA, Schönfelder G. A SNP in the flt-1 promoter integrates the VEGF system into the p53 transcriptional network. *Proc Natl Acad Sci USA* 2006; 103:1406-11; PMID:16432214; <http://dx.doi.org/10.1073/pnas.0508103103>
28. Carroll JS, Brown M. Estrogen receptor target gene: an evolving concept. *Mol Endocrinol* 2006; 20:1707-14; PMID:16396959; <http://dx.doi.org/10.1210/me.2005-0334>
29. Gruber CJ, Gruber DM, Gruber IML, Wieser F, Huber JC. Anatomy of the estrogen response element. *Trends in Endocrinology & Metabolism* 2004; 15:73-8
30. Joshi SR, Ghattamaneni RB, Scovell WM. Expanding the paradigm for estrogen receptor binding and transcriptional activation. *Mol Endocrinol* 2011; 25:980-94; PMID:21527498; <http://dx.doi.org/10.1210/me.2010-0302>
31. Cheok CF, Verma CS, Baselga J, Lane DP. Translating p53 into the clinic. *Nat Rev Clin Oncol* 2011; 8:25-37; PMID:20975744; <http://dx.doi.org/10.1038/nrclinonc.2010.174>
32. Huang DW, Sherman BT, Lempicki RA. Systematic and integrative analysis of large gene lists using DAVID bioinformatics resources. *Nat Protoc* 2008; 4:44-57; <http://dx.doi.org/10.1038/nprot.2008.211>
33. Kuhn M, Szklarczyk D, Franceschini A, Campillos M, von Mering C, Jensen LJ, et al. STITCH 2: an interaction network database for small molecules and proteins. *Nucleic Acids Res* 2010; 38(Database issue):D552-6; PMID:19897548; <http://dx.doi.org/10.1093/nar/gkp937>

34. Jin YJ, Wang J, Qiao C, Hei TK, Brandt-Rauf PW, Yin Y. A novel mechanism for p53 to regulate its target gene ECK1 in signaling apoptosis. *Mol Cancer Res* 2006; 4:769-78; PMID:17050670; <http://dx.doi.org/10.1158/1541-7786.MCR-06-0178>
35. Menendez D, Shatz M, Azzam K, Garantzios S, Fessler MB, Resnick MA. The Toll-like receptor gene family is integrated into human DNA damage and p53 networks. *PLoS Genet* 2011; 7:e1001360; PMID:21483755; <http://dx.doi.org/10.1371/journal.pgen.1001360>
36. Brummelkamp TR, Bernards R, Agami R. A system for stable expression of short interfering RNAs in mammalian cells. *Science* 2002; 296:550-3; PMID:11910072; <http://dx.doi.org/10.1126/science.1068999>
37. Subik K, Lee JF, Baxter L, Strzepek T, Costello D, Crowley P, et al. The Expression Patterns of ER, PR, HER2, CK5/6, EGFR, Ki-67 and AR by Immunohistochemical Analysis in Breast Cancer Cell Lines. *Breast Cancer (Auckl)* 2010; 4:35-41; PMID:20697531
38. Munster PN, Carpenter JT. Estradiol in breast cancer treatment: reviving the past. *JAMA* 2009; 302:797-8; PMID:19690316; <http://dx.doi.org/10.1001/jama.2009.1223>
39. Azmi AS, Banerjee S, Ali S, Wang Z, Bao B, Beck FW, et al. Network modeling of MDM2 inhibitor-oxaliplatin combination reveals biological synergy in wt-p53 solid tumors. *Oncotarget* 2011; 2:378-92; PMID:21623005
40. Deng XS, Wang S, Deng A, Liu B, Edgerton SM, Lind SE, et al. Metformin targets Stat3 to inhibit cell growth and induce apoptosis in triple-negative breast cancers. *Cell Cycle* 2012; 11:367-76; PMID:22189713; <http://dx.doi.org/10.4161/cc.11.2.18813>
41. Jiang Z, Jones R, Liu JC, Deng T, Robinson T, Chung PE, et al. RB1 and p53 at the crossroad of EMT and triple-negative breast cancer. *Cell Cycle* 2011; 10:1563-70; PMID:21502814; <http://dx.doi.org/10.4161/cc.10.10.15703>
42. Troester MA, Hoadley KA, Parker JS, Perou CM. Prediction of toxicant-specific gene expression signatures after chemotherapeutic treatment of breast cell lines. *Environ Health Perspect* 2004; 112:1607-13; PMID:15598611; <http://dx.doi.org/10.1289/ehp.7204>
43. Liu Q, Dumont DJ. Molecular cloning and chromosomal localization in human and mouse of the SH2-containing inositol phosphatase, INPP5D (SHIP). Amgen EST Program. *Genomics* 1997; 39:109-12; PMID:9027494; <http://dx.doi.org/10.1006/geno.1996.4374>
44. Kerley-Hamilton JS, Pike AM, Li N, DiRenzo J, Spinnella MJ. A p53-dominant transcriptional response to cisplatin in testicular germ cell tumor-derived human embryonal carcinoma. *Oncogene* 2005; 24:6090-100; PMID:15940259; <http://dx.doi.org/10.1038/sj.onc.1208755>
45. Badock V, Steinhilber U, Bommert K, Wittmann-Liebold B, Otto A. Apoptosis-induced cleavage of keratin 15 and keratin 17 in a human breast epithelial cell line. *Cell Death Differ* 2001; 8:308-15; PMID:11319614; <http://dx.doi.org/10.1038/sj.cdd.4400812>
46. Bailey ST, Shin H, Westerling T, Liu XS, Brown M. Estrogen receptor prevents p53-dependent apoptosis in breast cancer. *Proc Natl Acad Sci USA* 2012; 109:18060-5; PMID:23077249; <http://dx.doi.org/10.1073/pnas.1018858109>
47. Kooistra SM, Helin K. Molecular mechanisms and potential functions of histone demethylases. *Nat Rev Mol Cell Biol* 2012; 13:297-311; PMID:22473470
48. Mund A, Schubert T, Staeger H, Kinkley S, Reumann K, Kriegs M, et al. SPOC1 modulates DNA repair by regulating key determinants of chromatin compaction and DNA damage response. *Nucleic Acids Res* 2012; 40:11363-79; PMID:23034801; <http://dx.doi.org/10.1093/nar/gks868>
49. Sulli G, Di Micco R, d'Adda di Fagagna F. Crosstalk between chromatin state and DNA damage response in cellular senescence and cancer. *Nat Rev Cancer* 2012; 12:709-20; PMID:22952011; <http://dx.doi.org/10.1038/nrc3344>
50. Lee DY, Northrop JP, Kuo MH, Stallcup MR. Histone H3 lysine 9 methyltransferase G9a is a transcriptional coactivator for nuclear receptors. *J Biol Chem* 2006; 281:8476-85; PMID:16461774; <http://dx.doi.org/10.1074/jbc.M511093200>
51. An W, Kim J, Roeder RG. Ordered cooperative functions of PRMT1, p300, and CARM1 in transcriptional activation by p53. *Cell* 2004; 117:735-48; PMID:15186775; <http://dx.doi.org/10.1016/j.cell.2004.05.009>
52. Cloos PA, Christensen J, Agger K, Helin K. Erasing the methyl mark: histone demethylases at the center of cellular differentiation and disease. *Genes Dev* 2008; 22:1115-40; PMID:18451103; <http://dx.doi.org/10.1101/gad.1652908>
53. Garcia-Bassets I, Kwon YS, Teles F, Prefontaine GG, Hutt KR, Cheng CS, et al. Histone methylation-dependent mechanisms impose ligand dependency for gene activation by nuclear receptors. *Cell* 2007; 128:505-18; PMID:17289570; <http://dx.doi.org/10.1016/j.cell.2006.12.038>
54. Huang J, Sengupta R, Espejo AB, Lee MG, Dorsey JA, Richter M, et al. p53 is regulated by the lysine demethylase LSD1. *Nature* 2007; 449:105-8; PMID:17805299; <http://dx.doi.org/10.1038/nature06092>
55. Tsai WW, Nguyen TT, Shi Y, Barton MC. p53-targeted LSD1 functions in repression of chromatin structure and transcription in vivo. *Mol Cell Biol* 2008; 28:5139-46; PMID:18573881; <http://dx.doi.org/10.1128/MCB.00287-08>
56. Espinosa JM, Emerson BM. Transcriptional regulation by p53 through intrinsic DNA/chromatin binding and site-directed cofactor recruitment. *Mol Cell* 2001; 8:57-69; PMID:11511360; [http://dx.doi.org/10.1016/S1097-2765\(01\)00283-0](http://dx.doi.org/10.1016/S1097-2765(01)00283-0)
57. Hanstein B, Eckner R, DiRenzo J, Halachmi S, Liu H, Searcy B, et al. p300 is a component of an estrogen receptor coactivator complex. *Proc Natl Acad Sci USA* 1996; 93:11540-5; PMID:8876171; <http://dx.doi.org/10.1073/pnas.93.21.11540>
58. Collavin L, Lunardi A, Del Sal G. p53-family proteins and their regulators: hubs and spokes in tumor suppression. *Cell Death Differ* 2010; 17:901-11; PMID:20379196; <http://dx.doi.org/10.1038/cdd.2010.35>
59. Poyurovsky MV, Katz C, Laptchenko O, Beckerman R, Lokshin M, Ahn J, et al. The C terminus of p53 binds the N-terminal domain of MDM2. *Nat Struct Mol Biol* 2010; 17:982-9; PMID:20639885; <http://dx.doi.org/10.1038/nsmb.1872>
60. Berteaux N, Lottin S, Monté D, Pinte S, Quatannens B, Coll J, et al. H19 mRNA-like noncoding RNA promotes breast cancer cell proliferation through positive control by E2F1. *J Biol Chem* 2005; 280:29625-36; PMID:15985428; <http://dx.doi.org/10.1074/jbc.M504033200>
61. Wang J, Fu L, Gu F, Ma Y. Notch1 is involved in migration and invasion of human breast cancer cells. *Oncol Rep* 2011; 26:1295-303; PMID:21785827
62. Noetzel E, Rose M, Sevinc E, Hilgers RD, Hartmann A, Naami A, et al. Intermediate filament dynamics and breast cancer: aberrant promoter methylation of the Synemin gene is associated with early tumor relapse. *Oncogene* 2010; 29:4814-25; PMID:20543860; <http://dx.doi.org/10.1038/ncr.2010.229>
63. Cai Z, Sanchez A, Shi Z, Zhang T, Liu M, Zhang D. Activation of Toll-like receptor 5 on breast cancer cells by flagellin suppresses cell proliferation and tumor growth. *Cancer Res* 2011; 71:2466-75; PMID:21427357; <http://dx.doi.org/10.1158/0008-5472.CAN-10-1993>
64. Cowin P, Rowlands TM, Hatsell SJ. Cadherins and catenins in breast cancer. *Curr Opin Cell Biol* 2005; 17:499-508; PMID:16107313; <http://dx.doi.org/10.1016/j.ccb.2005.08.014>
65. Udayakumar D, Zhang G, Ji Z, Njauw CN, Mroz P, Tsao H. EphA2 is a critical oncogene in melanoma. *Oncogene* 2011; 30:4921-9; PMID:21666714; <http://dx.doi.org/10.1038/ncr.2011.210>
66. Zhang G, Njauw CN, Park JM, Naruse C, Asano M, Tsao H. EphA2 is an essential mediator of UV radiation-induced apoptosis. *Cancer Res* 2008; 68:1691-6; PMID:18339848; <http://dx.doi.org/10.1158/0008-5472.CAN-07-2372>
67. Salomoni P, Pandolfi PP. The role of PML in tumor suppression. *Cell* 2002; 108:165-70; PMID:11832207; [http://dx.doi.org/10.1016/S0092-8674\(02\)00626-8](http://dx.doi.org/10.1016/S0092-8674(02)00626-8)
68. Luo JM, Liu ZL, Hao HL, Wang FX, Dong ZR, Ohno R. Mutation analysis of SHIP gene in acute leukemia. *Zhongguo Shi Yan Xue Ye Xue Za Zhi* 2004; 12:420-6; PMID:15363123
69. Zhou MN, Kunttas-Tatli E, Zimmerman S, Zhouzheng F, McCartney BM. Cortical localization of APC2 plays a role in actin organization but not in Wnt signaling in Drosophila. *J Cell Sci* 2011; 124:1589-600; PMID:21486956; <http://dx.doi.org/10.1242/jcs.073916>
70. Shetty PJ, Movva S, Pasupuleti N, Vedicherla B, Vattam KK, Venkatasubramanian S, et al. Regulation of IGF2 transcript and protein expression by altered methylation in breast cancer. *J Cancer Res Clin Oncol* 2011; 137:339-45; PMID:20422427; <http://dx.doi.org/10.1007/s00432-010-0890-z>
71. Uhlen M, Oksvold P, Fagerberg L, Lundberg E, Jonasson K, Forsberg M, et al. Towards a knowledge-based Human Protein Atlas. *Nat Biotechnol* 2010; 28:1248-50; PMID:21139605; <http://dx.doi.org/10.1038/nbt1210-1248>
72. Breitling R, Armengaud P, Amtmann A, Herzyk P. Rank products: a simple, yet powerful, new method to detect differentially regulated genes in replicated microarray experiments. *FEBS Lett* 2004; 573:83-92; PMID:15327980; <http://dx.doi.org/10.1016/j.febslet.2004.07.055>
73. Vandesompele J, De Preter K, Pattyn F, Poppe B, Van Roy N, De Paeppe A, et al. Accurate normalization of real-time quantitative RT-PCR data by geometric averaging of multiple internal control genes. *Genome Biol* 2002; 3(research0034.1-research.11):H0034; PMID:12184808; <http://dx.doi.org/10.1186/gb-2002-3-7-research0034>
74. Thomas-Chollier M, Defrance M, Medina-Rivera A, Sand O, Herrmann C, Thieffry D, et al. RSAT 2011: regulatory sequence analysis tools. *Nucleic Acids Res* 2011; 39(suppl):W86-91; PMID:21715389; <http://dx.doi.org/10.1093/nar/gkr377>

Lion et al., Supplemental figure legends, supplemental figures and tables

Figure S1. Cell Index Analysis to follow up treatment-specific toxicity. Impact of the chemicals and drugs used for our experimental approach was tested using the Real-Time Cell Analyzer (RTCA) DP supplied by Roche Applied Science, Milan, Italy. Cells were seeded onto an E-Plate 16 and allowed to reach 70–80% of confluence (checked by cell index value at ~22-24 hours) before treating them with drugs as described in *Materials and Methods*. The proliferation rate was checked in the first 10 hours of treatment. A cell index normalization was imposed at the time point before drug administration. Mock condition was used as baseline. Presented are the average and standard deviation of three replicates for each condition. A) 1.5 μ M doxorubicin B) 375 μ M 5-fluorouracil, C) 10 μ M nutlin-3a +/- 10⁻⁹ M 17 β -estradiol (E2).

Figure S2. Known and predicted associations for the 16 genes selected from the DOX + E2 DEGs with p53, ERs or the treatment drugs. The online Search Tool for Interactions of Chemicals (STITCH) network was used (<http://stitch.embl.de/>) (Kuhn et al., Nucleic Acids Research 2010). The confidence view is shown. Stronger associations are represented by thicker lines. The network nodes are either chemicals (represented as pills) or proteins (represented as spheres) and the network edges represent the predicted functional associations. Protein-protein interactions are shown in blue, chemical-protein interactions in green and interactions between chemicals in red. The prediction is based on text-mining obtained from the literature. The established p53 and ER targets CDKN1A, TFF1 and GREB1 were included for comparison. The connection with p53 and/or ER for most of the chosen 16 genes is novel or largely unexplored.

Figure S3. Treatment-induced changes in total histone 3 levels at TLR5A, INPP5D and KRT15 promoter regions. Chromatin Immunoprecipitation was performed using the anti-Histone H3 (06-755) (Millipore) antibody. IgG was used as control (sc-2027, Santa Cruz). Two or three regions of the promoter containing established or predicted p53 REs and EREs and the TSS were examined by quantitative PCR analysis. The distance from TSS of the promoter portions is indicated (see also Figure 6A). Presented for each amplicon are average and standard deviation of changes relative to the mock condition. PCR was carried out in 384-well plates in a final volume of 10 μ l –see Methods for details-. The colors of

the bars indicate the promoter regions that were amplified and match the boxes that are placed in the schematic drawing of the genes on the top of each figure. The distance from TSS of the promoter regions that were examined is indicated.

Figure S1

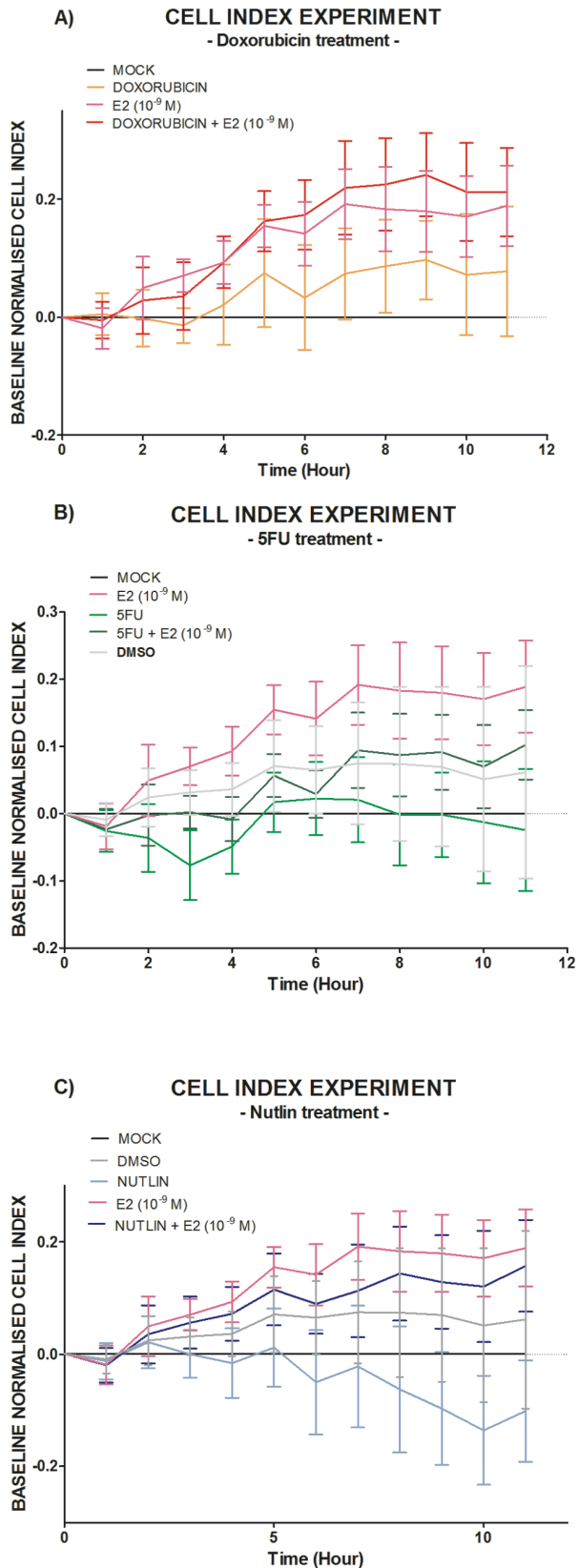


Figure S2

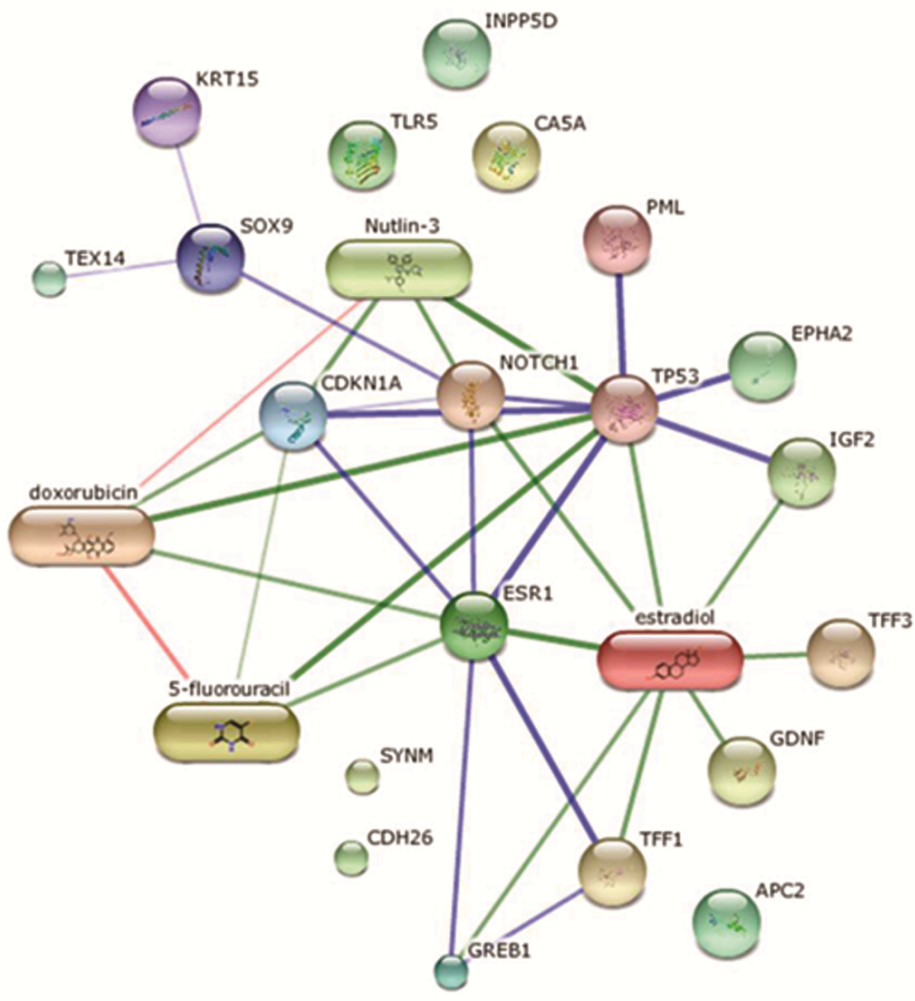


Figure S3

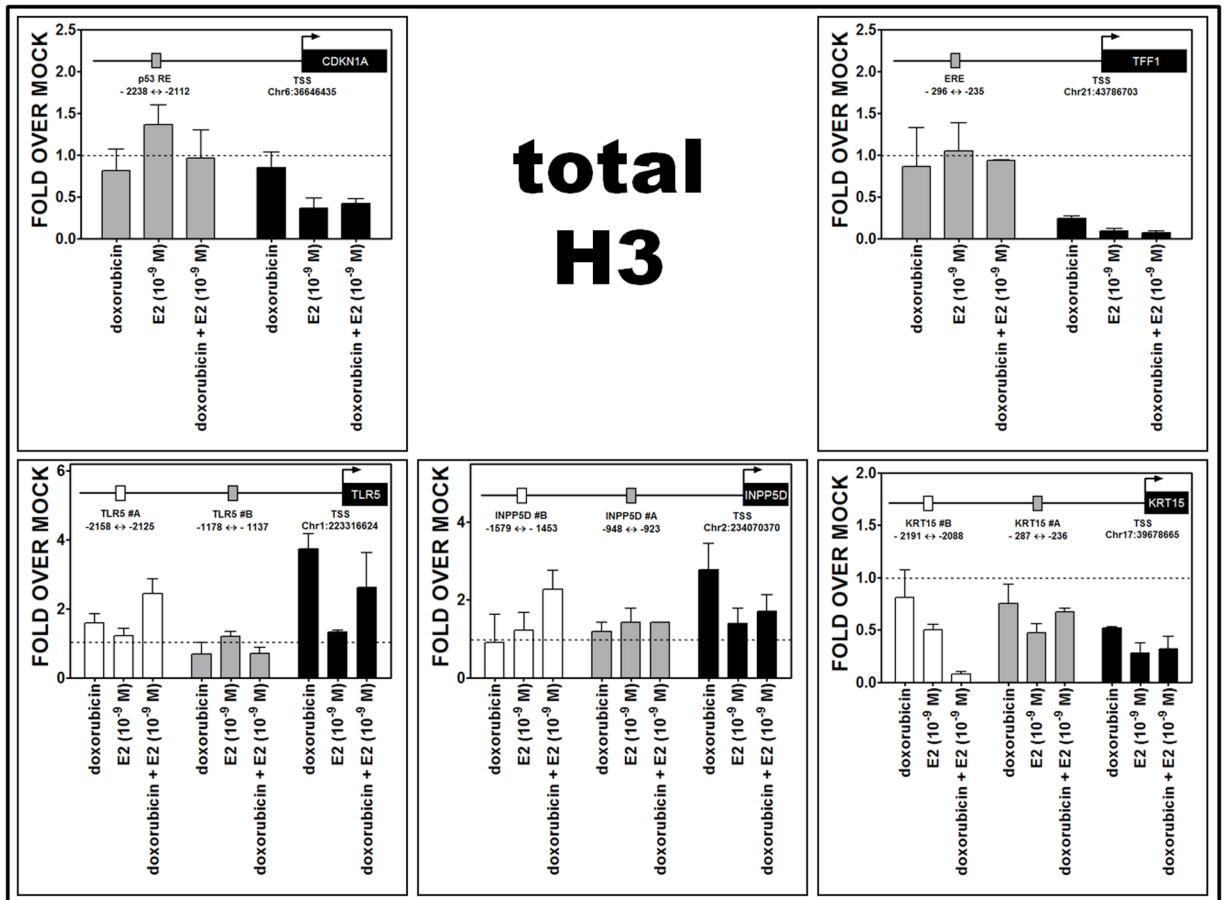


Table S1. Functional annotation clustering. Analyses were performed using the Ingenuity Pathway Analysis (IPA, <http://www.ingenuity.com>) as well as DAVID (<http://david.abcc.ncifcrf.gov/>; Huang et al., Nat. Protocols 2008) (enrichment score ≥ 1.5 , medium classification stringency) with default settings starting from the lists of differentially expressed genes corresponding to the treatment: A) E2 (10^{-9} M), B) E2 (10^{-7} M), C) doxorubicin (1.5 μ M), D) DOX + E2 (10^{-9} M), E) 66 unique up-regulated genes upon DOX + E2 (10^{-9} M) treatment, F) 167 unique down-regulated genes upon DOX + E2 (10^{-9} M) treatment, G) 27 up-regulated genes shared by DOX, E2 (10^{-9} M) and DOX+E2 (10^{-9} M), H) 54 repressed genes shared by DOX, E2 (10^{-9} M) and DOX+E2 (10^{-9} M), I) 201 genes with an additive effect in DOX + E2 (10^{-9} M) up-regulation condition, J) 142 genes with an additive effect in DOX + E2 (10^{-9} M) down-regulation condition. Results from DAVID functional cluster are summarized as a Table with the indicated enrichment score. Results from IPA Canonical Pathways and Upstream Regulators are presented as screen snapshots.

S 1A)**DAVID ANALYSIS**

E2 (10⁻⁹ M) FUNCTIONAL ANNOTATION CLUSTER	
Annotation Cluster	score
regulation of ossification	4.00
response to hormone stimulus	3.47
Bcl-2 proteins (BH domain)	3.46
regulation of apoptosis	3.41
negative regulation of apoptosis	3.08
insulin-like growth factor binding proteins (IGFBPs)	2.95
DNA replication	2.52
mesoderm development / morphogenesis	2.44
cytokine binding and control of the survival, growth and differentiation of tissues and cells	2.19
positive regulation of cell differentiation/cell development	2.16
chordate embryonic development	2.07
regulation of locomotion/cell migration	2.03
positive regulation of inflammatory response/ response to external stimulus	2.00
proteins with HLH domains	1.83
nucleotide-binding	1.78
protein dimerization activity	1.70
vasculature/blood vessel development	1.68
tube development	1.64
components of membrane fraction	1.62
positive regulation of ossification	1.53
proteins with SH ₂ domains	1.52

S 1A)

IPA UPSTREAM REGULATOR ANALYSIS

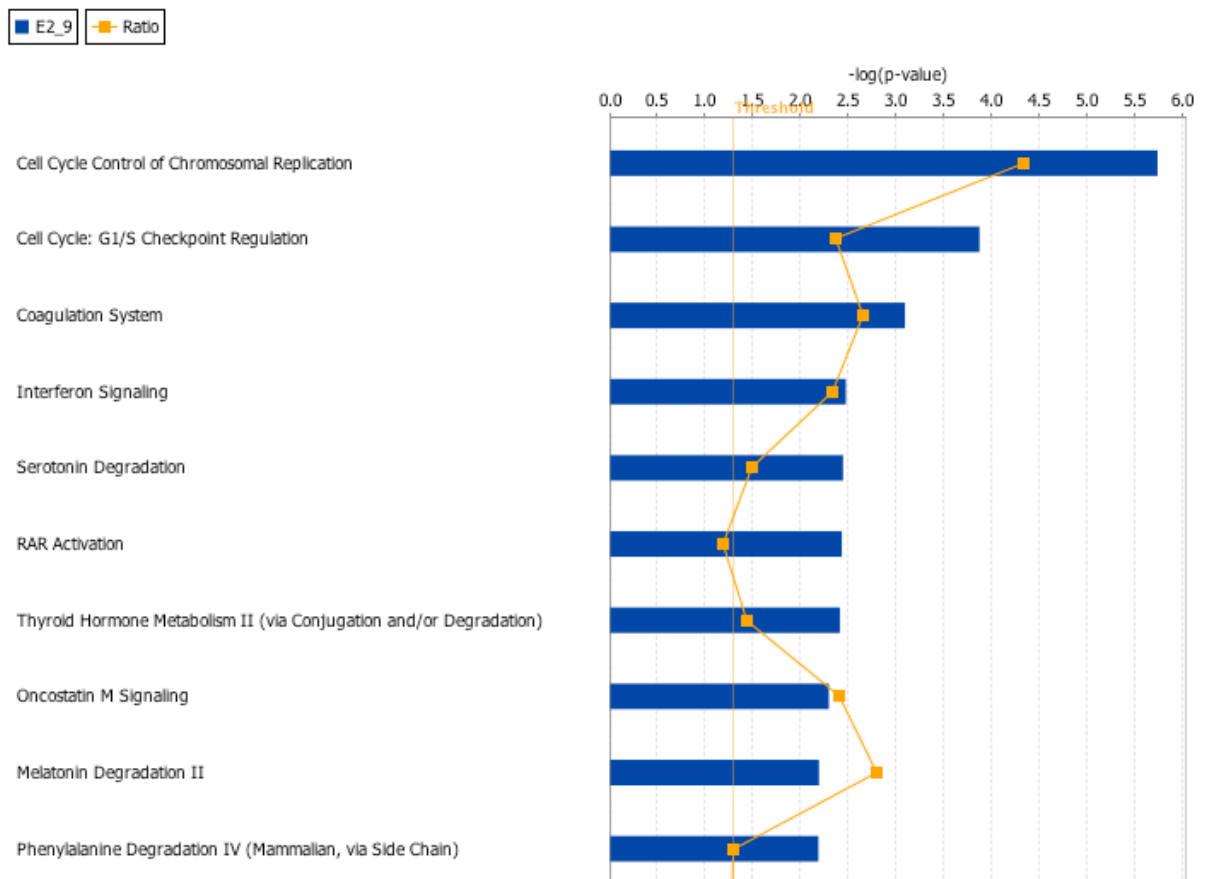
Presented in the first three columns are the names, function of upstream regulators that may be responsible for gene expression changes and their relative expression (Fold Change) observed in the data set. Predicted activity of these regulators with IPA-provided statistical assessment is included in column 4 and 5. A partial list of gene names and the total number in each group is also provided along with the Fisher's Exact Test results of the extent of overlap between DEGs and total number of genes considered as targets of the upstream regulator

Upstream Regulator	Log Ratio	Molecule Type	Predicted Activation State	Activation z-score	p-value of overlap	Target molecules in dataset
ESR1	↑ -0.545	ligand-dependent nuclear receptor	Activated	2.166	1.10E-11	↑ABCC5, ↑ADORA1, ↑BCL2, ↑CCNG2, ↑CXCL12, ↑DDIT4, ↑EFEMP1, ↑EF... ..all 28
ZNF217	↑ -0.837	transcription regulator	Activated	2.000	4.22E-05	↑ANK3, ↑CDKN2B, ↑FRK, ↑GAD1 (includes EGJ10000588), ↑GFEBP3, ↑MWC, ...all 10
LEF1	↑ 1.031	transcription regulator	Activated	2.213	7.95E-05	↑BCL2, ↑CASP9, ↑FGF18, ↑MTF, ↑MVC, ↑S6K1 ...all 8
NC0A3	↑ -0.862	transcription regulator	Activated	2.207	1.70E-03	↑BCL2, ↑CDC25A, ↑CDC6 (includes EG23834), ↑MCM7, ↑RGR ...all 5
TP53 (includes EG22059)	↑ 0.164	transcription regulator	Inhibited	-3.272	2.69E-05	↑AEN, ↑BIRC3, ↑BCL2, ↑BIK, ↑BRCA3, ↑BTG1, ↓DTG2, ↓CCNG2, ↓CDC25A, ...all 39
R81	↑ 0.128	transcription regulator	Inhibited	-2.470	8.94E-05	↑BCL2, ↑CDC25A, ↑CDC6 (includes EG23834), ↓CTED2, ↑TOS, ↓D1, ↑M... ..all 16
SMARCB1	↑ -0.027	transcription regulator	Inhibited	-2.789	6.20E-03	↑CDC6 (includes EG23834), ↑CKCR4, ↑HEV1, ↑MCM10 (includes EG307126), ...all 8
CDKN2A	↑ -0.915	transcription regulator	Inhibited	-2.155	2.06E-02	↑BCL2, ↑CDC25A, ↓CTED2, ↑E2F2, ↑MCM4, ↑MCM7, ↑PMEPA1, ↑TP63 ...all 8

S 1A)

IPA CANONICAL PATHWAYS

Canonical Pathways are displayed as bar chart. The $-\log(p \text{ value})$ results of a right-tailed Fisher's Exact Test is indicated. The ratio, calculated as number of genes in a given pathways that meet cut-off criteria divided by the total number of genes that make up the pathway, is overlaid as an orange line. The first 10 top pathways are shown.



S 1B)

DAVID ANALYSIS

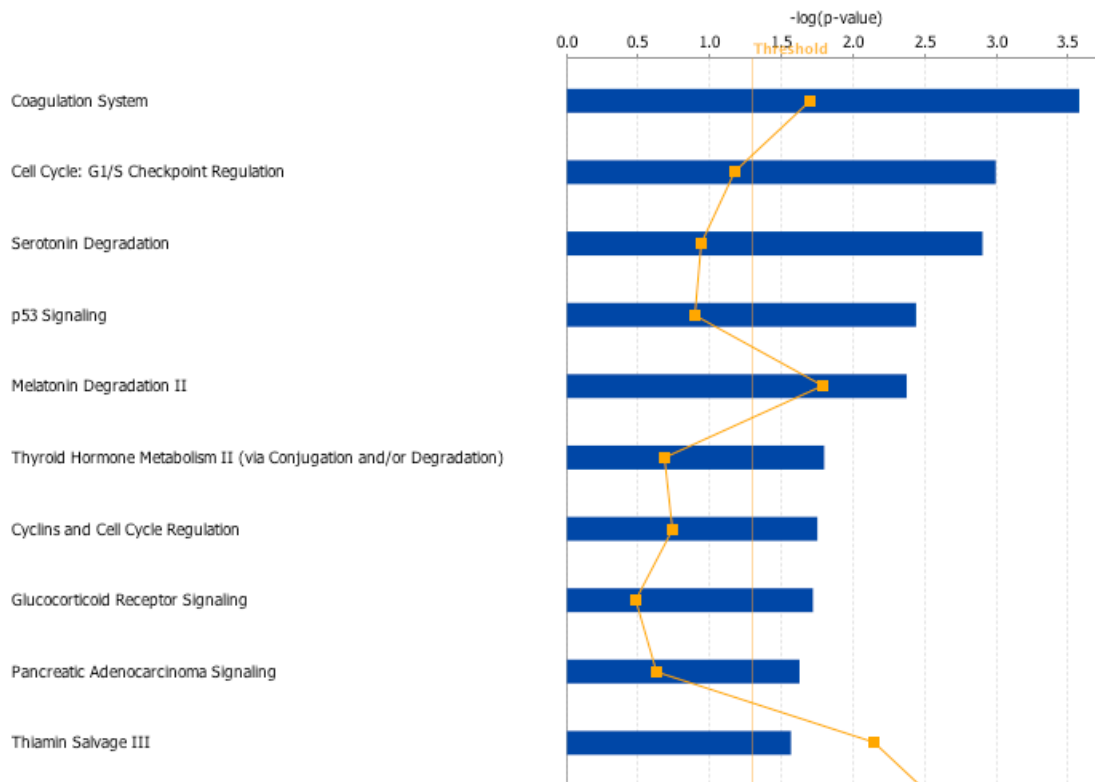
E2 (10⁻⁷ M) FUNCTIONAL ANNOTATION CLUSTER	
Annotation Cluster	score
response to hormone stimulus	4.34
regulation of locomotion/cell migration	2.84
constituent parts of the plasma membrane	2.49
proteins with SH₂ domains	2.35
glycoproteins	2.34
components of membrane fraction	2.34
developmental maturation	2.32
response to hypoxia	2.31
Bcl-2 proteins (BH domain)	1.97
vasculature/blood vessel development	1.90
lipoproteins	1.89
negative regulation of cell growth	1.85
response to wounding/inflammatory response	1.64
regulation of phosphate metabolic process	1.59
positive regulation of apoptosis	1.58
proteins with Pleckstrin homology-type domain (PH domain)	1.55
components of the extracellular region part	1.52

S 1B)
IPA UPSTREAM REGULATOR ANALYSIS

<input type="checkbox"/>	Upstream Regulator	Log Ratio	Molecule Type	<input type="checkbox"/>	Predicted Activation State	Activation z-score	Notes	p-value of overlap	Target molecules in dataset
<input type="checkbox"/>	ZNF217	↑ -0.784	transcription regulator	<input checked="" type="checkbox"/>	Activated	2.449	bias	5.00E-05	↑ANK3, ↑CDKN2B, ↑EPHX4, ↑FRK, ↑GFPB3, ↑MIZ12, ↑MVO1B, ↑RCAN1, ...all 9
<input type="checkbox"/>	HFE1A	↑ 0.540	transcription regulator	<input type="checkbox"/>	Inhibited	-2.734	bias	4.09E-05	↑CXCR4, ↑ESLN3, ↑EPAS1, ↑HILPDA, ↓ID2, ↑GFPB3, ↑NDRG1, ↓NOV1, ...all 16
<input type="checkbox"/>	CTNMB1	↑ -0.540	transcription regulator	<input type="checkbox"/>	Inhibited	-2.069	bias	2.26E-03	↑AXIN2, ↓DKK1, ↓ID2, ↓ID3, ↓LLR1, ↓MIZ12, ↓MSR2, ↑PLAU, ↓SEPR1, ...all 14
<input type="checkbox"/>	SP1	↑ -0.177	transcription regulator	<input type="checkbox"/>	Inhibited	-2.562	bias	5.39E-03	↑BBR3, ↑CDK6, ↑CDKN2B, ↑CTSD, ↑CXCL12, ↑GFPB3, ↓IL15 (includes: ..., all 16
<input type="checkbox"/>	TP53 (includes EG22059)	↑ 0.361	transcription regulator	<input type="checkbox"/>	Inhibited	-2.696		6.26E-03	↑BBR3, ↑BIRC, ↑BTG2, ↑CCNG2, ↑CDD2A, ↑CTSD, ↓DDIT4, ↓DKK1, ↓D..., ...all 27
<input type="checkbox"/>	SMARCA4	↑ 0.234	transcription regulator	<input type="checkbox"/>	Inhibited	-2.200	bias	1.65E-02	↑ABHD2, ↑CRL1, ↑CDD2A, ↑CDKN2B, ↑QIP4B, ↓DUX2, ↑HEYL, ↓D3, ...all 11
<input type="checkbox"/>	SMARCB1	↑ -0.025	transcription regulator	<input type="checkbox"/>	Inhibited	-2.425		2.70E-02	↑CXCR4, ↑HEYL, ↑MCM10 (includes EG307120), ↑OAS1, ↑PPARG, ↑RND3, ...all 6
<input type="checkbox"/>	NEK8A	↑ -0.617	other	<input type="checkbox"/>	Inhibited	-2.213		1.94E-01	↑BTG2, ↑CXCR4, ↓IL15 (includes EG10160), ↑PLAU, ↑IFGFC, ...all 5

S 1B)
IPA CANONICAL PATHWAYS

■ E2_7 ■ Ratio



S 1C)

DAVID ANALYSIS

DOXORUBICIN FUNCTIONAL ANNOTATION CLUSTER	
Annotation Cluster	score
regulation of transcription	8.53
components of cytoskeleton	7.59
cell cycle/mitosis	7.28
components of nuclear lumen/nucleoplasma	6.77
cellular response to stress/DNA damage stimulus	5.97
constituent parts of chromosomes / condensed chromosome kinethocore	5.07
proteins with zinc finger domain/C ₂ H ₂ -like	4.23
regulation of apoptosis	3.43
components of microtubule cytoskeleton	2.93
DNA damage / cell cycle checkpoint	2.74
components of chromosome segregation	2.68
positive regulation of transcription	2.66
basic-leucine zipper (bZIP) transcription factors	2.65
regulation of programmed cell death	2.62
negative regulation of transcription	2.57
proteins with BTB/POZ domain	1.95
GTPase regulator activity	1.93
regulation of meiotic cell cycle	1.90
p53/ATM cell signalling pathway	1.86
constituent parts of nuclear chromosomes	1.84
tube development	1.79
response to radiation	1.75
double-strand break repair	1.74
hemopoiesis / myeloid cell differentiation	1.74
negative regulation of transferase activity	1.68
positive regulation of cell migration	1.68
regulation of cell growth	1.66
nucleotide-binding	1.66
DNA damage response, signal transduction by p53 class mediator	1.62
growth factor activity	1.53
ovulation cycle process	1.51
regulation of DNA metabolic process / DNA replication	1.50

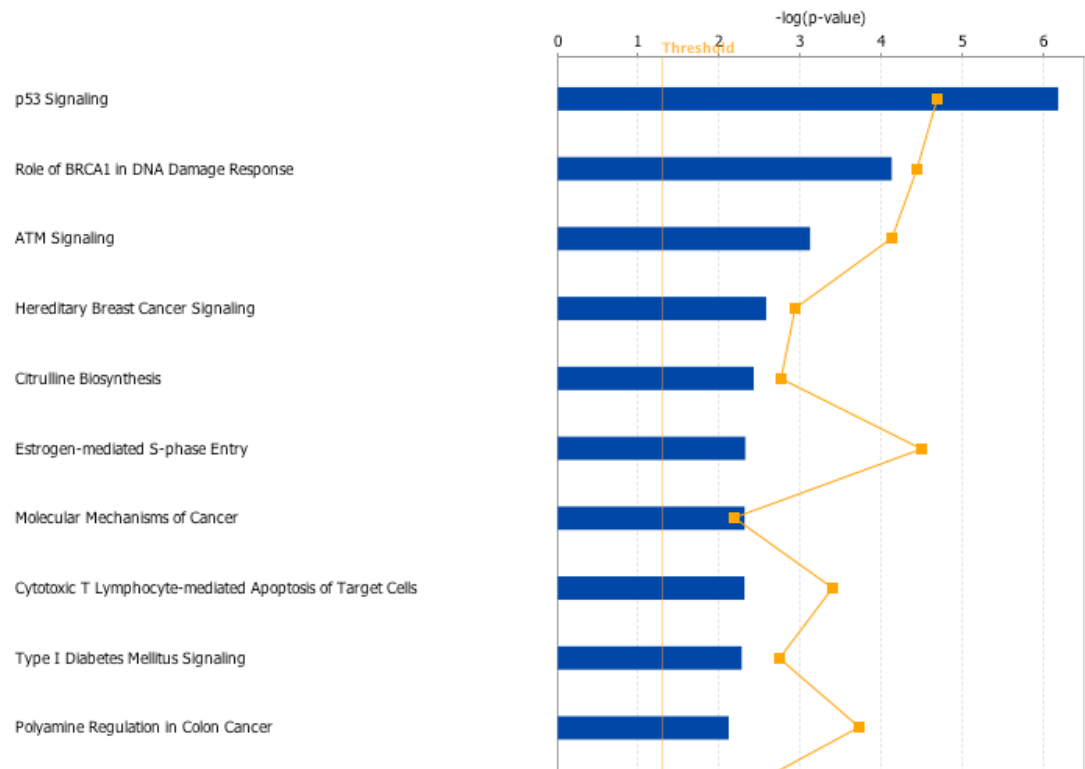
S 1C)

IPA UPSTREAM REGULATOR ANALYSIS

<input type="checkbox"/>	Upstream Regulator	Log Ratio	Molecule Type	<input type="checkbox"/>	Predicted Activation State	Activation z-score	p-value of overlap	Target molecules in dataset
<input type="checkbox"/>	TP53 (includes: EG:21059)	↑0.179	transcription regulator	<input checked="" type="checkbox"/>	Activated	6.084	7.45E-20	↑ACTA2, ↑ADA, ↑ADCK3, ↑AEN, ↑AK1, ↑ANLN, ↑ANXA4, ↑ARE, ... all 137
<input type="checkbox"/>	TP73	↑0.172	transcription regulator	<input checked="" type="checkbox"/>	Activated	3.163	2.27E-06	↑ADA, ↑AEN, ↑BAX, ↑BCL2L1L, ↑CDKN1A, ↑CDKN1C, ↑EGR1, ↑E, ... all 23
<input type="checkbox"/>	CDKN2A	↑0.590	transcription regulator	<input checked="" type="checkbox"/>	Activated	2.651	1.84E-05	↑ASF1B, ↑BAX, ↑BCL2, ↑BLM, ↑CCNA2, ↑CCNE1, ↑CDDC4, ↑CDC, ... all 26
<input type="checkbox"/>	FOXO4		transcription regulator	<input checked="" type="checkbox"/>	Activated	2.798	1.34E-04	↑CDC42EP3, ↑CDKN1A, ↑CTGF, ↑GADD45A, ↑GADD45B, ↑IAG1, ↑O, ... all 9
<input type="checkbox"/>	KDM5B	↑0.896	transcription regulator	<input checked="" type="checkbox"/>	Activated	2.575	1.44E-04	↑ANKRD36B, ↑AP4L, ↑BUB1B, ↑CAV1, ↑CDPT, ↑DLGAP5, ↑DPY1, ... all 22
<input type="checkbox"/>	HOXA5	↑0.983	transcription regulator	<input checked="" type="checkbox"/>	Activated	2.449	3.81E-04	↑CDKN1A, ↑EGR1, ↑GADD45B, ↑KLF10, ↑MDM2, ↑SAT1, ... all 6
<input type="checkbox"/>	SMAD4	↓-0.297	transcription regulator	<input checked="" type="checkbox"/>	Activated	3.003	5.58E-04	↑CCNE1, ↑CDC42EP3, ↑CDKN1A, ↑CTGF, ↑FOS, ↑GADD45A, ↑GA, ... all 23
<input type="checkbox"/>	FOXO3	↓-0.100	transcription regulator	<input checked="" type="checkbox"/>	Activated	2.933	2.39E-03	↑BCL2L1L, ↑CASP8, ↑CDC42EP3, ↑CDKN1A, ↑CTGF, ↑FBXO32, ↑G, ... all 17
<input type="checkbox"/>	PI3R	↓-0.465	ligand-dependent nuclear receptor	<input checked="" type="checkbox"/>	Activated	2.488	3.35E-02	↑CDKN1A, ↑CDKN1C, ↑CEBPB (includes: EG:1051), ↑DST, ↑GAS6, ↑, ... all 18
<input type="checkbox"/>	CREBBP	↑0.344	transcription regulator	<input checked="" type="checkbox"/>	Activated	2.768	3.50E-02	↑BCL2, ↑CDKN1A, ↑EGR1, ↑FGFR3, ↑FOS, ↑HLA-B, ↑INPP5D, ↑IRF, ... all 12
<input type="checkbox"/>	HIF1A	↑0.015	transcription regulator	<input checked="" type="checkbox"/>	Activated	3.248	3.87E-02	↑ANGPTL4, ↑BCL2, ↑CAV1, ↑CDKN1A, ↑CORO1A, ↑CKCR4, ↑EGLN3, ... all 27
<input type="checkbox"/>	RUVBL1	↓-0.837	transcription regulator	<input checked="" type="checkbox"/>	Activated	2.236	5.37E-02	↑FAM53C, ↑GADD45B, ↑HIST1H4A (includes: others), ↑PCNA, ↑PLAC8, ... all 7
<input type="checkbox"/>	STAT1	↑0.097	transcription regulator	<input checked="" type="checkbox"/>	Activated	2.598	6.42E-02	↑BCL2L1L, ↑CASP8, ↑CDKN1A, ↑FAS, ↑FOS, ↑FEI27, ↑IRF1 (include..., ... all 14
<input type="checkbox"/>	FTS1		transcription regulator	<input checked="" type="checkbox"/>	Activated	2.372	1.33E-01	↑CCNE1, ↑CDKN1A, ↑CSF1R, ↑CTGF, ↑EGR1, ↑HSPA6, ↑NCF1, ↑P, ... all 15
<input type="checkbox"/>	GATA1		transcription regulator	<input checked="" type="checkbox"/>	Activated	2.219	1.83E-01	↑ANK1, ↑BCL2L1L, ↑BMP6, ↑GP1BA, ↑NFE2, ↑PIN2, ... all 6
<input type="checkbox"/>	CEBPB (includes: EG:1051)	↑1.240	transcription regulator	<input checked="" type="checkbox"/>	Activated	2.188	3.25E-01	↑BCL2, ↑CDC42EP3, ↑CEBPB, ↑CSF1R, ↑F8, ↑FOS, ↑GADD45A, ↑ID1, ... all 13
<input type="checkbox"/>	EP300	↓-0.345	transcription regulator	<input checked="" type="checkbox"/>	Activated	2.753	3.60E-01	↑ACTA1, ↑BAX, ↑CCNE1, ↑CDKN1A, ↑CEBPB, ↑EGR1, ↑HIST1H4A, ... all 12
<input type="checkbox"/>	IRF3	↑0.613	transcription regulator	<input checked="" type="checkbox"/>	Activated	2.378	4.52E-01	↑ANXA4, ↑ARHG2 (includes: EG:11847), ↑CDH11, ↑HLA-F, ↑IRF7, ↑JUNB, ... all 8
<input type="checkbox"/>	MYCN	↓-1.475	transcription regulator	<input checked="" type="checkbox"/>	Activated	2.786	1.00E00	↑BAX, ↑CAV1, ↑CDH11, ↑CDKN1A, ↑CTGF, ↑HLA-A, ↑ID2, ↑INHBA, ... all 18
<input type="checkbox"/>	MDM2	↑1.050	transcription regulator	<input checked="" type="checkbox"/>	Inhibited	-2.073	7.81E-06	↑BAX, ↑BCL2, ↑CCNA2, ↑CCNA2, ↑CDKN1A, ↑KAT5B, ↑MDM2, ↑MDM4, ↑, ... all 12
<input type="checkbox"/>	E2F2	↓-1.612	transcription regulator	<input checked="" type="checkbox"/>	Inhibited	-2.121	2.01E-03	↑BCL2, ↑CCNA2, ↑CCNE1, ↑CDDC4, ↑CDKN1A, ↑MCM10 (include..., ... all 11
<input type="checkbox"/>	FOXM1	↓-0.348	transcription regulator	<input checked="" type="checkbox"/>	Inhibited	-2.628	8.80E-03	↑CAV1, ↑CCNA2, ↑CDKN1A, ↑CENPA, ↑KIF20A, ↑MYC, ↑NER2, ↑P, ... all 9
<input type="checkbox"/>	TCF4		transcription regulator	<input checked="" type="checkbox"/>	Inhibited	-2.000	8.38E-02	↑CDKN1A, ↑DKK1, ↑ID2, ↑MIA, ↑MYC, ↑SGK1, ... all 6
<input type="checkbox"/>	SP1 (includes: EG:20375)		transcription regulator	<input checked="" type="checkbox"/>	Inhibited	-2.200	2.91E-01	↑BAX, ↑CSF1R, ↑FEF, ↑FOS, ↑IL1R2, ↑NCF1, ↑PCNA, ↑TNFRSF14, ... all 8

S 1C)
IPA CANONICAL PATHWAYS

■ doxo.ipa - 2012-09-14 10:32 AM ■ Ratio



S 1D)

DAVID ANALYSIS

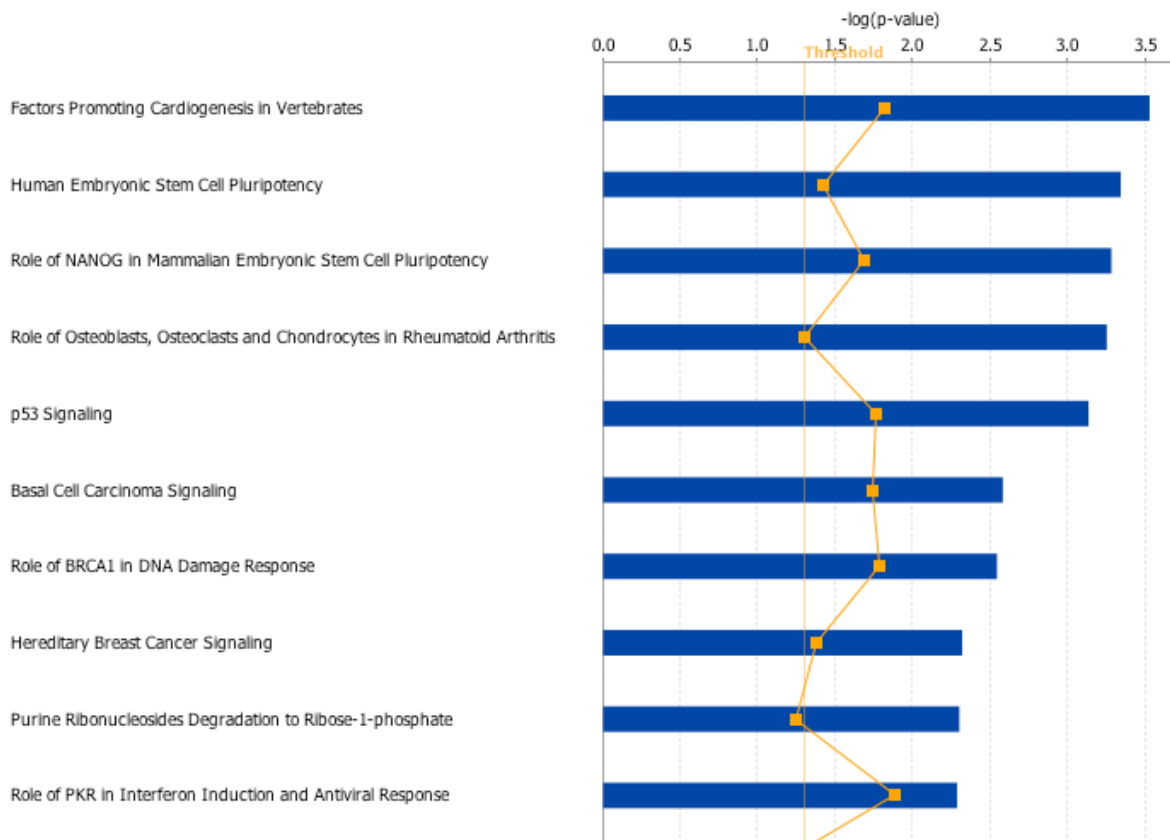
DOXORUBICIN + E2 (10⁻⁹ M) FUNCTIONAL ANNOTATION CLUSTER	
Annotation Cluster	score
regulation of transcription	6.48
proteins with BTB/POZ domain	4.42
basic-leucine zipper (bZIP) transcription factors	3.78
cell cycle/mitosis	3.27
components of microtubule cytoskeleton	3.63
cellular response to stress/DNA damage stimulus	3.09
proteins with zinc finger domain/C ₂ H ₂ -like	2.76
components of the nuclear chromosome part	2.69
proteins with sh3 domains	2.69
components of the condensed chromosome kinethocore	2.24
GTPase regulator activity	2.21
negative regulation of transcription from RNA pol II promoter	2.14
WNT receptor signalling pathway	2.12
components of nuclear lumen/nucleoplasma	2.10
regulation of apoptosis	2.03
positive regulation of transcription/macromolecule metabolic process	1.74
response to radiation/UV	1.62
proteins with SH ₂ domains	1.57
DNA-repair proteins/proteins with UmuC-like domain	1.53
proteins with BTB/POZ domain/Kelch-like proteins	1.52

S 1D)
IPA UPSTREAM REGULATOR ANALYSIS

<input type="checkbox"/>	Upstream Regulator	Log Ratio	Molecule Type	<input type="checkbox"/>	Predicted Activation St...	Activation z-score	Notes	p-value of overlap	Target molecules in dataset
<input type="checkbox"/>	TP53 (includes EG22059)	↑0.473	transcription regulator	<input type="checkbox"/>	Activated	4.605		4.31E-08	↑ACTA2, ↑ADA, ↓... all 66
<input type="checkbox"/>	ESR1	↓-1.210	ligand-dependent nuclear r	<input type="checkbox"/>	Activated	3.368		4.51E-07	↑ABCC5, ↓ABCC2, ... all 36
<input type="checkbox"/>	PGR	↑4.067	ligand-dependent nuclear r	<input type="checkbox"/>	Activated	2.043		2.67E-03	↑CDKN1A, ↑GAL, ... all 18
<input type="checkbox"/>	KDM5B	↑1.058	transcription regulator	<input type="checkbox"/>	Activated	2.341		5.90E-03	↑BUB1B, ↓DLGAP5 ... all 15
<input type="checkbox"/>	SMAD4	↓-0.260	transcription regulator	<input type="checkbox"/>	Activated	2.771		1.09E-02	↑CDCA2EP3, ↑CD... all 16
<input type="checkbox"/>	CDKN2A	↑0.447	transcription regulator	<input type="checkbox"/>	Activated	2.172		1.86E-02	↑BIM, ↓CCNA2, ↓... all 15
<input type="checkbox"/>	FOXM1	↓-0.233	transcription regulator	<input type="checkbox"/>	Inhibited	-2.224	bias	5.99E-03	↓ATF2, ↓CCNA2, ↑... all 8
<input type="checkbox"/>	MDM2	↑1.373	transcription regulator	<input type="checkbox"/>	Inhibited	-2.434		1.87E-02	↓CCNA2, ↑CDKN1A ... all 6

S 1D)
IPA CANONICAL PATHWAYS

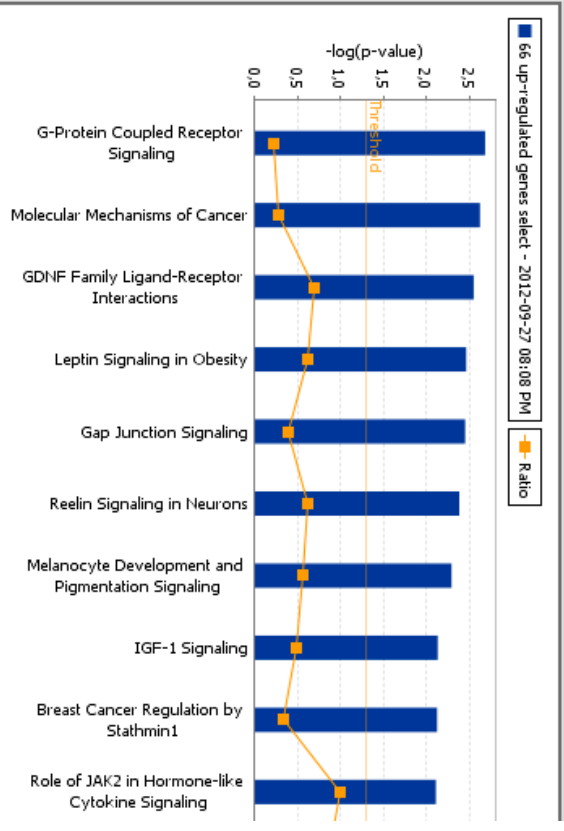
■ Dox + E2 ■ Ratio



S 1E)
DAVID ANALYSIS

DOXORUBICIN + E2 (10⁻⁹ M) FUNCTIONAL ANNOTATION CLUSTER	
Annotation Cluster (66 up-regulated genes selective responsiveness)	score
proteins with SH2 domain	2.21
response to hormone stimulus	1.87
adenylate cyclese activity	1.45
protease inhibitor	1.38

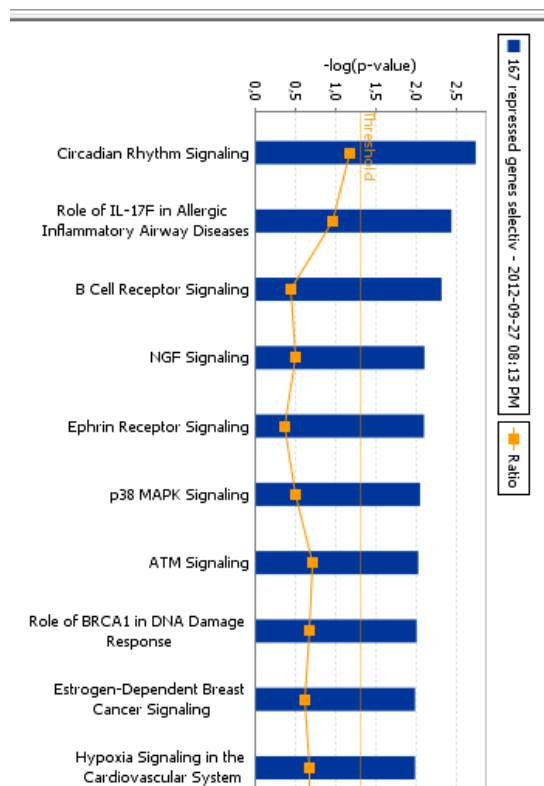
S 1E)
IPA CANONICAL PATHWAYS



S 1F)
DAVID ANALYSIS

DOXORUBICIN + E2 (10⁻⁹ M) FUNCTIONAL ANNOTATION CLUSTER	
Annotation Cluster (167 repressed genes selective responsiveness)	score
basic-leucine zipper (bZIP) transcription factors	2.04
zinc/metal transition ion binding proteins	1.86
regulation of transcription	1.60
proteins with SH3 domain	1.50

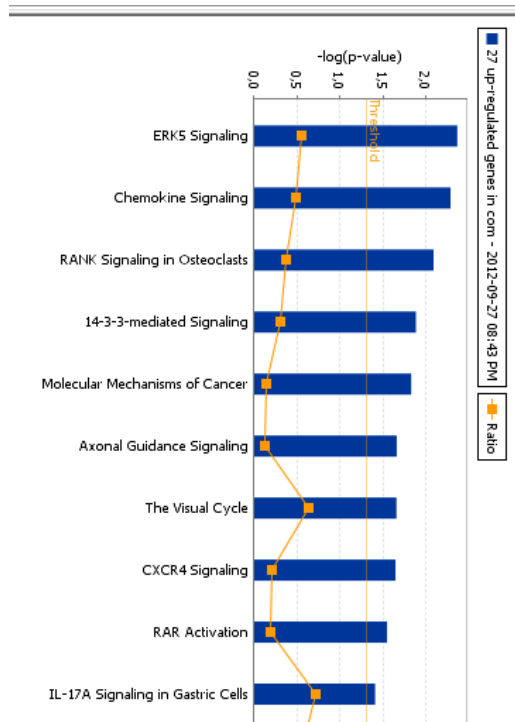
S II F)
IPA CANONICAL PATHWAYS



S 1G)
DAVID ANALYSIS

FUNCTIONAL ANNOTATION CLUSTER (27 up-regulated genes in common)	
Annotation Cluster	score
ossification / bone development	1.74
vasculature/blood vessel development	1.45
positive regulation of transcription	0.98
enzymes linked receptor protein signaling pathway	0.84
regulation of apoptosis	0.72
components of the extracellular matrix/growth factor	0.62

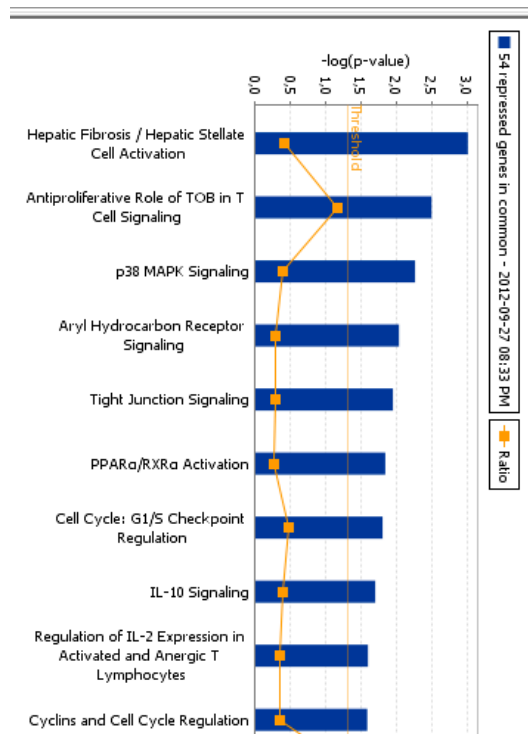
S 1G)
IPA CANONICAL PATHWAYS



S 1H)
DAVID ANALYSIS

FUNCTIONAL ANNOTATION CLUSTER (54 repressed genes in common)	
Annotation Cluster	score
cytokine-cytokine receptor interaction	1.65
regulation of ossification / skeletal system development	1.55

S 1H)
IPA CANONICAL PATHWAYS



S 11)

DAVID ANALYSIS

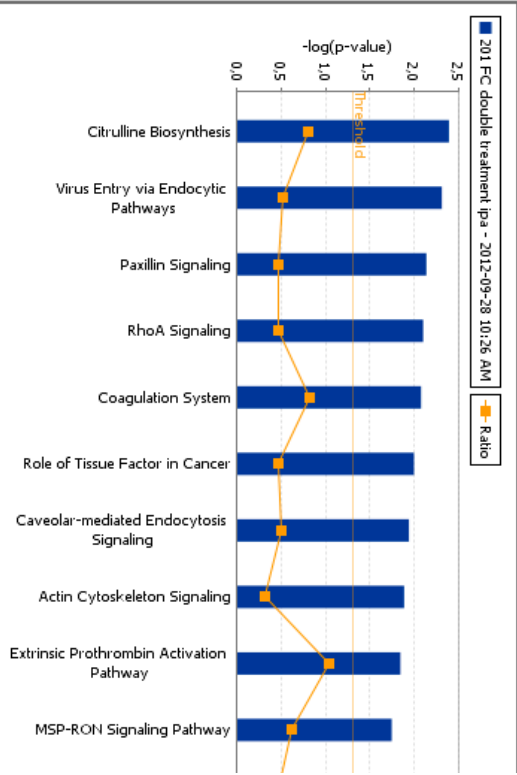
ADDITIVE EFFECT (DOXORUBICIN + E2 UP-REGULATION)	
FUNCTIONAL ANNOTATION CLUSTER	
Annotation Cluster (201 more than additive genes)	score
ectoderm development/epithelial cell differentiation	2.94
glycoproteins/proteins of the extracellular region	2.29
components of the plasma membrane	1.84
components of the extracellular matrix/cell adhesion proteins	1.59
inflammatory/defense response	1.55
mesenchymal/neural crest cells differentiation	1.54

S 11)

IPA UPSTREAM REGULATORS ANALYSIS

<input type="checkbox"/>	Upstream Regulator	Molecule Type	Predicted Activation State	Activation z-score	p-value of overlap	Target molecules in dataset
<input type="checkbox"/>	TP53 (includes EG:22059)	transcription regulator	Activated	3.163	8.19E-07	ACTA2, BTG2, EGRL, EPHA2, FDXR, FOSL, GADD45A, GPR87, H19, HBEGF
	...all 23					

S 11)
IPA CANONICAL PATHWAYS



S 1J)
DAVID ANALYSIS

ADDITIVE EFFECT (DOXORUBICIN + E2 DOWN-REGULATION)	
Annotation Cluster (142 genes with greater than additive down-regulation)	score
cell cycle/mitosis	1.75
mitotic spindle organization/mitotic cell cycle	1.59

S 1J)
IPA CANONICAL PATHWAYS

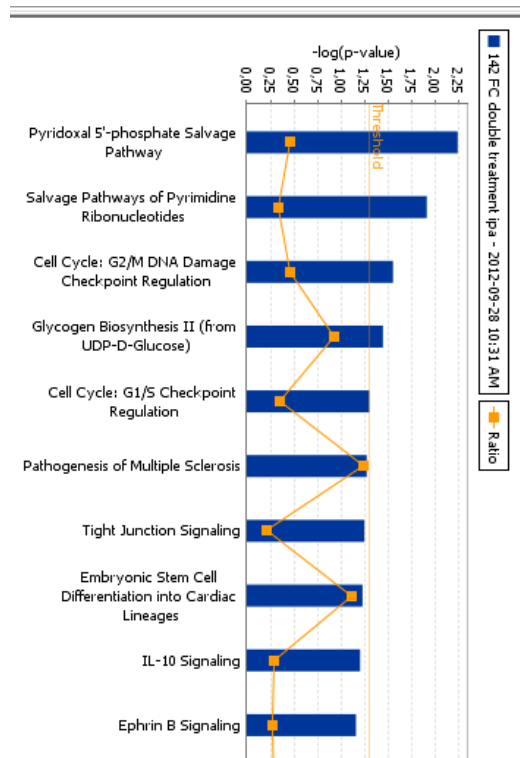


Table S2. Statistical analysis for synergistic impact of combined treatments.

The \log_2 of the fold of induction was considered. The means of two normally distributed populations composed of \log_2 [FC_{double treatment}] and \log_2 [FC_{DOX}] + \log_2 [FC_{E2}] were analyzed using a t-test approach ($p < 0.05$). Each population was composed of six values. A) doxorubicin B) 5FU C) Nutlin-3a (nutlin).

S 2A)

GENE NAME	\log_2 (DOX & E2)	\log_2 (DOX + E2)	p-value	Ref ¹	Ref ²
CA5A	-1.2673	1.4343	0.032620		(1)
CDH26	2.0860	3.3118	0.006878	(2, 3)	(4)
EPHA2	1.2677	2.2043	0.001083	(5)	
H19	0.6006	1.6148	0.000755		
INPP5D	1.5231	3.3450	0.027126	(6)	(7)
KRT15	1.2927	3.2635	0.000240		
NOTCH1	2.5643	2.6851	ns	(8-10)	(11)
PML	3.0089	2.7536	ns	(12)	
SOX9	3.0460	3.4651	ns	(13, 14)	(15)
SYNM	1.2360	2.4176	0.001560		
TEX14	2.0027	3.7901	0.003339		(16)
TLR5	1.3543	2.6876	0.000068	(17)	
GDNF	2.1639	3.7281	0.000451		(18)
TFF3	1.8022	1.7969	ns		(19)
APC2	-0.5028	-0.0014	ns		
IGF2	-0.9161	-0.3698	ns	(20)	

¹ Previous studies where a direct or indirect functional interaction with p53, with ER or among the selected genes has already been proposed.

2. Carroll JS, *et al.* (2006) Genome-wide analysis of estrogen receptor binding sites. *Nat Genet* 38(11):1289-1297.
3. Lin C-Y, *et al.* (2007) Whole-Genome Cartography of Estrogen Receptor α Binding Sites. *PLoS Genet* 3(6):e87.
5. Zhang G, *et al.* (2008) EphA2 Is an Essential Mediator of UV Radiation-Induced Apoptosis. *Cancer Research* 68(6):1691-1696.
6. Kerley-Hamilton JS, *et al.* (2005) A p53-dominant transcriptional response to cisplatin in testicular germ cell tumor-derived human embryonal carcinoma. *Oncogene* 24(40):6090-6100.
8. Kim SB, *et al.* (2006) Activated Notch1 interacts with p53 to inhibit its phosphorylation and transactivation. *Cell Death Differ* 14(5):982-991.
9. Hao L, *et al.* (2009) Notch-1 activates estrogen receptor-[alpha]-dependent transcription via IKK[alpha] in breast cancer cells. *Oncogene* 29(2):201-213.
10. Secchiero P, *et al.* (2009) Nutlin-3 up-regulates the expression of Notch1 in both myeloid and lymphoid leukemic cells, as part of a negative feedback antiapoptotic mechanism. *Blood* 113(18):4300-4308 .
12. Kurki, *et al.* (2003) Cellular stress and DNA damage invoke temporally distinct Mdm2, p53 and PML complexes and damage-specific nuclear relocalization. *J. Cell Science* 116:3917-3925.

13. Mead TJ, *et al.* (2009) Notch pathway regulation of chondrocyte differentiation and proliferation during appendicular and axial skeleton development. *Proceedings of the National Academy of Sciences* 106(34):14420-14425.
14. Muto A, *et al.* (2009) The group E Sox genes Sox8 and Sox9 are regulated by Notch signaling and are required for Müller glial cell development in mouse retina. *Experimental Eye Research* 89(4):549-558.
17. Menendez D, *et al.* (2011) The Toll-Like Receptor Gene Family Is Integrated into Human DNA Damage and p53 Networks. *PLoS Genet* 7(3):e1001360.
20. Zhang L, *et al.* (1998) p53 regulates human insulin-like growth factor II gene expression through active P4 promoter in rhabdomyosarcoma cells. *DNA Cell Biol* 17(2):125-131.

² Previous studies addressing expression of the genes in a different tissue type or implicating them in biological pathways that can represent an expansion of the p53/ER transcriptional master network.

1. Vullo D, *et al.* (2007) Carbonic anhydrase activators: An activation study of the human mitochondrial isoforms VA and VB with amino acids and amines. *Bioorganic & Medicinal Chemistry Letters* 17(5):1336-1340.
4. Li RW, *et al.* (2009) A temporal shift in regulatory networks and pathways in the bovine small intestine during *Cooperia oncophora* infection. *International Journal for Parasitology* 39(7):813-824.
7. Liu Q, *et al.* (1997) Molecular Cloning and Chromosomal Localization in Human and Mouse of the SH2-Containing Inositol Phosphatase, INPP5D(SHIP). *Genomics* 39(1):109-112.
11. Ferrando AA (2009) The role of NOTCH1 signaling in T-ALL. *ASH Education Program Book* 2009(1):353-361.
15. Staffler A, *et al.* (2010) Heterozygous SOX9 Mutations Allowing for Residual DNA-binding and Transcriptional Activation Lead to the Acampomelic Variant of Campomelic Dysplasia. *Human Mutation* 31(6):E1436-E1444.
16. Yatsenko AN, *et al.* (2010) The Power of Mouse Genetics to Study Spermatogenesis. *Journal of Andrology* 31(1):34-44.
18. Pascual A, *et al.* (2011) GDNF and protection of adult central catecholaminergic neurons. *Journal of Molecular Endocrinology*.
19. Takano T, *et al.* (2009) Trefoil Factor 3 (TFF3): A Promising Indicator for Diagnosing Thyroid Follicular Carcinoma. *Endocrine Journal* 56(1):9-16.

S 2B)

GENE NAME	log ₂ (5FU & E2)	log ₂ (5FU + E2)	p-value
CA5A	-1.4128	-1.5072	ns
CDH26	4.7005	4.3618	ns
EPHA2	-0.1362	0.1798	ns
H19	0.4730	1.1922	0.042541
INPP5D	1.2796	3.2618	0.000252
KRT15	1.6988	1.7465	ns
NOTCH1	0.7222	0.9498	ns
PML	-1.0537	-0.2178	ns
SOX9	-1.7045	-1.4752	ns
SYNM	-1.9345	-1.9135	ns
TEX14	-0.6878	-0.4685	ns
TLR5	-1.7295	-1.1135	ns
GDNF	-0.5720	0.6339	0.000526
TFF3	0.7461	0.3822	ns
APC2	-1.1356	-1.4878	ns
IGF2	-0.2356	-0.9762	ns

S 2C)

GENE NAME	log ₂ (nutlin & E2)	log ₂ (nutlin + E2)	p-value
CA5A	-1.1169	-0.2678	ns
CDH26	2.3298	2.3505	ns
EPHA2	0.9131	1.3605	0.000019
H19	1.0365	1.7015	0.009644
INPP5D	4.2265	5.1188	0.001312
KRT15	3.3848	2.9788	ns
NOTCH1	1.6481	1.7155	ns
PML	0.2631	0.5322	ns
SOX9	0.4598	0.6688	ns
SYNM	0.2915	0.4822	ns
TEX14	0.7431	0.6738	ns
TLR5	0.5498	0.6155	ns
GDNF	0.0508	0.1341	ns
TFF3	0.2928	0.1127	ns
APC2	-0.7422	-1.0940	ns

Table S3. List of the genes up-regulated by the concomitant treatment of doxorubicin and E2 (10⁻⁹ M) with more than an additive effect. To be part of this list the following conditions were satisfied: $\log_2[\text{FC}_{\text{double treatment}}] > 2$ and $\log_2[\text{FC}_{\text{double treatment}}] - \log_2[\text{FC}_{\text{DOX}}] - \log_2[\text{FC}_{\text{E2}}] > 0.1$

GENE	FOLD OF CHANGE (log ₂ treatment vs mock)			
	Doxorubicin + E2 (10 ⁻⁹ M)	Doxorubicin	E2 (10 ⁻⁹ M)	ADDITIVE EFFECT
CA5A*	1.30	1.19	-0.94	1.05
CDH26	4.30	0.09	3.22	1.00
EPHA2	2.62	1.62	0.10	0.90
H19	2.95	0.56	1.03	1.36
INPP5D	3.10	2.27	0.34	0.50
KRT15	3.24	-0.29	1.67	1.57
NOTCH1	3.25	2.31	0.56	0.38
PML	3.85	3.04	-0.68	0.81
SOX9	3.79	2.38	0.50	0.91
SYNM	3.27	2.01	-0.23	1.27
TEX14	3.52	2.16	-1.16	1.36
TLR5	2.88	1.08	0.06	1.74
GDNF	4.53	3.24	0.05	1.25
TFF3	2.53	0.70	1.04	0.80
APC2	2.88	1.80	-0.04	1.08
IGF2	2.27	1.24	-0.16	1.03
FAM63A	2.02	-0.21	0.32	1.70
KCNF1	3.91	0.66	1.55	1.69
KRT14	3.18	0.00	1.63	1.55
AHNAK2	3.61	2.30	-0.07	1.31
VWF	2.69	-0.02	1.38	1.31
FLJ45248	2.18	-0.24	0.88	1.30
XYLT1	2.63	0.94	0.42	1.27
KCNB1	3.26	2.03	-0.59	1.23
NEUROD2	4.04	2.84	-0.71	1.20
ITGB8	2.05	0.72	0.13	1.19
MERTK	2.32	1.05	0.16	1.11
MAMLD1	2.47	-0.23	1.45	1.01
COL27A1	2.08	0.74	0.37	0.98
POU3F1	3.24	2.29	-0.86	0.95
LOC646976	4.07	2.84	0.32	0.91
TNFAIP2	2.58	1.70	-0.54	0.88
RAB37	3.67	1.82	0.98	0.87
ICOSLG	3.03	2.06	0.13	0.84
FLJ42627	2.02	1.07	0.12	0.83
HEG1	3.07	-0.60	2.25	0.83
EFNB1	2.31	1.49	-0.07	0.83

C20orf132	2.48	1.66	-0.55	0.82
VWCE	4.24	3.21	0.23	0.80
DLX3	2.46	1.00	0.66	0.80
CDC42EP3	3.15	2.36	-0.35	0.79
NPTX1	4.25	2.87	0.59	0.79
FOSL1	3.18	2.39	-0.35	0.79
LOC390595	2.43	1.67	-0.08	0.77
PDE2A	4.12	3.08	0.30	0.74
AMZ1	3.18	-0.18	2.44	0.74
SIM2	2.24	1.49	0.01	0.74
SMPD3	3.43	2.71	-0.45	0.72
GLS	2.99	2.26	-0.39	0.72
HOXA11AS	2.06	1.12	0.23	0.71
INSM2	3.09	2.37	-0.09	0.71
IQCD	2.95	2.25	-0.14	0.70
MICALCL	2.65	0.67	1.29	0.70
MAF	2.35	1.67	-0.67	0.69
RGMA	4.87	3.25	0.94	0.68
ANK1	3.59	2.91	-0.35	0.67
DHRS3	2.35	1.68	-0.44	0.67
AOC3	2.73	2.06	-0.08	0.67
EGR1	2.30	1.63	-1.27	0.67
LRRC17	3.01	2.35	-0.50	0.66
PRDM2	2.60	1.94	-0.09	0.66
SPSB1	2.39	1.63	0.11	0.66
TMEM130	3.87	3.22	-1.27	0.66
AP3B2	2.16	1.51	-0.13	0.65
DLX2	2.70	2.06	-1.12	0.65
SERPINB9	3.19	2.54	-0.01	0.65
KLHL29	2.18	1.08	0.45	0.64
TGM2	3.12	-0.48	2.48	0.64
AMPD3	2.32	1.56	0.12	0.64
CHST6	2.53	1.90	-0.34	0.63
GGTA1	2.36	1.73	-0.33	0.63
MYO10	2.21	1.11	0.46	0.63
NUDT9P1	4.24	3.62	-0.25	0.62
POLH	3.27	2.53	0.12	0.62
AUTS2	3.32	2.34	0.35	0.62
FLJ26850	5.45	4.71	0.12	0.62
LOC402778	2.91	0.34	1.95	0.62
PRODH	2.11	1.50	-0.05	0.61
FGF18	2.82	1.13	1.08	0.60
ZCCHC24	2.44	1.85	-0.29	0.59
TMEM120B	2.17	0.38	1.19	0.59
HLA-DPB1	2.54	1.97	-0.40	0.57

RNF150	2.19	0.16	1.45	0.57
KIAA0562	2.97	1.99	0.44	0.55
RHOBTB1	3.17	1.04	1.59	0.54
RFC3	2.83	2.12	0.17	0.54
SLC8A3	3.14	2.61	-0.45	0.53
GGA2	2.14	1.31	0.30	0.53
DUSP5P	2.45	1.58	0.34	0.52
HES2	2.98	2.46	-0.79	0.52
C2orf27A	2.17	1.65	-0.72	0.52
KLRG2	2.27	1.48	0.29	0.51
LOC157562	3.24	2.73	-0.50	0.51
MIA	3.16	2.66	-0.19	0.50
FLJ13224	2.72	2.23	-0.72	0.50
RBPMS2	3.68	2.46	0.72	0.49
EPB41L4B	2.28	1.74	0.05	0.49
SLC6A8	4.39	3.76	0.14	0.48
HPS1	2.16	1.55	0.13	0.47
GRIN2C	4.60	4.14	-0.55	0.46
ASPRV1	2.01	1.55	-0.52	0.46
ETV7	3.96	3.20	0.30	0.46
MAFB	2.83	2.37	-0.52	0.46
SYTL4	3.01	0.44	2.11	0.46
STX6	2.12	1.67	-0.15	0.45
ACTA1	4.98	4.53	-0.09	0.45
CD46	2.25	1.68	0.13	0.44
PXK	2.10	0.73	0.94	0.43
RAB31	2.49	0.44	1.62	0.42
TP53I3	2.78	2.25	0.12	0.41
SIRPA	4.24	3.74	0.09	0.41
ELL2	2.81	2.40	-0.28	0.41
PRDM15	3.52	2.64	0.47	0.41
HGS	2.05	1.64	-0.07	0.41
RGS20	2.85	2.45	-0.23	0.40
PPP2R2D	2.42	2.02	-0.12	0.40
ZFP2	2.10	1.67	0.03	0.40
SERPINC1	4.04	3.60	0.06	0.38
FOXQ1	2.84	2.47	-0.65	0.37
LIMK2	2.35	1.99	-0.43	0.37
NTN1	3.55	2.41	0.78	0.36
CABYR	3.08	2.72	-0.06	0.36
RGAG4	2.55	2.19	-0.44	0.36
PAR6G	2.18	1.46	0.37	0.36
PLIN5	3.64	1.37	1.91	0.36
FLJ25006	2.48	1.41	0.72	0.35
KLK10	2.68	-0.13	2.33	0.35

PLEKHO2	2.36	1.93	0.09	0.35
FAM196A	7.27	6.70	0.22	0.35
SLC6A13	2.37	2.02	-0.86	0.35
RGS16	2.23	1.89	-0.11	0.34
OLFML2A	2.10	0.34	1.42	0.34
TFPI2	3.53	0.90	2.30	0.34
SPATA18	3.15	2.64	0.18	0.33
C20orf106	2.65	2.32	-0.02	0.33
COL12A1	2.31	0.34	1.64	0.33
SHANK3	2.92	1.84	0.76	0.32
C7orf53	2.14	1.78	0.03	0.32
THBD	2.41	1.62	0.47	0.32
PGLYRP2	3.15	-0.29	2.82	0.32
KRT13	3.29	0.09	2.88	0.32
GLIPR2	2.16	1.84	-0.55	0.32
GPR87	4.17	3.85	-0.35	0.31
CCDC96	2.35	2.04	-0.26	0.31
FDXR	2.91	2.60	-0.01	0.31
LAMP3	3.49	3.18	-0.11	0.31
PFKFB2	2.44	2.14	-0.32	0.30
ERO1LB	3.17	2.87	-0.63	0.29
ATP6V1C2	2.71	0.33	2.09	0.29
IRX2	2.37	1.80	0.29	0.29
C4orf49	3.30	3.01	-0.10	0.29
TNXB	3.02	2.74	-0.87	0.28
PRICKLE2	2.31	2.03	-0.63	0.28
SLC30A1	2.48	2.20	-0.02	0.28
MAN2A2	2.17	1.91	-0.22	0.26
RBM24	2.85	0.79	1.81	0.26
HSPA12A	2.12	1.41	0.45	0.25
GLDC	2.51	0.51	1.75	0.25
GADD45A	3.24	2.90	0.09	0.25
ACTA2	4.25	4.00	-0.28	0.24
C8G	2.66	2.42	-0.62	0.24
BAIAP2	2.80	2.39	0.17	0.24
AMIGO3	2.70	2.37	0.10	0.23
BTG2	2.40	2.18	-1.96	0.22
CCDC3	5.10	4.28	0.61	0.22
ADCY9	2.11	0.99	0.90	0.22
KCTD1	2.61	2.24	0.16	0.22
KDSR	2.00	1.54	0.25	0.21
FSCN1	2.61	2.29	0.11	0.21
GPR64	2.02	1.41	0.41	0.20
SLC47A1	2.84	0.91	1.74	0.19
DPYSL4	4.74	3.79	0.76	0.19

ONECUT2	2.33	1.60	0.54	0.19
FAM25A	2.76	0.55	2.03	0.18
LAMA3	3.02	0.08	2.77	0.18
CELF6	2.37	2.19	-0.49	0.17
NPL	2.27	1.78	0.32	0.17
PTPRH	2.38	2.12	0.09	0.17
TRIM7	2.46	2.08	0.21	0.17
PIK3CD	2.05	1.14	0.74	0.17
LOC727916	2.70	2.54	-0.89	0.16
RET	3.10	0.82	2.13	0.16
TTC13	2.03	1.46	0.42	0.15
HAS3	2.21	1.53	0.53	0.15
UNC5B	3.38	2.61	0.62	0.15
PLK3	4.99	4.62	0.22	0.15
LIF	2.53	2.04	0.34	0.15
PRSS23	2.15	0.53	1.47	0.15
GPR155	3.14	2.77	0.23	0.14
FLJ36031	2.36	2.22	-0.14	0.14
KANK3	2.08	1.95	-0.41	0.14
ITGA6	2.29	1.14	1.02	0.14
HBEGF	3.13	3.00	-0.44	0.13
INPP1	2.83	2.70	-0.10	0.13
NCR3	3.17	3.04	-0.25	0.13
LAT2	2.40	2.07	0.19	0.13
RNF122	2.29	2.16	-0.79	0.13
ZNF79	2.24	2.12	-0.05	0.12
SLC6A10P	3.26	2.79	0.35	0.12
LOC645277	2.17	2.06	-0.81	0.11
RNF170	2.54	2.43	-0.26	0.10
C13orf31	2.11	1.82	0.19	0.10

* = for CA5A $\log_2[\text{FC}_{\text{double treatment}}] > 2$ was based on data from DOX + E2 (10^{-7} M)

Table S4. Summary of the expression data obtained after single or combined drug treatment. “+” indicates a fold of induction greater than 1.5 after single drug or chemical treatment. Asterisks indicate that the combined treatment with E2 results in a more than additive effect that is statistically significant, as described in *Methods* section. Empty cell or missing symbol indicates that the above selection criteria are not fulfilled.

TREATMENTS	DOX / DOX+E2	5FU / 5FU +E2	Nutlin/ Nutlin + E2	E2	p53 [^]
Gene Name	Gene responsiveness by qPCR				
CA5A	+ / *				n.i.
CDH26	/ *	+ /		+ /	
EPHA2	+ / *		+ / *		+ /
H19	/ *	/ *	/ *	+ /	n.i.
INNP5D	+ / *	+ / *	+ / *		+ /
KRT15	/ *		+ /	+ /	+ /
NOTCH1	+ /	+ /	+ /		+ /
PML	+ /				n.i.
SOX9	+ /		+ /		+ /
SYNM	+ / *				n.i.
TEX14	+ / *		+ /		n.i.
TLR5	+ / *				+ /
GDNF	+ / *	/ *			+ /
TFF3					n.i.
APC2					n.i.
IGF2					n.i.

[^]p53 responsiveness is addressed based on experiments performed using the p53-deficient MCF7 cells. n.i. = gene expression was not investigated

p53 Transactivation and the Impact of Mutations, Cofactors and Small Molecules Using a Simplified Yeast-Based Screening System

Virginia Andreotti^{1,2,3*}, Yari Ciribilli^{2,3}, Paola Monti^{1,3}, Alessandra Bisio², Mattia Lion², Jennifer Jordan^{2,3b}, Gilberto Fronza¹, Paola Menichini¹, Michael A. Resnick^{3*}, Alberto Inga^{2*}

1 Unit of Molecular Mutagenesis, National Institute for Cancer Research, IST, Genoa, Italy, **2** Laboratory of Transcriptional Networks, Centre for Integrative Biology, CIBIO, Trento, Italy, **3** Chromosome Stability Group, Laboratory of Molecular Genetics, National Institute of Environmental Health Sciences, Durham, North Carolina, United States of America

Abstract

Background: The p53 tumor suppressor, which is altered in most cancers, is a sequence-specific transcription factor that is able to modulate the expression of many target genes and influence a variety of cellular pathways. Inactivation of the p53 pathway in cancer frequently occurs through the expression of mutant p53 protein. In tumors that retain wild type p53, the pathway can be altered by upstream modulators, particularly the p53 negative regulators MDM2 and MDM4.

Methodology/Principal Findings: Given the many factors that might influence p53 function, including expression levels, mutations, cofactor proteins and small molecules, we expanded our previously described yeast-based system to provide the opportunity for efficient investigation of their individual and combined impacts in a miniaturized format. The system integrates i) variable expression of p53 proteins under the finely tunable *GAL1,10* promoter, ii) single copy, chromosomally located p53-responsive and control luminescence reporters, iii) enhanced chemical uptake using modified ABC-transporters, iv) small-volume formats for treatment and dual-luciferase assays, and v) opportunities to co-express p53 with other cofactor proteins. This robust system can distinguish different levels of expression of WT and mutant p53 as well as interactions with MDM2 or 53BP1.

Conclusions/Significance: We found that the small molecules Nutlin and RITA could both relieve the MDM2-dependent inhibition of WT p53 transactivation function, while only RITA could impact p53/53BP1 functional interactions. PRIMA-1 was ineffective in modifying the transactivation capacity of WT p53 and missense p53 mutations. This dual-luciferase assay can, therefore, provide a high-throughput assessment tool for investigating a matrix of factors that can influence the p53 network, including the effectiveness of newly developed small molecules, on WT and tumor-associated p53 mutants as well as interacting proteins.

Citation: Andreotti V, Ciribilli Y, Monti P, Bisio A, Lion M, et al. (2011) p53 Transactivation and the Impact of Mutations, Cofactors and Small Molecules Using a Simplified Yeast-Based Screening System. PLoS ONE 6(6): e20643. doi:10.1371/journal.pone.0020643

Editor: Janine Santos, University of Medicine and Dentistry of New Jersey, United States of America

Received: January 12, 2011; **Accepted:** May 6, 2011; **Published:** June 2, 2011

This is an open-access article, free of all copyright, and may be freely reproduced, distributed, transmitted, modified, built upon, or otherwise used by anyone for any lawful purpose. The work is made available under the Creative Commons CC0 public domain dedication.

Funding: This work was supported by intramural research funds from NIEHS to MAR, project Z01-ES065079, and by the Italian Association for Cancer Research (AIRC IG#9086 to AI and AIRC IG#5506 to GF). The funders had no role in study design, data collection and analysis, decision to publish, or preparation of the manuscript.

Competing Interests: The authors have declared that no competing interests exist.

* E-mail: Resnick@niehs.nih.gov (MAR); inga@science.unitn.it (AI)

These authors contributed equally to this work.

^{2a} Current address: Department of Oncology, Biology and Genetics, University of Genoa, Genoa, Italy

^{2b} Current address: Center for Environmental Health Sciences, Massachusetts Institute of Technology, Cambridge, Massachusetts, United States of America

Introduction

The sequence-specific transcription factor p53 is a key tumor suppressor protein that can coordinate the expression of a large number of target genes involved in different cellular responses to stress conditions including cell cycle arrest, programmed cell death and DNA repair [1,2]. More recently, a role of p53 in a diverse spectrum of cellular pathways has been established, including angiogenesis, autophagy, as well as carbon and lipid metabolism [3,4,5]. p53 activity is finely tuned by a large number of signaling pathways which respond to alterations in cellular homeostasis or the microenvironment and result in the modulation of p53 protein

levels, the potential for protein:protein interactions and DNA binding affinity/specificity. Modulation of the p53 network mainly occurs via post-translational modifications of the p53 protein itself [6]. The critical importance of p53 in tumor suppression in humans is exemplified by the high frequency of human cancers showing alterations in the p53 pathway, including p53 mutations [7].

Many studies in a variety of cell lines and *in vivo* animal models have provided striking evidence that the reconstitution of p53 activity can lead to tumor cell death as well as to the regression of established tumors [8,9,10,11,12]. Over the past 15 years such results have spurred a number of studies aimed at developing the

means for restoring wild type p53 function in cells including viral delivery of p53 cDNAs and the rational design of small molecules or peptides that can stimulate p53 functions or reactivate tumor-associated mutant p53 proteins [13,14,15]. In tumors that retain wild type p53, the regulated pathway is frequently, if not always, impaired by other genetic events that result in higher expression and activity of the critical negative p53 regulator MDM2 or, to a lesser extent MDM4 and other modulators of p53 protein localization and activity [16,17,18,19]. The critical roles of MDM2 and MDM4 as negative modulators of p53, which have been elegantly established using knock-out models [20,21], as well as the over-expression of these proteins in several cancer types [17,22,23] raised expectations on the therapeutic potential of restoring p53 functions by MDM2/4 in tumors. However, the identification of chemicals that could disrupt protein:protein interactions or protein:DNA interactions involving p53 has proven challenging [24].

Small molecules that can inhibit the interaction between MDM2 and p53 can result in increased p53 protein levels and lead to p53-dependent growth suppression and apoptosis in different cell-based as well as *in vivo* models [25,26,27]. For example, Nutlin and the MI-43 compounds target the binding pocket for p53 in the MDM2 protein. RITA, which was identified in a cell-based screening assay, binds p53 and also inhibits the p53:MDM2 interaction [25]. Structural studies have identified similarities as well as shape differences between the p53-binding pockets in MDM2 and MDM4 [28], supporting the selectivity of Nutlin in p53:MDM2 interactions [29].

To investigate the impact of small molecules on p53 transactivation potential or on the functional interaction between p53 and cofactors, we have developed a highly defined dual-luciferase functional assay in the budding yeast *Saccharomyces cerevisiae*. This greatly expands our previous system designed to address functions of p53 mutants and target response elements by varying the level of p53 [30,31]. The assay exploits the variable expression of p53 proteins and utilizes the *Firefly* and *Renilla* luminescent reporters integrated as single copies at different chromosomal loci in haploid strains or at the same chromosomal location in diploid strains, *i.e.*, heteroalleles. While a common minimal promoter controls low-level constitutive expression of both reporters, p53-dependent expression of the *Firefly* reporter is attained through a specific p53 response element (RE) placed upstream of the minimal promoter [32,33].

The sensitivity and robustness of the assay system was investigated with various protocols for induction of wild type and mutant p53 protein as well as coincident measurement of the two luciferases. This was followed by an examination of the ability of the dual assay system to discern the functional interaction of wild type and mutant p53 when co-expressed with MDM2 or 53BP1 and the effects of RITA and Nutlin. Our results establish that the functional interactions as well as the impact of the small molecules were distinct and depend on the nature of the p53 mutants. The responsiveness to these chemicals did not extend to PRIMA-1 which has been reported to restore apoptotic activity of specific tumor-associated p53 missense mutants in engineered cancer cells [34,35,36]. We propose that our dual-luciferase yeast assay can be applied to the study of small molecules in order to investigate their differential impact on a large number of tumor-associated p53 mutations as well as partial inactivation of wild type p53 [37]. Furthermore, unlike other p53 screening systems, our genetically well-defined, cell-based assay can be applied to high-throughput screening (HTS) of chemicals toward a matrix of factors that can influence the p53 network including p53 protein levels, p53 mutations, nature of the p53 REs, and level of p53-interacting proteins.

Materials and Methods

Drugs, plasmids and media

RITA was purchased from Cayman Chemical (Cayman Europe, Tallinn, Estonia), Nutlin from Alexis Biochemicals (Enzo Life Sciences, Milan, Italy), and PRIMA-1 was obtained from Inalco (Inalco, Milan, Italy). Stock solutions of the compounds were prepared at the concentration of 10 mM; RITA and Nutlin were prepared in DMSO while PRIMA-1 was dissolved in water. Working dilutions were freshly prepared in yeast culture media immediately before treatment.

pTSG-hp53 was used to express human wild type or mutant p53 protein under the control of the *GAL1* inducible promoter. The plasmid is based on the centromeric pRS314 vector and contains the *TRP1* selection marker. Plasmids pRB254 and pRB759 were used to express MDM2 and 53BP1, respectively. These *HIS3*-marked plasmids were obtained from Rainer Brachmann (Irvine University, CA, USA) and contain full-length MDM2 or a 53BP1 fragment lacking the first 970 amino acids, that are constitutively expressed under the PGK1 and ADH1 promoter, respectively. Given that our luciferase reporter strains could not support *HIS3*-based plasmid selection due to a cryptic mutation in the histidine biosynthesis pathway, to conduct experiments with the co-expression of p53 and MDM2 or 53BP1 we constructed a diploid yeast reporter strain by mating our strain (whose construction is described below) yLFM-PUMA, RFM-M2, $\Delta pdr5$ [*Matx his-*, *leu2*, *trp1*, *ura3*, *ade2::cyc1-LUC*, *pdr5::cyc1-REN*] with the BY4704 strain (*Mata ade2::hisG*; *Dhis3-200*; *leu2- Δ 0*; *lys2- Δ 0*; *met15- Δ 0*; *trp1- Δ 63*, where “ Δ 0” indicates complete removal of the ORF sequence). The resulting diploid is heterozygous for $\Delta pdr5$. Plasmids were transformed into yeast cells using the standard LiAc protocol. Transformants were picked and purified on selective plates containing glucose as carbon source. To conduct the luciferase assays while exploiting variable induction of p53 proteins, yeast cells were cultured in liquid media containing 2% raffinose (Sigma-Aldrich, Milan, Italy) as carbon source or 2% raffinose supplemented with different amount of galactose (Sigma-Aldrich) as inducer of the *GAL1* promoter (as indicated in the Results section and Figure Legends) following the protocol developed previously [31,32,33,38]. All media components were obtained from BD-Bioscience (BD-Biosciences Italy, Milan, Italy) or Sigma-Aldrich. 5-Fluoroorotic Acid was purchased from Toronto Research Chemicals Inc. (North York, Ontario, Canada). The integrative plasmid pdr1DBD-repressor (*sin3*) was a generous gift of Dr. John Nitiss (St. Jude Children's Hospital, TN, USA) and was used to disrupt the regulator of the ABC transporter system *PDR1* gene by replacing it with a fusion construct whereby the *PDR1* DNA binding domain is fused with the *SN3* transcriptional repression domain [39].

Development of dual-luciferase yeast reporter strains

The *Renilla* luciferase open reading frame (ORF) was amplified from the pRL-SV40 vector (Promega, Milan, Italy) and integrated at the *ADE2* locus using the *delitto perfetto* approach [40] starting from the available y-FM-cyc1-ICORE strain [32]. This strain contains the targeting module, consisting of the I-SceI recognition site and GAL1-I-SceI expression cassette, that provides for generation of a single, site-specific double strand break by the homing endonuclease I-SceI. The targeting module also contains a *URA3* and a *KANMX4* marker, respectively, for counter-selection on plates containing 5-fluoro-orotic acid and forward selection for G418 resistance [41]. The *ICORE* was integrated by exploiting homologous recombination downstream of the minimal *CYC1*

promoter and in place of the *ADE2* ORF in the previously developed yAFM strains [38]. ICORE replacement with the *Renilla* ORF resulted in the yRFM (R = *Renilla*) strain which was further modified by introducing the ICORE cassette upstream of the minimal *CYC1* promoter. The resulting yRFM-ICORE strain was then used to develop desired p53 RE insertions upstream of the *CYC1* promoter by targeting the ICORE site with oligonucleotides containing the chosen RE sequences, as previously described [38]. To develop dual-luciferase yeast reporter strains two approaches were followed. To construct an isogenic diploid reporter, the yRFM strain, in which *Renilla* is expressed at basal levels, was transformed by pGAL-HO plasmid [42,43] and cultured in galactose to induce expression of the HO endonuclease in order to induce mating type switching. The yRFM, *Mata* derivatives were identified by crosses with mating type testers, purified and then used in a cross with the yLFM-PUMA p53 reporter strain. The resulting diploid strain is isogenic, but hetero-allelic at the *ADE2* locus, in that one chromosome contains the *Firefly* luciferase, while the other contains *Renilla*. The diploid version of the assay was used for the experiments investigating the impact of MDM2 or 53BP1 on p53 transactivation potential.

A haploid dual-luciferase reporter strain was also developed placing the *CYC1-Renilla* construct at the *PDR5* locus. First, we targeted the *PDR5* gene that codes for a p-glycoprotein whose disruption results in increased sensitivity to a broad spectrum of chemicals [44]. To this aim the *PDR5* gene was modified by PCR-mediated integration of the ICORE disruption cassette starting from the yLFM-PUMA strain. The resulting yLFM-PUMA *pdr5::ICORE* strain was then further modified by replacing the ICORE cassette with a PCR product obtained by amplifying the *Renilla* reporter cDNA starting from the yRFM strain and using PCR primers containing tails of homology for the ICORE integration flanking sites at the *PDR5* locus. Alternatively, the ICORE cassette was removed from the *PDR5* locus using a short oligonucleotide to simply recycle the cassette and leave a complete deletion of the targeted gene. Sequences of all primers for targeting and colony PCR analysis are available upon request.

Small volume dual luciferase assays in yeast

Yeast transformants were selected on plates selective for the presence of the *p53/MDM2/53BP1* expression vectors. Overnight cultures (1 ml) were grown in glucose liquid medium to keep p53 expression repressed. The cultures were then washed in selective medium containing 2% raffinose as carbon source and diluted to OD_{600nm} ~0.1 in media containing 2% raffinose and a desired amount of galactose (see Results section) for the induction of the *GAL1* promoter that drives p53 expression. 100 µl of cell suspensions were placed in 96-well plates. When needed the desired concentration of the small molecules RITA, Nutlin and PRIMA-1 were added to the cell suspension in the 96-well format. The 96-well plate was then incubated for 16 hrs at 30°C under moderate (150 rpm) orbital shaking. Immediately prior to the luciferase assays, cultures were resuspended and 10 µl were transferred to a white 384-well plate. OD₆₀₀ was directly measured in the 96-well plate. For the luciferase assay, 10 µl of PLB buffer 2X (Passive Lysis Buffer, Promega, Milan, Italy) were added to the 10 µl cell cultures, and the 384-well plate was placed on a thermomixer and incubated for 15 min at room temperature with the shaker set at 500 rpm. 10 µl of *Firefly* luciferase Bright Glo substrate (Promega, Milan, Italy) were then added to the cell suspension and light units were measured in a plate reader (Mithras LB940 plate reader -Berthold Technologies, Milan, Italy or Infinite M-200, Tecan, Milan, Italy). For the dual-luciferase assay, 5 µl of the *Firefly* luciferase substrate (Luciferase Assay

Reagent, LARII, Promega) followed by 5 µl of the Stop&Glow buffer were used instead of the Bright Glo, (Promega) to measure *Renilla* activity.

Larger volume luciferase assay in yeast

The results obtained with the newly developed small volume luciferase assay were compared to those obtained with an intermediate protocol that utilized 1 ml liquid cultures to induce p53 expression. Luciferase activity was determined without the laborious extraction of soluble proteins by mechanical lysis and centrifugation. To this aim, 0.5 ml of the cultures were collected by centrifugation after the 16-hour growth in the desired p53-inducing conditions. Cells were suspended in 0.5 ml of 1x PLB (or CCLR) lysis buffer and incubated for 15 min. at room temperature. 10 µl of cell suspensions were then transferred to a white 96-well plate and 50 µl of Bright Glo reagent were added for the luciferase assay. 100 µl of the cell suspension were also transferred to a transparent 96-well plate to measure the OD_{600nm} that was used as normalizing factor. The dual luciferase assay was developed similarly, except for the use of 10 µl of the *Firefly* substrate and 10 µl Stop&Glow® *Renilla* substrate.

Protein extraction and luciferase assay

The results obtained with the newly developed small volume luciferase assay were also compared with the previously developed protocol that relies on 1 to 2 ml liquid cultures of yeast transformants and soluble protein extraction [31,45]. Briefly, purified transformants with the desired p53 expression plasmids were cultured to induce p53 expression for 16 hrs in 2 ml of synthetic selective medium. Cells were then collected by centrifugation, washed in sterile water and suspended in 100 µl of GLO lysis buffer (Promega, Milan Italy) and an equal volume of pre-chilled glass-beads (~0.5 mm, Sigma-Aldrich) was added. Protein lysates were obtained from mechanical lysis of the cells obtained using a vortex mixer. Protein extracts were cleared by centrifugation (15 min at ~16000 g at 4°C) and quantified using the BCA Protein Assay (Pierce Biotechnology, Milan, Italy). Luciferase activity was measured using a multitable Mithras LB940 plate reader (Berthold technologies, Milan, Italy) or Infinite M-200 plate reader (Tecan) using 10 µl of extracts and 50 µl of the Bright-Glo assay reagent (Promega).

Western Blot

Yeast transformants were grown overnight in selective galactose-containing medium and an equivalent amount of cells, based on the culture absorbance measurement (OD_{600nm}), were collected the day after in 1.5 ml tubes by centrifugation (1 min ×14000 g). Cells were washed once with 1 ml of sterile water and harvested again by centrifugation. Pellets were then resuspended in 300 µl of lysis buffer (0.025 M Tris-HCl pH 6.8, 0.015 M NaCl, 10% glycerol, additioned with 0.01 M PMSF and 1x complete protease inhibitor cocktail (Roche, Milan, Italy). One volume of acid-washed glass beads (0.4–0.5 mm diameter, Sigma, Milan, Italy) was added to the cell suspension and lysis was obtained by 6 cycles of 30 sec. vortex at high setting, each followed by 30 sec. on ice. Soluble proteins were then obtained after centrifugation at 4°C for 10 min. at maximum speed. Supernants were transferred and proteins quantified using the BCATM method (Pierce, Thermo Scientific Milan, Italy). Protein extracts were boiled at 95°C for 5 min., resolved with SDS-Page on 7.5% BisTris Acrylamide gels using a Biorad MiniProtean III apparatus (Bio-Rad, Milan, Italy) and transferred to Nitrocellulose or PVDF membranes using the semidry iBlot system (Life Technologies, Milan, Italy). After blotting the quality as well as the equal loading and transfer of

protein blots was determined by Ponceau S staining. The membranes were probed with monoclonal or polyclonal antibodies specific for p53 (pAb1801 and DO-1, Santa Cruz Biotechnology) MDM2 (SMP14, Santa Cruz Biotechnology, D.B.A. Italia, Milan, Italy) and actin (I-19-R, Santa Cruz Biotechnology). The relative Molecular mass (M_r) of the immunoreactive bands was determined using molecular weight markers (Fermentas, Milan, Italy). After washing, blots were incubated with the appropriate IgG-horseradish peroxidase conjugated secondary antibody (Santa Cruz Biotechnology), and immune complexes were visualized with ECL plus reagent (GE Healthcare) using a Molecular Imager ChemiDoc XRS+ system (Bio-Rad). Band intensities were quantified using the Image-Lab software (Bio-Rad).

Results

Development of a small-volume, dual-luciferase assay to study p53 transactivation potential

In previous studies [30,31,32,33,38], we reported several modifications to the original yeast-based *ADE2* color (red/white) p53 functional assay [46]. The p53 gene was placed under the control of the finely-tuned inducible *GALI,10* promoter (“rheostatable”) to address transcriptional issues that are dependent upon protein levels. This system revealed subtle differences in p53 function at many target sequences and identified mutants with enhanced or altered transactivation capacity including change-of-spectrum mutants [47]. The *ADE2* reporter was replaced with the more quantitative *Firefly* luciferase and the system incorporated a convenient *in vivo* mutagenesis system based on oligonucleotides [40] that enabled us to easily create isogenic yeast reporter strains differing only in the p53 RE target sequence driving the luciferase reporter [38]. The resulting system provided opportunities to address the transactivation potential of p53REs, functional SNPs in p53 REs and noncanonical REs [30,31,32,33].

While very informative, the requirement for 1 to 2 ml cultures per experimental condition and soluble protein extraction to quantify *Firefly* luciferase activity limited the experimental opportunities. Thus, we sought to develop a miniaturized system that did not require protein extraction. As described in the following, we found that cells in growth phase as well as stationary of both the haploid and diploid strains we developed could be permeabilized for uptake of luciferase substrate if resuspended in Passive Lysis Buffer (PLB) or Cell Culture Lysis Reagent (CCLR) from Promega (Milan, Italy) without leading to the appearance of soluble protein in the solution. There was a time-dependent loss of viability in PLB buffer (survival was ~10% after 1 hr incubation at room temperature). Cells were incubated for 10 min in the PLB prior to the addition of the *Firefly* luciferase substrate. Since the permeabilized cells retained structural integrity, the optical densities (OD_{600nm}) of cell suspensions could be used for normalization. The assay provides robust measurement of p53-dependent transactivation, as shown in Figure 1A. The transactivation potential of wild type (WT) p53 and the $\Delta 368$ deletion mutant lacking the regulatory domain in the p53 carboxy terminus (C-ter) were determined using three reporter strains and four galactose concentrations to modulate p53 expression. The results are in agreement with our previous analysis of the same p53 proteins and REs using luciferase measurements following protein extraction [31].

We also examined the robustness of the system for detecting luciferase activity within small culture volumes (100 μ l) using 96-well plates and sampling 10 μ l aliquots. In these experiments both WT and the partially functional R282Q mutant were expressed at

variable levels under the inducible *GALI* promoter (Figure 1B and C) as well as under the constitutive *ADHI* promoter (Supporting Information S1). Relative transactivation potential was measured from four p53 REs: the strongly responsive P21-5', the moderate GADD45 and PUMA and the weaker AIP1 [38]. Again, the results were comparable to those obtained with the traditional protein extraction and luciferase protocol (compare Figure 1B with Figure 1C) supporting the use of luminescent reporters, permeabilized cells, and small volumes to assess p53 transcriptional functions as well as providing a high-throughput format.

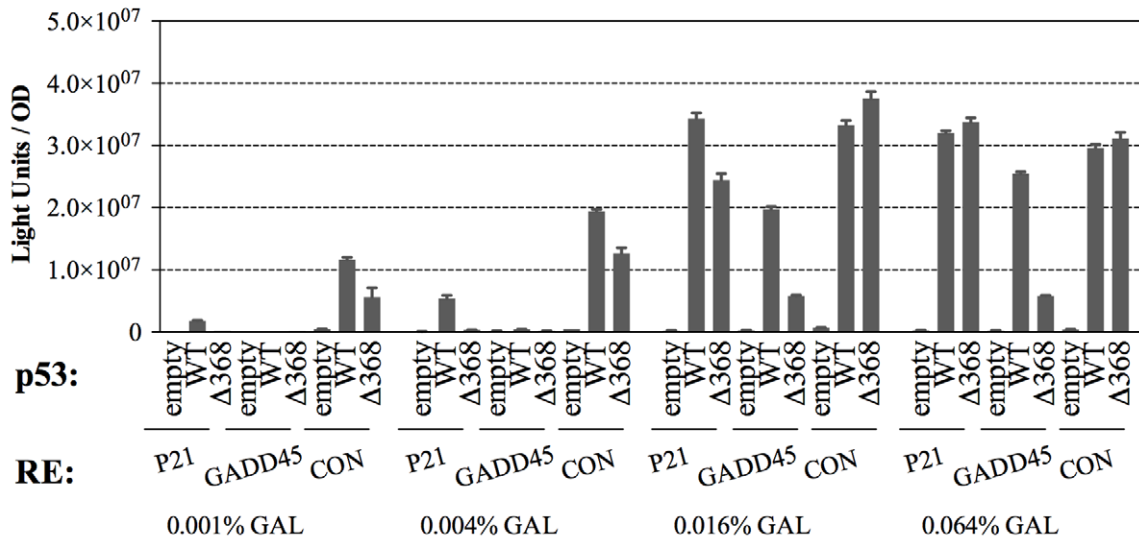
Genetic modification of reporter strains to improve drug accumulation

To make our assay more suitable to test different kind of molecules, we modified the ABC transporter genes to increase the accumulation of small molecules. Specifically, we took advantage of a disruption cassette for the *PDR1* (pleiotropic drug resistance) gene, a regulator of the ABC-transporter system, that replaces the WT gene with a chimeric construct in which the PDR1 DNA binding domain is fused to a transcriptional repressor domain. This chimeric gene provides dominant enhanced sensitivity to a variety of chemicals [39] in yeast. We also disrupted the p-glycoprotein gene *PDR5*, resulting in increased sensitivity to a broad spectrum of chemicals [44,48,49]. Growth of the ABC mutants was examined in liquid cultures under the same conditions used for the luciferase protocol described above (see Materials and Methods). As shown in Figure 1D, the growth rates appeared comparable to WT in raffinose and galactose-containing medium after an initial delay following transfer from glucose medium (Figure 1D). The same results were observed both in rich and synthetic, glucose-containing medium (Supporting Information S1 and data not shown). For all the galactose concentrations used in this study (up to 0.064%) we did not detect an impact of p53 expression on growth parameters of the yeast cultures nor a distinct impact of the genetic modifications targeting the ABC transporter system (not shown). To examine the impact of these genetic modifications on drug accumulation in our strain background, we evaluated the toxicity of cycloheximide [39] (Supporting Information S1). Results confirmed that both *PDR1* and *PDR5* disruption rendered the cells more sensitive to the drug. The *pdr5* mutant was the most sensitive although, surprisingly, the double mutant *pdr1, pdr5* exhibited a slightly reduced sensitivity compared to *pdr5*. Although the specific impact of the PDR1 or PDR5 deletions could be dependent on the nature of the small molecule tested [48], based on the observed relative sensitivity in this work we focused on the *pdr5* mutant to develop the modifications of the yeast-based assay.

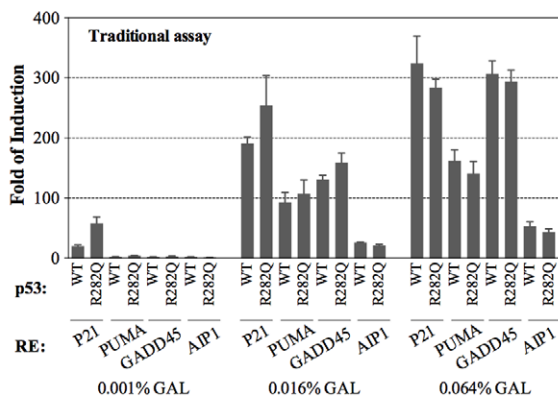
Dual-luciferase system to study p53-dependent transactivation

The system was further modified to include a *Renilla reniformis* cDNA luminescent reporter that could be used for internal normalization rather than relying on cell density. We established that *Renilla* activity can also be measured in cell suspensions prepared in PLB or CCLR lysis buffers by comparing p53-dependent transactivation potential in a pair of strains containing the *Firefly* or the *Renilla* reporters cloned downstream of the moderate p53 RE derived from the human PUMA target gene (the OD provided a normalizing parameter), as shown in Figure 2A. To develop the *Renilla* reporter as an internal standard, the *Renilla* cDNA was placed downstream from the minimal *CYC1* promoter, previously used for the *Firefly* luciferase [38] without the introduction of a p53 RE. This *CYC1-Renilla* minimal promoter-

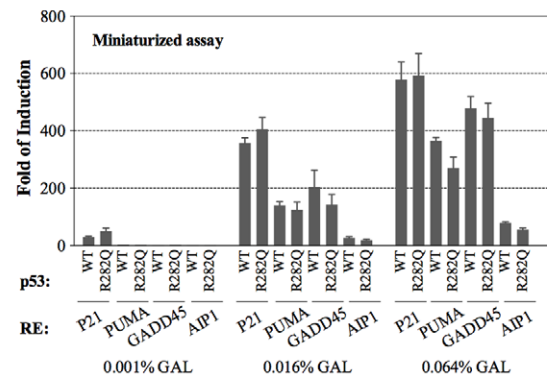
A



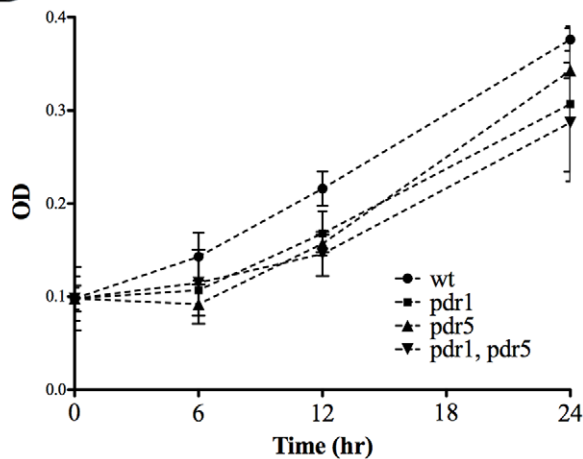
B



C



D



Time (hr)	wt	pdr1	pdr5	pdr1, pdr5
6	0.143	0.107	0.092	0.115
12	0.216	0.168	0.157	0.146
24	0.376	0.307	0.343	0.287

Figure 1. Generation of a small volume format for p53 functional assays. (A) Relative transactivation capacity of WT p53 and a carboxy terminal deletion measured in permeabilized cell cultures and normalized to optical density OD. p53 proteins were induced at different levels by varying the amount of galactose, as indicated. Three different p53 response elements (REs) that differed in relative transactivation capacity from very

strong (CON, an optimized consensus sequence), to strong (P21, corresponding to the p21-5' site) and to moderate (GADD45). OD of the cultures was used as normalizing factor. Presented are the average measurements and standard deviations of three biological replicates. (B, C) Small-volume yeast cultures can determine p53 transactivation capacity. Relative transactivation capacity of WT and the R282Q p53 have been compared towards four different REs obtained with the traditional assay based on 2ml liquid cultures in individual tubes (B) and with the permeabilized assay format based on 100 μ l cultures prepared directly in 96-well plates (C). p53 proteins were induced at different levels by varying the amount of galactose, as indicated. A strong (P21), two moderate (PUMA, GADD45) and a weak RE (AIP1) were compared. Cells collected from the two different culture protocols were used for the measurement of luciferase activity as described in the Materials and Methods section. Presented are the average fold-induction of luciferase by p53 proteins relative to the activity obtained with an empty vector; included is the standard deviations of three replicates. (D) Impact of genetic modifications of the ABC-transporter systems on yeast growth. Overnight liquid cultures in synthetic medium containing glucose were washed and resuspended in fresh medium containing raffinose (2%) as the carbon source and low levels of galactose (0.0032%) (time zero) to induce p53 protein expression. Cultures were diluted to ~ 0.1 OD_{600nm} as measured by a plate reader. OD was measured at the 6, 12, 24hr time intervals. Error bars plot the standard deviations of three biological replicates. The average absorbances are also presented to the right of the graph.

doi:10.1371/journal.pone.0020643.g001

reporter cassette, which provides constitutive basal (low-level) expression of the control luciferase, was cloned at the *PDR5* locus (*pdr5:REM*) in the γ LFM-PUMA reporter strain. The p53 responsiveness of this dual-luciferase system is depicted in Figure 2B. Luciferase activities could be detected using only 10 μ l of cell suspension and 5 μ l of standard luciferase substrate and were comparable to those obtained using our previous approaches that involved lysis by glass beads and larger volumes [31,33].

To directly compare the different approaches for detecting p53 transactivation, the WT p53 and the R282Q mutant were tested in the following manner: i) 2 ml cultures of cells were lysed with glass beads; ii) 500 μ l of the 2 ml cultures were transferred into 1.5 ml eppendorf tubes and permeabilized with 100 μ l of 1x lysis buffer; and iii) 100 μ l cultures were incubated in 96-well plates of which 10 μ l were transferred into 384-well plates and permeabilized by an equal volume of 2x PLB lysis buffer. As shown in Figure 2C, the miniaturized dual-luciferase assay provides a sensitive and robust system for addressing p53 dependent transactivation in a format that is amenable to high-throughput screens.

Functional interactions between p53 and MDM2 or 53BP1 using the yeast-based dual luciferase assay

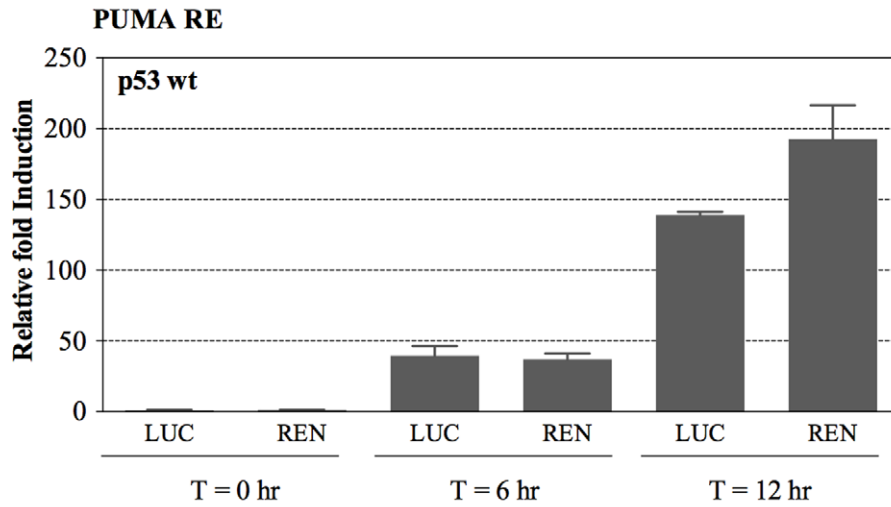
A goal in the development of the dual luciferase system was to obtain a suitable assay to address interactions of p53 with factors that determine its stability and to identify chemicals that could modify those interactions. Specifically, we addressed the functional interaction between p53 and MDM2 and the impact of small molecules targeting this interaction. MDM2 is a critical inhibitor of p53 functions that can bind p53 in the amino terminal (N-ter) region and lead to p53 protein degradation via its E3 ubiquitin-ligase activity in human cells [50]. For these experiments we generated diploid reporter strains that could select for the MDM2 expression vector (see Materials and Methods). The diploid cells were heterozygous for the *PDR5* deletion. Consistent with a previous report [51], we found that in yeast MDM2 co-expression resulted in a reduction of p53-dependent transactivation. Initially, we explored the impact of MDM2 on the ability of increasing amounts of p53 protein to transactivate the *ADE2* red/white reporter from an upstream p53 RE [30,38]. The MDM2 cDNA was expressed constitutively under the moderate *PGK1* promoter. Reduction of p53-dependent transactivation by MDM2 was observed only at very low levels of p53 expression (Supporting Information S1, raffinose only vs raffinose + galactose plates) and was affected by amino acid changes in the p53 N-ter mimicking post-translational modifications. The MDM2 inhibition of p53 activity in this semi-quantitative assay was dependent on the p53 RE examined and was observed only with the highest p53 affinity REs, p21-5' and CON, being suitable for the *ADE2* reporter assay.

The impact of MDM2 on p53 WT and mutants was subsequently evaluated using a luciferase-based assay. Specifically, serine/threonine residues in the N-terminal domain were mutated to mimic phosphorylation events in mammalian cells or to prevent phosphorylation; these residues are modified as part of the signaling pathways that activate p53 by influencing protein:protein interactions including that with MDM2 [52,53,54]. As shown in Figure 3A, we confirmed that MDM2 could inhibit p53-dependent transactivation from different p53 REs. The impact of the mutations was in part dependent on the nature of the p53 RE driving *Firefly* luciferase expression. In particular the T18E and S20D p53 mutants were less sensitive to MDM2-dependent inhibition of transcription at a moderate RE (Killer/DR5) than with a strong RE (p21-5'). On the contrary, transactivation at either RE by p53 mutants mimicking constitutive phosphorylation (referred to as "4D" and "6D" in the figure) was largely insensitive to co-expressed MDM2. The transactivation potential of those N-ter p53 mutants when expressed alone was comparable to WT p53 with the exception of the multiple mutant 6A, where the concomitant change of Ser 15, 20, 33, 37, 46 as well as of threonine 18 into alanine resulted in approximately three-fold higher activity (Supporting Information S1).

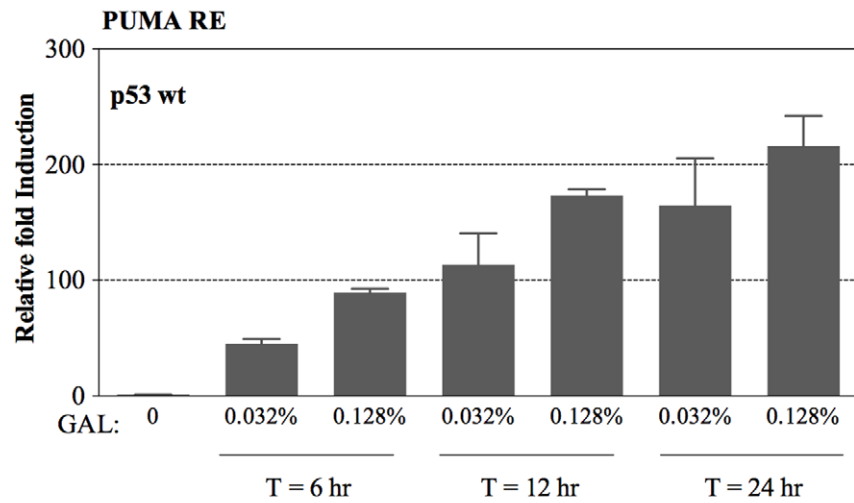
The impact of MDM2 co-expression on WT p53 protein levels was also assessed using western blot analysis (Figure 3B & C). p53 protein levels were determined from cells grown in glucose (steady-state) or from cells grown in galactose for 16 hrs to induce p53 and then transferred to glucose media to repress the transcription of the p53 cDNA to estimate the p53 protein half life in yeast. p53 protein amounts were quantified relative to β -actin loading control. A 10% reduction in steady-state p53 protein amount due to the co-expression of MDM2 was observed in the galactose-induced cultures (Figure 3B lanes 3 & 4). Furthermore, MDM2 appeared to reduce p53 half life in yeast, based on relative quantitation of the immunoblot at the various time points after the transfer of the cells to glucose medium. p53 half life was estimated to be ~ 2.5 hours in cells that express MDM2 and 5 hours when MDM2 was not expressed (Figure 3C). MDM2 protein levels also appeared to vary during the experiment, in relation to the growth phase of the cultures. A previous study reported that the *PGK1* promoter that controls MDM2 cDNA expression in the vector we used, could be severely repressed in stationary phase cells, while remaining largely unaffected by changes of carbon sources in the medium [55]. It is important to note that all the luciferase assays in our work were conducted in cultures grown for 16 hrs in galactose-containing medium, when cells are still in a late-logarithmic culture phase. A previous study in yeast where MDM2 and p53 were co-expressed under a *GAL* promoter reported a similar impact of MDM2 on p53 protein half life [56].

Overall, these results strongly suggest that the functional interaction between p53 and MDM2 is at least in part dependent

A



B



C

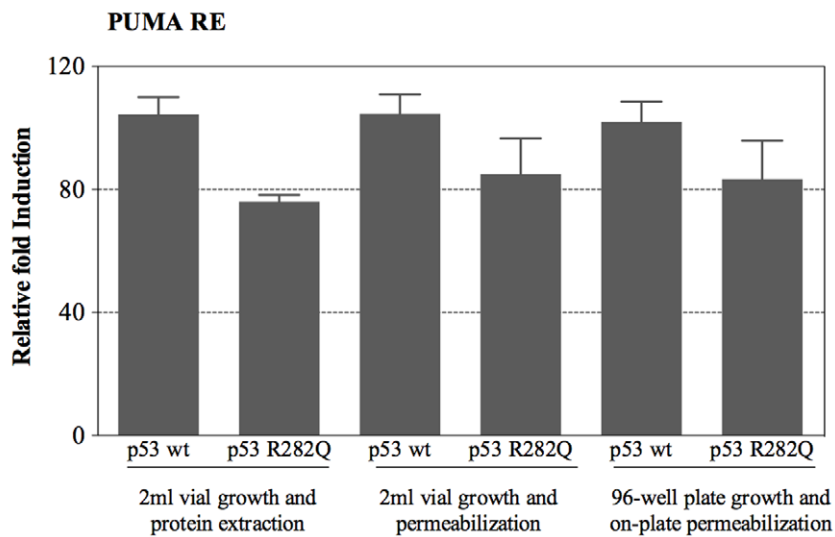


Figure 2. Either *Firefly* or *Renilla* luciferase can function as p53-dependent reporters. (A) The ability of *Firefly* and *Renilla* cDNAs to serve as reporters for p53 transactivation was examined by placing them downstream from the moderate p53 RE derived from the PUMA promoter in isogenic strains. The values indicate the fold induction measured over an empty vector. Presented are average and standard deviations of three replicates relative to optical density of the cultures measured at different times (T in hrs) after switching cultures to galactose-containing medium. (B) Dual luciferase reporter assay with a strain expressing WT p53 and containing the *Firefly* luciferase as p53 reporter gene and the *Renilla* luciferase as constitutive reporter. Presented are the average and standard error of the *Firefly* luciferase activities normalized for *Renilla* and compared to empty vector at various time points after shifting 100 μ l yeast cultures to galactose-containing media in the 96-well plate format. (C) Comparison of relative induction using measurement of protein from 2 ml cultures vs direct permeabilization of cells in a 384 well format following transfer from a 96-well growth plate, as described in the text and the Materials and Methods section. Relative transactivation capacities of WT p53 and the R282Q mutant in the "2 ml vial" experimental set-ups were measured using either protein extraction or permeabilization. Experiments were conducted using 0.032% galactose inducer, unless specified otherwise. Error bars plot the standard error of four biological replicates. doi:10.1371/journal.pone.0020643.g002

on the same amino acids in the p53 N-ter domain as in mammalian cells but does not lead to a strong reduction in p53 protein stability. Thus, the impact of MDM2 in yeast is likely due to a competing effect for p53 binding to components of the transcription machinery, as suggested previously [51].

We extended the study of p53 interactors in the dual-luciferase system to 53BP1 using a yeast-expression vector containing a 53BP1 clone with N-ter deletion of the first 970 amino acids [51]. 53BP1 was identified in a 2-hybrid screen by its ability to bind the DNA binding domain (DBD) of p53 through the BRCT domains present in the C terminal region (C-ter) of 53BP1 [57]. While 53BP1 was shown to act as a positive cofactor for p53 function in human cells [58], its co-expression with p53 (WT or mutant) in our yeast-based assay led to a reduction in p53-dependent transactivation (Figure 4 and 5C), consistent with a previous study [51]. This result indicates that 53BP1 might compete with p53 for sequence-specific binding to DNA. Unlike the general inhibition by MDM2, the impact of 53BP1 differed towards specific partial-function p53 missense mutants, consistent with the p53:53BP1 physical interaction. For example, transactivation by the R181L and R282Q mutant proteins were slightly or not affected by 53BP1, while the transactivation by A119V, P219L and R283H was reduced by co-expression of 53BP1 (Figure 4).

The small molecules Nutlin and RITA can reduce the inhibitory effects of MDM2 and 53BP1

Using the dual luciferase system we then investigated the impact of two well-known small molecules than can affect p53, namely Nutlin and RITA. The former can disrupt the interaction between p53 and MDM2 by binding to MDM2 while RITA can interfere on the same interaction by targeting p53, possibly leading to conformational changes [59]. As summarized in Supporting Information S1, we did not observe a significant impact on yeast growth under the conditions used for the WT strain or for the ABC-transporter mutants, although the mutants experienced a delay in growth following the shift in media (also described in Figure 1). While Nutlin had little impact on transactivation by p53 alone it counteracted the negative impact of MDM2 (Figure 5A).

Treatment with RITA led to a severe reduction in p53-dependent *Firefly* luciferase activity (Figure 5B). However, also the basal luciferase activity was affected by RITA, indicating that the effect might not be related to p53. A negative impact of RITA on *Firefly* luciferase activity was previously reported in mammalian cells [60]. However, RITA had no impact on the basal activity of the *Renilla* luciferase. We, therefore, constructed a dual luciferase reporter strain in which the *Renilla* luciferase was placed under p53 transcriptional control. In this strain, treatment with RITA had no effect on p53-induced transactivation detected by the *Renilla* luciferase (Supporting Information S1). After taking into account the impact of RITA on basal *Firefly* luciferase activity, we were able to show that RITA could partially relieve the inhibition of

p53-dependent transactivation by MDM2 (Figure 5C). The impact of Nutlin and RITA on the p53/53BP1 functional interaction was also examined. Treatment with Nutlin did not modify the 53BP1-dependent inhibition of p53-dependent transactivation (Figure 5C). However, the inhibition was partially relieved by RITA. Western blot analysis confirmed that MDM2 co-expression had little impact on p53 protein levels after culturing cells for 16 hrs in 0.012% galactose. Interestingly, treatment with Nutlin but not RITA appeared to reduce MDM2 expression/stability (Figure 5D).

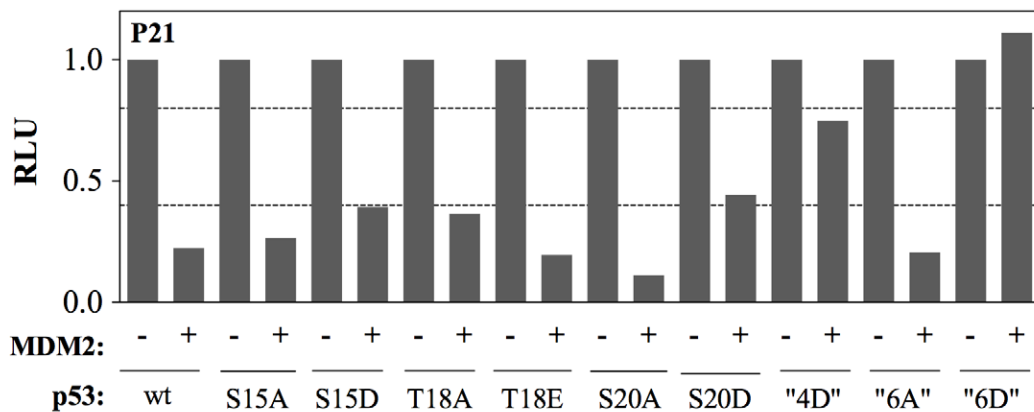
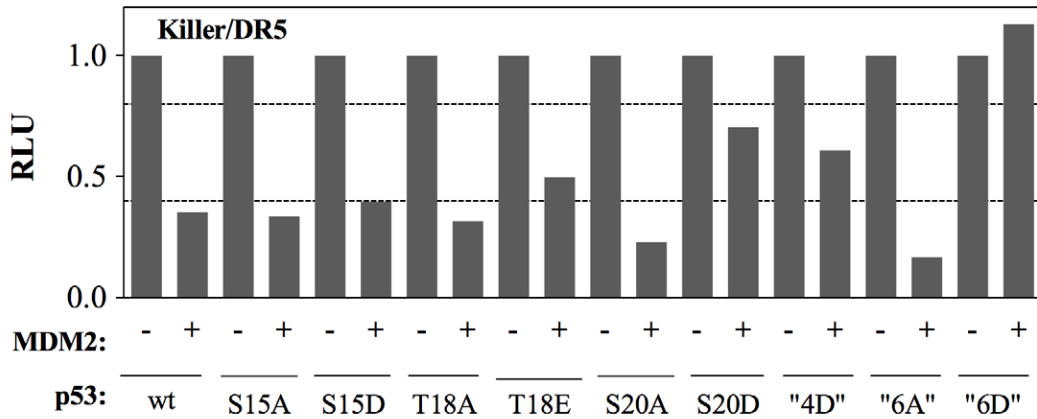
PRIMA-1 exhibited an apparent lack of impact on p53 mutants

The dual luciferase system was investigated for its responsiveness to PRIMA-1, a small molecule identified in a mammalian cell-based screen for chemicals that could induce apoptosis in a mutant p53-dependent manner [35]. PRIMA-1 restored sequence-specific DNA-binding and transcriptional transactivation to mutant p53 *in vitro*, possibly through altering mutant p53 conformation or folding stability [61] although the precise mechanism remains to be determined. To examine the impact of PRIMA-1, we chose a panel of p53 mutations that differ in their relative transactivation capacity in the yeast-based assay. Four loss-of-function mutants were tested, including the two cancer hotspot mutants R175H and R273H that were shown to be responsive to PRIMA in human cells [35]. We also examined 5 partial function p53 mutations since they could register negative and positive impacts of small molecules. The transactivation potential of the p53 mutants ranged from 50 to 80% of the WT protein in the reporter strain containing the PUMA p53 RE under moderate expression from the *GALI* promoter. As described in the supplementary material, we were unable to detect any effect of PRIMA-1 on transcription by WT or mutant p53 in WT (not shown) or in *ptr5* mutant cells (Supporting Information S1).

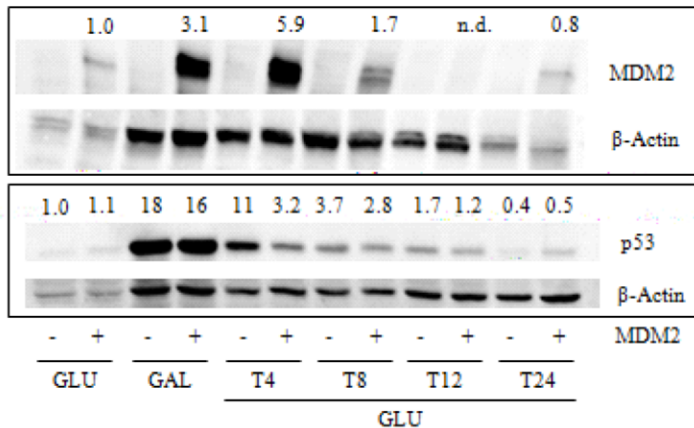
Discussion

In this study we have greatly expanded the features of our previously described yeast strains for assessing p53 and p53 RE function in order to develop a system that is both more efficient and miniaturized. The system provides for rapid assessment of p53 transactivation potential as well as the impact of p53 mutations, cofactors and small molecules. In particular, it integrates variable expression of p53 proteins under the finely tunable *GALI* promoter, single copy luminescence reporters that are chromosomally located with opportunities to co-express p53 alleles along with chosen cofactor proteins coded from selectable low copy number plasmids. Furthermore, the assay is based on a small-volume format for p53 expression, treatment with chemicals, and quantification of the reporter expression and is compatible with high-throughput screening.

A



B



C

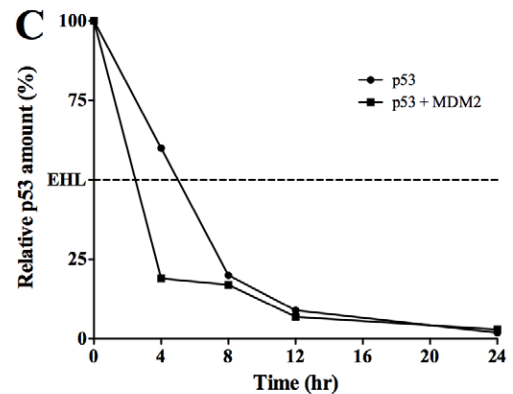


Figure 3. MDM2 co-expression reduces WT and mutant p53-dependent transactivation and can impact p53 protein level and stability. (A) The functional interaction between p53 and MDM2 was examined using two different reporter strains, as indicated. Transformants were cultured in 0.012% galactose to achieve low expression of p53 for 16 hours. MDM2 is expressed under the constitutive PGK1 promoter. Besides WT p53, several mutants at Ser/Thr in the p53 N-ter were tested. The activity of each p53 mutant was set to one to better focus on the relative impact of MDM2 co-expression on p53 transactivation capacity. The relative transactivation potential of the various p53 mutants is presented in Supporting Information S1; 4D refers to a quadrupole mutant with S15D, T18E, S20D, S33D changes in p53. 6A indicates a multiple mutant with alanine changes at S15, T18, S20, S33, S37, S46. 6D indicates a multiple mutant with aspartic acid changes at S15, S20, S33, S37, S46 and a glutamic acid change at T18. Presented are the average fold-inductions by p53 proteins compared to empty vector and normalized using the *Renilla* control luciferase. These assays were conducted with diploid strains that were obtained by crossing the indicated yLFM- p53 reporter strains with the BY4704 strain (see Materials and Method section) using the permeabilized format. (B) Western blot analyses of p53 and MDM2 protein levels. O/N cultures in synthetic glucose medium (GLU) were washed and shifted to medium containing raffinose and 0.012% galactose (GAL) to achieve low expression of p53. The p53 was expressed under the inducible *GAL1* promoter while MDM2 was expressed at constitutive levels from a moderate *PGK1* promoter. After

16 hrs of growth in galactose-containing medium, cells were washed and transferred to glucose medium to repress the *GAL1* promoter. Samples were collected at the indicated time points to prepare protein extracts for western blot. 100 μ g (MDM2 and actin, top panel) and 20 μ g (p53 and actin, lower panel) of extract was loaded in each lane. The DO-1, SMP14 and I-19-R antibodies (Santa Cruz) were used for the immunodetection of p53, MDM2 and actin, respectively. Actin levels were used as a normalization factor to estimate relative MDM2 and p53 amounts. Consistent with a previous study [55], we observed that MDM2 expression under the *PGK1* promoter was affected by the culture state and was particularly reduced when cell approached the stationary phase (O/N in glucose; T8 and T12 time points; at T12 cells were diluted for the additional 12 hr time point). The relative changes in MDM2 and p53 protein amounts compared to the level observed in glucose cultures are indicated above the immunoblot. (C) Quantification of p53 expression relative to the amount observed after 16 hrs in 0.012% galactose, normalized to actin levels. A 10% reduction in steady-state p53 protein amount due to the co-expression of MDM2 was observed in the galactose-induced cultures. To better visualize the impact of MDM2 on the estimated p53 half life (EHL) the relative amount of p53 observed after 16 hrs in galactose was set to 100%, both for extracts of cells expressing only p53 or p53 + MDM2. doi:10.1371/journal.pone.0020643.g003

Interactions with p53-cofactor proteins

Specifically, we have established that the new, dual-luciferase based protocol can assess p53-dependent transactivation and the impact of single amino acid changes in the p53 DBD. We found that co-expression of MDM2 can lead to reduced p53 transactivation at low levels of p53 protein expression. p53 mutants at the DBD that have partial transactivation function were also inhibited by MDM2, whereas mutations introduced into the p53 N-ter domain that mimic phosphorylation events could relieve p53 from the MDM2-dependent inhibition. Those same amino acid changes did not alter significantly the transactivation potential of the p53 protein, when expressed alone. This suggests that the assay can be used to reveal ectopic p53:MDM2 physical interactions that are likely to occur at the p53 N-ter region, similar to the endogenous interaction in higher eukaryote cells. The assay also revealed a modest impact of MDM2 on p53 protein stability in yeast. Although MDM2 was recently found to bind p53 at the DNA binding domain (DBD) and at the C-ter [62], the primary site of interaction occurs at the transactivation domain (TAD) in the p53 N-ter region [63].

We also examined the impact on p53 transactivation of another important p53 cofactor, the protein 53BP1. The BRCT domains present in the 53BP1 C-ter are required for the interaction with p53 as well as with other important proteins such as BRCA1 [57]. The physical and functional interactions between p53 and 53BP1

in the context of DNA damage response appears to be complex. Following DNA damage, 53BP1 can localize to nuclear foci in mammalian cells, is rapidly phosphorylated in an ATM-dependent manner [64], and is essential for DNA double strand break repair [65]. Furthermore, 53BP1 appears to be an important mediator of the induction of senescence and cell death pathways elicited by BRCA1 deficiency in mice [66]. A crystal structure of p53 DBD bound to the human 53BP1 BRCT domains led to the identification of amino acids in the p53 DBD involved in such interaction [67]. More recently, the Tudor domain of 53BP1 was shown to interact with p53 proteins dimethylated in the p53 C-ter region at lysine 382 [68]. The generation of p53 dimethylated at Lys382 promotes the accumulation of p53 protein that occurs upon DNA damage but this accumulation is dependent on 53BP1 [69]. These results suggest that the positive coactivator function of 53BP1 towards p53 in mammalian cells [58] may be related to its positive impact on p53 protein amount. Possibly, 53BP1 reduces the interaction between p53 and MDM2 (G. Selivanova, unpublished results).

The co-expression of 53BP1 with p53 leads to a reduction in p53-dependent transactivation, similar to previously reported findings in yeast [51]. Unlike MDM2, the impact of 53BP1 was lost or greatly reduced with specific partial function p53 mutants in the DBD. For example the p53 R181L mutant was not sensitive to 53BP1. Structural studies showed that p53 R181 formed both a

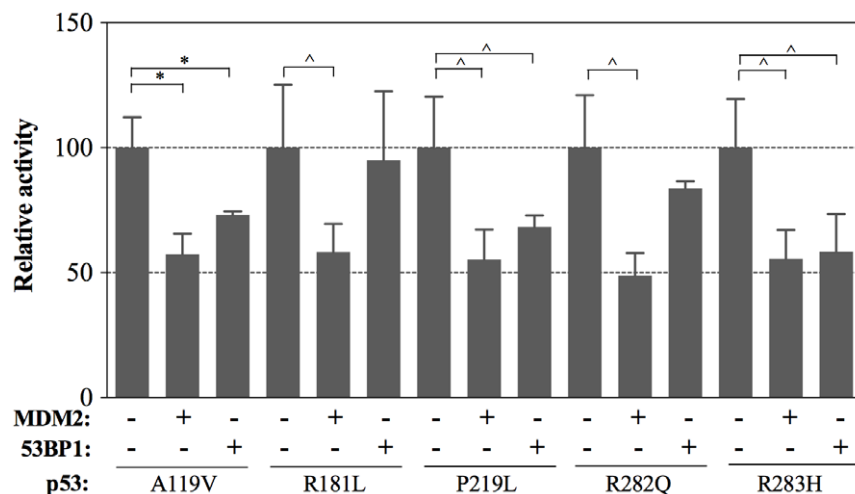
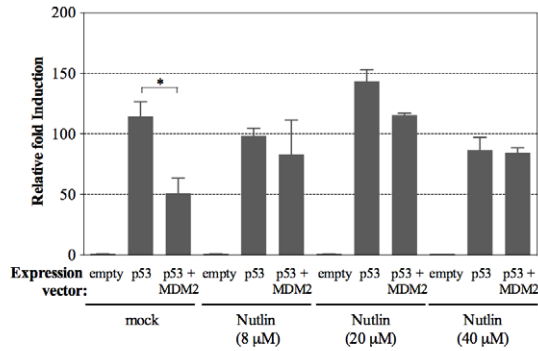
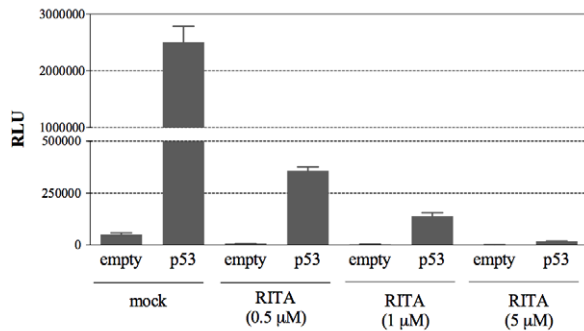


Figure 4. Functional interactions between partial function p53 mutants and MDM2 or 53BP1. Mutant p53 expression was under the control of the *GAL1* promoter while MDM2 or 53BP1 (a clone containing a N-ter deletion of the first 970 amino acids) were expressed at constitutive levels under the *PGK1* and *ADH1* promoters, respectively. p53 expression was induced for 16 hrs in medium containing 0.012% galactose. Presented are results describing the impact of MDM2 or 53BP1 on transactivation of various p53 mutants that are capable of partial transactivation toward the PUMA RE. To better visualize the impact of MDM2 and 53BP1, the activity of each p53 mutant alone is set to 100%. The relative light units of the various mutants in this experiment were WT p53, 2.1×10^5 ; A119V, 1.3×10^5 ; R181L, 0.86×10^5 ; P219L, 0.87×10^5 ; R282Q, 0.79×10^5 ; R283H, 0.53×10^5 . Significant differences in activity relative to p53 alone are shown (*: $p < 0.01$; ^: $p < 0.05$, Student's t-test). doi:10.1371/journal.pone.0020643.g004

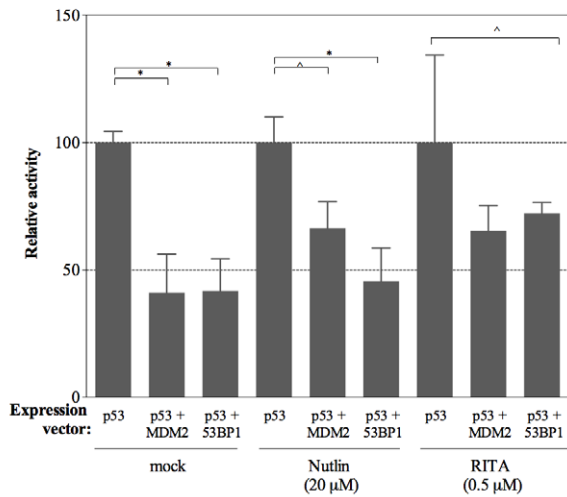
A



B



C



D

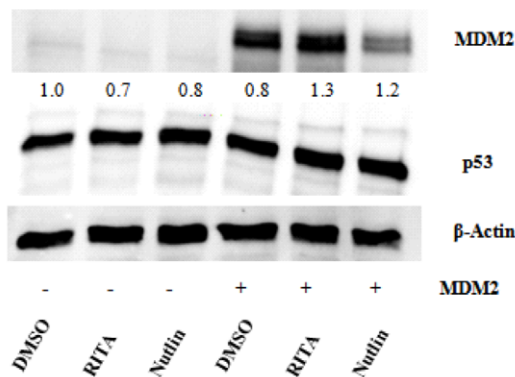


Figure 5. Functional interactions between wild type p53 and MDM2 or 53BP1 and the impact of Nutlin and RITA. WT p53 was expressed at low-level achieved by culturing cells in medium containing 0.012% galactose for 16 hrs in the 96-well plate format. MDM2 was expressed from the moderate PGK1 promoter. (A) The impact of MDM2 on p53-dependent transactivation was examined in the presence of different concentrations of Nutlin added to the medium at the time of the switch to galactose-containing medium using a reporter strain containing the moderate PUMA p53 RE. The average transactivation relative to the basal level of reporter activity measured in cells that do not express p53 and standard deviations of three biological repeats are presented. Significant differences in activity relative to p53 alone are shown (*: $p < 0.01$, Student's t-test). (B) Firefly luciferase activities normalized using the control luciferase *Renilla* are presented for empty vector and wild type p53 in the presence of different amounts of RITA. (C) Nutlin and RITA impact on the functional interactions between p53 and MDM2 or 53BP1. Nutlin (20 μM) or RITA (0.5 μM) were added at the time of switching cultures to galactose-containing medium. The luciferase activity by wild type p53 alone, normalized using the *Renilla* control luciferase, is set at 100%. Both MDM2 and 53BP1 co-expression reduced p53-dependent transactivation. Nutlin partially relieved the functional impact of MDM2, but not that of 53BP1. RITA partially relieved p53 from the inhibition by both MDM2 and 53BP1. Significant differences are shown (*: $p < 0.01$; Δ : $p < 0.05$, Student's t-test). (D) MDM2 and p53 immunoblot in mock-, RITA- and Nutlin-treated yeast cells. Proteins were prepared from cells grown in medium containing 0.012% galactose for 16 hrs and treated with DMSO solvent control 0.5 μM RITA or 20 μM Nutlin. 25 μg were loaded to detect p53 and 100 μg of protein extracts were loaded to probe for MDM2. Actin was used as a loading control.

doi:10.1371/journal.pone.0020643.g005

hydrogen bond and stacking interactions with 53BP1 residues in the BRCT domains [67]. The reduced interaction between the p53 mutant R282Q and 53BP1 could not be linked to the reported physical interaction between the two proteins.

Overall, our results indicate that the dual-luciferase yeast-based assay can be used to study the interaction between p53 and cofactor proteins. While the functional interaction appears dependent on conserved physical interactions, the outcomes of the co-expression on p53-dependent transactivation in the yeast assay does not always reflect expectations from mammalian cells, although such discrepancies can be reasonably explained and related to the defined nature of the assay, as proposed above for the impact of 53BP1.

Impact of small molecules

Having established that the yeast-based assay can reveal a functional interaction between p53 and its cofactors MDM2 or 53BP1, we explored the impact of small molecules targeting those interactions using Nutlin and RITA. Nutlin had been isolated as a small molecule that interacts with the p53-binding pocket in MDM2, resulting in accumulation of p53 protein and possibly inhibition of MDM2 activity towards other of its targets [10,59,70]. Treatment with Nutlin led to p53 accumulation in a variety of cancer cell lines, without significant induction of p53 post-translational modifications, and resulted mainly in cell cycle arrest, although apoptosis was also detected. The compound showed p53-dependent growth suppression in *in vivo* experiments without much evidence for toxicity in nude mice. The small molecule RITA (reactivation of p53 and induction of tumor cell apoptosis) was obtained in a cell-based assay screening for induction of WT p53-dependent apoptosis [25]. Its mechanism of action appears to be at least in part related to a direct interaction with the p53 protein and inhibition of the p53-MDM2 binding. Differently from Nutlin, which directly affects the binding of MDM2 to the amino-terminal region of p53, RITA was reported to bind the p53 N-ter region and indirectly affect the

functional interaction with MDM2 [59,70]. RITA could induce p53-dependent apoptosis in a variety of tumor cell lines [25].

Our results establish that treatment of yeast cells with the small molecules Nutlin or RITA could partially relieve WT p53 from the MDM2-dependent inhibition, similar to what is observed in mammalian cells. Furthermore, while Nutlin treatment had no impact on the functional interaction between p53 and 53BP1, RITA was also able to target the p53/53BP1. Combined with the observation that 53BP1 appeared to interact with p53 mutants in a manner that is mutant-specific, our results suggest that the yeast-based assay could be used to screen a large panel of tumor-associated p53 mutations for differential impact of these chemicals on p53 functional interaction with cofactors.

Attempts to modify WT or mutant p53 function by PRIMA-1 were unsuccessful. PRIMA-1 was reported to restore the sequence-specific DNA-binding and transcriptional transactivation of some p53 mutants *in vitro* and to suppress tumor-cell growth in mice by inducing apoptosis (Bykov *et al.*, Nat Med. 2002). Interestingly, PRIMA-1 inhibited the growth of cell lines derived from various human tumor types in a mutant p53-dependent manner [71]. The precise mechanism of action of this compound is not clear; moreover its selectivity for mutant p53 remains to be fully established and may also be related to indirect effects on p53 folding and nuclear localization. For example PRIMA-1 induced the expression of heat shock protein 90 (Hsp90) in breast cancer cells, restored the p53-Hsp90 interaction and enhanced the translocation of the p53-Hsp90 complex to the nucleus [72]. Recently the ability of PRIMA-1 to induce nucleolar localization and degradation of mutant p53 protein has been demonstrated [73], suggesting the existence of a complex mode of action, likely cell-type specific, that can be independent from the restoration of transactivation functions to mutant p53. Indeed, PRIMA-1 fails to stimulate the DNA binding potential of isolated mutant p53 DBD *in vitro* [59]. The apparent lack of effect of PRIMA-1 in our assay might be due to poor uptake, even in the *pdr5* mutant, or modification of the chemical in yeast. It has been shown that PRIMA-1 is converted to compounds that forms adducts with thiols on mutant p53 and such p53 protein modifications can trigger apoptosis [61]. It might well be that these activating modifications are impaired in yeast.

Overview

Cell-based functional assays are expected to be useful tools for identifying molecules targeting mutant p53 or impacting on the interaction between p53 and cofactors. They can provide unbiased screening opportunities for leads that act beyond steric hindrance of protein:protein interactions including allosteric modifiers of protein folding or stability. Allosteric modulators could be combined potentially with rationally designed drugs to increase potency or overcome single agent resistance *in vivo* [74]. In this regard initial studies suggest that the combination of Nutlin and RITA might provide additional stimulation of p53-induced responses, consistent with the different broad transcriptional responses induced by the two compounds when given as single agents [75]. However, off-target effects that impact the biological endpoints being measured, such as the induction of apoptosis, can hamper identification of mechanisms of action of molecules scoring positively in cell-based screening assays. This potentially limiting feature is especially relevant in the case of proteins like p53, whose functions are wired into many cell-signaling pathways. Furthermore, the tremendous variability in tumor-associated p53 mutations and in expression levels of distinct p53-interacting proteins and p53 splice and promoter variants as well as p53-related proteins p63 and p73 could significantly affect the outcome

of small molecule treatments. The yeast-based assay described here has the advantage of generally being free of p53 biological consequences. Alternatively, assays have been developed that exploit the impact of moderate/high levels of p53 expression on the growth of yeast [76,77]. This type of assay provides the opportunity to score the effect of cofactors or small molecules that may also act on p53 transcriptional-independent functions. However, the exact mechanisms of p53-mediated growth retardation in yeast are not well-defined. The growth retardation could be, in part, dependent on effects on transcriptional complexes, based on our previous identification of toxic p53 alleles in yeast that at low expression levels result in enhanced transactivation capacity and on the loss of the toxicity caused by second-site loss-of-function missense mutations in p53 ([47,78].

The spectrum of missense p53 mutations associated with sporadic and familial cancer comprises more than 1200 distinct sporadic and ~110 germline mutations (www.iarc.fr/P53/) [79]. Furthermore, biochemical, and functional assays have revealed that the degree of thermodynamic as well as folding instability caused by the mutations and their impact on sequence-specific transactivation function can vary greatly [30,80,81]. These differences could impact the activity of small molecule modifiers. Furthermore, the efficacy of allosteric modifiers could be significantly affected by the cellular/nuclear amounts of p53 mutant proteins or by the ratio between wild type p53 and specific negative cofactors, such as MDM2 or MDM4. Finally, the impact of small molecules could be, in part, influenced by the nature of the interaction between p53 and its many different cognate response elements located in the large number (hundreds) of human p53 target genes [82,83,84].

In summary, we propose that the miniaturized yeast dual luciferase system we developed provides a genetically well-defined, robust and cost-effective assay that can be used in parallel to mammalian cell-based assays to screen molecules or further evaluate leads that target p53 functions. A specific advantage of the assay is the potential for high-throughput assessment of a matrix of factors that include low and variable levels of p53 proteins, nature of the p53 response elements and specific, disease-associated p53 mutations. All these variables could impact the activity of small-molecule modifiers of p53 functions. Our assay system could be particularly relevant for further characterization of small molecules that may act as allosteric modifiers of p53 functions or p53-cofactor interactions.

Supporting Information

Supporting Information S1 1. Small-volume yeast functional assay with constitutive expression of p53 proteins. Presented is the comparison of the relative transactivation capacity of wild type (WT) and the R282Q p53 towards four different response elements (REs) obtained with the traditional assay based on 2 ml liquid cultures in individual tubes (A, traditional assay) and with the permeabilized assay format based on 100 μ l cultures prepared directly in 96-well plates (C, miniaturized assay). p53 proteins were expressed under the moderate, constitutive ADH1 promoter. Cells collected from the two different culture protocols were used for the measurement of luciferase activity as described in the Materials and Methods section. Presented are the average fold-induction of luciferase by p53 proteins relative to the activity obtained with an empty vector; included is the standard deviations of three replicates. In these experiments the light units per OD for WT p53 and the p21-5' RE were 2.8×10^6 for the 2 ml cultures and 2.5×10^7 for the 100 μ l cultures. **2. Impact of genetic modifications at**

the ABC transporter system on cell sensitivity to cycloheximide. Based on the experiments described by Stepanov *et al.* [39] we used cycloheximide treatment to evaluate whether the disruption of *PDR1* and replacement with the *PDR1*-repressor construct, the disruption of *PDR5*, or the combined modifications would result in enhanced toxicity in our reporter strain background. Cells from the indicated strains were resuspended in sterile water and transferred to a 96-well plate. Serial dilutions (1:5) were prepared and cells were transferred to plates containing synthetic medium (SD) with different concentrations of cycloheximide using a 48-pin replicator. A rich (YPDA) and an SD control plates were also spotted for comparison. Plates were incubated for two days at 30°C. **3. Phenotypic analysis of the impact of MDM2 on WT and mutant p53 transactivation.** The ADE2-based red/white assay was used to examine p53 dependent transactivation and the impact of MDM2. p53 was expressed at low levels under the *GALI* promoter in media containing only raffinose (2%), or raffinose plus 0.002%, 0.004% or 0.016%, galactose. MDM2 was expressed from the constitutive *PGK1* promoter. p53 transactivation was examined from three REs upstream of ADE2-based p53 reporter strains as indicated. The optimized consensus (CON) and P21-5' p53 RE yield levels of high transactivation while the NOXA RE is weaker [38]. In the ADE2-based p53 functional assays, cells grown on plates containing a low-amount of adenine (5 mg/L) result in small red colonies when p53 is not present or not transcriptionally active. p53-dependent expression of ADE2 results in the appearance of colonies with a color ranging from light red to white, depending on the level of transactivation. To reveal the dependency of the phenotype on p53 expression levels, streaks are prepared on glucose plates containing high amount of adenine (200 mg/L) and the plates are incubated for two days at 30°C, resulting in the appearance of white colonies. These plates are then replica-plated to a stack of plates containing 2% raffinose plus various levels galactose along with the low-level of adenine. The replica plates are then incubated at 30°C for 2-3 days. Images of a section of the replicas are presented. For each image the upper section corresponds to colonies expressing p53 alone, while in the lower section the colonies also express MDM2. Various multiple mutants were tested, as indicated. **4. Relative transactivation capacity of p53 phosphorylation-site mutants.** The activity of the p53 mutants described in Figure 4 is presented as relative light units in two p53 reporter strains using the Killer/DR5 or the p21-5' REs upstream of a luciferase reporter. Results were obtained with the traditional assay format and are normalized to amount of soluble proteins. 4D refers to a quadruple mutant with the S15D, T18E, S20D, S33D changes in p53. 6A indicates a multiple mutant with alanine changes at S15, T18, S20, S33, S37, S46. 6D indicates a multiple mutant with aspartic acid changes at S15, S20, S33, S37, S46 and a glutamic acid change at T18. **5. Impact of small molecules Nutlin and RITA on the growth of WT yeast reporter strains or the isogenic derivatives with modified chemical uptake.** Overnight cultures grown in synthetic glucose medium were washed and diluted to ~0.1 OD_{600nm} as measured by a plate reader. (A) The WT strain was treated with 40 μM or 80 μM Nutlin (indicated as nutlin 1 and

nutlin 2 respectively) and 1 μM or 2 μM RITA (indicated as rita1 and rita2). (B) The indicated mutant ABC-transporter strains were treated with 1 μM RITA (or DMSO solvent control). OD was measured at the following times: 2, 4, 8, 12 and 24 hrs. Error bars correspond to the standard deviations of three biological replicates. **6. Negative impact of RITA on the *Firefly* luciferase but not the *Renilla* luciferase.** To confirm that the negative impact of RITA on the *Firefly* reporter was not dependent on modulation of p53 transactivation, an isogenic derivative strain was developed containing the PUMA p53 RE upstream of the *Renilla* luciferase. Wild-type p53-dependent transactivation was examined in cultures treated with DMSO control solvent or with 1 μM RITA. Presented are relative light units normalized to OD_{600nm} of the cultures. The error bars correspond to standard deviations for three biological repeats. **7. Apparent lack of PRIMA-1 effects on yeast growth or p53-dependent transactivation.** (A) *The small molecule PRIMA-1 does not affect yeast growth.* Overnight cultures grown in synthetic glucose medium were washed, diluted to ~0.1 OD_{600nm}, as measured by a plate reader, and treated with 200 μM PRIMA-1. Growth curves were compared for the wild type strain or the indicated ABC-transporter mutants. OD_{600nm} was measured at the 2-, 4-, 8-, 12- and 24-hr time points. Presented are standard deviations for three biological repeats. (B) *The small molecule PRIMA-1 does not impact wild type p53 transactivation capacity.* Cells were grown in glucose-containing media to keep p53 expression repressed and transferred to galactose-containing media followed by the addition of PRIMA-1. Dual luciferase assays were conducted 16 hrs after the treatment. *Renilla* luciferase was used as normalization factor. There was no significant effect of PRIMA-1 on WT p53 transactivation. The same result was obtained with a diploid yeast strain, in which both the p53-dependent reporter (*Firefly*) and the control luciferase (*Renilla*) were placed at the ADE2 chromosomal locus (*i.e.*, heteroalleles), thus removing potential chromatin effects on reporter expression. The diploid strain was obtained starting from two isogenic isolates of our yLFM strain background that differ for the mating type locus. Presented is the fold-induction of the *Firefly* reporter over the *Renilla* reporter relative to strains that do not express p53, as they contain an empty expression vector. (C) *The small molecule PRIMA-1 does not affect mutant p53 transactivation capacity.* Different p53 alleles were expressed at moderate levels using medium containing 0.128% galactose. PRIMA-1 (200 μM) was added to the cultures at the time of the switch to galactose-containing medium. Presented are the average fold-induction by p53 proteins compared to empty vector and normalized using the *Renilla* control luciferase. Presented are standard deviations for three biological repeats. (DOC)

Author Contributions

Conceived and designed the experiments: VA YC PM MAR AI. Performed the experiments: VA YC PM AB ML JJ AI. Analyzed the data: VA YC PM AB ML JJ GF PM MAR AI. Contributed reagents/materials/analysis tools: GF PM. Wrote the paper: VA YC PM JJ MAR AI.

References

- Riley T, Sontag E, Chen P, Levine A (2008) Transcriptional control of human p53-regulated genes. *Nat Rev Mol Cell Biol* pp 402–412.
- Menendez D, Inga A, Resnick MA (2009) The expanding universe of p53 targets. *Nature Rev Cancer* 9: 724–737.
- Lane D, Levine A (2010) p53 Research: The Past Thirty Years and the Next Thirty Years. *Cold Spring Harb Perspect Biol* 2: a000893.
- Vousden KH, Ryan KM (2009) p53 and metabolism. *Nat Rev Cancer* 9: 691–700.
- Gottlieb E, Vousden KH (2010) p53 regulation of metabolic pathways. *Cold Spring Harb Perspect Biol* 2: a001040.
- Perry ME (2010) The regulation of the p53-mediated stress response by MDM2 and MDM4. *Cold Spring Harb Perspect Biol* 2: a000968.

7. Olivier M, Hollstein M, Hainaut P (2010) TP53 mutations in human cancers: origins, consequences, and clinical use. *Cold Spring Harb Perspect Biol* 2: a001008.
8. Christophorou MA, Martin-Zanca D, Soucek L, Lawlor ER, Brown-Swigart L, et al. (2005) Temporal dissection of p53 function in vitro and in vivo. *Nat Genet* 37: 718–726.
9. Kastan MB (2007) Wild-type p53: tumors can't stand it. *Cell* 128: 837–840.
10. Farnebo M, Bykov VJ, Wiman KG (2010) The p53 tumor suppressor: a master regulator of diverse cellular processes and therapeutic target in cancer. *Biochem Biophys Res Commun* 396: 85–89.
11. Xue W, Zender L, Miething C, Dickins RA, Hernando E, et al. (2007) Senescence and tumour clearance is triggered by p53 restoration in murine liver carcinomas. *Nature* 445: 656–660.
12. Ventura A, Kirsch DG, McLaughlin ME, Tuveson DA, Grimm J, et al. (2007) Restoration of p53 function leads to tumour regression in vivo. *Nature* 445: 661–665.
13. Blagosklonny MV, el-Deiry WS (1996) In vitro evaluation of a p53-expressing adenovirus as an anti-cancer drug. *Int J Cancer* 67: 386–392.
14. Foster BA, Coffey HA, Morin MJ, Rastinejad F (1999) Pharmacological rescue of mutant p53 conformation and function [see comments]. *Science* 286: 2507–2510.
15. Komarov PG, Komarova EA, Kondratov RV, Christov-Tselkov K, Coon JS, et al. (1999) A Chemical Inhibitor of p53 That Protects Mice from the Side Effects of Cancer Therapy. *Science* 285: 1733–1737.
16. Michael D, Oren M (2002) The p53 and Mdm2 families in cancer. *Curr Opin Genet Dev* 12: 53–59.
17. Toledo F, Wahl GM (2007) MDM2 and MDM4: p53 regulators as targets in anticancer therapy. *Int J Biochem Cell Biol*. pp 1476–1482.
18. Toledo F, Wahl GM (2006) Regulating the p53 pathway: in vitro hypotheses, in vivo veritas. *Nat Rev Cancer*. pp 909–923.
19. Kaustov L, Lukin J, Lemak A, Duan S, Ho M, et al. (2007) The conserved CPH domains of Cul7 and PARC are protein-protein interaction modules that bind the tetramerization domain of p53. *J Biol Chem*. pp 11300–11307.
20. Montes de Oca Luna R, Wagner DS, Lozano G (1995) Rescue of early embryonic lethality in mdm2-deficient mice by deletion of p53. *Nature* 378: 203–206.
21. Eischen CM, Lozano G (2009) p53 and MDM2: antagonists or partners in crime? *Cancer Cell* 15: 161–162.
22. Han X, Garcia-Manero G, McDonnell TJ, Lozano G, Medeiros LJ, et al. (2007) HDM4 (HDMX) is widely expressed in adult pre-B acute lymphoblastic leukemia and is a potential therapeutic target. *Mod Pathol* 20: 54–62.
23. Valentin-Vega YA, Barboza JA, Chau GP, El-Naggar AK, Lozano G (2007) High levels of the p53 inhibitor MDM4 in head and neck squamous carcinomas. *Hum Pathol* 38: 1553–1562.
24. Arkin MR, Wells JA (2004) Small-molecule inhibitors of protein-protein interactions: progressing towards the dream. *Nat Rev Drug Discov* 3: 301–317.
25. Issaeva N, Bozko P, Enge M, Protopopova M, Verhoef LG, et al. (2004) Small molecule RITA binds to p53, blocks p53-HDM-2 interaction and activates p53 function in tumors. *Nat Med* 10: 1321–1328.
26. Vassilev LT, Vu BT, Graves B, Carvajal D, Podlaski F, et al. (2004) In vivo activation of the p53 pathway by small-molecule antagonists of MDM2. *Science* 303: 844–848.
27. Sun SH, Zheng M, Ding K, Wang S, Sun Y (2008) A small molecule that disrupts Mdm2-p53 binding activates p53, induces apoptosis and sensitizes lung cancer cells to chemotherapy. *Cancer Biol Ther* 7: 845–852.
28. Popowicz GM, Czarna A, Holak TA (2008) Structure of the human Mdmx protein bound to the p53 tumor suppressor transactivation domain. *Cell Cycle* 7: 2441–2443.
29. Shangary S, Ding K, Qiu S, Nikolovska-Coleska Z, Bauer JA, et al. (2008) Reactivation of p53 by a specific MDM2 antagonist (MI-43) leads to p21-mediated cell cycle arrest and selective cell death in colon cancer. *Mol Cancer Ther* 7: 1533–1542.
30. Resnick MA, Inga A (2003) Functional mutants of the sequence-specific transcription factor p53 and implications for master genes of diversity. *Proc Natl Acad Sci U S A* 100: 9934–9939. Epub 2003 Aug 9938.
31. Jordan JJ, Menendez D, Inga A, Nourredine M, Bell D, et al. (2008) Noncanonical DNA motifs as transactivation targets by wild type and mutant p53. *PLoS Genet* 4: e1000104.
32. Tomso DJ, Inga A, Menendez D, Pittman GS, Campbell MR, et al. (2005) Functionally distinct polymorphic sequences in the human genome that are targets for p53 transactivation. *Proc Natl Acad Sci U S A* 102: 6431–6436.
33. Jegga AG, Inga A, Menendez D, Aronow BJ, Resnick MA (2008) Functional evolution of the p53 regulatory network through its target response elements. *Proc Natl Acad Sci U S A* 105: 944–949.
34. Selivanova G, Iotsova V, Okan I, Fritsche M, Strom M, et al. (1997) Restoration of the growth suppression function of mutant p53 by a synthetic peptide derived from the p53 C-terminal domain. *Nat Med* 3: 632–638.
35. Bykov VJ, Issaeva N, Shilov A, Hultcrantz M, Pugacheva E, et al. (2002) Restoration of the tumor suppressor function to mutant p53 by a low-molecular-weight compound. *Nat Med* 8: 282–288.
36. Wiman KG (2010) Pharmacological reactivation of mutant p53: from protein structure to the cancer patient. *Oncogene* 29: 4245–4252.
37. Komarov PG, Komarova EA, Kondratov RV, Christov-Tselkov K, Coon JS, et al. (1999) A chemical inhibitor of p53 that protects mice from the side effects of cancer therapy. *Science* 285: 1733–1737.
38. Inga A, Storic F, Darden TA, Resnick MA (2002) Differential transactivation by the p53 transcription factor is highly dependent on p53 level and promoter target sequence. *Mol Cell Biol* 22: 8612–8625.
39. Stepanov A, Nitiss KC, Neale G, Nitiss JL (2008) Enhancing drug accumulation in *Saccharomyces cerevisiae* by repression of pleiotropic drug resistance genes with chimeric transcription repressors. *Mol Pharmacol* 74: 423–431.
40. Storic F, Resnick MA (2006) The delitto perfetto approach to in vivo site-directed mutagenesis and chromosome rearrangements with synthetic oligonucleotides in yeast. *Methods Enzymol* 409: 329–345.
41. Storic F, Durham CL, Gordenin DA, Resnick MA (2003) Chromosomal site-specific double-strand breaks are efficiently targeted for repair by oligonucleotides in yeast. *Proc Natl Acad Sci U S A* 100: 14994–14999.
42. Kolodkin AL, Klar AJ, Stahl FW (1986) Double-strand breaks can initiate meiotic recombination in *S. cerevisiae*. *Cell* 46: 733–740.
43. Tran HT, Keen JD, Krickler M, Resnick MA, Gordenin DA (1997) Hypermutability of homonucleotide runs in mismatch repair and DNA polymerase proofreading yeast mutants. *Mol Cell Biol* 17: 2859–2865.
44. Meyers S, Schauer W, Balzi E, Wagner M, Goffeau A, et al. (1992) Interaction of the yeast pleiotropic drug resistance genes PDR1 and PDR5. *Curr Genet* 21: 431–436.
45. Reamon-Buettner SM, Ciribilli Y, Traverso I, Kuhls B, Inga A, et al. (2009) A functional genetic study identifies HAND1 mutations in septation defects of the human heart. *Hum Mol Genet* 18: 3567–3578.
46. Flaman JM, Frebourg T, Moreau V, Charbonnier F, Martin C, et al. (1995) A simple p53 functional assay for screening cell lines, blood, and tumors. *Proc Natl Acad Sci U S A* 92: 3963–3967.
47. Inga A, Monti P, Fronza G, Darden T, Resnick MA (2001) p53 mutants exhibiting enhanced transcriptional activation and altered promoter selectivity are revealed using a sensitive, yeast-based functional assay. *Oncogene* 20: 501–513.
48. Golin J, Ambudkar SV, Gottesman MM, Habib AD, Szczepanski J, et al. (2003) Studies with novel Pdr5p substrates demonstrate a strong size dependence for xenobiotic efflux. *J Biol Chem* 278: 5963–5969.
49. Mitterbauer R, Weindorfer H, Safaie N, Krška R, Lemmens M, et al. (2003) A sensitive and inexpensive yeast bioassay for the mycotoxin zearalenone and other compounds with estrogenic activity. *Appl Environ Microbiol* 69: 805–811.
50. Freedman DA, Wu L, Levine AJ (1999) Functions of the MDM2 oncoprotein. *Cell Mol Life Sci* 55: 96–107.
51. Wang T, Kobayashi T, Takimoto R, Denes AE, Snyder EL, et al. (2001) hADA3 is required for p53 activity. *Embo J* 20: 6404–6413.
52. Alarcon-Vargas D, Ronai Z (2002) p53-Mdm2—the affair that never ends. *Carcinogenesis* 23: 541–547.
53. Chao C, Saito S, Anderson CW, Appella E, Xu Y (2000) Phosphorylation of murine p53 at ser-18 regulates the p53 responses to DNA damage. *Proc Natl Acad Sci U S A* 97: 11936–11941.
54. Dumaz N, Meek DW (1999) Serine15 phosphorylation stimulates p53 transactivation but does not directly influence interaction with HDM2. *Embo J* 18: 7002–7010.
55. Gasch AP, Spellman PT, Kao CM, Carmel-Harel O, Eisen MB, et al. (2000) Genomic expression programs in the response of yeast cells to environmental changes. *Mol Biol Cell* 11: 4241–4257.
56. Di Ventura B, Funaya C, Antony C, Knop M, Serrano L (2008) Reconstitution of Mdm2-dependent post-translational modifications of p53 in yeast. *PLoS One* 3: e1507.
57. Ward JM, Minn K, van Deursen J, Chen J (2003) p53 Binding protein 53BP1 is required for DNA damage responses and tumor suppression in mice. *Mol Cell Biol* 23: 2556–2563.
58. Iwabuchi K, Bartel PL, Li B, Marraccino R, Fields S (1994) Two cellular proteins that bind to wild-type but not mutant p53. *Proc Natl Acad Sci U S A* 91: 6098–6102.
59. Selivanova G (2010) Therapeutic targeting of p53 by small molecules. *Semin Cancer Biol* 20: 46–56.
60. Grinkevich VV, Nikulenkova F, Shi Y, Enge M, Bao W, et al. (2009) Ablation of key oncogenic pathways by RITA-reactivated p53 is required for efficient apoptosis. *Cancer Cell* 15: 441–453.
61. Lambert JM, Gorzov P, Veprintsev DB, Soderqvist M, Segerback D, et al. (2009) PRIMA-1 reactivates mutant p53 by covalent binding to the core domain. *Cancer Cell* 15: 376–388.
62. Poyurovsky MV, Katz C, Laptchenko O, Beckerman R, Lokshin M, et al. (2010) The C terminus of p53 binds the N-terminal domain of MDM2. *Nat Struct Mol Biol* 17: 982–989.
63. Kussie PH, Gorina S, Marechal V, Elenbaas B, Moreau J, et al. (1996) Structure of the MDM2 oncoprotein bound to the p53 tumor suppressor transactivation domain. *Science* 274: 948–953.
64. FitzGerald JE, Grenon M, Lowndes NF (2009) 53BP1: function and mechanisms of focal recruitment. *Biochem Soc Trans* 37: 897–904.
65. Shibata A, Barton O, Noon AT, Dahm K, Deckbar D, et al. (2010) Role of ATM and the damage response mediator proteins 53BP1 and MDC1 in the maintenance of G(2)/M checkpoint arrest. *Mol Cell Biol* 30: 3371–3383.

66. Cao L, Xu X, Bunting SF, Liu J, Wang RH, et al. (2009) A selective requirement for 53BP1 in the biological response to genomic instability induced by Brca1 deficiency. *Mol Cell* 35: 534–541.
67. Derbyshire DJ, Basu BP, Serpell LC, Joo WS, Date T, et al. (2002) Crystal structure of human 53BP1 BRC1 domains bound to p53 tumour suppressor. *Embo J* 21: 3863–3872.
68. Kachirskaia I, Shi X, Yamaguchi H, Tanoue K, Wen H, et al. (2008) Role for 53BP1 Tudor domain recognition of p53 dimethylated at lysine 382 in DNA damage signaling. *J Biol Chem* 283: 34660–34666.
69. Roy S, Musselman CA, Kachirskaia I, Hayashi R, Glass KC, et al. (2010) Structural insight into p53 recognition by the 53BP1 tandem Tudor domain. *J Mol Biol* 398: 489–496.
70. LaRusch GA, Jackson MW, Dunbar JD, Warren RS, Donner DB, et al. (2007) Nutlin3 blocks vascular endothelial growth factor induction by preventing the interaction between hypoxia inducible factor 1alpha and Hdm2. *Cancer Res* 67: 450–454.
71. Bykov VJ, Issaeva N, Selivanova G, Wiman KG (2002) Mutant p53-dependent growth suppression distinguishes PRIMA-1 from known anticancer drugs: a statistical analysis of information in the National Cancer Institute database. *Carcinogenesis* 23: 2011–2018.
72. Rehman A, Chahal MS, Tang X, Bruce JE, Pommier Y, et al. (2005) Proteomic identification of heat shock protein 90 as a candidate target for p53 mutation reactivation by PRIMA-1 in breast cancer cells. *Breast Cancer Res* 7: R765–774.
73. Russo D, Ottaggio L, Penna I, Foggetti G, Fronza G, et al. (2010) PRIMA-1 cytotoxicity correlates with nucleolar localization and degradation of mutant p53 in breast cancer cells. *Biochem Biophys Res Commun* 402: 345–350.
74. Zhang J, Adrian FJ, Jahnke W, Cowan-Jacob SW, Li AG, et al. (2010) Targeting Bcr-Abl by combining allosteric with ATP-binding-site inhibitors. *Nature* 463: 501–506.
75. Rinaldo C, Prodosmo A, Siepi F, Moncada A, Sacchi A, et al. (2009) HIPK2 regulation by MDM2 determines tumor cell response to the p53-reactivating drugs nutlin-3 and RITA. *Cancer Res* 69: 6241–6248.
76. Coutinho I, Pereira C, Pereira G, Goncalves J, Corte-Real M, et al. (2011) Distinct regulation of p53-mediated apoptosis by protein kinase C α , δ , ϵ , and ζ : Evidence in yeast for transcription-dependent and -independent p53 apoptotic mechanisms. *Exp Cell Res*.
77. Coutinho I, Pereira G, Leao M, Goncalves J, Corte-Real M, et al. (2009) Differential regulation of p53 function by protein kinase C isoforms revealed by a yeast cell system. *FEBS Lett* 583: 3582–3588.
78. Inga A, Resnick MA (2001) Novel human p53 mutations that are toxic to yeast can enhance transactivation of specific promoters and reactivate tumor p53 mutants. *Oncogene* 20: 3409–3419.
79. Petitjean A, Achatz MI, Borresen-Dale AL, Hainaut P, Olivier M (2007) TP53 mutations in human cancers: functional selection and impact on cancer prognosis and outcomes. *Oncogene* 26: 2157–2165.
80. Bullock AN, Henckel J, DeDecker BS, Johnson CM, Nikolova PV, et al. (1997) Thermodynamic stability of wild-type and mutant p53 core domain. *Proc Natl Acad Sci U S A* 94: 14338–14342.
81. Kato S, Han SY, Liu W, Otsuka K, Shibata H, et al. (2003) Understanding the function-structure and function-mutation relationships of p53 tumor suppressor protein by high-resolution missense mutation analysis. *Proc Natl Acad Sci U S A* 100: 8424–8429.
82. Shakked Z (2007) Quaternary structure of p53: the light at the end of the tunnel. *Proc Natl Acad Sci U S A* 104: 12231–12232.
83. Kitayner M, Rozenberg H, Kessler N, Rabinovich D, Shaulov L, et al. (2006) Structural basis of DNA recognition by p53 tetramers. *Mol Cell* 22: 741–753.
84. Kitayner M, Rozenberg H, Rohs R, Suad O, Rabinovich D, et al. (2010) Diversity in DNA recognition by p53 revealed by crystal structures with Hoogsteen base pairs. *Nat Struct Mol Biol* 17: 423–429.

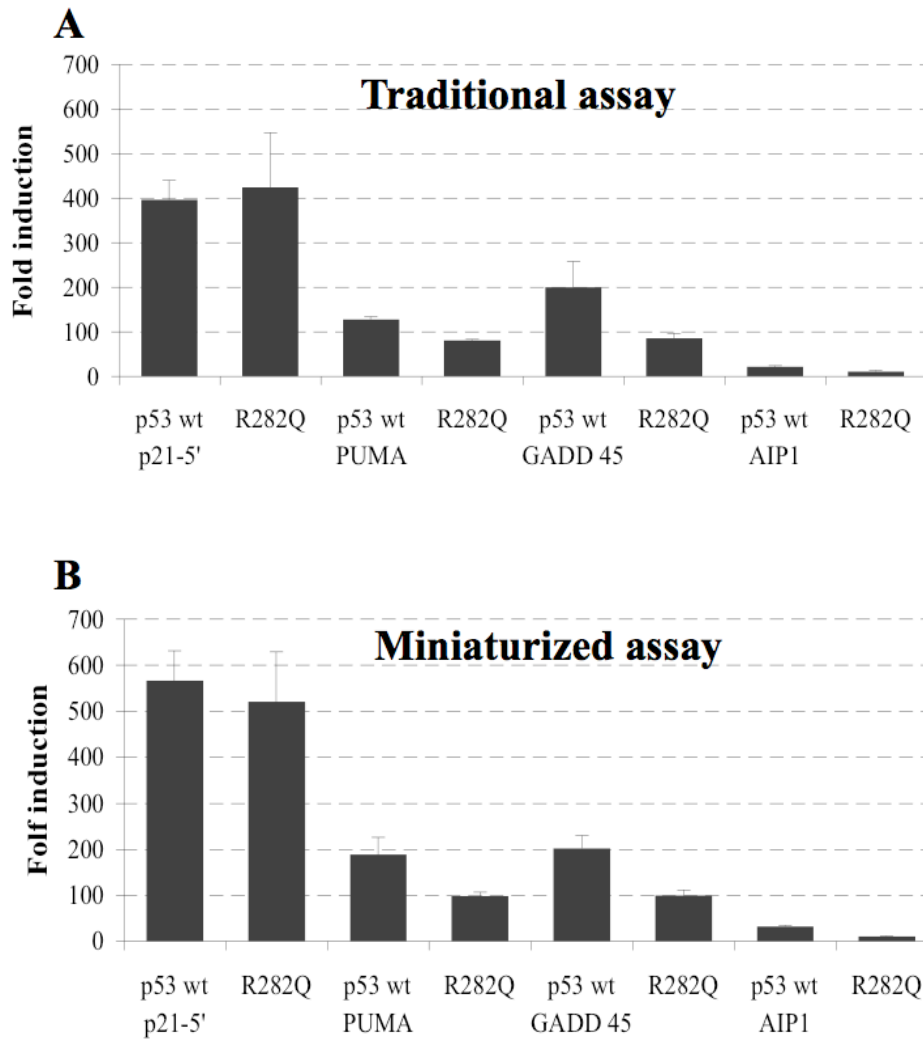
Supporting Information

1. Small-volume yeast functional assay with constitutive expression of p53 proteins. Presented is the comparison of the relative transactivation capacity of wild type (WT) and the R282Q p53 towards four different response elements (REs) obtained with the traditional assay based on 2 ml liquid cultures in individual tubes (A, traditional assay) and with the permeabilized assay format based on 100 μ l cultures prepared directly in 96-well plates (C, miniaturized assay). p53 proteins were expressed under the moderate, constitutive ADH1 promoter. Cells collected from the two different culture protocols were used for the measurement of luciferase activity as described in the [Materials and Methods](#) section. Presented are the average fold-induction of luciferase by p53 proteins relative to the activity obtained with an empty vector; included is the standard deviations of three replicates. In these experiments the light units per OD for WT p53 and the p21-5 \square RE were 2.8×10^6 for the 2 ml cultures and 2.5×10^7 for the 100 μ l cultures. **2. Impact of genetic modifications at the ABC transporter system on cell sensitivity to cycloheximide.** Based on the experiments described by Stepanov *et. al.* [39] we used cycloheximide treatment to evaluate whether the disruption of *PDR1* and replacement with the *PDR1*-repressor construct, the disruption of *PDR5*, or the combined modifications would result in enhanced toxicity in our reporter strain background. Cells from the indicated strains were resuspended in sterile water and transferred to a 96-well plate. Serial dilutions (1:5) were prepared and cells were transferred to plates containing synthetic medium (SD) with different concentrations of cycloheximide using a 48-pin replicator. A rich (YPDA) and an SD control plates were also spotted for comparison. Plates were incubated for two days at 30°C. **3. Phenotypic analysis of the impact of MDM2 on WT and mutant p53 transactivation.** The ADE2-based red/white assay was used to examine p53 dependent transactivation and the impact of MDM2. p53 was expressed at low levels under the *GAL1* promoter in media containing only raffinose (2%), or raffinose plus 0.002%, 0.004% or 0.016%, galactose. MDM2 was expressed from the constitutive *PGK1* promoter. p53 transactivation was examined from three REs upstream of ADE2-based p53 reporter strains as indicated. The optimized consensus (CON) and P21-5 \square p53 RE yield levels of high transactivation while the NOXA RE is weaker [38]. In the ADE2-based p53 functional assays, cells grown on plates containing a low-amount of adenine (5 mg/L) result in small red colonies when p53 is not present or not transcriptionally active. p53-dependent expression of ADE2 results in the appearance of colonies with a color ranging from light red to white, depending on the level of transactivation. To reveal the dependency of the phenotype on p53 expression levels, streaks are prepared on glucose plates containing high amount of adenine (200 mg/L) and the plates are incubated for two days at 30°C, resulting in the appearance of white colonies. These plates are then replica-plated to a stack of plates containing 2% raffinose plus various levels galactose along with the low-level of adenine. The replica plates are then incubated at 30°C for 2-3 days. Images of a section of the replicas are presented. For each image the upper section corresponds to colonies expressing p53 alone, while in the lower section the colonies also express MDM2. Various multiple mutants were tested, as indicated. **4. Relative transactivation capacity of p53 phosphorylation-site mutants.** The activity of the p53 mutants described in [Figure 4](#) is presented as relative light units in two p53 reporter strains using the Killer/DR5 or the p21-5 \square REs upstream of a luciferase reporter. Results were obtained with the traditional assay format and are normalized to amount of soluble proteins. 4D refers to a quadruple mutant with the S15D, T18E, S20D, S33D changes in p53. 6A indicates a multiple mutant with alanine changes at S15, T18, S20, S33, S37, S46. 6D indicates a multiple mutant with aspartic acid changes at S15, S20, S33, S37, S46 and a glutamic acid change

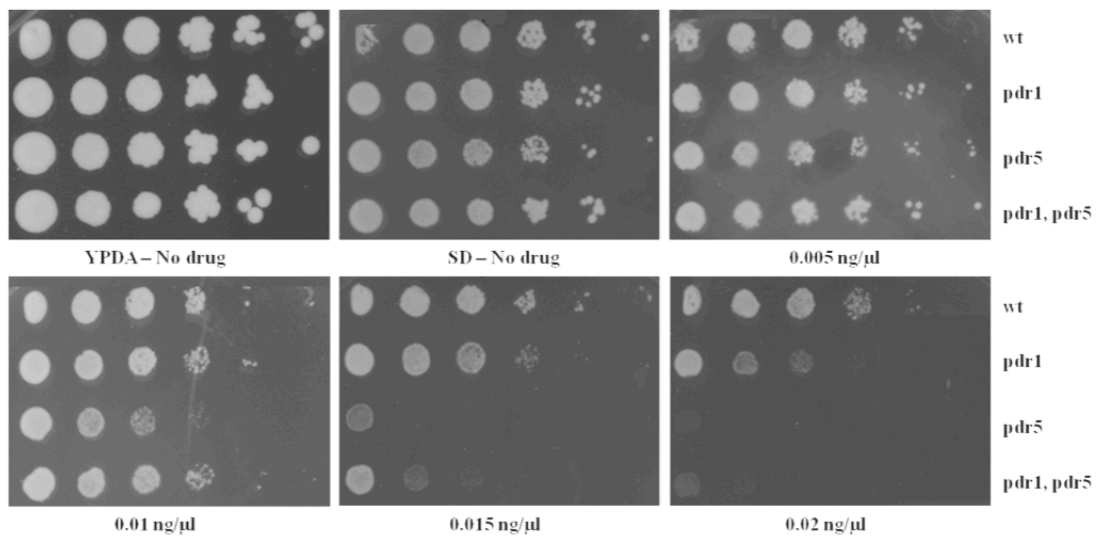
at T18. **5. Impact of small molecules Nutlin and RITA on the growth of WT yeast reporter strains or the isogenic derivatives with modified chemical uptake.** Overnight cultures grown in synthetic glucose medium were washed and diluted to ~ 0.1 OD_{600nm} as measured by a plate reader. (A) The WT strain was treated with 40 μ M or 80 μ M Nutlin (indicated as nutlin 1 and nutlin 2 respectively) and 1 μ M or 2 μ M RITA (indicated as rita1 and rita2). (B) The indicated mutant ABC-transporter strains were treated with 1 μ M RITA (or DMSO solvent control). OD was measured at the following times: 2, 4, 8, 12 and 24 hrs. Error bars correspond to the standard deviations of three biological replicates. **6. Negative impact of RITA on the *Firefly* luciferase but not the *Renilla* luciferase.** To confirm that the negative impact of RITA on the *Firefly* reporter was not dependent on modulation of p53 transactivation, an isogenic derivative strain was developed containing the PUMA p53 RE upstream of the *Renilla* luciferase. Wild-type p53-dependent transactivation was examined in cultures treated with DMSO control solvent or with 1 μ M RITA. Presented are relative light units normalized to OD_{600nm} of the cultures. The error bars correspond to standard deviations for three biological repeats. **7. Apparent lack of PRIMA-1 effects on yeast growth or p53-dependent transactivation.** (A) *The small molecule PRIMA-1 does not affect yeast growth.* Overnight cultures grown in synthetic glucose medium were washed, diluted to ~ 0.1 OD_{600nm}, as measured by a plate reader, and treated with 200 μ M PRIMA-1. Growth curves were compared for the wild type strain or the indicated ABC-transporter mutants. OD_{600nm} was measured at the 2-, 4-, 8-, 12- and 24-hr time points. Presented are standard deviations for three biological repeats. (B) *The small molecule PRIMA-1 does not impact wild type p53 transactivation capacity.* Cells were grown in glucose-containing media to keep p53 expression repressed and transferred to galactose-containing media followed by the addition of PRIMA-1. Dual luciferase assays were conducted 16 hrs after the treatment. *Renilla* luciferase was used as normalization factor. There was no significant effect of PRIMA-1 on WT p53 transactivation. The same result was obtained with a diploid yeast strain, in which both the p53-dependent reporter (*Firefly*) and the control luciferase (*Renilla*) were placed at the *ADE2* chromosomal locus (*i.e.*, heteroalleles), thus removing potential chromatin effects on reporter expression. The diploid strain was obtained starting from two isogenic isolates of our γ LFM strain background that differ for the mating type locus. Presented is the fold-induction of the *Firefly* reporter over the *Renilla* reporter relative to strains that do not express p53, as they contain an empty expression vector. (C) *The small molecule PRIMA-1 does not affect mutant p53 transactivation capacity.* Different p53 alleles were expressed at moderate levels using medium containing 0.128% galactose. PRIMA-1 (200 μ M) was added to the cultures at the time of the switch to galactose-containing medium. Presented are the average fold-induction by p53 proteins compared to empty vector and normalized using the *Renilla* control luciferase. Presented are standard deviations for three biological repeats.

Supporting Information S1

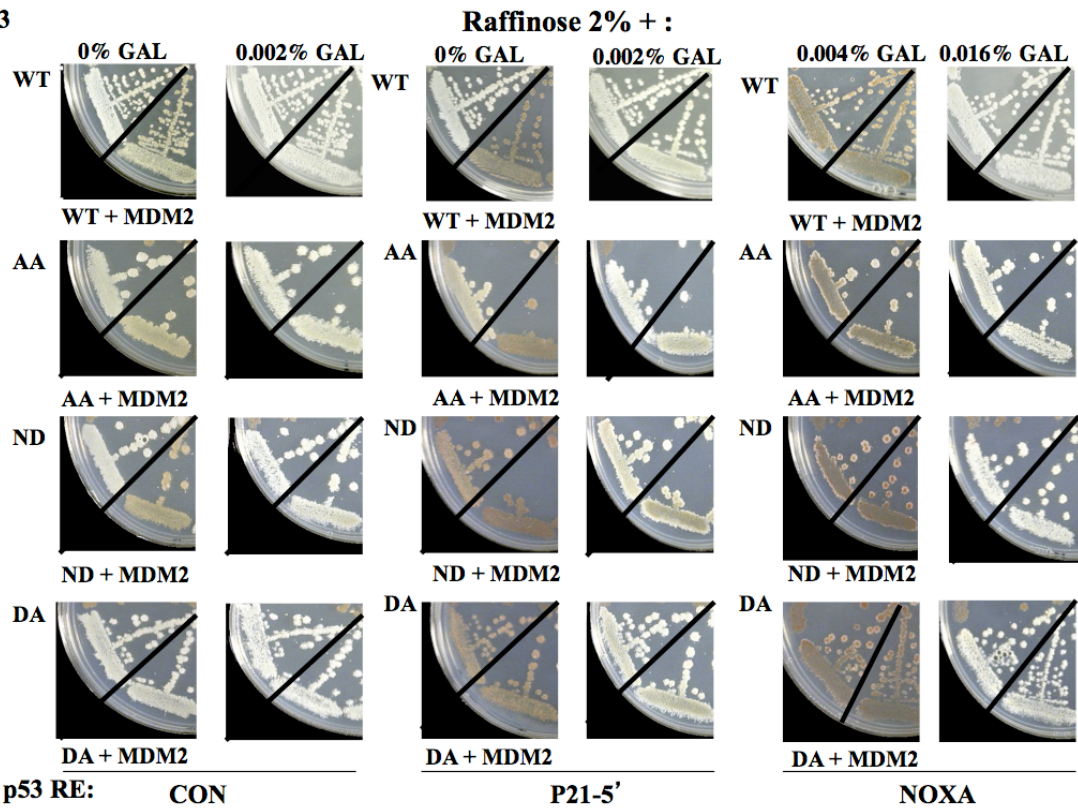
1)



2)



3



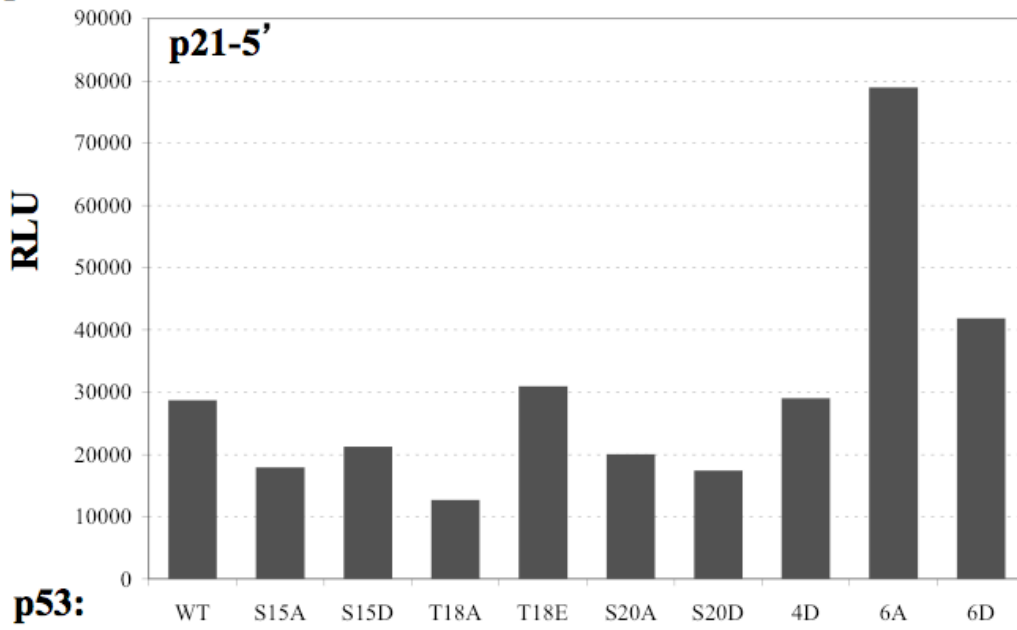
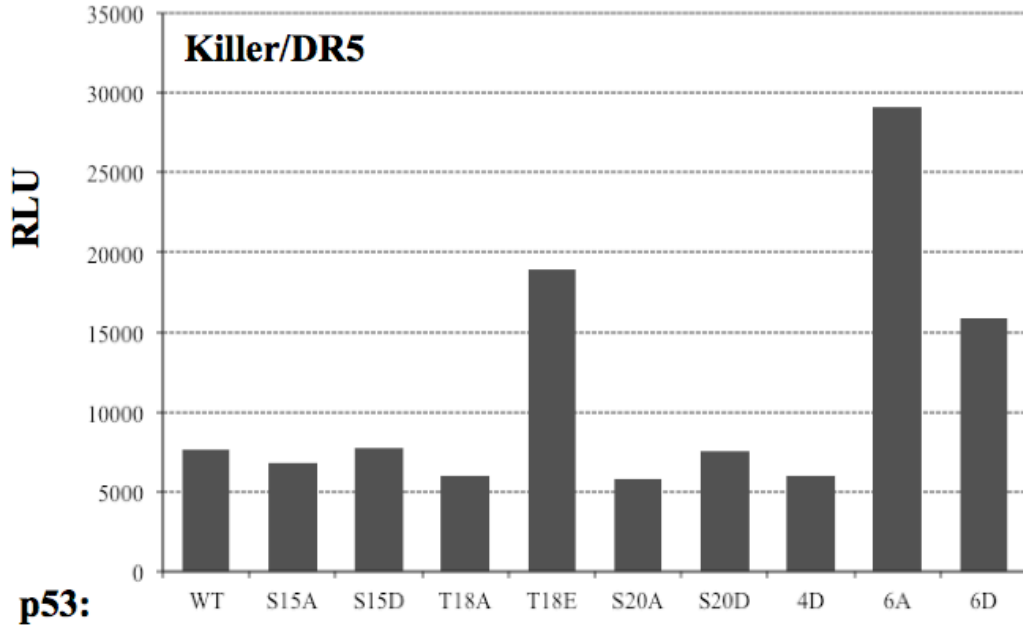
p53 RE: CON

P21-5'

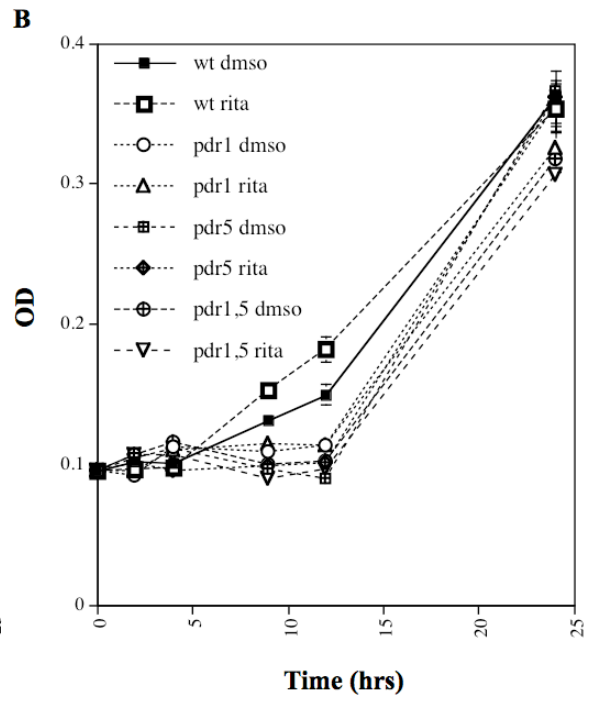
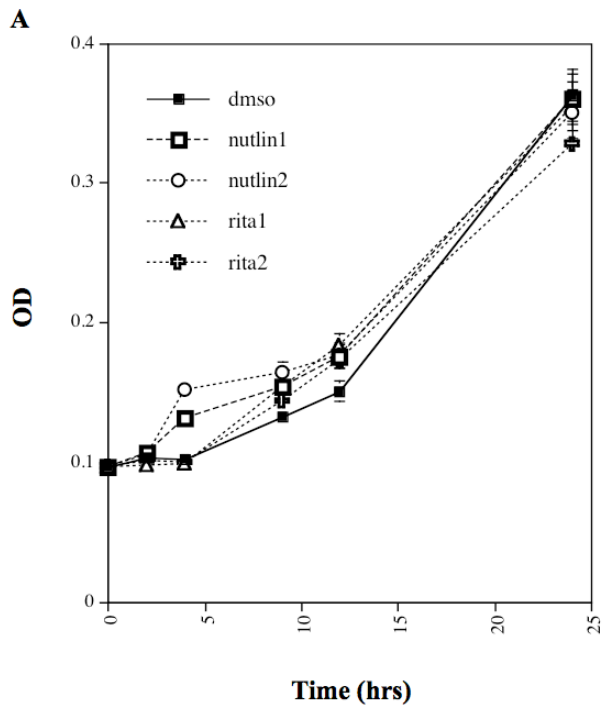
NOXA

53 mutant proteins: AA = Ser15, Thr18, Ser20, Ser33, Ser37, Ser46 -> Ala ND = Ser33, Ser37, Ser46 -> Asp
 DA = Ser15, Thr18, Ser20 -> Asp; Ser33, Ser37, Ser46 -> Ala

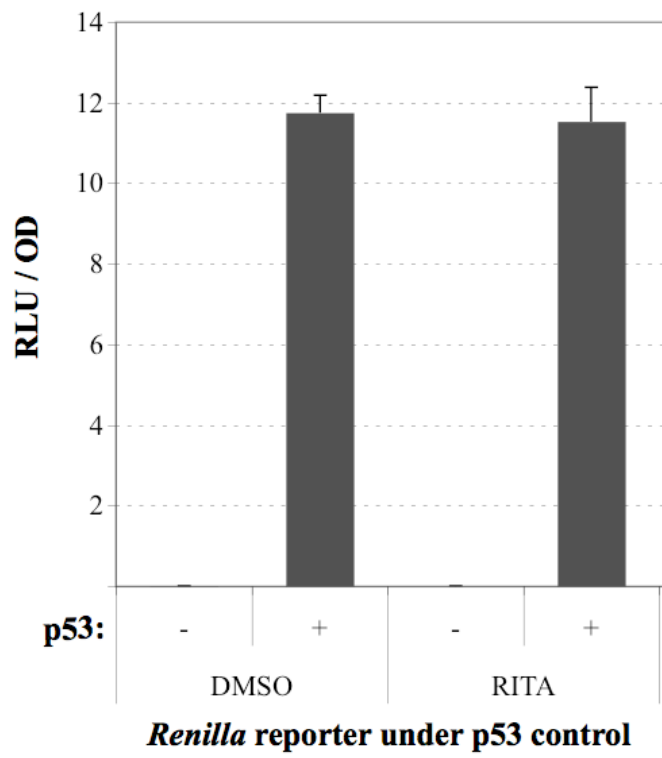
4)



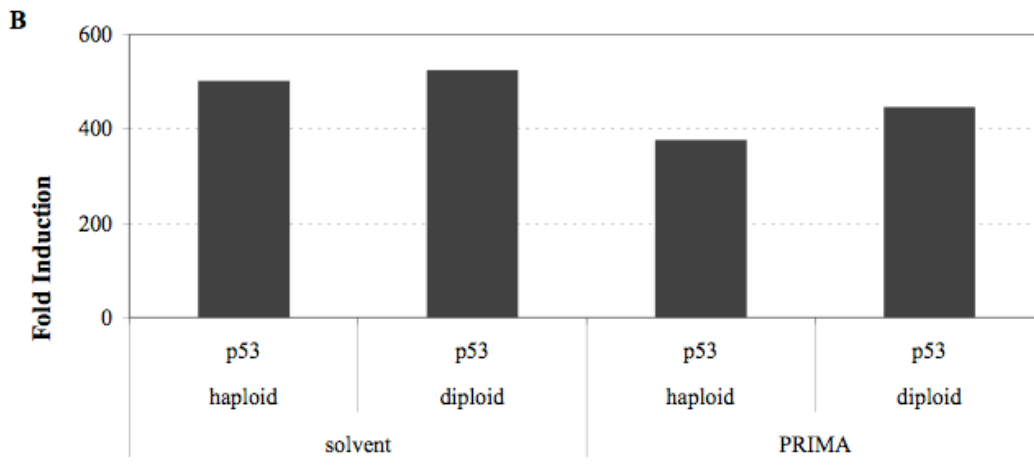
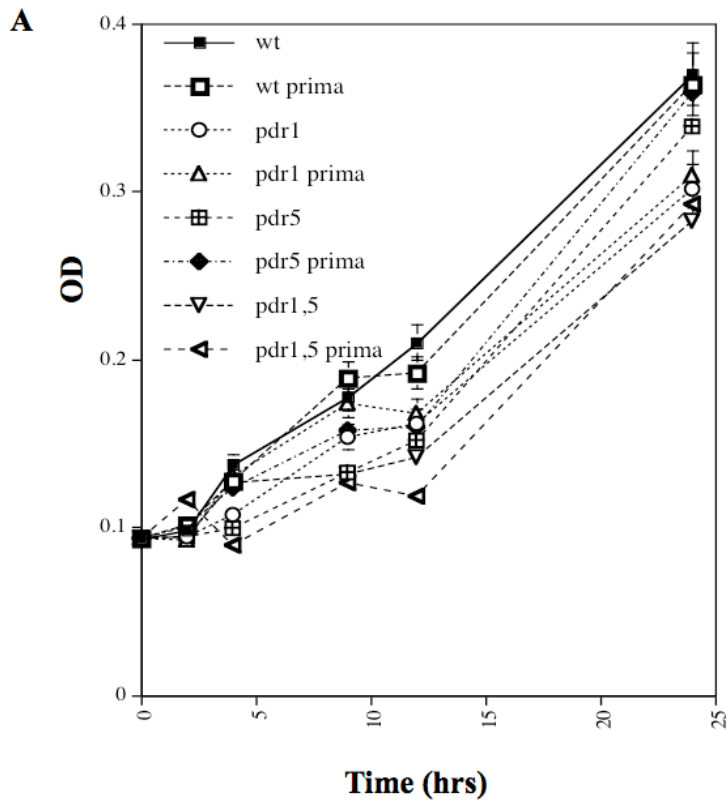
5)



6)



7)



C

